Technical Developments for the Geomorphological Reconstruction of Palaeo Ice Sheets from Remotely Sensed Data

Michael Johnson Smith

A Thesis Submitted for the Degree of Doctor of Philosophy

Department of Geography
University of Sheffield

Submitted: May 2003

Title:

Technical Developments for the Geomorphological Reconstruction of Palaeo Ice Sheets from Remotely Sensed Data

Summary:

Ice sheet reconstructions are concerned with an understanding of the dynamics of palaeo ice sheets through time. This involves ascertaining the configuration of ice domes and flow patterns, as well as the evolution of glaciation and deglaciation. The use of remotely sensed data (radar and visual/near infra-red imagery) has been a key development in these studies, allowing the rapid mapping of individual landforms over large areas. These data sources record electro-magnetic reflectance of an illuminated landscape which leads to the introduction of random and systematic bias'. This research explores the propagation of these bias' and recommends that, in order to obtain optimum imagery, sensor spatial resolution is <30m and solar elevation is <20º at acquisition. More problematic is the selective bias introduced by the solar azimuth in relation to the orientation of linear landforms. This cannot be removed and requires a good knowledge of the study area or an additional primary data source (e.g. radar or digital elevation model).

DEMs are rapidly supplementing, and in many cases replacing, satellite imagery in landform mapping. However as they record surface elevation, rather than surface reflectance, they should be able to provide a bias-free data source for landform mapping. Methods by which the landscape can be visualised are explored with the purpose of providing a bias free method, although no single visualisation was found to be satisfactory. A suitable mapping strategy was developed through the application of these methods to the mapping of glacial landforms from a DEM of the Lake District.

Once landform mapping has been completed it is common for mapped landform data to be generalised in order to reduce their complexity and so aid interpretation. This is usually a manual technique that involves reducing several thousand individual lineaments to summary lines. The thesis concludes with the development of a set of tools to help with this manual process, as well as provide quantitative verification. This is then applied to the landforms mapped from the Lake District in the previous chapter. A method for the automation of this procedure is also suggested.

Acknowledgements

Many people have been involved in the long toil of the past 6 years, all of whom I would like to thank for their help and support. In particular, thanks to Chris Clark. Your honesty and high standards are a breath of fresh air in the academic world. During my time, I have just about seen Jane, Coomeran, Chris and Paul come and go. You have all provided help in many ways (including data) and, as a research group, it's been great to have discussions.

Others who have helped include Paul Cole, Wishart Mitchell and Steve Wise. Graham and Paul put up with me throwing maps at them for printing. Many thanks to Steve and Kamie who have piqued my interest in DEMs; hopefully more work looms on this front. Rachel and Rut at Erdas have fielded (far too) numerous support calls from me.

A variety of data have been used in this project. The OS have provided free academic use of their DEM data, MIMAS have made available SPOT and Landsat TM satellite imagery, whilst Clas Hättestrand allowed access to the Russian ETM+ imagery. ERA-Maptec kindly forgot to invoice the project for the fantastic Landsat TM data.

Finally, my wife and children have formed a large part of this work. I thank them for their patience and long suffering, and maybe Daddy won't be locked away typing through the long evenings.

Table of Contents

1 Introduction

1.1 Introduction

Palaeo-environmental studies are an important part of geography as they provide a means by which we can understand our surroundings. By using our understanding of current processes we can look at landforms generated in the past and then infer the environment in which they were created. Although this assumes that current processes are good proxies for past ones, it is a powerful method as it not only allows us to provide a history, one which may inform us of singular events, but we can then use that information to help predict how our environment might operate in the future.

1.2 Use of Ice Sheet Reconstructions

The most widely publicised predictive studies are based around global environmental issues, such as global warming. General circulation models attempt to enter current environmental variables and predict future climatic states. Clearly the development of such models is based upon an understanding of contemporary processes, however there is great utility in calibrating or testing them using palaeo-environmental data. The reconstruction of past glacial environments clearly falls within this remit

Ice sheet reconstructions specifically try to recreate dynamics through time. This deals with the location and migration of ice sheets and divides, as well as the dating of changes in their configuration. It can then be postulated what were the causes of these changes. Ice sheets can be an important aid in determining the extent and degree of interaction between the atmosphere, geosphere and cryosphere and are believed to be the one of the most important feedback mechanisms that have modulated climate change over the last 2 million years. Once an ice sheet has been reconstructed in time and space, this can be compared with known or inferred behaviours of the ocean and atmosphere. Given the current poor level of knowledge of the dynamical change of the cryosphere, an ice sheet reconstruction should provide more insight into climate change through the combined inputs of the atmosphere (particularly changing

precipitation patterns), ocean (particularly the switching on and off of the oceanic deep water currents), cryosphere (particularly the extent and cause of Heinrich events) and external forcing (Milankovitch cycles).

1.3 Techniques for Ice Sheet Reconstruction

The use of remotely sensed data to perform ice sheet reconstructions is a relatively new technique. Prior to this, field mapping and aerial photography were the primary data sources. Using these techniques, it was difficult to acquire ice-sheet wide landform evidence and, as a result, processes inferred as operating over small areas of investigation were scaled up to the ice sheet level and extrapolated to cover wider regions. Ice sheet reconstructions tended to be syntheses combining evidence from different researchers who used different techniques and methodologies.

Mapping from remotely sensed data solved the issue of acquiring ice sheet wide landform evidence, however it introduced methodological problems concerning their integration and interpretation. Methods have gradually been developed to solve these issues, whilst newer, and better, primary data sources have been made available. Figure 1.1 presents a broad outline of the steps involved in an ice sheet reconstruction. After acquisition of a primary data source, glacial landforms are mapped by an observer. These are then generalised into summary flow patterns so that their interpretation into flow sets (glaciologically plausible scenarios) is easier. This then allows the production of a final, or several, reconstructions.

The last 20 years have seen a major shift in the way ice sheet reconstructions are performed. Rather than using piecemeal evidence that is hung together using an authors preferred interpretation, there is now an explicit methodology, with flow sets the key building blocks to data synthesis. Figure 1.2 shows a space-time diagram for an idealised region that has been glaciated. The top surface represents the present day land surface that has imprinted upon it evidence of former ice flow. Using this evidence it should be possible to infer the dynamics of an ice sheet through time. Geomorphologically based ice sheet reconstructions aim to do this.

Although the methodology by which these reconstructions are produced is well established (e.g. Clark, 1997), the primary source data can contain random or systematic errors which then become reproduced in the research. Additionally, the techniques used involve subjective or qualitative stages which can introduce biases through their application. At best this makes comparison between researchers and regions difficult, at worst it can make the results unreliable.

1.4 Aims and Objectives

The research for this PhD began with the intention of producing an ice sheet reconstruction for the United Kingdom and Ireland. Being an almost self-contained unit, Ireland was an obvious location to begin landform mapping. This was initially pursued using ERS-1 SAR imagery (satellite based radar) and later extended to include limited Landsat TM (satellite based visual/near infra-red) and digital elevation model (DEM) data. It quickly became apparent that not only were there differences between the different data sources, but in certain locations there was little similarity. It was clear that further landform mapping could not be pursued until these issues were resolved and this also called into question previous landform mapping exercises.

This research has therefore developed into an understanding of the above problems, as well as a refinement to some of the techniques used as part of a glacial reconstruction. This work can be divided into three broad research topics:

- **Aim 1: Investigate the presence of bias within satellite imagery**

Satellite imagery depicts topographic glacial landforms through the recording of reflected light on an illuminated surface. The detail of the images, and the manner in which the landscape is illuminated, controls how these landforms are depicted. This introduces both random and systematic biases into the imagery. The nature of this biasing is explored, with recommendations for their mitigation.

- **Aim 2: Explore visualisation techniques for DEM data**

DEMs are rapidly becoming an important primary data source for landform mapping. They have traditionally been visualised through relief shading, however this introduces biasing in a manner similar to those identified for satellite imagery. This section explores and assesses a variety of techniques for visualising DEMs.

- **Aim 3: Improvement of techniques for lineament generalisation**

The final part of the thesis is concerned with the generalisation of landform data from individually mapped landforms to coherent patterns that can be interpreted as part of ice-sheet wide events. This stage has traditionally been performed visually by the researcher and can introduce subjective bias at an early stage. A technique for quantitatively verifying this manual generalisation stage is introduced.

1.5 ThesisStructure

The next chapter introduces the broad methodology by which an ice sheet reconstruction is performed, introducing the reader to the technical and methodological techniques currently in use, as well as familiarising them with how an understanding of the processes that created landforms can be used to infer conditions in past environments. This is followed by a review of satellite imagery based ice sheet reconstructions (Chapter 3), with a particular emphasis on the techniques and methodologies used. Chapter 4 goes on to introduce the key research issues highlighted in Chapter 3 and how they might be investigated. Chapter 5 investigates the problems in using both VIR and radar satellite imagery in landform mapping exercises and concludes with recommendations for best practice. Chapter 6 goes on to review and develop different DEM visualisation techniques, with suggestions for performing mapping exercises. The final research chapter develops techniques to aid the generalisation of landforms into flow patterns. These can be iteratively refined and quantitatively verified.

Although this research began as an ice sheet reconstruction, it has developed into a refinement of the techniques used to perform them. Initial exploratory

work clearly identified weaknesses in current approaches. It is hoped that these improvements will allow better mapping, a greater take up in the use of DEM data and the better development of flow patterns and the resultant reconstructions.

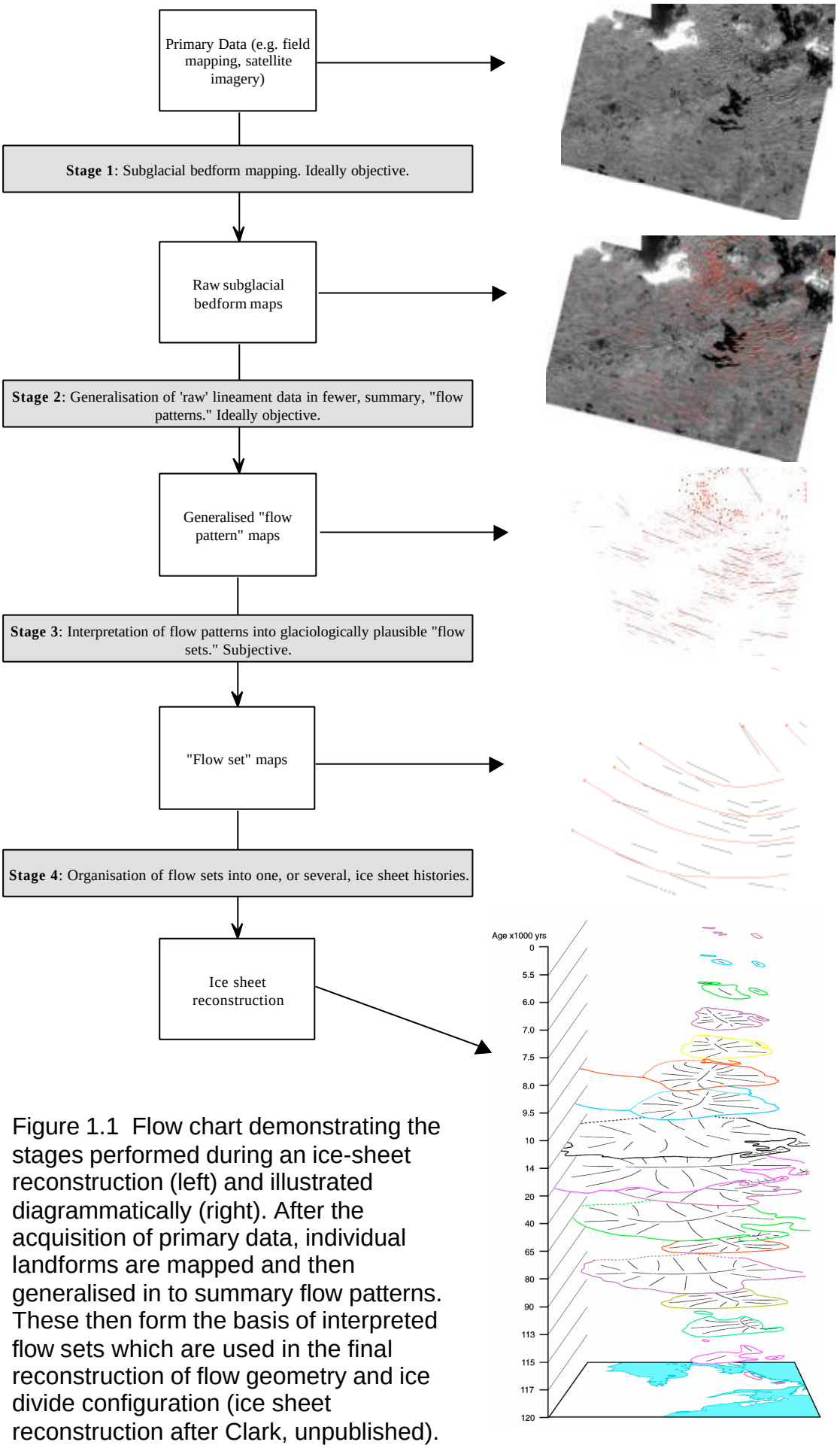

Figure 1.1 Flow chart demonstrating the stages performed during an ice-sheet reconstruction (left) and illustrated diagrammatically (right). After the acquisition of primary data, individual landforms are mapped and then generalised in to summary flow patterns. These then form the basis of interpreted flow sets which are used in the final reconstruction of flow geometry and ice divide configuration (ice sheet reconstruction after Clark, unpublished).

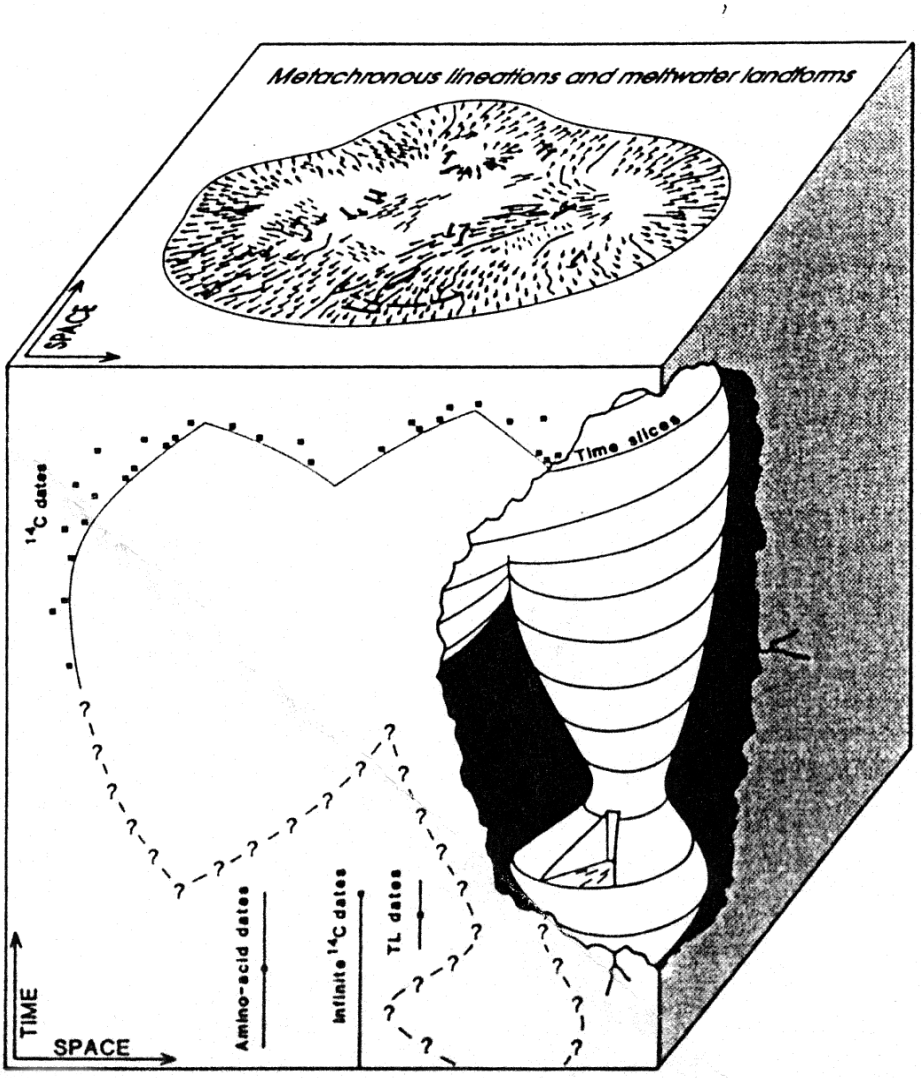

Figure 1.2 Space-Time cube showing the current geomorphological surface (top of cube) and the postulated ice sheet behaviour required to have generated this (Kleman *et al*, 1996). The “vase” in the centre of the cube provides an hypothesised reconstruction of the ice sheet through time. The front face shows how landform evidence can be used to mark the maximum extent of the ice sheet through time, whilst, where available, dating indicators match this to an absolute time scale.

2 Overview of Ice Sheet Reconstruction from Geomorphological Evidence

2.1 Introduction

Satellite images can be used to map glacial landforms and have been a good supplement to aerial photography due to their wide coverage and synoptic scale. A reconstruction of the glacial history of a region involves four stages:

- mapping individual landforms from satellite imagery.
- generalisation of individual landforms into distinctive flow patterns
- interpretation of flow patterns into distinctive flow sets
- palaeo-glacial interpretation of all glacial landform data to produce a reconstruction of ice sheet geometry, extent and changes through time.

This chapter will outline the image processing and mapping techniques currently used by researchers, as well as the methodological framework for landform interpretation. This is followed by a discussion of the palaeo-evidence provided by different landforms, the use of relative chronological data and the variation in interpretation of landforms and their implications for ice sheet reconstructions. The chapter is concluded with an example of an ice sheet reconstruction.

2.2 MethodologicalOverview

Ice sheet reconstructions have been a focus for research since the late 1800's and involve the collection and interpretation of landform data related to ice flow direction and marginal positions. It is an incremental procedure whereby knowledge slowly accumulates as more landforms are mapped. Researchers tend to collect and interpret their own geomorphological evidence (primary data), augmenting it with published literature (secondary data).

The acquisition of primary data was originally achieved through field work (e.g. striae mapping), later augmented with aerial photography and digital satellite imagery. Satellite imagery is particularly useful for ice sheet reconstructions as it allows a synoptic scale view of former glaciated areas and provides global

coverage. Interpretation relies upon the use (and development) of theories concerning landform formation.

Geomorphology attempts to provide further understanding of the real world through a “systematic process of investigation” (Rhoads and Thorn, 1993). This invariably takes place through observation of the physical system (or part thereof) being studied and the creation or testing of theory. Theory that is able to model the full complexity of the real world is closest to achievement on very small temporal and spatial scales, such as fluid dynamics (e.g. Jackson and Steyn, 1993). For larger spatial and temporal scales less information is available, leading to a greater subjective assessment of data. It is this problem that faces glacial reconstruction. More specifically, relict features are used to infer possible processes, through indirect empirical methods or, as Rhoads and Thorn (1993) state, historical retrodictive abduction.

Geomorphological landforms are formed through the interaction of one, or several, physical processes on the Earth’s surface. By studying currently active processes it is possible to learn the conditions and controls on landform development. When relict landforms are discovered we can then use this knowledge to infer the environmental conditions at the time of their formation. An example is the formation of striae through the abrasion of rocks embedded in the base of a warm based ice sheet as it passes over bedrock. The direction of ice flow can be inferred by striae orientation. However this method cannot be extended to landforms where their formational processes have not been observed. Drumlins fall into such a category and consequently theoretical development is reliant upon the study of relict landforms. These landforms are also used in the reconstruction of former ice sheets.

Boulton *et al* (2001) describe this area of research as *palaeoglaciology* and suggest that the following steps are required:

- characterise ice sheet dynamic elements
- identify geological features that reflect these elements
- interpret and integrate these features to recreate the behaviour of former ice sheets.

These steps can specifically be applied to reconstructions based upon satellite imagery (Figure 1.1) and are principally accomplished through the mapping of glacial lineaments (particularly drumlins and mega-lineaments). This technique is well established, having been used by Punkari (1982), Boulton and Clark (1990), Knight (1996), Dongelmans (1996) and discussed in detail by Clark (1997). Once complete, the lineament data is generalised. This is a data reduction stage designed to make the interpretation of regional ice flow patterns easier. Once a series of ice flow patterns are delimited, the observer finally produces a single, or series of, ice sheet reconstructions. There is a well developed theoretical framework for the reconstruction of past glacial environments (Clark, 1994,1999 and Kleman *et al*, 1996) using geomorphological landforms. These stages are discussed in more detail in the following sections. It should be born in mind that these techniques apply specifically to satellite imagery based investigations, however they are directly applicable to aerial photography, DEM and field work investigations. Aerial photography is still a valuable resource and satellite imagery should be viewed as a supplement to these data. Their higher resolution and ability to view terrain stereoscopically are used effectively by many researchers (e.g. Kleman *et al*, 1996), however these benefits must be weighed against the relative large scale (in general) of images (typically 1:40000 or less). The financial and labour investment often means that aerial photography is not a cost effective method for mapping glacial landforms over large areas.

2.3 MethodologicalTechniques

2.3.1 Satellite Imagery and Image Processing

The mapping of glacial landforms requires the acquisition of appropriate imagery for the area of interest. Although there are many active earth resources sensors, there are only a handful that are suitable for landform mapping (Table 2.1). There are two main types of sensor; Visible and Infra-Red (VIR) or Synthetic Aperture Radar (SAR). The former images are in the VIR part of the electromagnetic (EM) spectrum, whilst the latter images are in the microwave part of the EM spectrum. Landsat Multi-Spectral Scanner (MSS) has been used extensively as it has been available the longest, however its low spatial

resolution makes it unsuitable for detecting individual landforms. Landsat Thematic Mapper (TM) provides good resolving capabilities, whilst both Landsat Enhanced Thematic Mapper (ETM+) and SPOT Panchromatic sensors provide excellent imaging of glacial landforms. Landsat ETM+ is the most desirable VIR imagery at present and is relatively inexpensive. Landsat MSS is very cheap and consequently provides an economical medium for low cost landform mapping. SAR imagery provides a good resolution, however more knowledge is required during image processing due to technical considerations. In addition interpretation is more difficult, requiring an experienced observer.

For VIR imagery, representation of linear landforms can be enhanced by obtaining images during periods of low solar elevation so that fore slopes are illuminated slightly more than lee slopes (Slaney, 1981), highlighting topographic differences. It may also be possible to highlight moisture differences (spectral differentiation) between lineaments and the surrounding terrain (*geobotanical method*) through the use of band combinations (e.g. Punkari, 1982). Figure 2.1 shows two Landsat TM images of Lough Gara, Ireland. These images illustrate the advantages of using winter (bottom) imagery with low solar elevation, over summer (top) imagery.

VIR imagery require cloud free conditions in order to image the Earth. The use of low solar elevation to enhance lineaments, places constraints upon the timing of image acquisition. For mid-latitude regions this will be in mid-winter, making cloud free images difficult to obtain. This becomes more complex in high latitudes where it is also desirable to obtain snow free images so that landforms are not obscured.

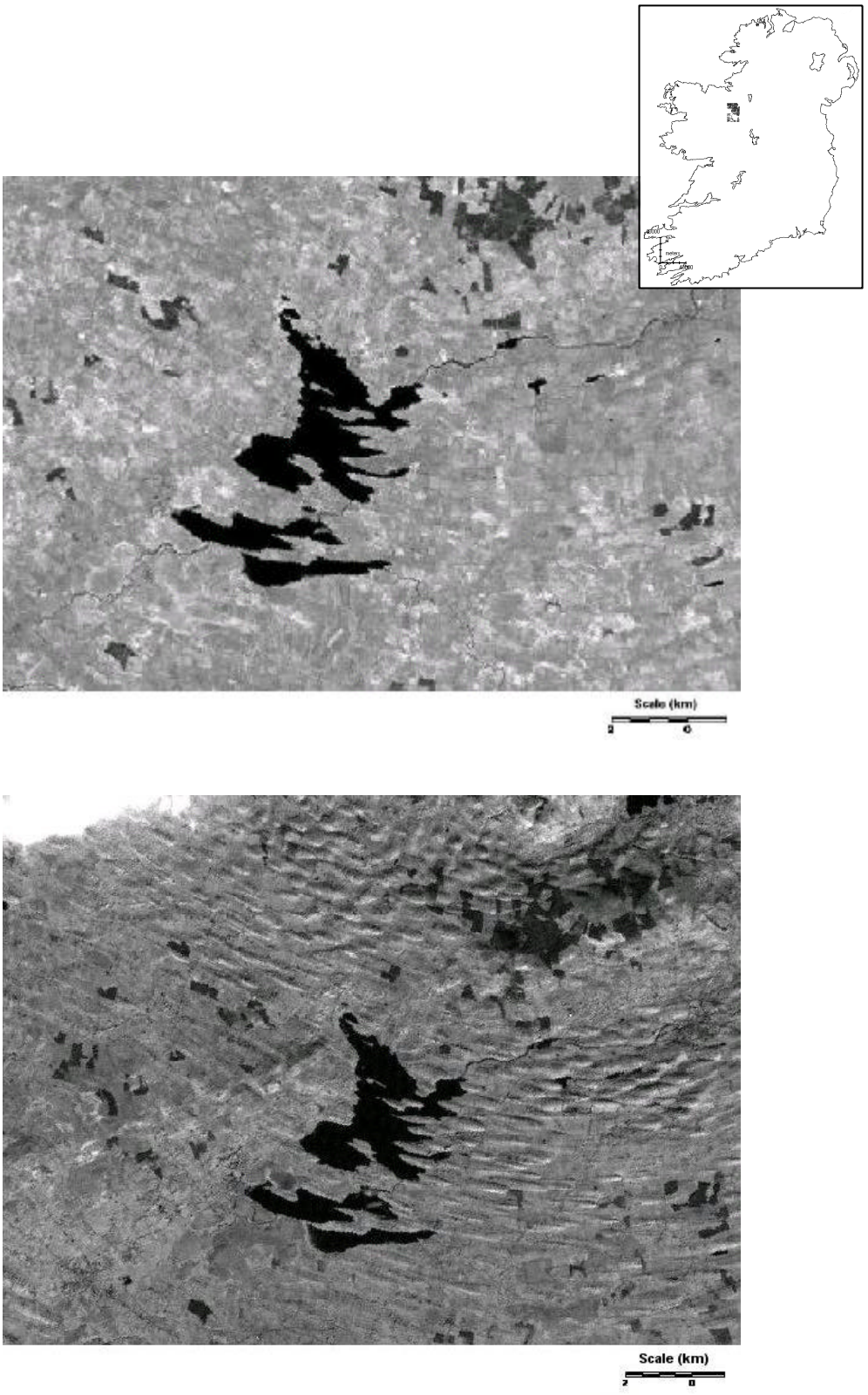

Figure 2.1a and b Landsat TM images of Lough Gara, Ireland, with a summer image (top; high solar elevation angle) and winter image (bottom; low solar elevation angle).

Satellite	Sensor	Nominal Resolution (m)	Image Size (km)
Landsat	MSS	80	185×185
Landsat	TM	30	185×185
Landsat	ETM+	15/30	185×185
SPOT	XS	20	60×60
SPOT	Pan	10	60×60
SEASAT	SAR	25	100×100
ERS	SAR	25	100×100
Radarsat	SAR	9-100	Swath width 50-500
Terra	Aster	15	60×60

Table 2.1 Earth resources satellites used in glacial reconstructions.

Clark (1997) reviews image pre-processing techniques used to enhance glacial landforms. For VIR images these include contrast stretching, convolution filtering and de-striping, as well as experimentation with colour composites in areas with mixed surface cover. Processing techniques for SAR are different as it is a microwave, rather than optical sensor. Vencatasawmy *et al* (1998) and Clark (1997) report specific recommendations for geomorphological applications. These involve de-speckling, data reduction and contrast improvements.

Pre-processing is followed by the geocorrection of the imagery to known geographic co-ordinates. For sub-pixel accuracy in geocorrection, topographic maps with high spatial accuracy are required and, if in mountainous terrain, a high resolution digital elevation model (DEM) is required to correct for relief displacement. Often neither of these requirements are met in glaciated terrain and so accuracy of the order of 5 pixels is attained. If topographic maps are not available for the selected region then it will require the simple correction using the corner co-ordinates supplied with the image; this will provide an accuracy of the order of 15-20 pixels. This order of accuracy is satisfactory for the synoptic

mapping of glacial landforms in the production of generalised flow events for a region.

2.3.2 Palaeoglaciological Landform Mapping

Once geocorrection is complete, glacial landforms, particularly lineaments, eskers, ribbed moraine, moraines and hummocky bedforms, need to be identified and mapped. This can be achieved by hand, on paper print-outs of the imagery and then manipulated on paper or later entered into a Geographic Information System (GIS). Alternatively landforms can be digitised on-screen within a GIS using thematic layers. This latter approach is more flexible as it allows viewing of the imagery at all scales and later digital manipulation.

Identification and digitisation is best performed at different scales to allow the recognition of different size landforms, although this is dependent upon the nominal resolution of the imagery. For Landsat MSS the most detailed mapping scale is 1:120,000, however for other imagery it is desirable to initially map at 1:75,000. This is followed by mapping at 1:150,000, with less intensive mapping at 1:300,000 and even 1:600,000. Once completed, a single image can contain several thousand lineaments. It is then important to check against the broad regional geology for spurious correlations with fault lines, drift covered rock ridges (scarps), bedding and major changes in lithology.

Mapping can be viewed as the initial interpretation (or abstraction) of the observations of an unknown surface imaged by a satellite sensor. It is the qualitative (manual) identification of landforms within an image and an appraisal of their significance. In addition, the observer requires experience at interpreting satellite imagery as well as in the subject area of interest.

2.3.3 Flowset Construction (Figure 2.2)

Before the interpretation of lineament patterns can begin, the original mapped lineaments are generalised or grouped into summary lines, termed **flow patterns**. Flow patterns represent groups of glacial lineaments, with high parallel conformity and similar morphometry (e.g. length, spacing), reducing the amount of data for interpretation. Spatially coherent flow patterns are then taken and interpreted into distinct flow events termed **flow sets** (Boulton and Clark,

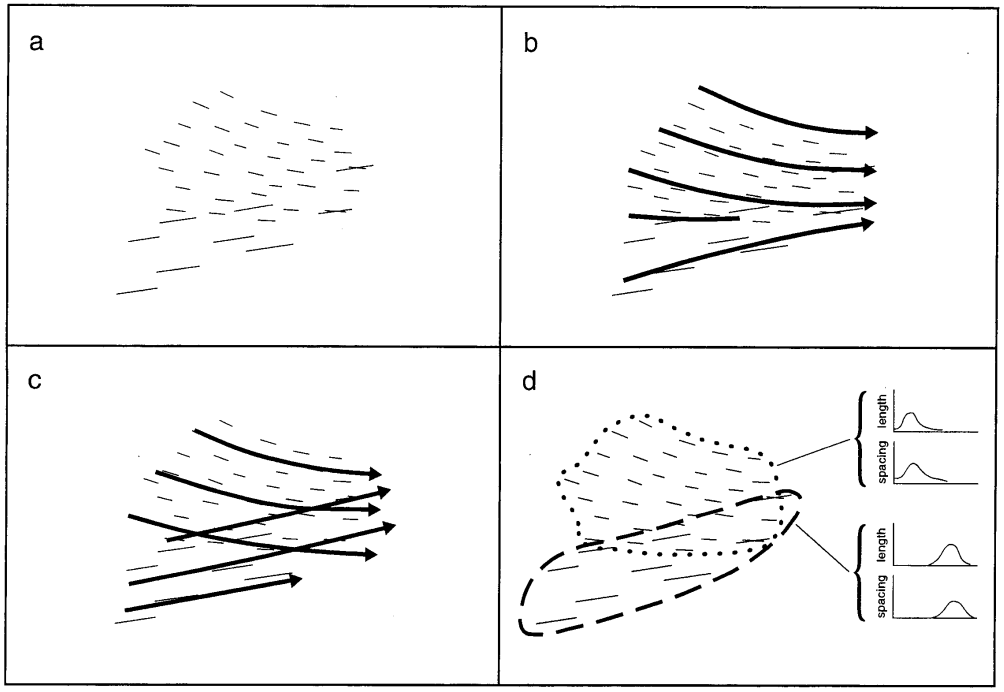

Figure 2.2 (a) shows individual mapped lineaments, whilst (b) and (c) show two alternative interpretations of their formation. (d) illustrates that by grouping lineaments and reviewing their characteristics (e.g. spacing and length), there can be a basis for interpretation (Clark, 1993).

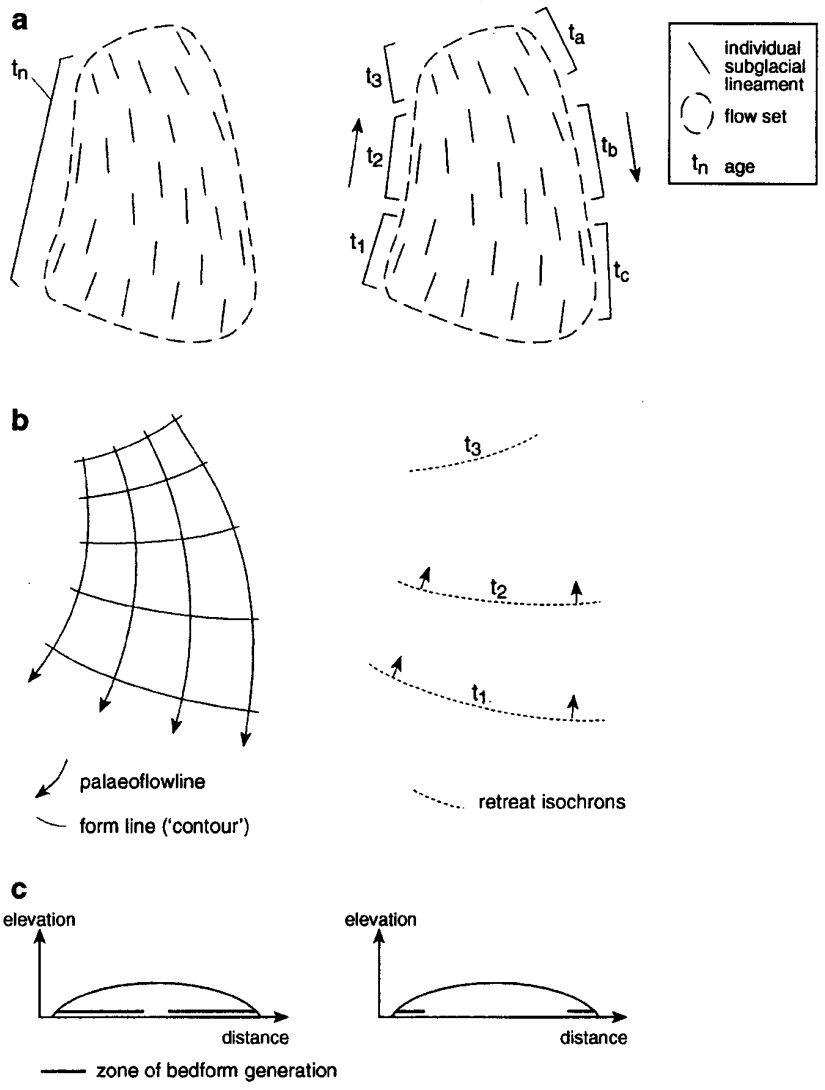

Figure 2.3 Illustration of isochronous (left) and time-transgressive (right) flow set formation. The isochronous lineaments are formed at time t_n (a) and can be represented by palaeo ice flow lines (b). Time transgressive lineaments are shown in (a), with the retreat pattern they represent at t_1, t_2 and t_3 (b). Their location of formation is shown in (c) (Clark, 1999).

1990). As flow sets are interpreted features, it is important to consider all glaciologically plausible scenarios in their grouping. The construction of flowsets is a process that devolves landform assemblages into flow event building blocks from which a reconstruction can be based.

2.3.4 Synchroneity of Formation

Once flow sets have been created their mode of emplacement needs to be ascertained. This can be categorised (Figure 2.3) as either **time transgressive** (formed over a period of time) or **synchronous** (formed at a point in time). Synchronous flow sets exhibit high parallel conformity and similarity of morphology over small areas, with gradual and systematic changes over larger areas.

Time transgressive flow sets are formed during periods of *varying* flow patterns and consequently display obvious discordancy, with lower parallel conformity, changes in morphology and unsystematic cross-cutting (Clark, 1999). Lineament patterns formed time transgressively typically form behind a retreating ice margin.

2.3.5 Cross-cutting flow traces

With the establishment of ice sheet wide flow sets, cross-cutting data (see §2.3.6) are extrapolated from individual landforms to flow sets and then used to establish a **relative chronology** of flow sets. This provides information on the changing ice dynamics through time. Clark (1993) stresses that it is not possible to asses relative age by assuming the newest lineations produce the dominant or “freshest” patterns. The appearance of cross-cutting sets is controlled by sediment supply to a re-advancing ice sheet margin. If there is a ready supply of sediment then one flow set can be **superimposed** upon another. However if there is a small, or no, sediment supply then **re-moulding** of the pre-existing flow set will occur. Clark (1993) suggests that the degree of re-moulding is dependent upon ice velocity (Figure 2.4) and consequently can be used to determine the velocity zones of former ice sheets (i.e. lineaments are related to relative high velocity zones which are located at the ice sheet margin). Other researchers (e.g. Sugden and John, 1976) arrive at similar conclusions.

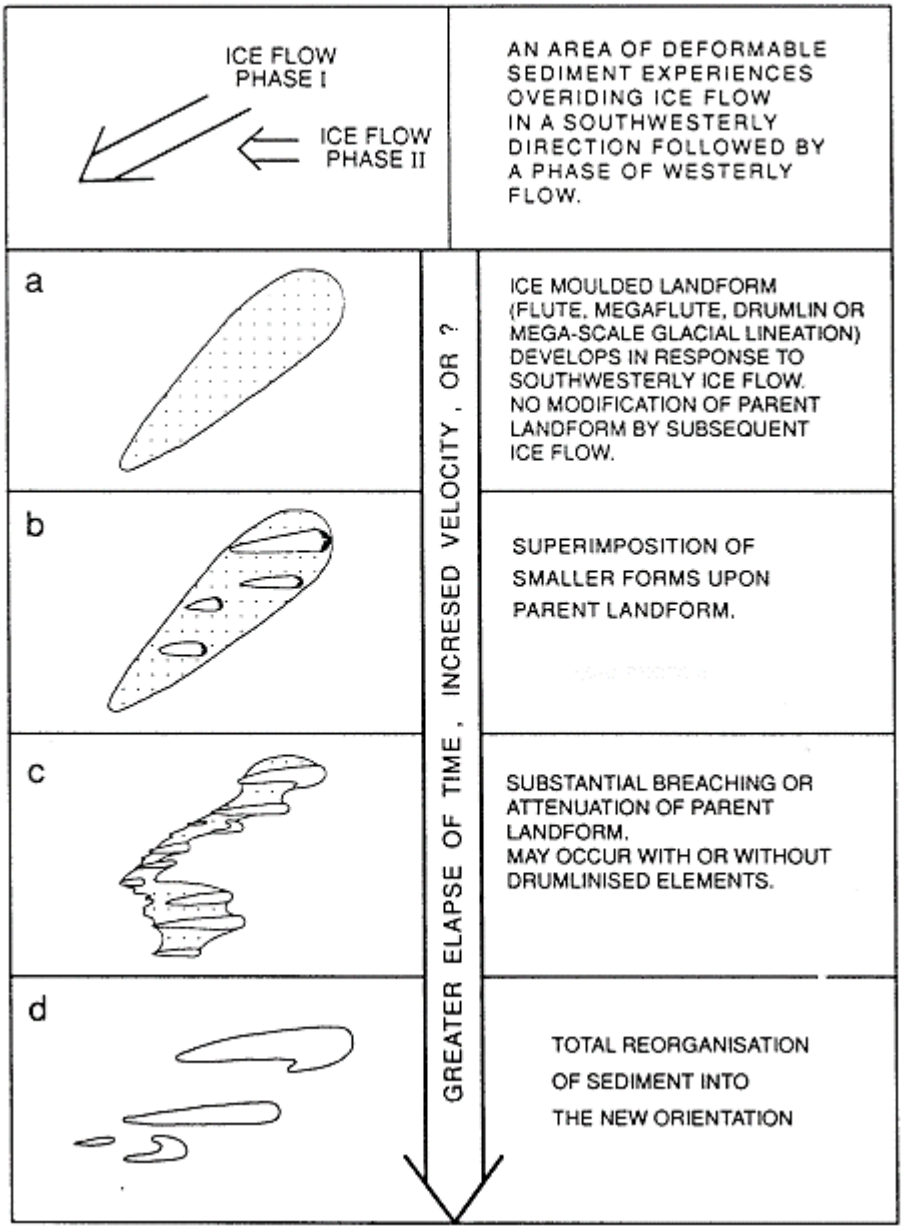

Figure 2.4 The glacial record shows that cross-cutting lineaments form a variety of shapes with superimposed and remoulded forms as end members. The greater the residence time and velocity of the ice sheet, in addition to a low sediment supply, the more likely remoulding is to occur (Clark, 1993).

Published field studies that provide dating evidence for landforms mapped from the satellite imagery can also be used (e.g. radio carbon dates for till horizons). These allow the determination of an absolute age for a particular site, so providing an **absolute age assessment**. This information can be combined with the relative age assessment, however it is unlikely that all the flow sets will be constrained by absolute dates. Rather, it is likely that some sites will be dated and so provide broad dates between which certain flow events are known to have occurred.

2.3.6 Relative Age

Boulton and Clark (1990) noted that glacial lineaments often exhibit cross-cutting relationships (e.g. Figure 2.5). It had previously been thought that all glacial lineaments were formed during the last glacial advance, however the discovery of cross-cutting relationships demonstrates that older patterns can be preserved (see §3.7.8). Figure 2.2 shows how flow patterns would originally have been explained and how they can subsequently be interpreted with reference to cross-cutting. Cross-cutting patterns of bedforms, in a single glaciation, can occur due to (refer to Figure 2.6):

1. **Ice Divide Migration** - movement of the ice divide position changes ice flow geometries and as a result causes cross-cutting. In general the closer to the current ice divide that cross-cutting patterns are found, the greater the angular difference between cross-cuts. This theory was used as sole explanation for cross-cutting patterns by Boulton and Clark (1990) in their reconstruction of the Laurentide ice sheet.

2. **Ice Stream Activation** – ice streams are fast flowing channels of ice, that initially converges from an ice sheet interior. They exhibit a strictly confined zone of parallel flow. Once an ice stream is activated it may cross-cut previously formed lineaments.

3. **Lobate Margin Retreat** - as an ice sheet recedes, lobate margins will pull back in a slow, irregular, manner. Retreat patterns can be complex and may

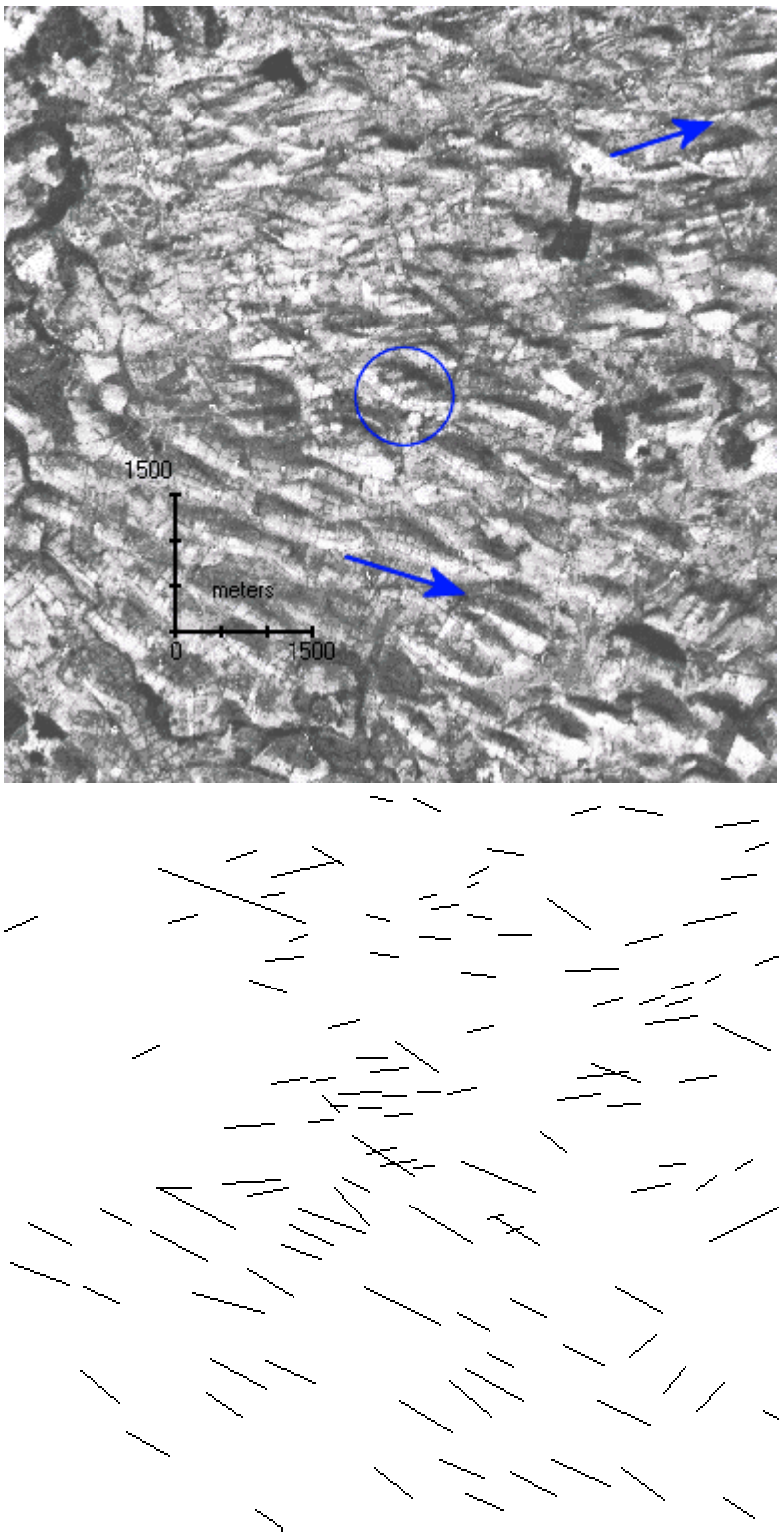

Figure 2.5 a. Example of cross-cutting lineaments depicted on SPOT satellite imagery (Lough Gara, Ireland). The arrows in the top diagram highlight two dominant lineament directions. The circled region shows cross-cutting lineaments. The image is 8.5km across. b. The bottom diagram shows lineaments that have been mapped from the above image.

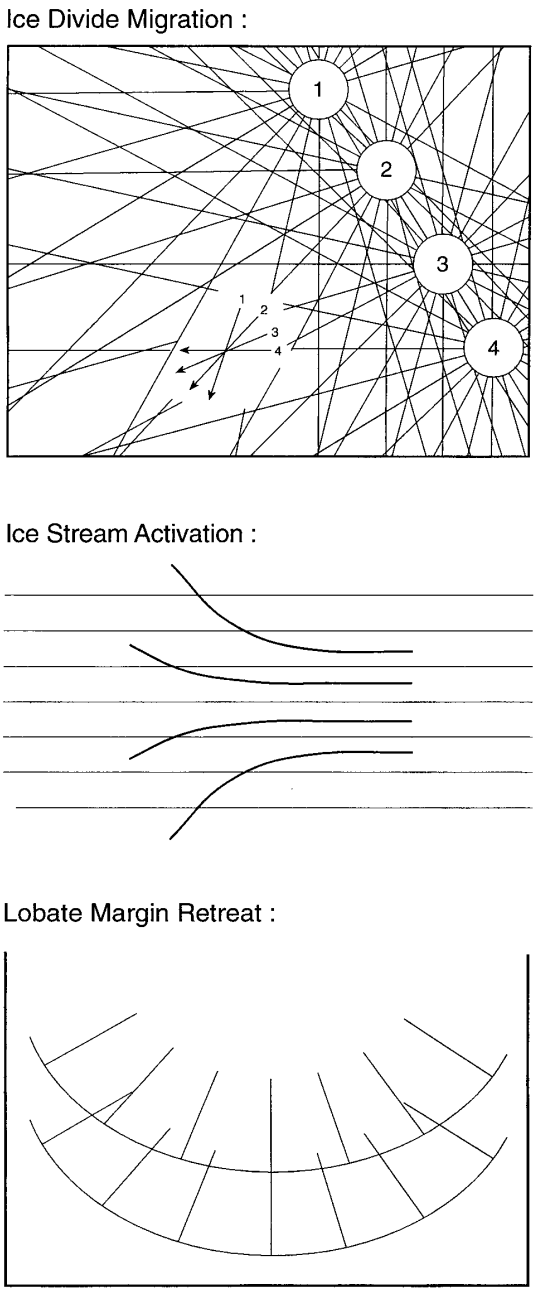

Figure 2.6 Three main glaciological scenarios through which cross-cutting lineaments can be generated (Clark, 1997). Ice divide migration, ice stream activation and lobate margin retreat all allow for the change in ice flow direction.

leave a record of flow patterns if still drumlin forming. In the latter case, cross-cutting lineaments will mark the retreat of the margin. In an idealised situation, towards the central axis of a lobe lineaments will be aligned conformably, whilst towards the edges of the margin there will be a greater angular difference (Figure 2.6). However, this hides what will actually appear to be a very complicated area of flow; the resulting pattern will be a complex mix of cross-cutting lineaments with little appearance of conformity as ice sheets rarely retreat in a steady, orderly, pattern. Sections of the ice will retreat faster than others and then re-advance, further complicating the flow trace.

2.3.7 Summary

This section has presented the different types of satellite imagery appropriate for mapping glacial landforms to be used in a full ice sheet reconstruction. The methods by which these are mapped and then identified as contiguous landform assemblages was described. Flow sets are the final part of this process. Using this information, and given the constraints of topography, the position of cold-based regions and ice divides can be inferred (i.e. areas where no lineations were formed and preservation of pre-existing landforms occurs). The evidence can finally be pieced together to provide a single reconstruction or, more likely, a number of alternative reconstructions. These reconstructions are based upon mapped and published geomorphological and sedimentary evidence. Table 2.2 provides a summary of how this evidence can be used to infer the conditions that were prevalent during glaciation. The following section illustrates how all the stages of a ice sheet reconstruction fit together through the use of a case study.

2.4 Reconstruction Case Study – The Irish Midlands

This section provides an example of an ice sheet reconstruction for the Irish Midlands, based upon Clark and Meehan (2001).

2.4.1 Methodology

Ireland has perhaps one of the longest traditions in glacial research owing to the presence of one of Europe's largest drumlin fields in the Midlands. However it is

Table 2.1 Description of palaeo-glaciological evidence used in the reconstruction of ice sheet dynamics.

Palaeo-glaciological Feature	Formation	Evidence for	Alternative Hypotheses
Glacial lineaments	Streamlining of drift parallel to ice flow direction.	• Warm based conditions. • Ice flow parallel to lineament.	Subglacial mega-floods.
Striae	Rock scouring due to debris laden ice flowing over bedrock.	• Movement of entrained debris. • Warm based conditions. • Ice flow parallel to striation.	
Erratic travel:			
Surficial	Deposition of supra-glacial material during ice stagnation.	• Time-integrated aggregate flow patterns. • Nunataks or mechanism for bringing subglacial material to surface.	
Subglacial	Entrainment of bedrock into basal ice or deforming layer.	• Bedrock erosion and entrainment.	
Till fabric	Orientation of actively deposited till clasts.	• Movement of debris. • Warm based conditions. • Palaeo ice flow direction.	
Esker	Deposition of glacio-fluvial material subglacially, normal to the glacier snout; typically formed during ice recession.	• Active glacier. • Receding glacier. • Warm based conditions.	Synchronous esker deposition along length.
Kame	Meltwater deposits in front of, or alongside, an active glacier.	• Deglaciation	
Ice-contact channels:			
Ice marginal	Channels formed along the margins of glaciers.	• If solitary retreat patterns then cold based conditions.	
Overflow	Incisions cut by marginal channels overflowing low cols.		
Sedimentation:		• **Warm based conditions.** • **Ice free region.**	
Glacio-fluvial	Pro-glacial fluvial deposits (e.g. deltas).	• Absence of pro-glacial lake. • Topographically downhill.	
Glacio-lacustrine	Sedimentation in pro-glacial lakes.	• Ice dammed lake.	
Glacio-marine	Sedimentation in marine environments that are in direct contact with the ice margin.	• Marine conditions.	
Moraines:			
Lateral	Debris deposited at the side of a valley glacier.	• Formed adjacent to glacier margin.	
End	Linear till ridge accumulated at the glacier snout.	• Ice limit or still stand during recession.	
De Geer	Small subaqueous ridges formed subglacially, transverse to flow close to an ice sheet margin (marine or lake).	• Ice margin position concurrent with sea or lake.	
Ribbed (Rogen)	Large, transverse, complex ridges.	• Warm based conditions.	Formed at the cold/warm based interface.
Hummocky	Complex transverse ridges formed by dead ice wastage.	• Stagnation rather than active retreat.	

poorly mapped due to fragmented research from a variety of authors. The lack of a glacial map for Ireland has hindered research and the authors attempt to help redress this balance. The authors used a high quality Landsat TM image (180km by 180km) and a high resolution (25m pixel) DEM (100km by 100km) for the Irish Midlands. These two data sources were used to produce a glacial landform map for this region. Both data sets were provided in digital form allowing on-screen digitising of landforms. Initial investigations identified the presence of a large number of ribbed moraines, in addition to the lineaments. These were mapped as polygons (marking the break of slope) and single lines (marking ridge crests) respectively on the DEM (Figure 2.7). The Landsat TM image involved mapping broad lineament and ribbed moraine patterns rather than individual landforms. The primary data were supplemented with field mapping and sedimentology, as well as selected erratic trains.

With the mapping phase complete, the authors go on to describe the broad characteristics and pattern of ribbed moraine and drumlins. The former comprises two separate patterns. The first, a single contiguous field, covers almost the entire area, whilst the second is oriented transverse to the first and occupies a small region in the NW corner. Drumlins occur across the entire region with considerable overprinting on the ribbed moraine. Indeed the close association between the two suggests the drumlins were formed shortly after the ribbed moraine. They argue that the strong parallel conformity of drumlins (and association with the ribbed moraine) in this area suggests they form a single phase of drumlin creation that was probably isochronous (flowing from the NW to SE). Drumlins also overtop relief up to 200m, without deflection, which negates their creation at a receding margin. They identify two further patterns in the NW (flowing SW to NE) and SE (flowing SW to NE) respectively which are identified by a marked change in orientation (although no cross-cutting is present) and drumlin morphometry. Traditional stoss and lee relationships for drumlins were used to identify flow direction.

2.4.2 Ice Sheet Reconstruction

With the creation of flow patterns complete, the authors go on to develop drumlin and ribbed moraine flow sets (Figure 2.8) identifying 6 lineament and 8

ribbed moraine flow sets based upon parallel conformity and morphometry. These are then sorted into known relative ages based upon cross-cutting relationships noted on the original imagery (Table 2.3).

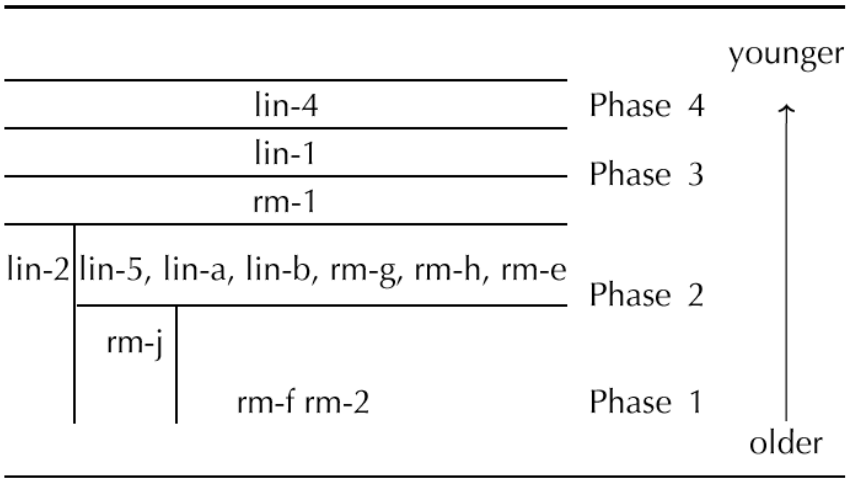

Table 2.3 Relative chronology of interpreted flow sets and how they relate to the different Phases of the ice sheet reconstruction.

Using this information the authors suggests four main phases based upon their evidence (refer to Table 2.3 and Figure 2.9). These are:

Phase 1 – rm-2 and rm-f form the earliest phase representing ice flow from the NE. As relief (up to 200m) has little effect on their creation, they cannot have formed under thin ice or close to the margins. They infer these forms as representative of expansion of an ice cap centred upon NE Ireland, possibly after invasion by Scottish ice.

Phase 2 – seven flow sets comprise this phase; some are not influenced by topography, whilst others are. They are grouped together (due to their orientation) as representative of this period, not because they all formed synchronously. Their orientation suggests a linear N-S ice divide. This position of cold based ice beneath the divide would have also helped preserve the flow sets in Phase 1. From this evidence they infer a worsening in climatic conditions leading to the development of a large ice cap. Given the landforms record a large ice cap at a relatively southern latitude, it is assumed this represented the Last Glacial Maximum (LGM).

Phase 3 – the flow sets identified here are the most dominant in Ireland. The drumlins closely match the ribbed moraine, as well as cross-cutting them. They can safely be grouped together, with the drumlins formed shortly after the

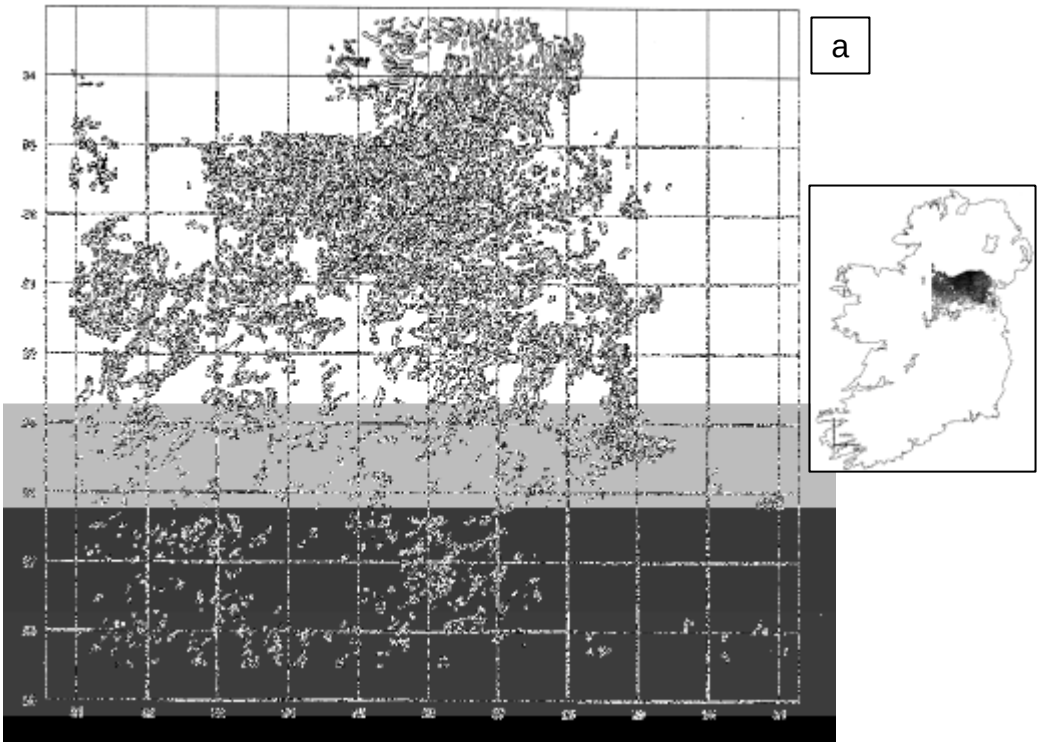

Figure 2.7 Ribbed moraine (a) and lineaments (b) mapped from DEM data of Ireland (inset) by Clark and Meehan (2001). Mapping based upon Irish National Grid squares.

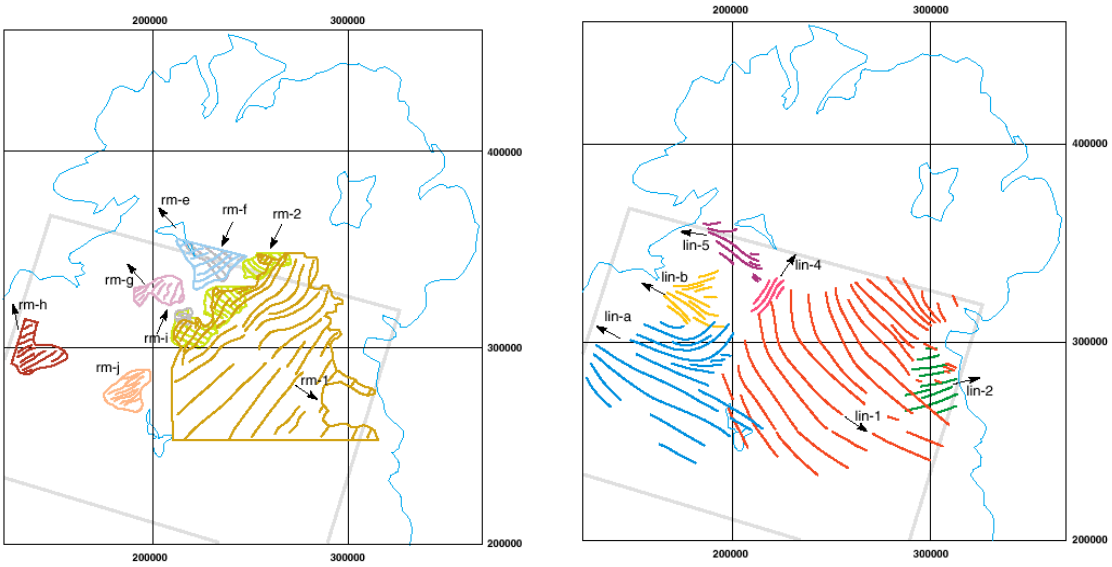

Figure 2.8 Ribbed moraine (rm) flow sets (left) and drumlin (lin) flow sets (right) interpreted from original landform data mapped from high resolution DEM data and Landsat TM satellite imagery (Clark and Meehan, 2001).

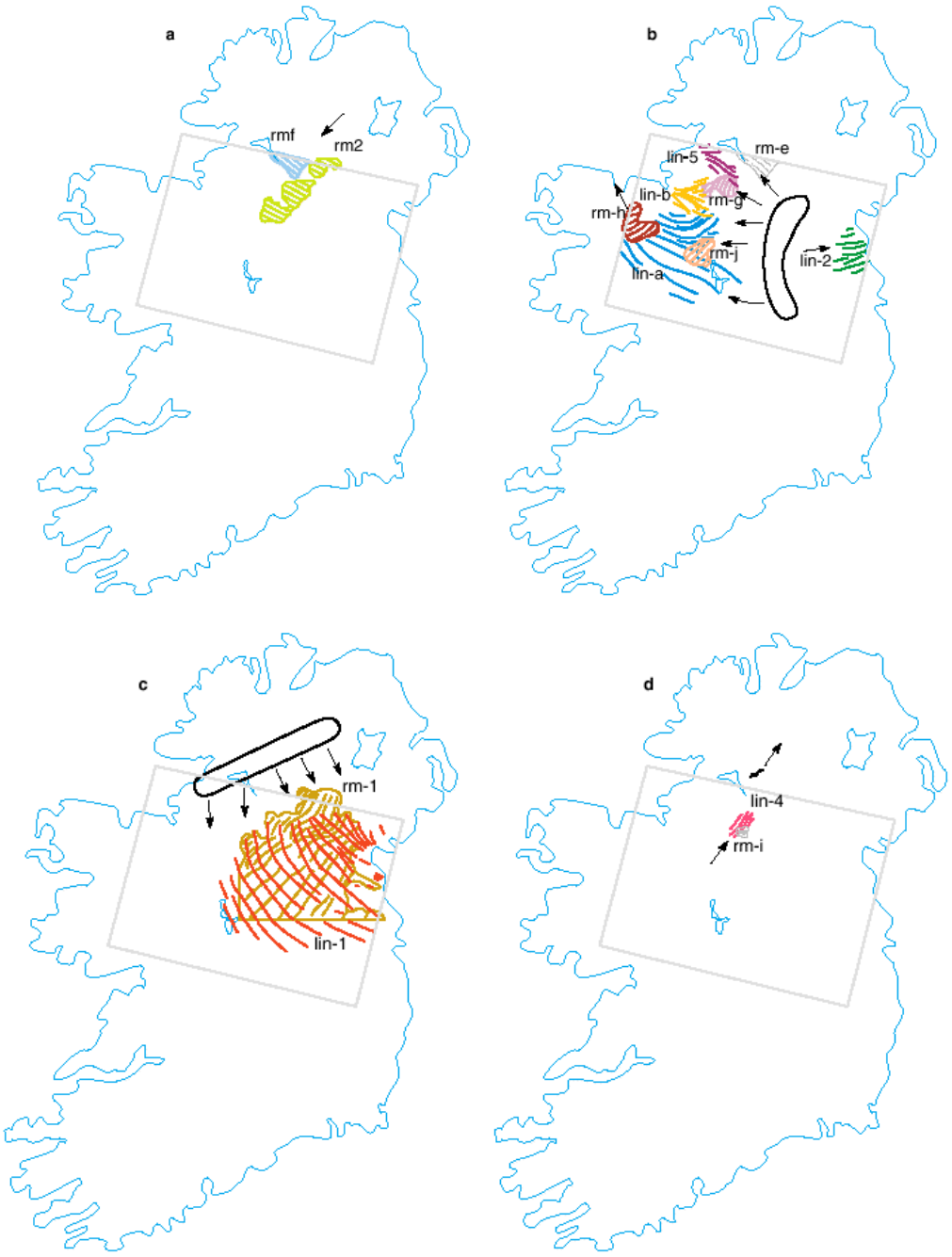

Figure 2.9 Four phases of ice sheet reconstruction developed by Clark and Meehan (2001) developed for the Irish Midlands. Phase 1 (a) represents a build of ice from the north, probably due to an incursion by Scottish ice. Phase 2 (b) shows a fully developed ice divide (Last Glacial Maximum) over the Midlands. This ice divide migrates to the NW in Phase 3 (c). The remaining flow sets probably represent the fragmentation of the Irish Ice Sheet (d).

ribbed moraine. This then infers an ice divide located in NW Ireland, possibly extending out on to the continental shelf. This was a major phase of drumlinisation which would have erased all older landforms beneath it.
Phase 4 – the final, and youngest, drumlin pattern is left, being strongly controlled by topography. This appears to indicate ice flow *towards* the NE, almost a complete reversal of the previous phase. The two inferences are that a Galloway based ice cap invaded and extended towards the north or, more likely, this phase represented a fragmentation of the ice sheet into smaller ice caps and that this simply records deglaciation.

The above phases represent the authors' preferred interpretation of the available primary evidence. However it is discussed in relation to existing literature and there is room, within these phases, for flexibility. They suggest that the relative age of events is stable, although absolute ages are far less so. To this extent, they provide an alternative interpretation which would equally fit evidence. This suggests that Phases 1 and 2 represent the build of ice and that Phase 3 is representative of the LGM. Once sea ice was established in the Irish Sea, it is possible that the ice divide migrated towards the higher northern region helped by precipitation from the Atlantic.

The above section represents the application of the four main stages of an ice sheet reconstruction by Clark and Meehan. That is, the mapping of individual landforms from satellite imagery and DEM data, following by their generalisation into distinctive flow patterns. Once completed the authors used these patterns to generate distinctive flow sets which could be placed within a relative chronology and assessed as to whether they were time-transgressive or isochronous. Using all this evidence a reconstruction of ice sheet geometry, extent and changes through time was produced. This is completed with a discussion of implications relating to the surrounding regions that are not directly evidenced in the research. In addition, previous literature needs to be examined in order to note and explain differences between conclusions.

2.5 Summary

This chapter has discussed the techniques and methodology currently used in ice sheet reconstructions. Although the diversity of satellite imagery is still relatively restricted, the current variability provides a wide range in the quality of data available and consequently the interpretation of any landforms that are mapped. The methodology described above allows the implementation of techniques to integrate diverse palaeo-evidence, recognising the importance of cross-cutting data and the alternative scenarios of interpretation. Indeed the methods are specifically designed to embrace all data and interpretations. This reduces data precision but highlights strong synoptic trends such that complementary evidence can be used to discard improbable or implausible scenarios. Although the work of Sugden (1976), Boulton and Clark (1990) and Kleman and Börgstrom (1996) have made significant improvements to these methods, there are still weaknesses which are highlighted in the following chapter through a review of previous satellite imagery based glacial reconstructions. Chapter 4 then goes on to formulate specific key issues on which the research of this thesis is based.

3 Review of Ice Sheet Reconstructions based on Geomorphology Mapped from Remotely Sensed Data

3.1 Introduction

The advent of remote sensing allowed the rapid mapping of glacial landforms over large areas, initially using aerial photography (e.g. Prest *et* al, 1968) and later satellite imagery (e.g. Punkari, 1982). They provided a synoptic view, often over remote regions, allowing the identification of small scale features that were unrecognisable from the ground. With the wider availability of these data, theoretical (e.g. Sugden and John, 1976), methodological (e.g. Clark, 1993) and technical (e.g. Clark, 1997) advances in the way glacial reconstructions are performed have been achieved.

The theory used in glacial reconstructions is well developed and practised by several researchers in areas of former ice sheets. Chapter 2 introduced the data sources, techniques and methods employed by these researchers. This chapter aims to make the reader familiar with a range of glacial reconstructions from these different authors. These papers are broadly reviewed by research groups that the principal author falls in (e.g. Punkari in one section and Clark in another). Within each section papers are generally reviewed in chronological order, highlighting methodological advances and discussing particular weaknesses. The chapter concludes with a review of papers that developed the methodological techniques of ice sheet reconstruction.

3.2 EarlyGlacialReconstructions

Glacial reconstructions date to the beginnings of glaciology in the early 1800's (e.g. Agassiz, 1840). Within the UK (my initial study area) it was the geological mapping programmes in the latter half of the 1800's that provided researchers with regional glacial landform data. For example, in Ireland, Close (1867) and Hull (1878) provided early countrywide reconstructions, with numerous other Geological Survey workers discussing regional trends in the memoirs

accompanying geological map sheets. However it was not until the 1950's, with the wide spread use of aerial photography by national mapping programmes, that fieldwork was superseded as the predominant tool for mapping glacial landforms over large areas. The mapped data could form the basis of glacial landform maps of entire former ice sheets and so lead on to interpretation and reconstruction. Prest *et al* (1968) used such a method in the reconstruction of the dynamics of the Laurentide Ice Sheet.

The advent of digital imagery, particularly satellite based, later supplemented these data. The relatively low cost and large areal coverage were ideally suited to regional glaciology. Landsat MSS (1:1,000,000 photomosaics) images were first used within a glaciological context by Sugden (1978) to map areas of areal scouring in North America, however it was not until Punkari (1982) that the full potential of satellite imagery for ice sheet reconstruction was implemented.

3.3 Punkari (various), Dongelmans (1997) and Boulton *et al* (2001)

Punkari (1982) used Landsat MSS data (1:100,000 to 1:400,000 paper prints) to map a variety of different glacial landforms in Finland and surrounding areas providing the first satellite based glacial reconstruction. Mapped landforms included lineaments, eskers, end moraines, hummocky moraine, rogen moraines and marginal moraine, incorporating striae, till fabric, erratics and sediment type from the published literature (Figure 3.1). He made particular use of different EM band combinations to highlight vegetational differences (*geobotanical method*) and so enhance lineaments. Due to the restrictions in the sensor spatial resolution (nominally 80m) individual ridge features were difficult to determine, however a general trend (co-linear texture) was apparent. Mapped lineaments were nominally assigned to a flow type of *time transgressive* or *lobate marginal retreat*. Punkari's initial research also highlighted an older flow event which he suggested was preserved under cold based ice. Figure 3.2 illustrates his lineament map and final reconstruction. Punkari (1985) extended his work into Soviet Karelia using the same technical methods. He was able to use winter imagery, noting the particular utility of low solar elevation in detecting lineaments. Soviet airborne radar was found to be

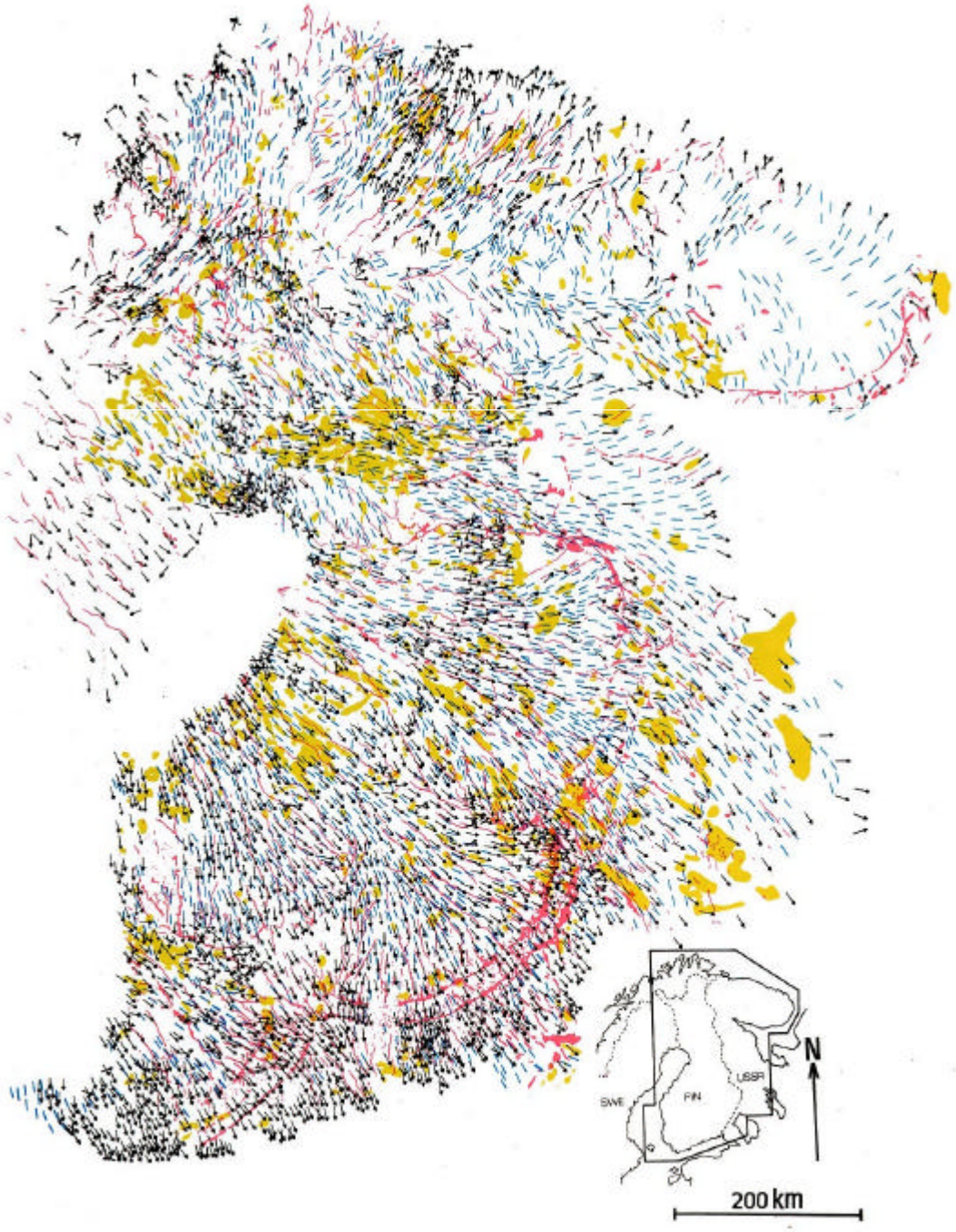

Figure 3.1 Glacial landforms mapped from Landsat MSS satellite imagery (Punkari, 1982) for a large part of Fennoscandia. Landforms are lineaments (blue), end moraines/eskers (red), hummocky moraine (yellow) and striae (black).

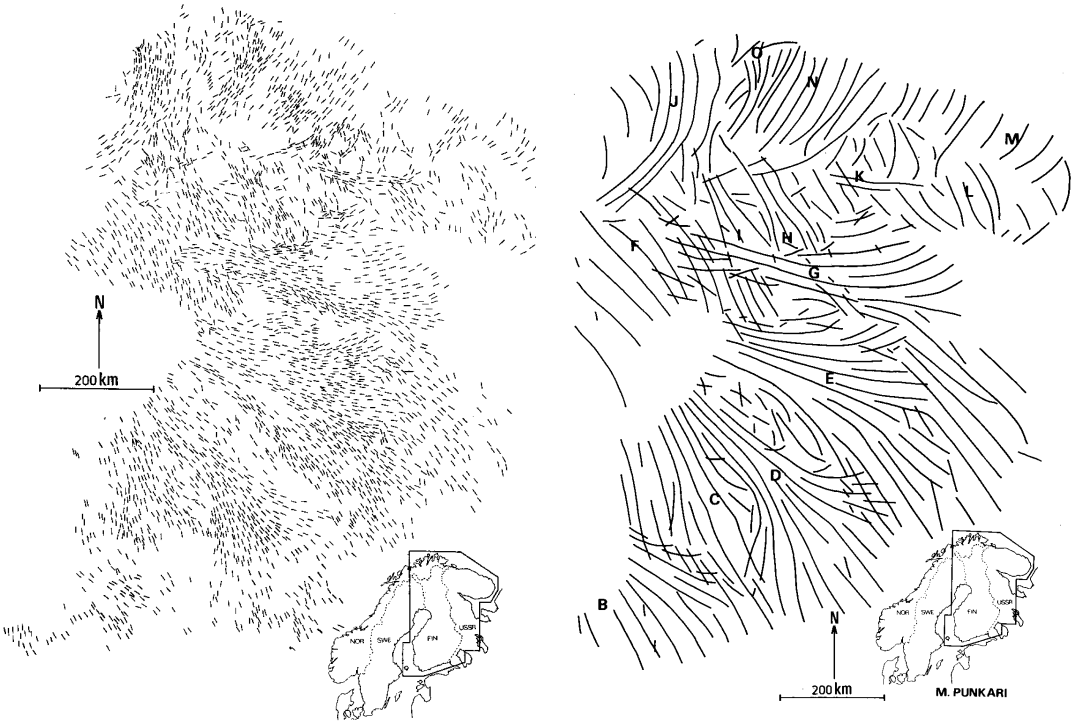

Figure 3.2 Lineaments mapped from Landsat MSS satellite imagery (left) and their corresponding flow patterns (right) for parts of Fennoscandia (Punkari, 1982). Flow patterns are the key element to establishing flow sets prior to a full ice sheet reconstruction. The methods used to produce flow patterns from lineaments are not detailed.

better at detecting glacial lineaments than Landsat MSS, although coverage was limited. This confirmed early work by Ford (1981) that had already shown the usefulness of radar images in detecting glacial landforms. In exceptional cases Punkari was able to extract cross-cutting relationships from superimposed lineaments. Other practical enhancements included cross checking for geological misinterpretation, the use of field work for ground control and the explicit need to consider topography in any reconstruction. Conceptual notions of time transgressive and synchronous flow events were implicitly used.

Punkari (1989) consolidated the above work to produce an overall glacial reconstruction of Scandinavian and Russian Karelia, with the methodology explained in detail in Punkari (1993). This latter report indicated that “general scale” satellite mapping (1:500,000 to 1:1,000,000) was predominantly used (utilising Landsat and SPOT imagery), but incorporated detailed scale (1:20,000) mapping from south-western Finland. This latter mapping was able to identify individual landforms by using topographic maps and aerial photography, supplemented by some field work (principally for logging till fabrics and striae). As a consequence any general scale maps of lineaments are *generalised* from the first stage of mapping, and only in the detailed area of south-western Finland, are individual lineaments identified. Cross-cutting relationships are therefore only available for striae and these are extrapolated and applied to other glacigenic landforms. This work also incorporated the first explicit use of a GIS in ice sheet reconstruction, to digitise landforms and plot histograms of landform orientation.

Punkari (1995) later expanded his mapping of glacial landforms into north-western Russia, again using Landsat MSS 1:300,000 to 1:1,000,000 photomosaics. An explicit theoretical methodology was used and individually mapped features were now digitised and imported into a GIS. Lineaments were directly generalised from the imagery to the map, subjectively taking into account lineament orientation, density and length. In order to analyse lineament orientation, the entire area was segmented into 50km squares and rose diagrams produced (Figure 3.3), following the techniques of Broadgate (1997).

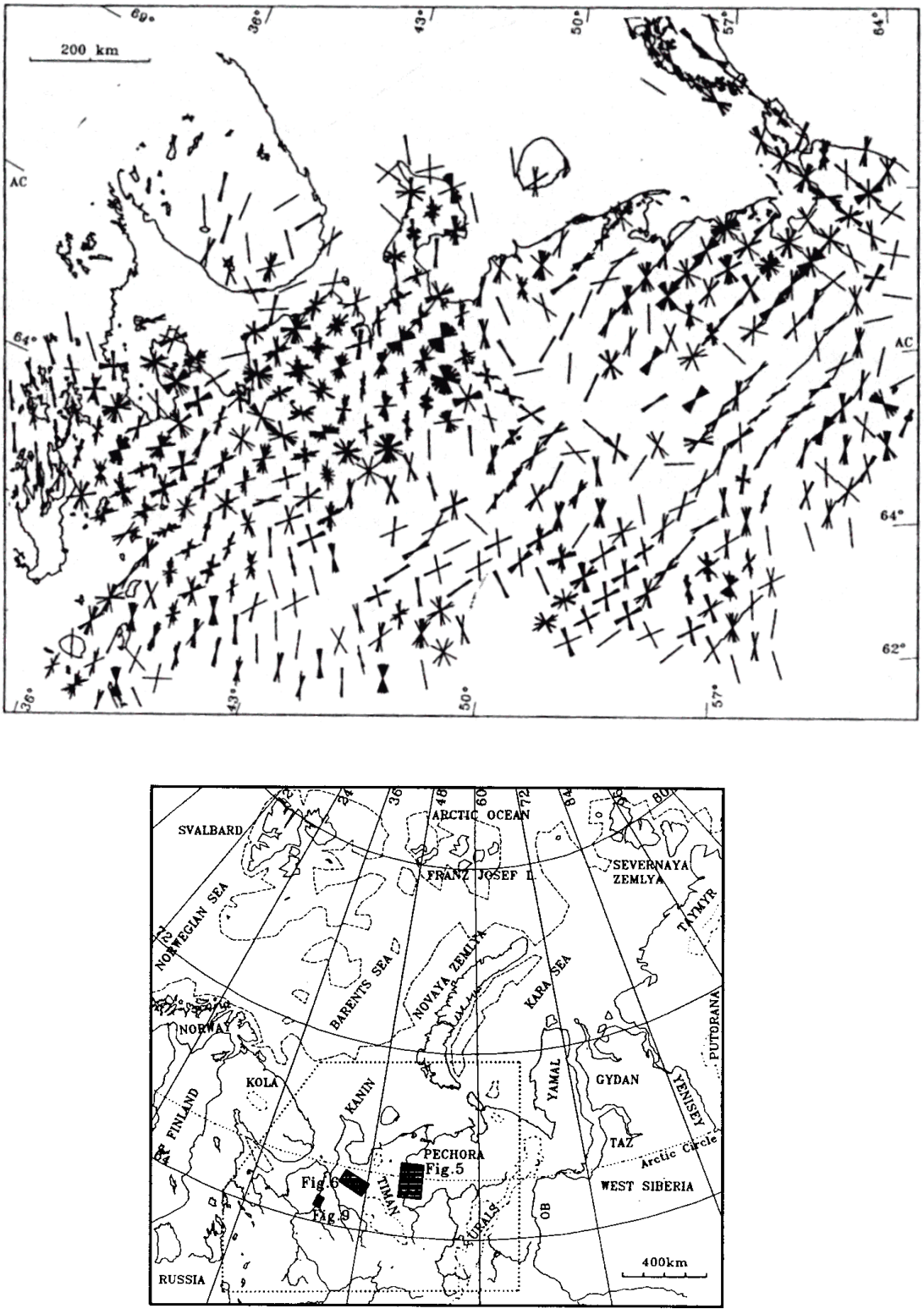

Figure 3.3 Rose diagrams of lineament orientation in NW Russia for 50km^2 grids (Punkari, 1995). Although graphically representing a lot of lineament data, it is difficult to interpret.

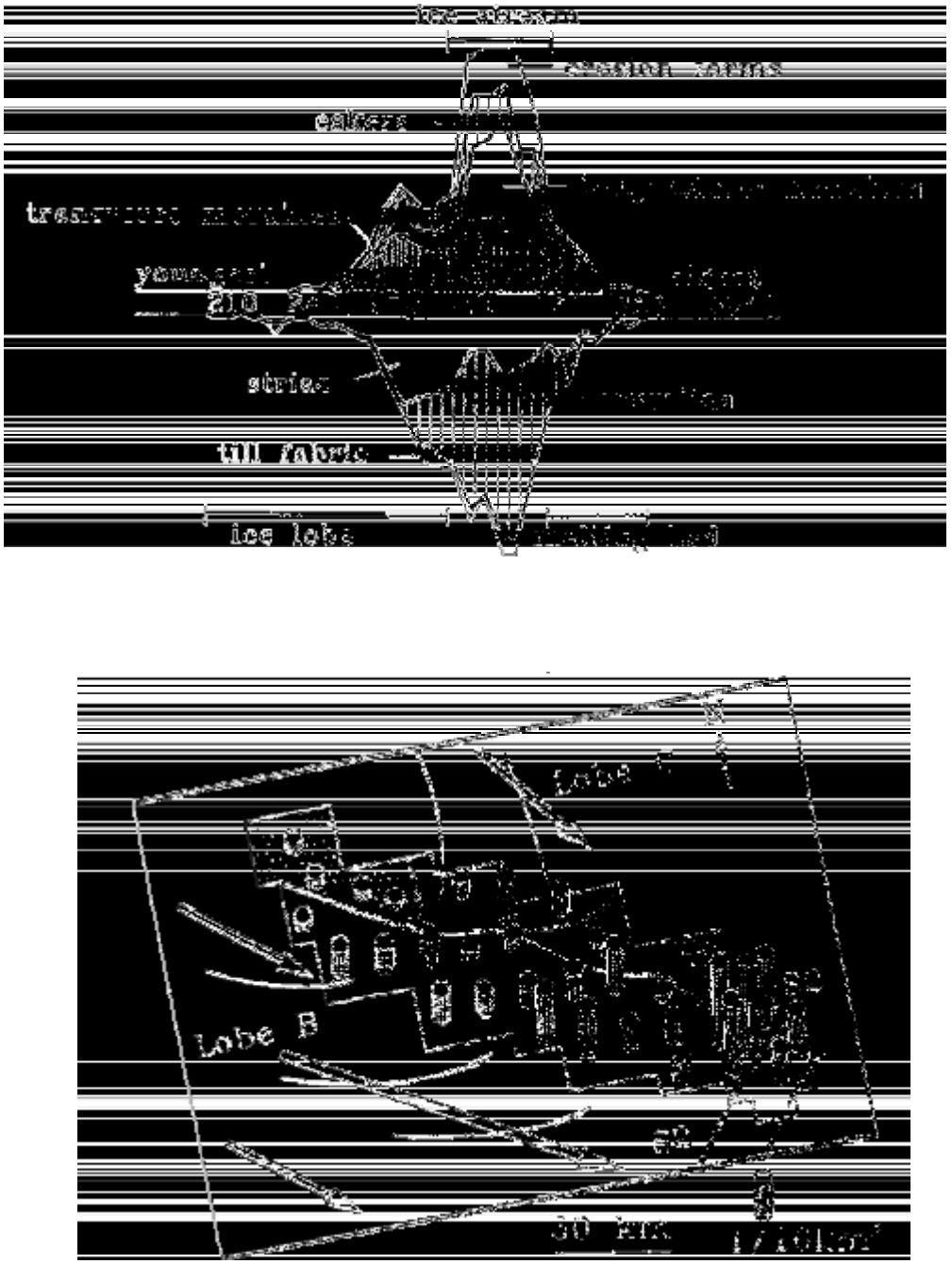

Figure 3.4 Frequency histogram (top) of orientation for different glacial landforms, illustrating the use of GIS based data (Punkari, 1993). Bar chart (bottom) of lineament frequency in part of Scandinavia (Punkari, 1993).

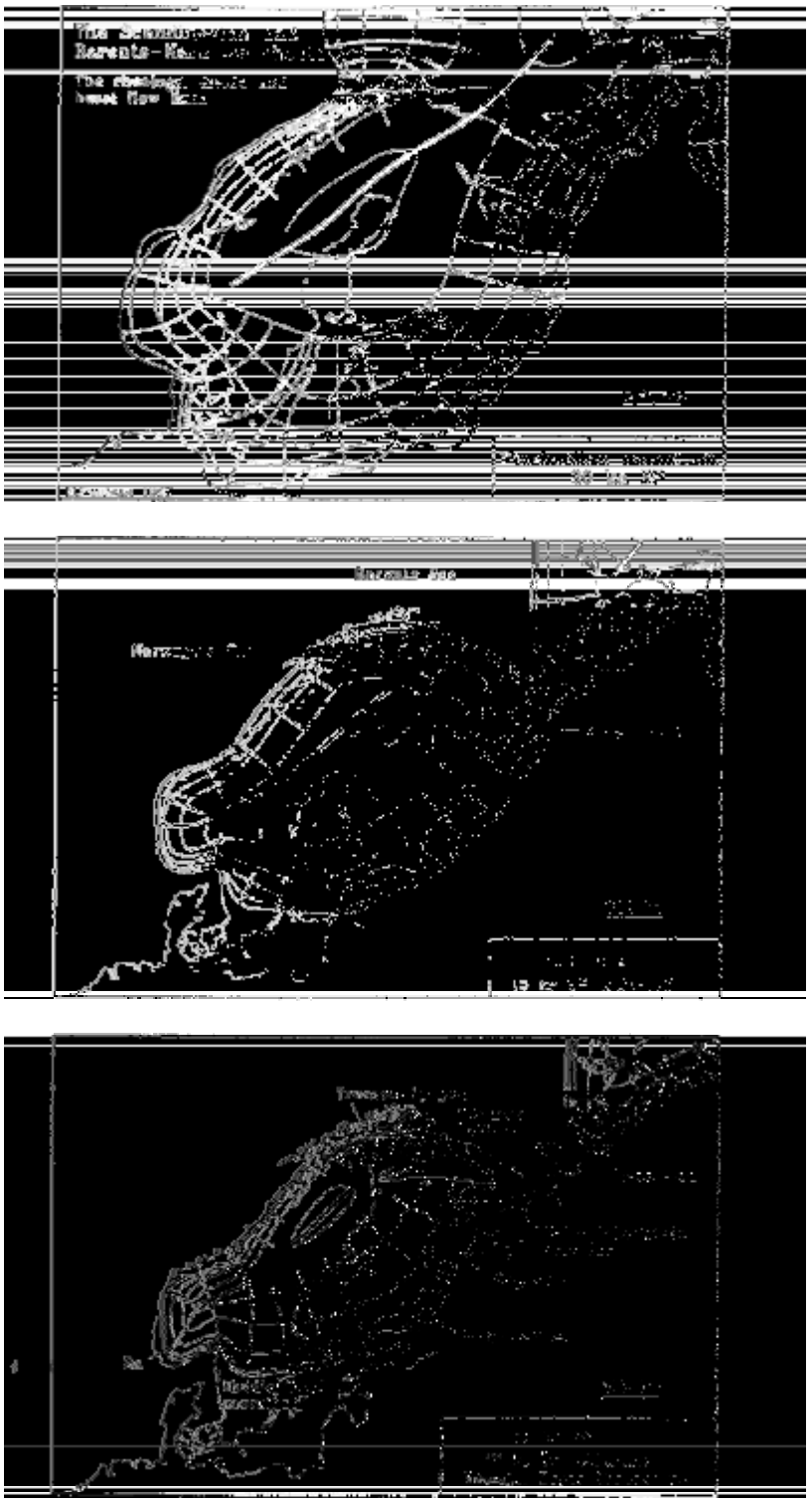

Figure 3.5 Glacial reconstruction of the Scandinavian ice sheet during the last glaciation (Punkari, 1993). Ultimately, glacial landform mapping and interpretation aims to produce a coherent history of the evolution of an ice sheet.

These then aided a reconstruction of the glacial history (e.g. Figure 3.4) to produce a full glacial reconstruction (Figure 3.5). His results concurred with the prevailing view that ice sheet lobes discharged eastwards from the Gulf of Bothnia, however he assumed that evidence of deglaciation was simply imprinted or "stamped" upon the landscape. He did not recognise that retreating ice lobes must be time transgressive and, assuming that lineations are continually formed, cross-cutting must result.

Dongelmans (1997) and Boulton *et al* (2001) produced a reconstruction of the Fennoscandian ice sheet using Landsat MSS 1:1,000,000 photomosaics and a mixture of Landsat MSS (27) and TM (4) scenes. For selected areas where relative chronology was important, 1:150,000 aerial photographs were incorporated. Like Punkari (1982), near-infrared images were used to detect lineaments by highlighting vegetational differences. They mapped eskers, moraines and drumlins (Figure 3.6a), but admit that the Landsat MSS imagery is unable to sufficiently resolve eskers and moraines to perform mapping accurately. Dongelmans does not discuss the process of generalisation, although original interpretations and summary maps are provided. When establishing a "flow" (flow set equivalent) Dongelmans requires lineaments to be "spatially continuous", although this is never defined. Rather than developing methods to cross-check "flow" creation, Boulton *et al* required each author to create their own "flows" and then compared the results. They found no substantive differences and so accepted these results. For display purposes Boulton *et al* performed four iterations of gradual generalisation, ultimately producing a final, ice-sheet wide, generalised map. The lineament and moraine data were linked to the Swedish varve chronology data to allow the authors to infer timescales of ice sheet retreat (Figure 3.6b). The original mapped lineaments were also used to identify major ice sheet structural elements, as idealised in Figure 3.7.

Discussion

Punkari (1982) was the first researcher to attempt to map many different glacial landforms from satellite imagery over a large area and integrate the data with published material in order to develop a glacial reconstruction. Initially the

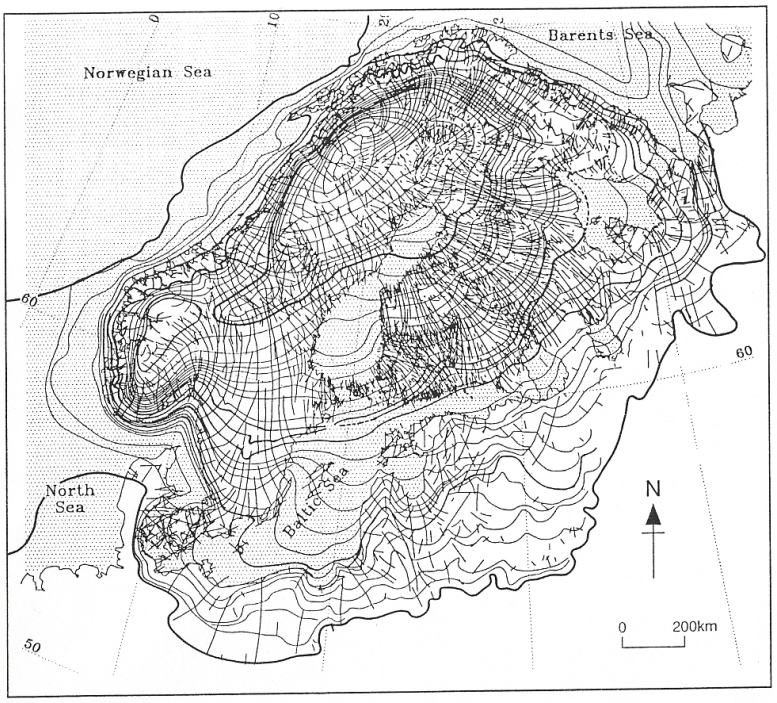

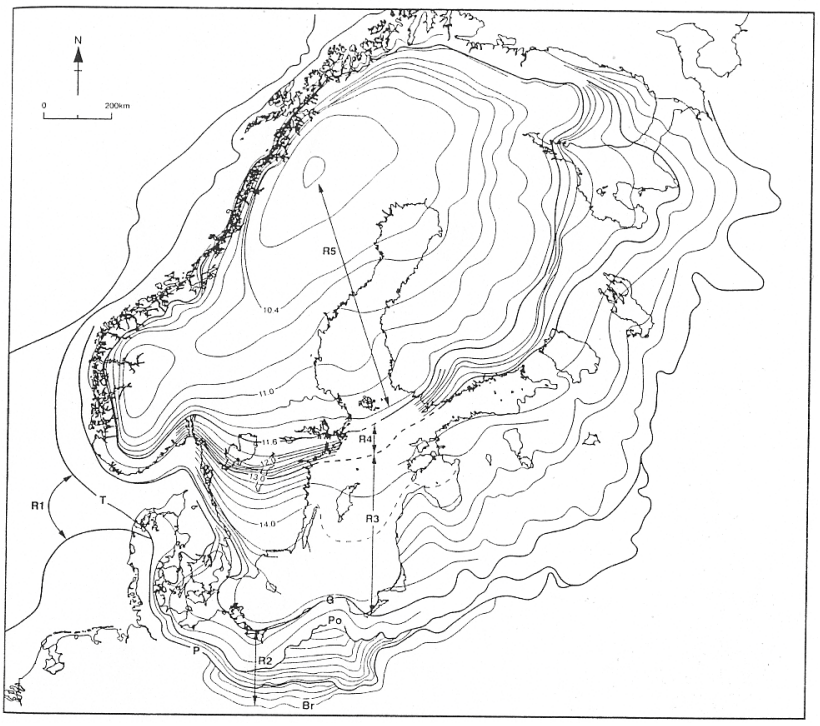

Figure 3.6 a. Major lineament patterns and inferred ice front retreat for the Fennoscandian ice sheet. b. Isochrons of retreat for the last Fennoscandian ice sheet (Boulton *et al*, 2001)

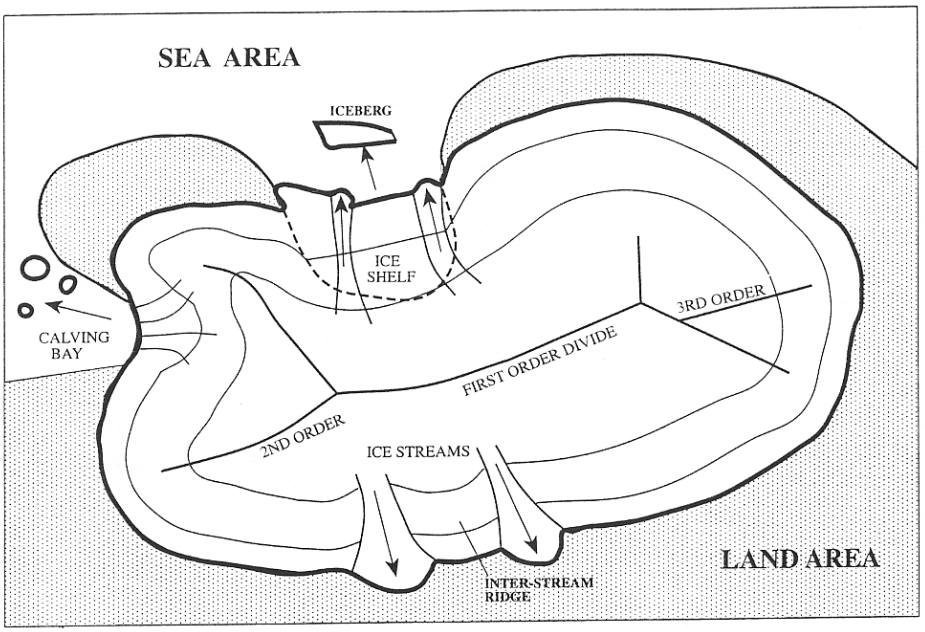

Figure 3.7 Idealised ice sheet structural elements (Boulton *et al*, 2001).

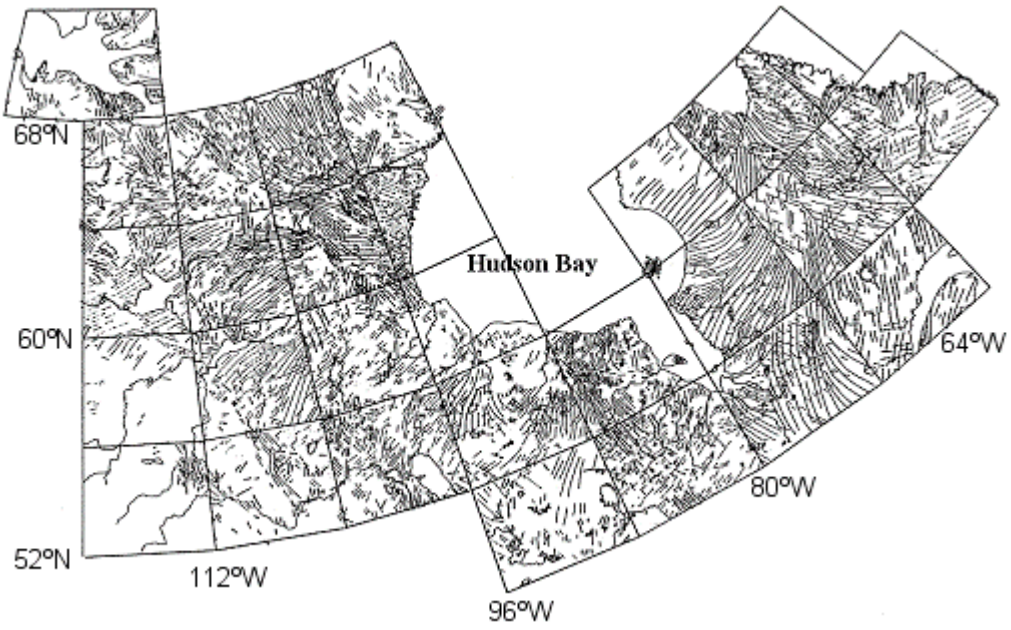

Figure 3.8 Summary lineament mapping for the Laurentide ice sheet (Boulton and Clark, 1990) based upon Canadian NTS (National Topographic System) quadrants.

author had several practical and technical limitations to overcome, exploring many image processing techniques in order to map different landforms. No explicit theoretical methodology was stated, although there were several implicit assumptions concerning the formation of different landforms (e.g. lineaments form subglacially, parallel to flow) and how these combined to produce a glacial reconstruction (e.g. time transgressive). Importantly, he recognised the existence of landforms from the penultimate glaciation, suggesting that these were preserved under cold based ice, however he didn't consider the possibility of multiple flow events within a single glaciation recorded in the morphological record and the implied changes in ice sheet dynamics. As a result he wasn't able to take advantage of developing a chronological history by correlating ice flow indicators across wide areas and using cross-cutting relationships. His ongoing experimentation with SAR and winter imagery was forward thinking, along with the input of mapped data into a GIS. This allowed the integration of a range of published data sources, as well as the development of analysis tools (Broadgate, 1997).

The technical developments implemented by Punkari were not matched by methodological developments. The lack of a framework through which mapped data was interpreted was a weakness in comparison with the methodological advances discussed by Boulton and Clark (1990) and Kleman *et al* (1996). In addition he failed to discuss the assumptions required in his interpretations of the landform evidence, as well as the procedures used to map and generalise the data prior to interpretation. Unfortunately mapping introduces bias into the final dataset used for interpretation. The original satellite image is not fully representative of the landforms on the surface (this is described in more detail in Chapter 4), whilst the observer is biased in the landforms that are mapped. The generalisation of these data, prior to interpretation, also introduces bias. In general, researchers have failed to recognise these deficiencies and account for them.

Dongelmans (1997) and Boulton *et al* (2001) used the same technical and methodological techniques as Punkari, applying them to the Fennoscandian Ice Sheet. Although they introduce the use of cross-cutting lineaments in

developing a relative chronology, their discussion fails to incorporate some of the extensive developments made by Boulton and Clark (1990), Kleman *et al* (1996) and Clark (1999). They also do not map the extensive Fennoscandian rogen moraines or discuss the interpretation of these landforms with respect to the thermal regime of the ice-bed interface .

Their reliance upon Landsat MSS imagery is a major deficiency, a general point noted by Clark (1997, p1074) who states that early researchers:

> *used hardcopy prints at small scales and it is likely that many flow patterns were missed and some others erroneously interpreted or confused with geological structure.*

Landsat MSS is also unable to resolve all but the largest cross-cutting relationships. Boulton *et al* did have access to some Landsat TM and selected small scale aerial photography, however the widespread use of Landsat MSS is surprising.

Boulton *et al* (2001) rely upon the interpretation of lineaments as being heavily imprinted on the landscape and more densely grouped in submarginal zones and that this represents the retreat phase of an ice sheet. In addition where divergence of flow is observed at the former ice sheet margins, this is assumed to be indicative of land based ice streaming. They do not consider other glacial interpretations of the data and do not discuss other geomorphological criteria that may be indicative of ice streaming (see Stokes and Clark, 1999 for further discussion).

3.4 Clark (1990), Boulton and Clark (1990), Knight (1996), Clark *et al* (2000) and Clark and Meehan (2001)

Boulton and Clark (1990) used Landsat MSS (1:1,000,000 photomosaics) to map the glacial geomorphology of the former Laurentide ice sheet (Figure 3.8), however for each of the Canadian NTS (National Topographic System) quadrants they mapped, they acquired sample aerial photography to verify relative chronologies (see Chapter 2). Boulton and Clark developed the

theoretical ideas of Sugden and John (1976; see §3.7), establishing that traces of previous flow events were visible and were cross-cut by traces of the final event in an area. The cross-cutting relationship provided a relative chronology which could be correlated across large areas. Assuming that previous flow events were preserved under ice divides, divide locations could be estimated and so the dynamics of the ice sheet, through time, constructed (Figure 3.9). Regions where cross-cutting information wasn't available were fitted into different glaciological scenarios to provide a variety of alternative reconstructions. Particular events within a reconstruction could be anchored to time if absolute dates of individual landforms were available. Whereas Boulton and Clark (1990) discuss technical methodological advances in glacial reconstruction, Clark (1993) goes on to describe the geomorphological implications of their results. This approach is later used by Knight (1996) and described in a review by Clark (1997).

In the PhD thesis of Knight (1996), and the subsequent published paper (Clark *et al,* 2000), ERS-1 SAR imagery was used to map glacial lineaments from the Labrador Sector of the Laurentide ice sheet (Figure 3.10). Image hardcopies (unspecified scale) were used to map lineaments. These were digitised, imported into a GIS and added to digitised vector or scanned raster data from published sources. Additional ancillary layers, such as coastlines, rivers and the Canadian National Topographic Grid (Figure 3.11), were also combined. Ground truthing was carried out through the use of 1:50,000 aerial photos (checking drift cover and lineament orientation), selected fieldwork (checking lineament orientation and gathering striae data), image re-interpretation (human interpretation error) and the use of SAR ascending/descending scenes to minimise errors introduced by illumination azimuth.

Individual lineaments were visually generalised into *ice flow trend lines*, with an idealised and actual example shown in Figure 3.12. In the case of multiple lineament patterns, trend lines were grouped into *ice flow line sets*. Although the GIS provided the ability to work seamlessly over the study area at any scale, Knight chose to work with digitised data within the spatial restrictions imposed by the imagery scenes. The creation of *flow sets* involved the extension of ice

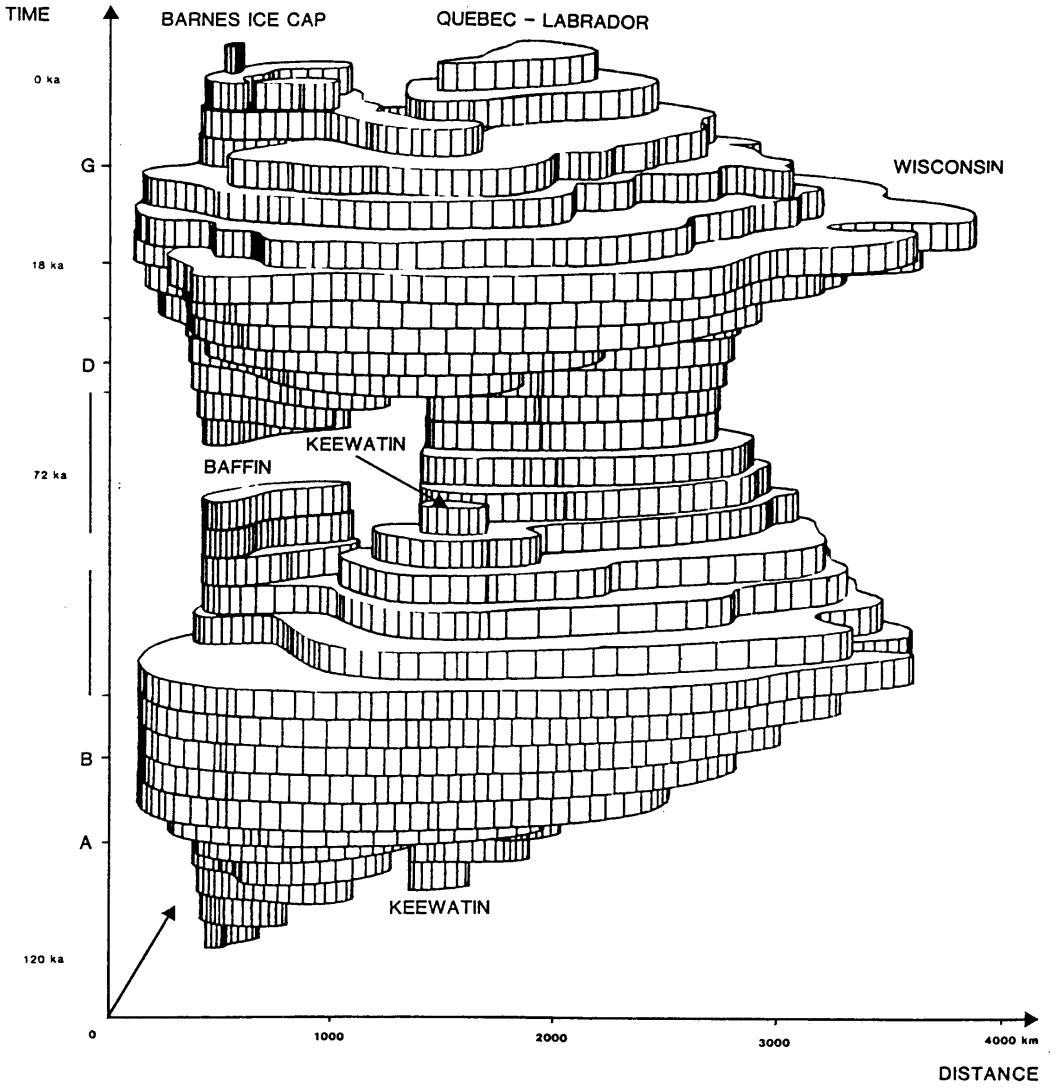

Figure 3.9 Postulated dynamics of the Laurentide ice sheet through the last glacial cycle (Boulton and Clark, 1990), showing the ice sheet border and its waxing and waning.

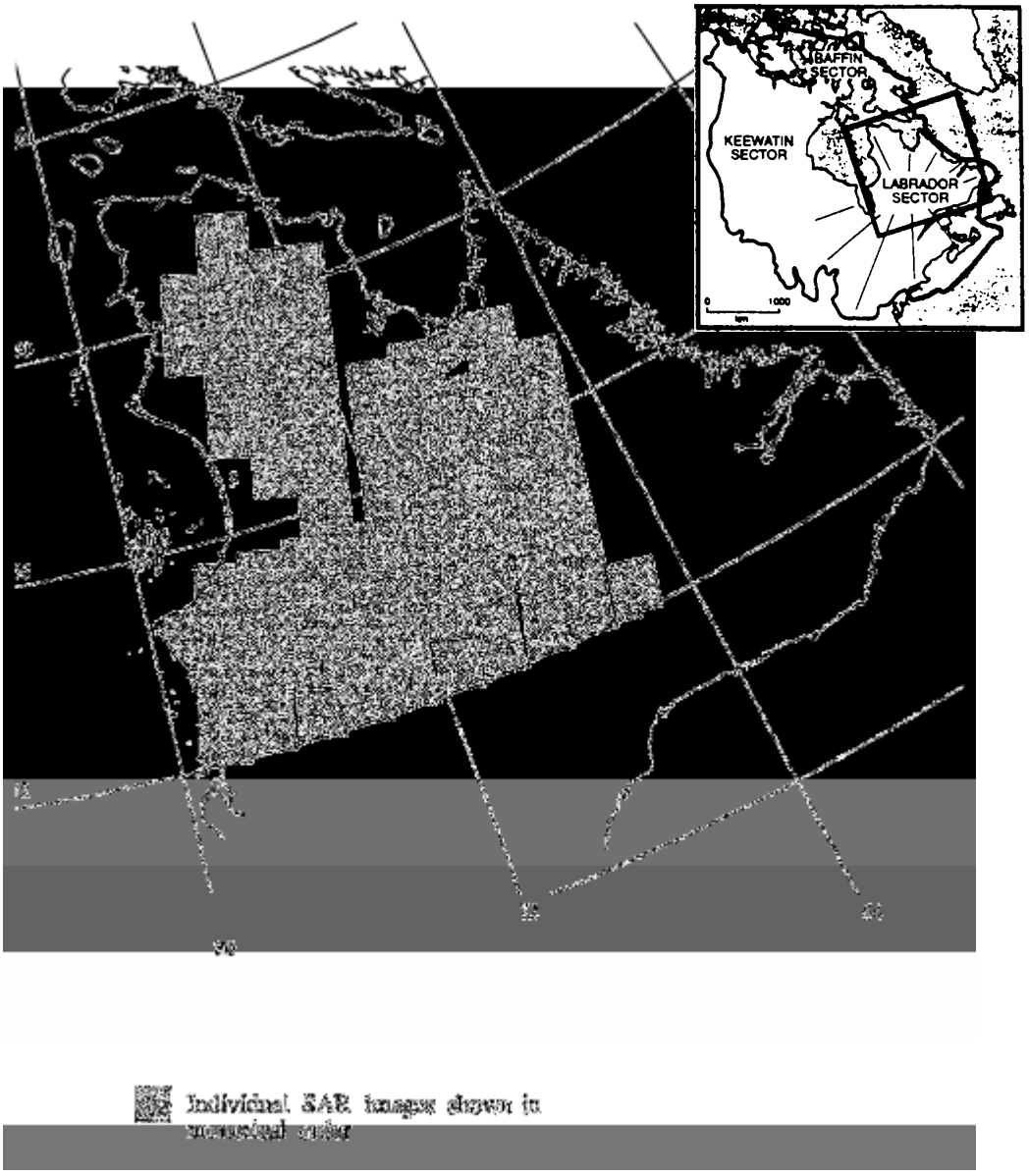

Figure 3.10 Coverage of ERS-1 SAR imagery used to map lineaments for the Labrador sector of the Laurentide ice sheet (after Knight, 1996)

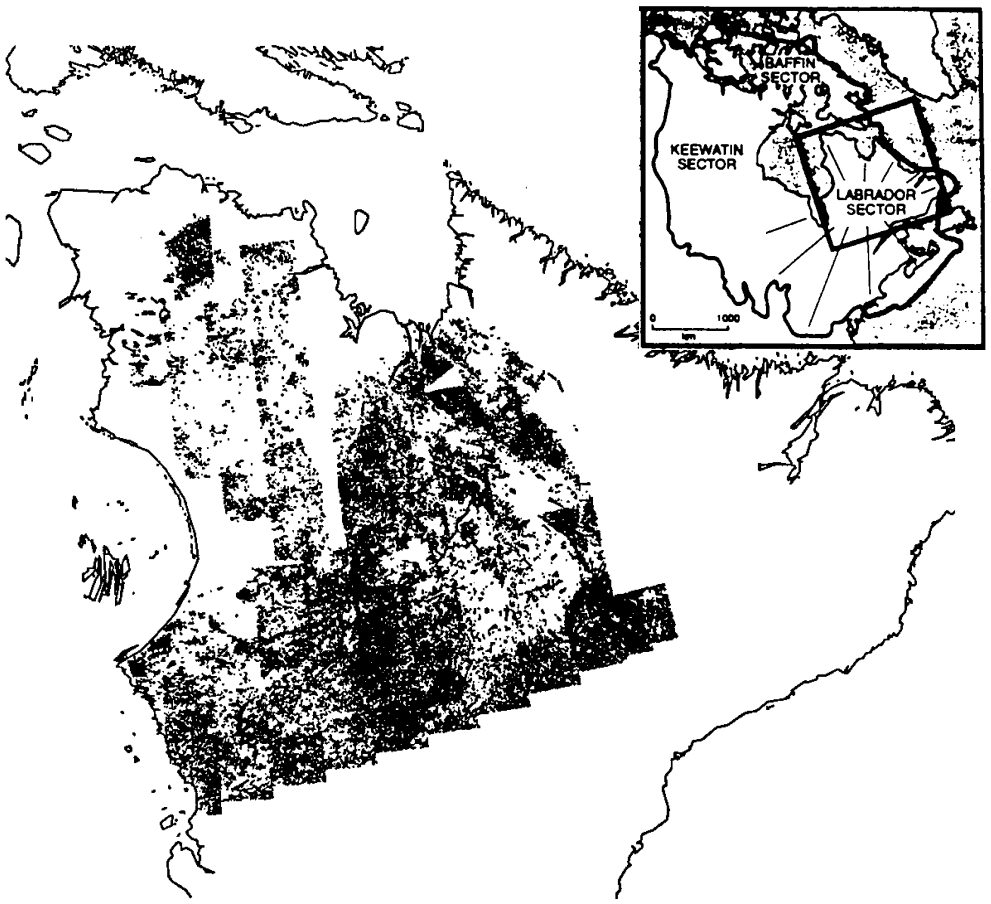

Figure 3.11 Lineaments mapped from the Labrador sector of the Laurentide ice sheet (after Knight, 1996)

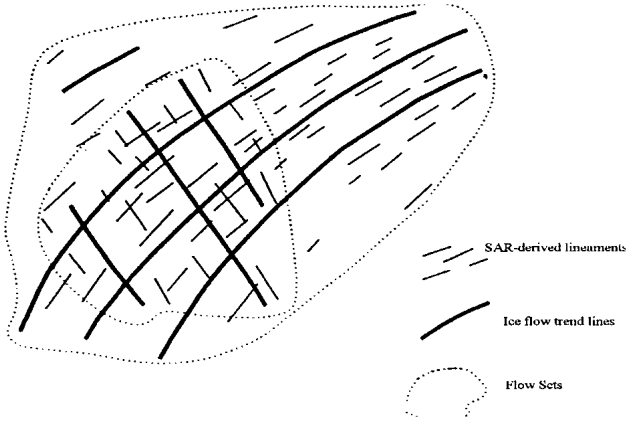

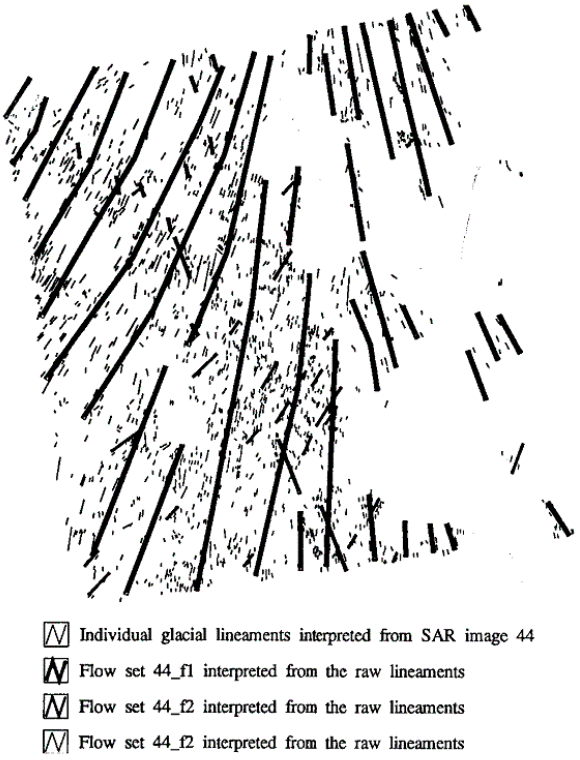

Figure 3.12 Idealised ice flow line creation from raw lineament data (top) and an example of flow lines created from lineaments mapped from one SAR image (Knight, 1996)

flow line sets into adjacent images in an attempt to distinguish discrete palaeo-ice flow events over large areas. The criteria used to establish both ice flow trend lines and flow sets required lineaments to be similarly oriented or with smooth, gradual, continuous change in orientation and no cross-cutting. Knight states that all residual ice flow lines that could not be included in flow sets were disregarded, however their proportion of total lineaments is not recorded. Drift cover and structural geology maps were compared to flow sets to filter out non-glacial data. The glacial reconstruction used lineament (primary data), ribbed moraine and esker (from Prest *et al*, 1968) data.

In her glacial reconstruction. Knight had three main assumptions:
1. Lineaments form synchronously or time transgressively, by subglacial deformation, parallel to ice flow.
2. Eskers form time transgressively recording ice margin retreat.
3. Ribbed moraine form synchronously in ice divide locations.

Knight then assigned flow sets as either synchronous or time transgressive based upon morphological criteria:
1. Synchronous - high parallel alignment and conformity.
2. Time Transgressive - less coherent lineament pattern, with localised cross-cutting, and often a strong alignment with eskers.

Relative ages were then assigned by looking at individual landforms within a flow set and extrapolating their cross-cutting relationships to that of the flow set. Although Knight was able to use SAR, she found aerial photography, fieldwork and published data more reliable. It would have been useful to break down the total number of relative age data points, by category, per flow set and so provide a quality assessment on relative age assignments.

Clark and Meehan (2001) go on to reconstruct different phases of the Irish Ice Sheet using a mixture of satellite imagery and DEMs (see also §2.4). Landform mapping was performed from a high resolution DEM, that was further supplemented by satellite imagery and field mapping. Using the methods of

Clark (1997) they went on to create flow sets from the mapped lineaments and ribbed moraine, before producing a reconstruction.

Discussion

Like the work of Punkari, Boulton and Clark (1990) made use of Landsat MSS photomosaics: they accepted that individual lineaments were usually not visible, but were able to make use of lineament "grains". Consequently aerial photography was used to determine cross-cutting relationships. Although the photomosaics were a mixture of MSS imagery from different seasons and years, they did not discuss the potential for low solar elevation to aid detecting glacial lineaments. Boulton and Clark made significant methodological advances, recognising the preservation of glacial landforms in the landscape and using this evidence to build a chronology of events. They also discussed the effect that assumptions about landform development have on the interpreted sequence of events. By providing the original data, the known chronology and the assumptions used in their interpretation, the work was open to scrutiny and re-interpretation by other researchers. Their work was also able to take advantage of the large Canadian aerial photography archives in order to verify cross-cutting relationships.

Knight (1996) and Clark *et al* (2000) were the first researchers to make use of SAR data for lineament mapping, whilst Clark and Knight (1994) assessed the utility of SAR for lineament mapping and Vencatasawmy (1998) developed SAR image processing techniques for geomorphological mapping. Knight explicitly states the techniques employed in the research, making full use of aerial photos, fieldwork, ascending/descending SAR scenes and image re-interpretation in order to minimise bias and increase accuracy, however no assessment of the accuracy was performed. The methods of generalisation to provide the final dataset for interpretation are also discussed.

Finally, Clark and Meehan (2001) are one of the first users of high resolution DEM data for mapping glacial landforms and interpreting that data to produce a glacial reconstruction. In addition, they supplement this data with a Landsat TM

purposefully acquired to have low solar elevation in order to enhance topographic features. They also briefly discuss (and highlight) some of the processing required of the DEM data in order to avoid mapping landforms from a biased dataset.

3.5 Hättestrand (1997) and Kleman *et al* (1997)

Hättestrand (1997) made use of 1:150,000 panchromatic aerial photographic coverage of central and northern Sweden to map glacial landforms. The small scale, high altitude photography made the project similar to mapping carried out from satellite imagery. These included ribbed moraine, De Geer moraine, end and lateral moraines, Veicki moraine, eskers, meltwater channels and lineations. The aerial photography coverage was 35km by 35km (although less for stereopairs) with a nominal spatial resolution of 5m. The author was able to make good use of the stereoscopic viewing and high resolution, however the small areal coverage per stereopair meant that many photos were required in order to map large areas. A mirror stereoscope was used for mapping and, although not providing the accuracy of an analytical plotter, was adequate for the requirements of geomorphological mapping, particularly in low lying areas where the effect of relief displacement is minimal.

The above work formed part of a wider research project that culminated in the reconstruction of the Fennoscandian ice sheet (Kleman, *et al*; 1997). In addition to the above mapping, they also utilised stereoscopic satellite prints of the Kola peninsula and incorporated much published literature, including the mapping performed by Punkari for Finland and Russia. Once the data had been mapped, cross-cutting relationships were established (Figure 3.13). This was achieved through reference to published striae and till fabric data, as well as their own observations of cross-cutting landforms.

Discussion

The methodology used in this research is clearly defined with an explicit set of assumptions, following Kleman *et al* (1996). However there were many details concerning the precise techniques used that were not discussed. As noted above, the method of generalisation is vital to the delineation of flow sets (or

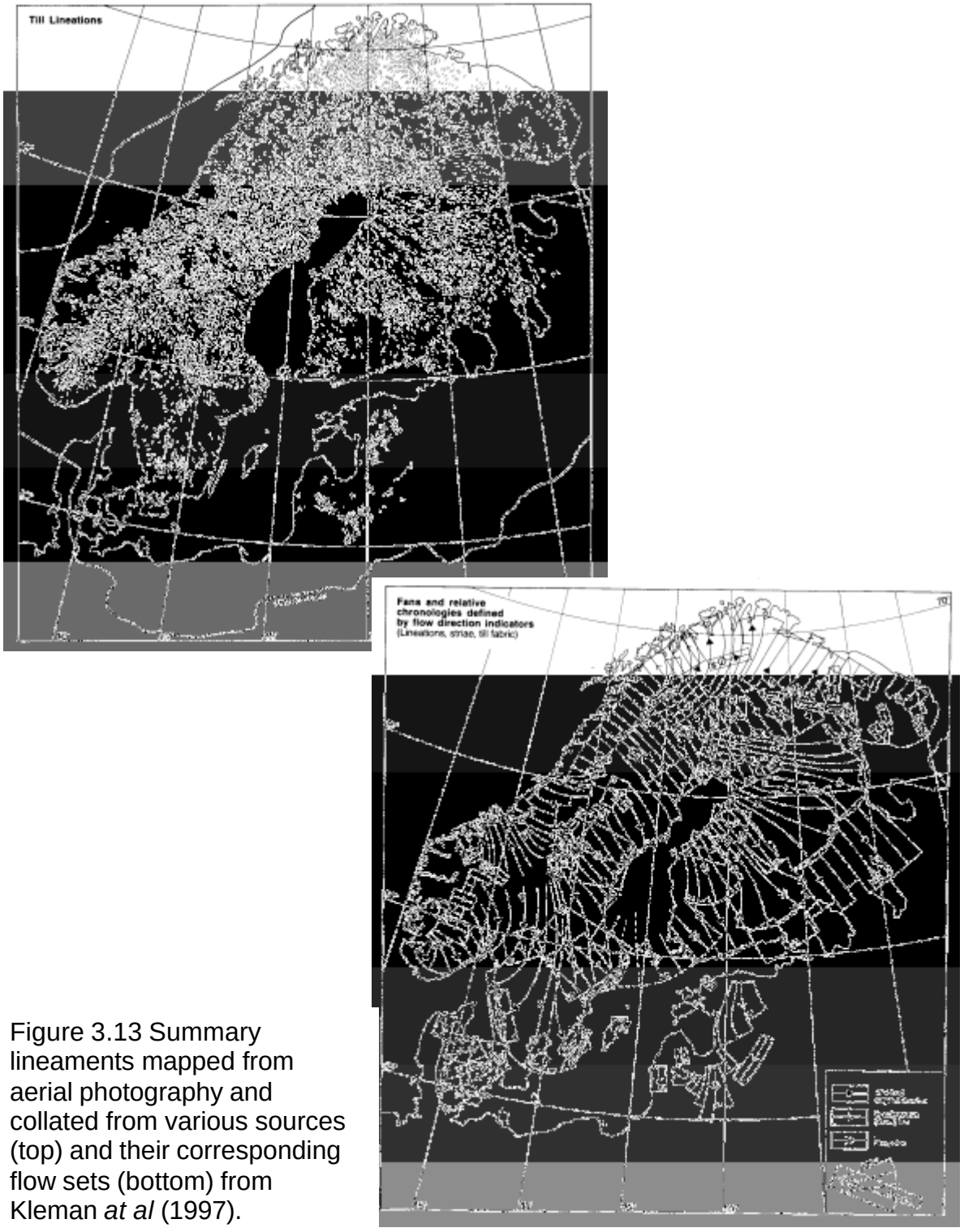

Figure 3.13 Summary lineaments mapped from aerial photography and collated from various sources (top) and their corresponding flow sets (bottom) from Kleman *at al* (1997).

fans), yet it was not clear what methods were used. The construction of relative chronologies was also problematic as there was little information on how this was performed from the fan data. Intriguingly Kleman *et al* (1997) discuss only 29 of the stated 56 fans. Relative chronologies were assigned according to individual landform evidence, relying heavily on striae data. In areas of low relief with few flow directions, correlating cross-cutting striae with other palaeo-flow indicators is acceptable, however in areas of high relief and many flow directions this is not satisfactory. Some relative chronologies were assigned purely on the basis of till fabric data. These can only be used reliably if one till sheet overlies another (e.g. Hill and Prior, 1968). Clast orientation is not strongly correlated to ice flow direction (Syverson, 1994) and may be misleading if there have been multiple ice flow events. Strong glaciotectonism may also alter clast orientation.

As part of Hättestrand's work, Goodwillie (1995) mapped and interpreted lineaments in the Kiruna region of northern Sweden. This work gave a fuller account of the procedures used in their reconstruction. Part of this work involved the division of the study area into 50km grid squares and the production of a lineament orientation histogram per square. These were used to identify dominant lineament orientations. This technique was used by Boulton and Clark (1990) and Punkari (1995). Clark (pers. comm, 1997) discarded its use as it simply identified visually dominant lineament orientations.

3.6 Knight and McCabe (1997a, 1997b) and McCabe *et al* (1998)

Knight and McCabe (1997a) utilised satellite imagery (Landsat MSS 1:250,000 paper prints) to map lineaments in Donegal Bay, Ireland, presenting a generalised diagram (Figure 3.14). They were concerned with the relationship between individual lineament morphology and sedimentology in order to infer the depositional environment. They recognised the presence of cross-cutting lineaments and that lineament morphology is composed of a continuum of forms that vary according sediment supply and depositional environment. The authors therefore use the concept of a relative chronology and that this requires a mechanism for lineament preservation.

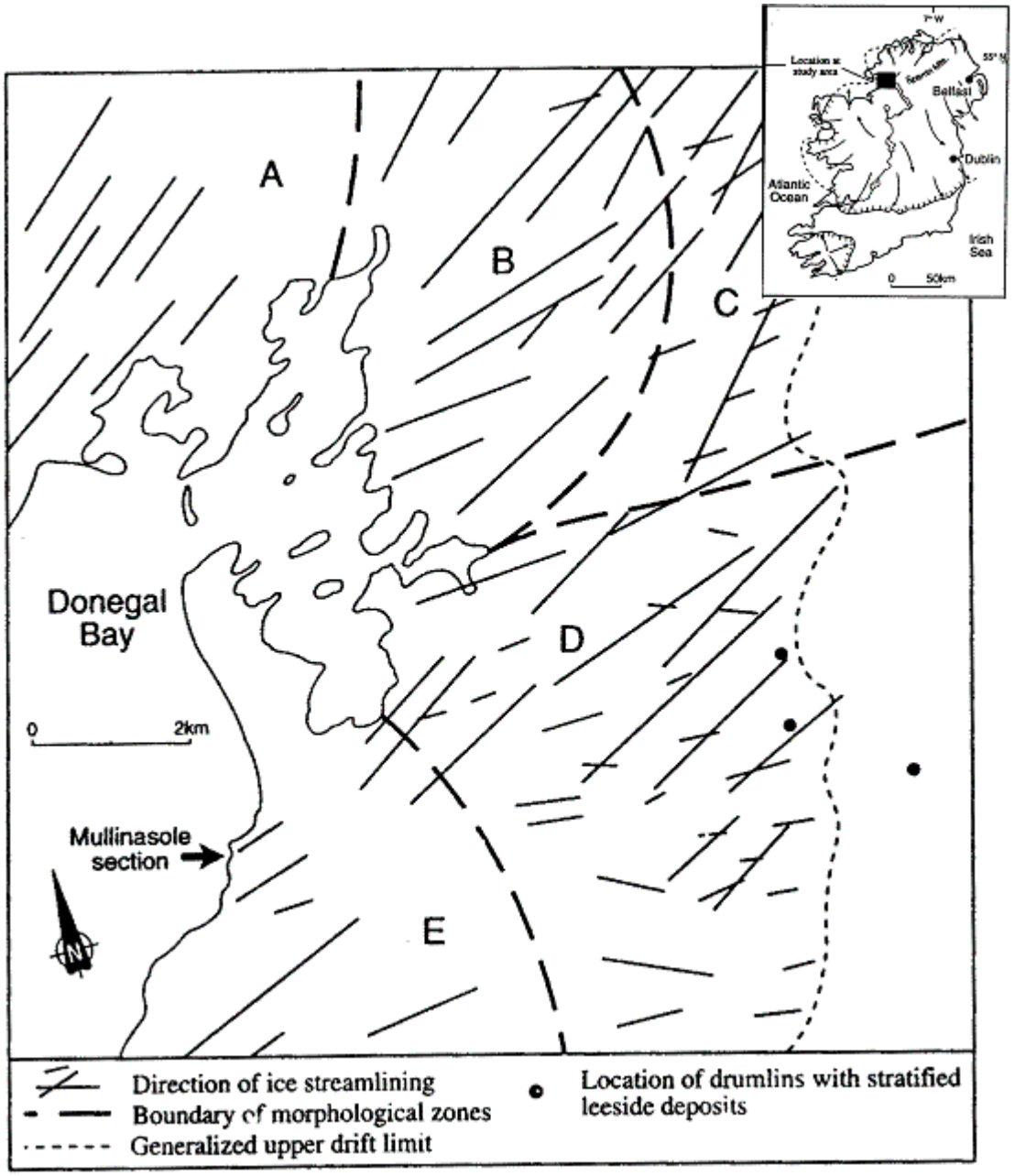

Figure 3.14 Generalised lineaments mapped from Landsat TM satellite imagery (Knight *et al*, 1997).

Knight and McCabe (1997b) extended the above mapping into the Irish Midlands, using a Landsat TM 1:250,000 paper print to map glacial landforms. Image mapping was used to complement detailed field surveying, although they were for two separate field areas. For illustration they presented satellite mapped data (ribbed moraine) of their field area and a sample image of a different area.

McCabe *et al* (1998) used Landsat TM paper prints to map glacial bedforms in north-central Ireland, this is supplemented by an unspecified use of aerial photography and field work. Their reconstruction uses mapped data and published evidence, to describe four distinct ice flow stages, however they do not use the methodological techniques (e.g. flow set creation) developed by Clark (1993) and Kleman *et al* (1996). The lack of a rigorous methodological basis from which landform data can be interpreted to flow sets does not provide a solid morphological base from which to interpret their data. They also fail to discuss the distinction between time transgressive and synchronous flow sets; for example they describe a pattern of curving flow as indicative of ice streaming, however this flow pattern can be explained by either flow set type, each providing a different glacial scenario.

Initially they interpret landform data purely as directional indicators, however they assume that ice sheet marginal bedforms are indicators of fast ice flow and consequently representative of net-erosional processes. This is used to develop the idea of transverse ridge erosion followed by streamlining. They go on to suggest that ribbed moraine cross-cut by lineaments are representative of a change in basal thermal regime, the former explained by Lundqvist's (1989) theory of ribbed moraine formation, and the latter evidenced by coastal moraines representative of the high erosional processes.

Discussion

It is disappointing that the papers of Knight and McCabe do not follow the methodological techniques of Boulton and Clark (1990) and Clark (1993, 1994) for their glacial reconstructions. No assumptions are outlined and the conclusions are based around discussion points, rather than providing an

objective review of the evidence and the production of alternative interpretations.

3.7 TheoreticalandTechnicalMethodologicalDevelopment

The traditional method of reconstructing palaeo-glacial environments involves the up-scaling of processes that form individual landforms, within a study area, to that of the ice sheet. This approach usually involves *a priori* assumptions concerning landform processes, as well as their scalability. In addition, it assumes that all landforms within the study area were created similarly and that this can be extrapolated to other regions. The weaknesses introduced by the above assumptions become more apparent at smaller and smaller scales and consequently the methodology has evolved into an approach that uses appropriately scaled techniques to reconstruct former ice sheets. These techniques are based around two main approaches, or models, to geomorphology. The first, termed the ***landsystems model*** is defined by Benn and Evans (1998) as an:

> *holistic approach to terrain evaluation, wherein the geomorphology and subsurface materials that characterise a landscape are genetically related to the processes involved in their development.*

This is distinct from the ***process-form model*** where spatial variation in morphology are used to infer changes in process. The palimpsest landscapes investigated by the glaciologist will display morphological variations that are a result of both *landsystems* and *process-form* changes and an understanding of these models and their implications will allow a more complete study of past glacial environments.

Sugden and John (1976) used the process-form model to investigate ice sheet reconstructions within the context of the Laurentide ice sheet. They idealised an ice cap in cross-section (Figure 3.15a) with two broad zones; a *wastage zone* towards the ice cap margins where sediments are deposited and an *active zone* where faster flowing ice both erodes and deposits, shaping the landscape. The wastage zone identifies moraine, dumping and melt-out landforms. The active zone is dominated by deposition towards its margins, with erosion towards the

ice cap centre. They briefly discussed the effect of multiple glaciations on the landscape, but concentrated on sedimentary sequences rather than morphology. It is natural to develop associations between different processes and changes in landform morphology. Indeed, given a morphological association in their genesis, this link can feed back into an understanding of the processes that formed them. Sugden and John (1976) concluded with a generalised model of drift landscapes that moves from erosion, to active, to wastage zones, with transition areas between, and the landforms associated with those zones (Figure 3.15b).

The advent of satellite imagery allowed the expansion of landform mapping to larger areas and so closer scrutiny of landform associations. It was not until Boulton and Clark (1990), Clark (1993) and Clark (1994) that an attempt at an objective methodology was explicitly implemented. This incorporated assumptions about landform formation, the discovery and use of a relative chronology from cross-cutting landforms, a discussion of “grain” features and the discovery of mega-scale glacial lineations. Perhaps most importantly the glaciological implications of cross-cutting lineations were explored. This included the method of cross-cutting (superimposition or remoulding) and how this related to ice velocity, residence time and sediment supply. Clark (1993) envisaged a continuum from a lineament with no modification, through superimposition and minor remoulding to complete realignment (Figure 2.4). The degree of modification is reliant upon a combination of ice velocity and time of exposure in relation to sediment availability. Within an ice sheet, velocity is very low at the divide, with no supply of sediment. Towards the margins velocities increase and so the potential for strong deformation is high. Using lineament correlation over large areas and relative and absolute dating, Boulton and Clark (1990) considered the majority of cross-cutting landforms in the Laurentide Ice Sheet could only occur if the ice divide had shifted. This assumes all lineaments are from one glaciation, the alternative a result of multiple glaciations. This work provided evidence of dynamically shifting ice divides and how this is reflected in the landscape. This model assumes that lineaments are formed synchronously, however many cross-cutting lineaments in marginal areas would require a complex series of re-advances in order to

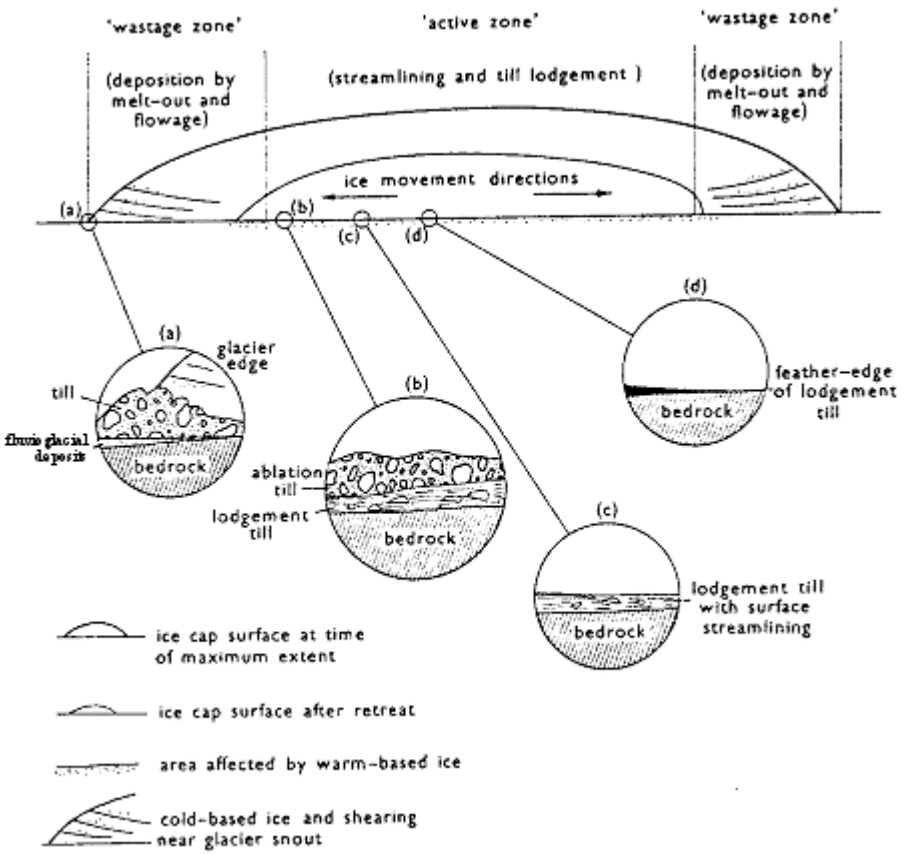

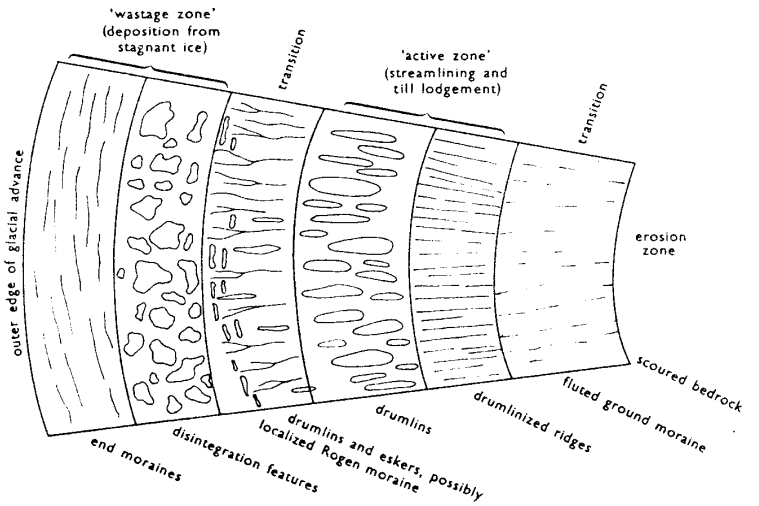

Figure 3.15 a. Generalised model of drift landscapes (Sugden and John, 1976). There is erosion in subcentral parts of the ice sheet (the “active” zone) that changes to deposition in submarginal regions (the “wastage” zone) b. Landforms associated with these zones.

explain such patterns. Clark (1997) suggests that the “on-off” activation of ice streams may produce cross-cuts (Figure 2.6). He also provides a detailed discussion of the type of imagery suitable for lineament mapping and the image processing techniques that are available.

Clark (1999) focuses more specifically on the interpretation of mapped lineament data by asking the following questions:

- *What were the processes of generation?*
- *What was the glaciodynamic context?*

Investigations into landform generation have been numerous, but are inhibited by problems in directly studying these processes. At the lowest level, glacial landforms provide information on palaeo-ice flow direction. Any further inferences are based directly upon theoretical assumptions.

Understanding of the *context of generation* has received little attention. Although both inquiries are linked, geometric and contextual landform data can be used to provide a great deal of information on the location of formation.

Whereas flow patterns are simply the large scale grouping of landforms (in this instance lineaments), flow sets operate over much larger areas where there are often several different interpretations available to the researcher (§2.3.6). These interpretations are strongly influenced by the assessment of lineament formation as isochronous or time-transgressive (§2.3.4). Clark goes onto develop seven glacial contexts where lineaments may be formed, primarily classified as time-transgressive or isochronous (Figure 3.16). The application of a context within specific situations is intended to provide a further tool for understanding the dynamics of previous ice sheets.

This discussion highlights the necessity to distinguish between time-transgressive and isochronous lineament patterns. Clark considers ice thickness, flow topology and stability to be the main controlling variables, visualised in the following manner:

- **Time-transgressive** - formed close behind retreating ice margin and consequently unstable conditions, thin ice and variable flow conditions.
- **Isochronous** - formed some distance from the ice margin and consequently beneath thicker ice, with a more stable flow pattern.

Clark goes on to list distinguishing parameters for each type of configuration. Isochronous flow events will display lineaments with similar orientation and morphometry, whereas time-transgressive events will produce a less well ordered pattern, perhaps with obvious discontinuities. A special case of this latter event is that produced at a retreating ice margin. This produces a distinctive pattern of splayed lobes that accrue as the margin retreats. The low profile of the ice produces landforms that are partially controlled by topography. These factors produce a complex record of cross-cutting lineaments, broadly emplaced within splayed lobes.

Although these criteria are a good starting point, visually identifying such flow sets and separating them from isochronous ones is difficult. The assignment of flow set type is a procedure concurrent with the creation of those flow sets and as such this tandem process is somewhat iterative as it attempts to account for as many flow sets as possible within a single scenario.

Building on the methodology outlined above, Kleman *et al* (1996) further developed glacial reconstruction methodology, following techniques originally developed for striae data (Kleman, 1990) and investigations into the morphological record of landforms and methods of preservation (Kleman, 1994). The space-time cube (Figure 3.17) depicts the present day suite of glacial landforms (the top surface of the cube). Each “layer” within the cube represents the state of the surface during earlier periods. The area covered by ice constantly changes, as does the type, number and magnitude of landforms “recorded” on the surface. Relict landforms will also be present, but can be combined with contemporary landforms forming composite ones or entirely removed.

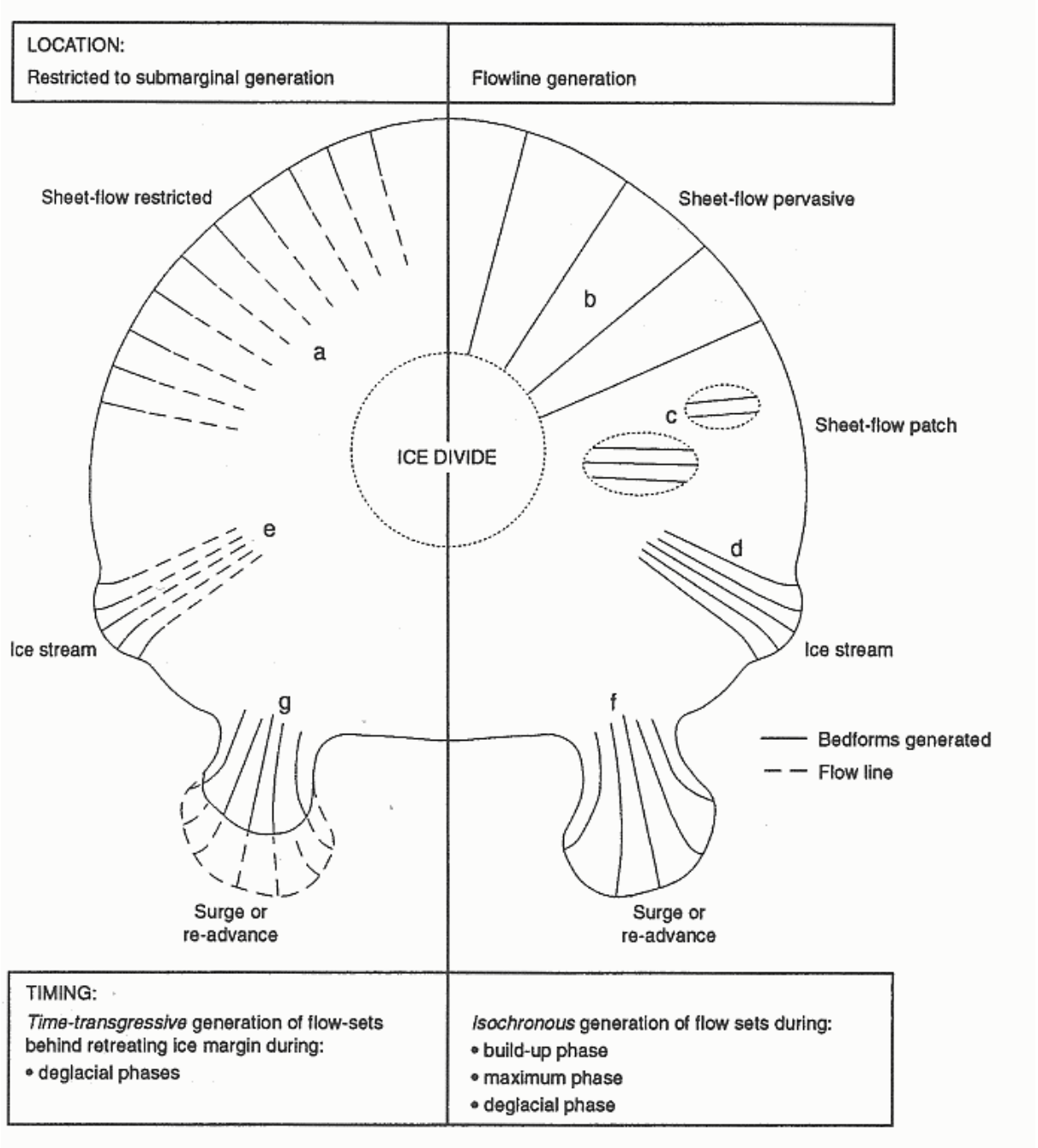

Figure 3.16 a. Different glaciodynamic contexts under which lineaments can be generated (Clark, 1999). These can be grouped under generation *isochronously* or *time-transgressively*.

Ice sheet reconstructions were originally based upon interpreting all landform data (the top surface) as representative of conditions at the last glacial maximum (LGM). However the challenge now is to unravel the history of a region by interpreting landform suites into individual landforms and the events that formed them. This can be further aided by the use of dating methods to constrain both the extent of glaciation through time and individual events.

After the grouping of landforms into flow events, the associations between landforms within these events and whether they are synchronous or time-transgressive, allows their classification into one of five categories (Figure 3.18). Although this methodology aims to provide an overall theoretical and techniques based framework for further work, Kleman *et al* (1997) state that it is less suitable for areas with mountainous terrain. This is because one of the assumptions for the conglomeration of features into fans is their spatial continuity, which cannot be maintained in high relief areas, a point noted by Punkari (1985). However this element can be incorporated through the use of relief (i.e. a DEM) to help assess spatial continuity, a task suited to a GIS. This example highlights the problems involved in the methodology.

Benn and Evans (1998) prefer a landsystems approach (Eyles, 1985) to reconstruction, suggesting that bed strength and hydraulic conductivity, basal thermal regime, meltwater availability, ice velocity, shear stress and effective overburden pressure influence the formation of subglacial sediments and landforms. This complex interaction produces the palimpsest terrain viewed today, which typically produces distinct landform zonation, although this can later be modified by further advances and retreats of the ice margin. An integrated, small scale, methodology remains to be developed, that can combine the landform mapping from satellite imagery with detailed sediment logging.

3.8 Conclusions

Remotely sensed images have been used within palaeo-glaciology for nearly 25 years and during this time remarkable changes in their use have been made. These developments have been made in tandem with technological ones

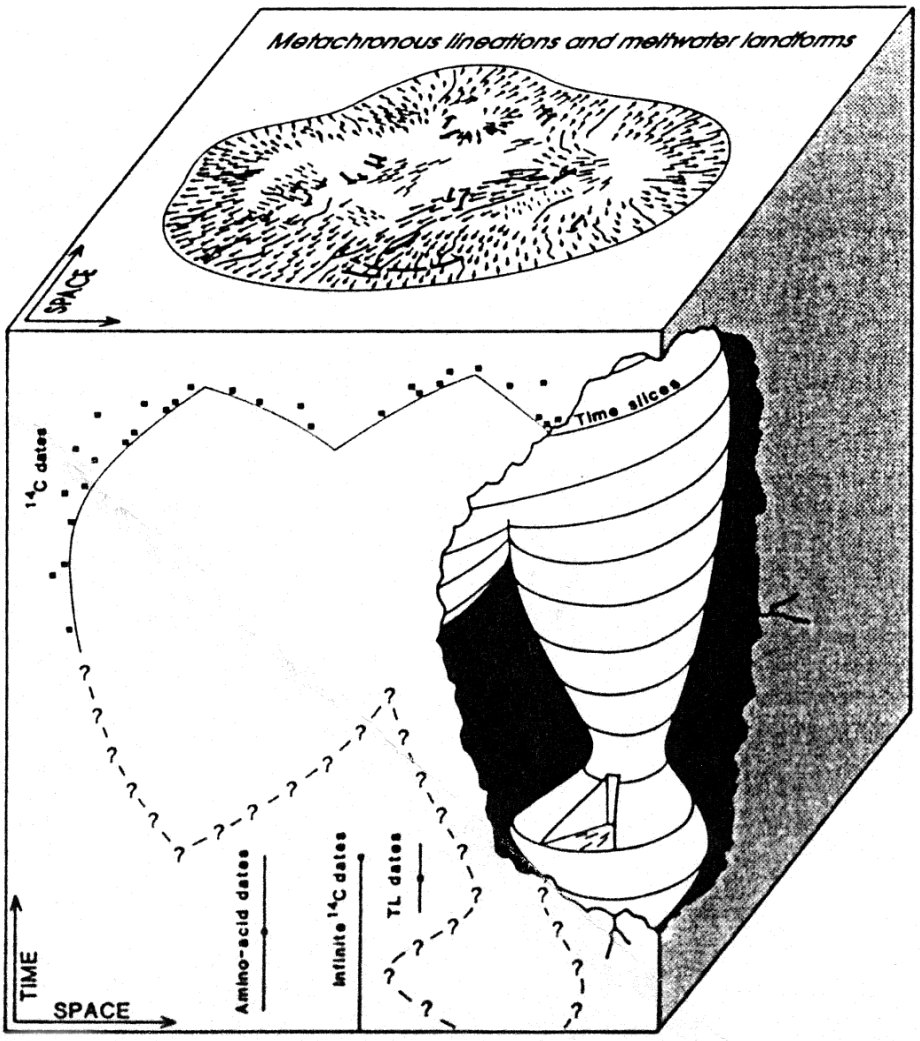

Figure 3.17 Space-Time cube showing an idealised, contemporary, geomorphological surface (top of cube) and the inferred ice sheet behaviour required to have generated this (Kleman *et al*, 1996).

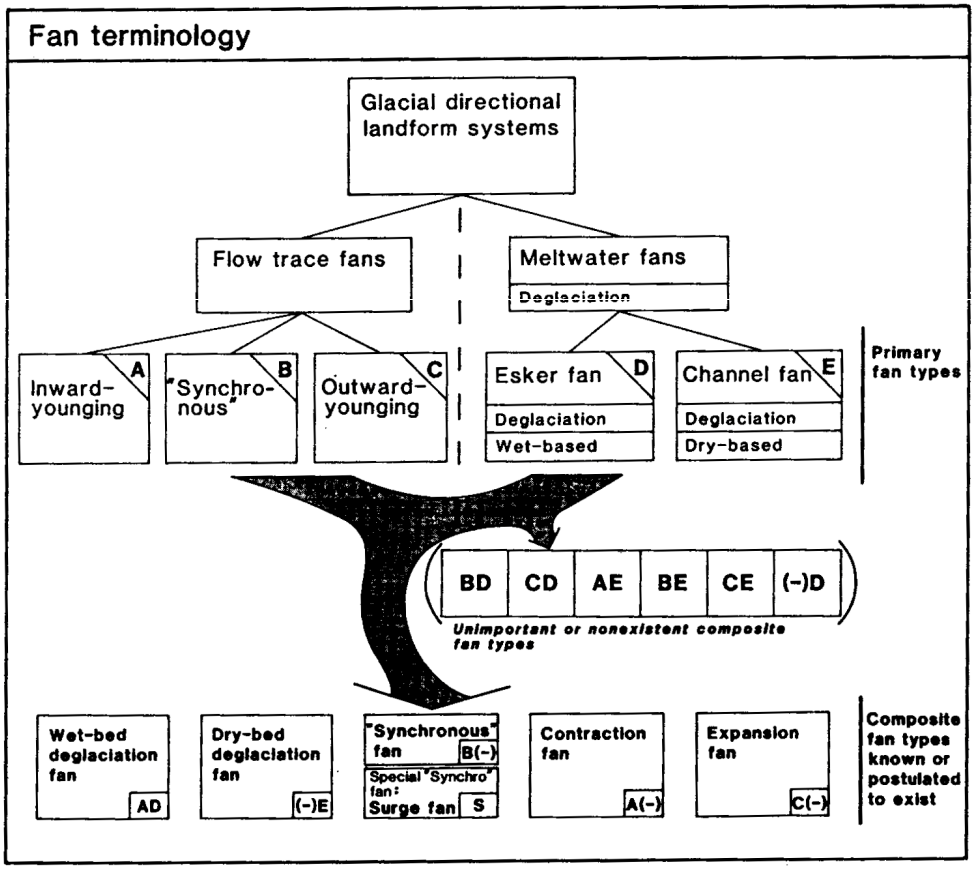

Figure 3.18 Table showing postulated fans that can logically exist (top) and those that are known or postulated to exist (bottom) (both diagrams after Kleman *et al*, 1996).

deriving from the launch of new satellites. More detailed data are being collected, allowing the morphological mapping of glacial landforms, over large areas, at relatively economic costs. Until the advent of such technology, the mapping of landforms across an area previously covered by an ice sheet, was almost unheard of due to the scale of project needed to complete such a task. Indeed this work unequivocally showed that the present day landform assemblages can record multiple ice flow events. This realisation has forced a complete re-evaluation of the way in which palimpsest data are interpreted. Unfortunately, these methodological developments require the *process* of landform generation to be understood, as well as its *context*. Given the difficulty in studying sub-glacial processes beneath present day ice sheets, these are purely hypothesised and will require on-going refinement.

This chapter has highlighted the importance of satellite imagery within ice sheet reconstruction research and traced the technological and methodological developments that have taken place. It has also emphasised the weaknesses and inconsistencies, within research, that need addressing. Unfortunately this is not confined to earlier research, but equally affects more recent work. It is important that any future research is able to acquire appropriate satellite imagery and map glacial landforms in a consistent and appropriate manner. These data then need to be generalised into a simpler information set that can be interpreted. The following chapter highlights areas of weakness within this current workflow and these are then addressed later in this thesis.

4 Key Research Topics

4.1 Introduction

During my research into the reconstruction of the Irish ice sheet, it became clear that the results obtained by mapping from remotely sensed imagery may vary according to the nature of the imagery used, and the skill and experience of the observer. If this method is to yield reliable results which are comparable between different regions, mapped by different observers, then there needs to be a greater understanding of the sensitivity of the results to the exact methodology employed.

Ice sheet reconstructions require the mapping of individual glacial landforms from imagery. The results from this stage will depend on the *detectability* of the landforms, a term which incorporates the following two elements:

1. **Image:** the degree to which the physical and spectral characteristics of the sensor allow the landforms to be distinguished from other features on the image
2. **Observer:** the success with which an observer can record these differences and thus map the landforms.

The second stage involves summarising the landform information into meaningful patterns by grouping the individual landforms into sets of features which can be assumed to have been derived by a single glacial event. This is a subjective technique, which resembles the process by which cartographers generalise information from large scale maps to produce small scale ones.

Although remotely sensed images were the main source of data for my original mapping of the Irish ice sheet, they are rapidly being supplemented and, in many instances, replaced, by digital map data, principally digital elevation models (DEMs). Within the restrictions set by data collection and DEM creation,

these are accurate representations of a surface and are ideal data sources for morphological mapping.

This chapter discusses methodological problems arising from both the mapping (using satellite imagery and DEM data) and generalisation stages. These topics then become the main foci of this research and the thesis is structured around them. The following three chapters describe the methodology used to investigate these topic areas and present results from these investigations. The thesis concludes with a review of the results.

4.2 Detectability

Scientific investigation can be based around experimentation involving the collection of measurements and their analysis. This can then lead to the creation of a framework through which a phenomenon can be understood. For ice sheet reconstruction, the location of landforms created during the last glaciation is required. Their location (or measurement of their position) is recorded through field mapping or remote sensing. As Chapter 2 has illustrated, this can effectively be achieved through the use of satellite imagery. However the recording of surface reflectance is not a surrogate for the location of glacial landforms. For this to occur, meaning must be assigned to features depicted in the image. This process is termed *landform detection* and is dependent upon the representation of a landform on an image and the ability of an observer to assign meaning to it. That is to say, for a landform to be successfully detected it must be fully represented upon the image and the observer must be able to locate it. This section will discuss the factors that affect these two variables.

4.2.1 Landform Representation

The representation of a landform upon an image depends upon the characteristics of the sensor, the characteristics of the landform, the illumination conditions and sometimes the meteorological conditions prior to and during acquisition. The interaction of these categories combine to produce the following variables:

1) **Relative size:** the relationship of lineament length to sensor spatial resolution. The higher the spatial resolution the greater the ability to resolve shorter lineaments (Figure 4.1).

2) **Azimuth Biasing:** a bias in landform detectability arising from the difference between the lineament orientation and the illumination orientation (azimuth angle). Landforms are known to appear differently when they have different solar illumination directions (Figure 4.2). For example, a drumlin viewed side-on will look like a drumlin, but when viewed head-on can look like a circular hill (Aber *et al* (1993) and Lidmar-Bergström *et al* (1991)).

3) **Landform Signal Strength:** the degree to which the landform can be distinguished from other features by tonal and textural information in the image. These variations are caused by differences between the surface cover of a lineament and its surroundings (Figure 4.1b shows drumlins highlighted by inter-drumlin waterbodies), and the relief effect arising from slopes appearing lighter or darker depending upon the height of the sun in the sky (solar elevation; Figure 4.3). High illumination angles cause lee slopes to be illuminated (so reducing textural information), whilst low illumination obscures lee slope with shadow (also reducing textural information, but highlighting the presence of the lineament). Several authors have investigated the conditions through which high contrast images depicting lineaments are obtained (e.g. Slaney, 1981). In general they conclude that a low solar elevation produces ideal imaging conditions.

Synthetic aperture radar (SAR) imagery is also used for mapping landforms but here the controls on detectability are different because of the different viewing geometry. SAR imagery is good at detecting topographic variation due to the oblique viewing angle of the sensor, as opposed to the near-vertical viewing angle of visible and near infra-red (VIR) sensors (Figure 4.4). An advantage of SAR data is that it is acquired with fixed illumination and azimuth angles providing a consistent data source. This is unlike optical data (e.g. Landsat) which will have varying angles on different images according to the date and time of day (i.e. the sun position varies).

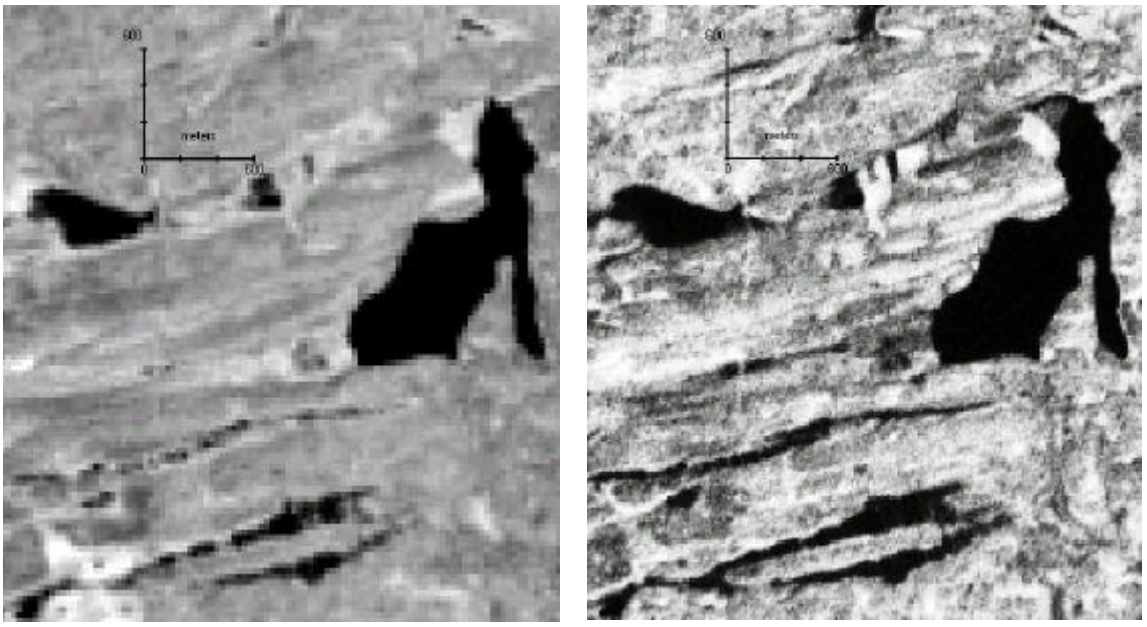

Figure 4.1a and b Landsat ETM+ Multispectral (left) and Panchromatic (right) images showing the effect of sensor spatial resolution (15m and 30m respectively) on lineament detection.

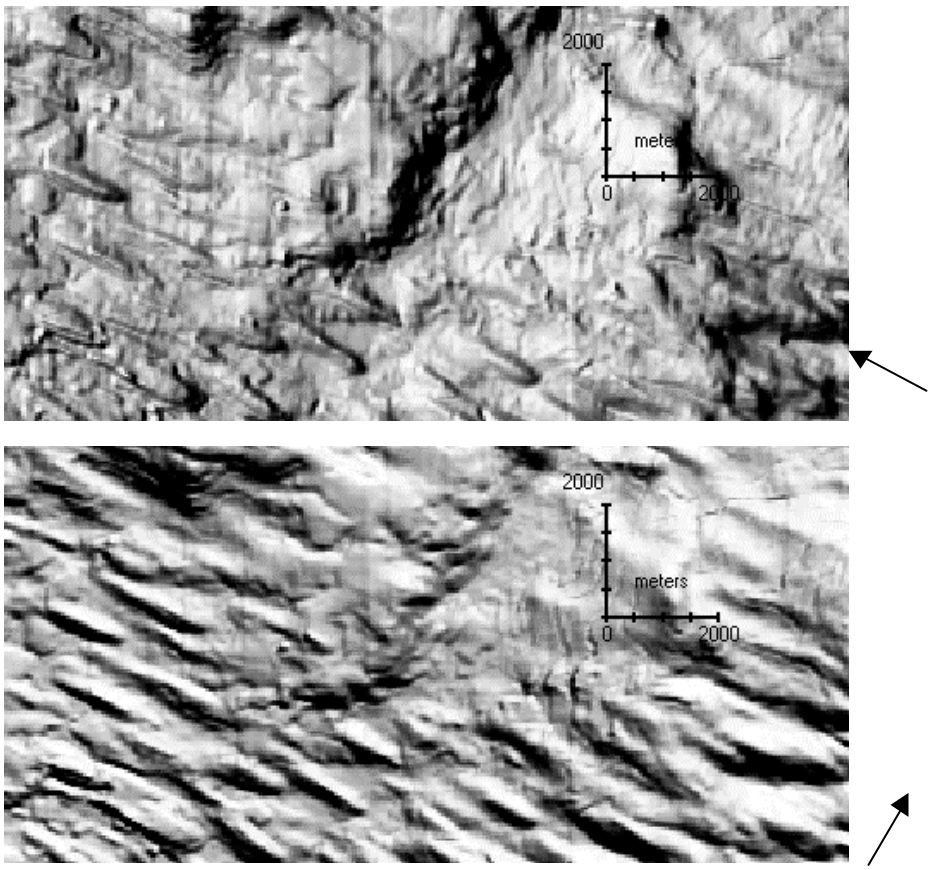

Figure 4.2 Illustration of the effect of azimuth biasing on landform detection. The two images are extracted from a relief shaded DEM (Lough Gara, Ireland), illuminated from different azimuths. Arrows indicate azimuth angle.

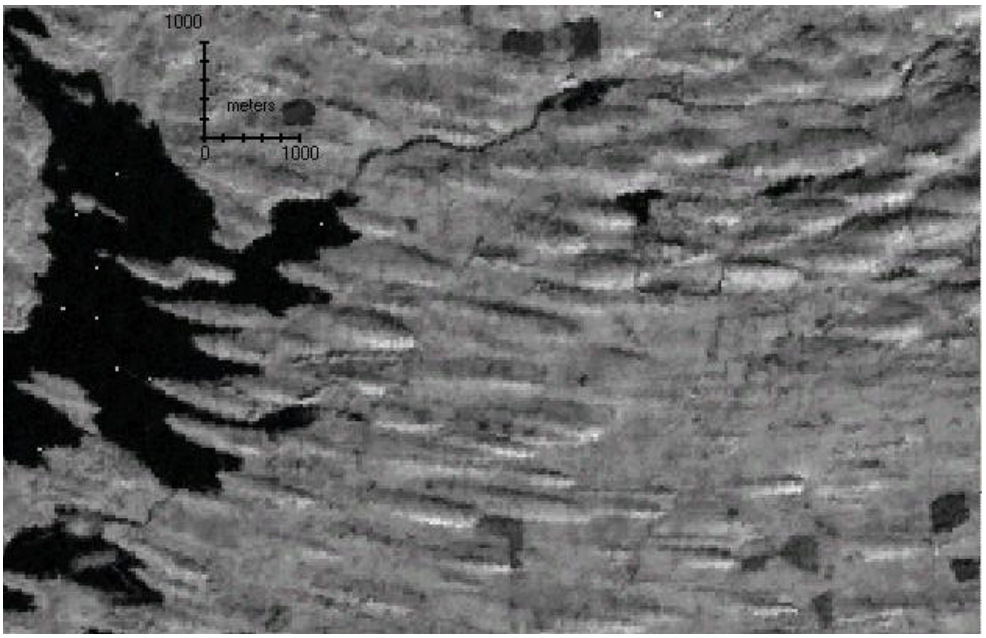

Figure 4.3 Illustration of the effect of the relief effect on landform detection. The image shows lineaments highlighted by the shadows they cast, a result of low solar elevation. Arrow indicates azimuth angle.

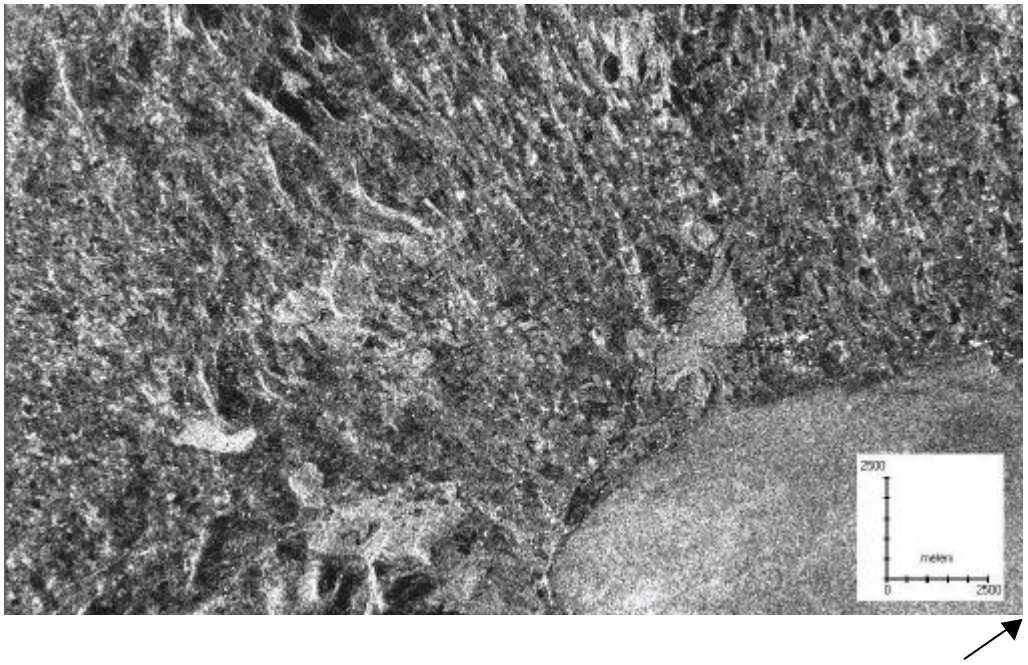

Figure 4.4 ERS-1 SAR image highlighting lineaments on the right hand side oriented north-south. Note the rollover effect the side-looking radar has on the steep, mountainous terrain in the centre. Arrow indicates azimuth angle.

The greater the difference in reflectance properties of the surface cover of the lineament when compared to surrounding terrain and the greater the relief effect (for VIR imagery), the greater the tonal differentiation of the lineament on the image (see Clark, 1997 and Aber et al, 1993 for further discussion). As lineaments are often composed of the same material as the surrounding terrain, spectral differentiation is of limited use in these situations. However, Punkari (1982) and Dongelmans (1996) have successfully used spectral differentiation by taking advantage of certain regions where drumlinised terrain enhances the collection of moisture in inter-drumlin areas. This variability in surface moisture affects surface cover (i.e. inter-drumlin regions become boggy) and allows drumlin identification.

Meteorological conditions can also be important for landform representation in VIR imagery. Atmospheric interference can reduce the sharpness of imagery by diffusing direct radiation, whilst antecedent conditions may affect surface reflectance properties and so alter lineament tonal differentiation. This is especially true for SAR data which is highly sensitive to variations in moisture such as from rainfall events or dew.

The interaction of the above variables produce a complex representation of an imaged surface. In order to interpret data mapped from imagery it is essential to understand the nature of the imagery from which that data has been acquired so that inherent errors can be accounted for. This is dependent upon the aims of the research and consequently the level of spatial accuracy and completeness required. If a morphological map of a selected region is required, then mapping with high spatial accuracy and completeness is necessary. Conversely, generalised flow patterns of a palaeo-ice sheet require lower spatial accuracy and completeness.

In summary, there is a minimum resolvable landform size and a range of lineament orientations that an individual sensor will be able to represent. In addition, the *definition* of these landforms is dependent upon the surface cover (affected by antecedent meteorological conditions) and relief effect (for VIR

imagery). Optimum conditions for definition (e.g. Aber *et al*, 1993) will allow the representation of some landforms and easier interpretation of others.

4.2.2 Observer Ability

Image interpretation is the qualitative (manual) identification of features of interest within an image and an appraisal of their significance. The ability of an observer to interpret a remotely sensed image is dependent upon the experience in using interpretive techniques, as well as specialist information pertaining to the area of interest.

Different interpretive techniques have been developed since the availability of aerial photography and have consequently been the focus of much research (e.g. Colwell, 1960). With the advent of infra-red and radar photography these techniques were expanded (e.g. Oslon, 1960) and this process continued with the introduction of space photography and digital imagery (e.g. Colwell, 1983). Traditional techniques (Colwell, 1960) include the assessment of shape, size, tone, texture, shadow, pattern, location and association. A “convergence of evidence” allows the successful identification of an object. Estes *et al* (1983) ordered the above techniques, so providing a hierarchical framework to image interpretation methodology. This was extended by Black (1995) who categorised this hierarchy, suggesting that higher order techniques provided the most effective methods of identification and so should form the basis of an image enhancement strategy (Figure 4.5). Black suggests traditional interpretation techniques allow “perception” and “cognition”, however higher order techniques lead to “recognition” and ultimately “identification.” By focusing lineament mapping and image enhancement techniques on these higher orders, high accuracy mapping should be attainable. His principal datasets were Landsat TM imagery and DEM data created from 1:10560 and 1:50000 digitised contour data. The latter were used to create slope and aspect maps, as well as alternately relief shaded images. Although he recommends image processing techniques for satellite imagery, he states that the DEM and derived data were the best primary data source, however the exact technique used for mapping from the DEM data is not explained.

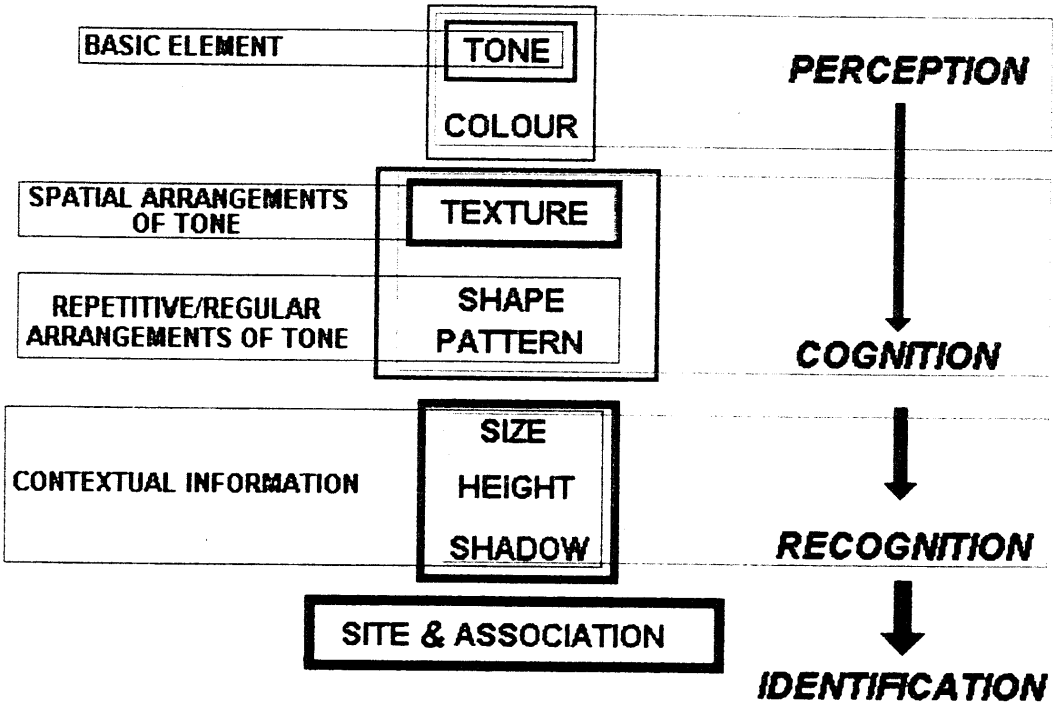

Figure 4.5 Hierarchical ordering of elements used in image interpretation (Black, 1995). Image enhancement aimed at the *Recognition* and *Identification* stages should lead to higher accuracy mapping.

The specialist experience of an observer is central to their ability to interpret imagery. In glaciology, the ability to identify glacial landforms in different locations and environments is fundamental to the achievement of complete mapping.

Lineament mapping has formed a major area of research, particularly during early geologic applications of Landsat MSS imagery (Pohl *et al*, 1998). This has attracted work on the enhancement of lineaments within imagery (e.g. Clark, 1997; Black, 1995), as well as the reproducibility of results by one observer and between observers. The former topic was briefly described above, whilst the latter topic will now be touched upon.

Siegal (1977) built a scaled model of a landscape and used vertical photographs (with four different illumination azimuths) to test the variability between specialist geological observers. He explicitly focused on geological lineaments and chose to provide no definition of “lineament” to the observers. Given that observer variability is expected, it is not surprising that his results reflect this. He found that there was high variability in the number of lineaments mapped, with 22% of the variation of total lineament length attributable to observer variability, whilst illumination azimuth accounted for just 2%. The remaining variability is a result of observer-azimuth interaction and other unaccountable errors. Siegal went on to perform a comparison of lineament coincidence between observers and found that there was less than 5% coincidence between all 5 observers, with 50% of all mapped lineaments not coincident at all. However overall accuracy could not be gauged as a higher accuracy map was not used to test against.

Podwysocki (1975) compared the lineament mapping of four geologists using Landsat MSS imagery, having provided them with an explicit definition of a lineament beforehand. Less than 1% of lineaments were coincident between all four operators, however Podwysocki had no access to higher quality data and admitted that the study area was not ideal.

These results are perhaps not surprising given the very broad remit with regard to mapping. Within geological lineaments both topographic and non-topographic forms will be mapped, with lineament lengths often varying across several orders of magnitude. This can result in the inclusion of nearly all linear features as requiring mapping. The lineaments mapped will therefore depend on the mapping style and experience of each individual observer. Within the context of a glacial environment, lineaments (i.e. drumlins) are purely topographic forms, principally spanning the 200-2000m range, although longer and shorter lineaments do exist. Given their topographic representation, other ancillary evidence often exists with which to corroborate an identification. For detailed morphological mapping, it is desirable to perform break-of-slope mapping and then subsequently identify lineaments. With careful mapping procedures operator inter-variability should be minimal.

4.2.3 Summary

Landform detectability is dependent upon the representation of a surface by a satellite sensor and the ability of an observer to map those landforms. This then raises the following questions:

- Does the available image represent all, or a large proportion, of the landforms present?
- Is the observer able to map these landforms or are errors of omission and commission present?

The latter question has been briefly touched upon above, but is yet to receive specific examination with respect to glacial landforms. Indeed, recent research (e.g. Vencatasawmy, 1997) has looked at the ability to automate the process of lineament mapping. Chapter 5 aims to investigate the former question and whilst observer variability in mapping is a problem, this is assumed to be minimal through consistency produced by one observer.

4.3 DEM Visualisation

4.3.1 Introduction

The two-dimensional visualisation of three-dimensional terrain has been a common problem within geography, dating back to early map making. Perspective views (Figure 4.6a) are a common method used to introduce a sense of depth, however it is not appropriate for maps as they are generally orthographic (i.e. scale invariant with a vertical view). Map makers came up with alternative methods which included hachuring, contours and relief shading (Figure 4.6). Other less common techniques that were developed included vacuum-formed maps (i.e. three-dimensional surface models created using the vacuum-formed process), illuminated contours (relief shading with contours), physiographic diagrams and inclined contours (perspectively viewed contours which are planimetrically correct). These are depicted in Figure 4.7.

Since the advent of computer graphics and computer based mapping, the graphical recreation of a real word scene through numerical modelling and visualisation on a computer monitor has been the focus of much research (See Appendix 1 for further discussion). A number of techniques have been developed to perform this and are broadly referred to as *rendering*. These are either predominantly physically or visually based and can provide an orthographic or perspective view. The more complex techniques produce photo-realistic results which are designed to be indistinguishable from real landscapes, as evidenced by computer based special effects used by film makers. The simpler techniques leverage their ability to produce results very quickly and so allow real-time, interactive, visualisation. Aircraft flight simulators clearly fall within this category.

Within map based disciplines, these latter methods are predominant as they allow rapid evaluation of terrain for a variety of purposes. For example Tragheim (1996) illustrates the use of digital photogrammetry within the British Geological Survey. After the acquisition of standard aerial photography, the photos are scanned into a digital photogrammetric workstation and a DEM produced. This can then have the original rectified image draped over it and allow the operator to “fly” through the landscape. Interactive viewing can allow

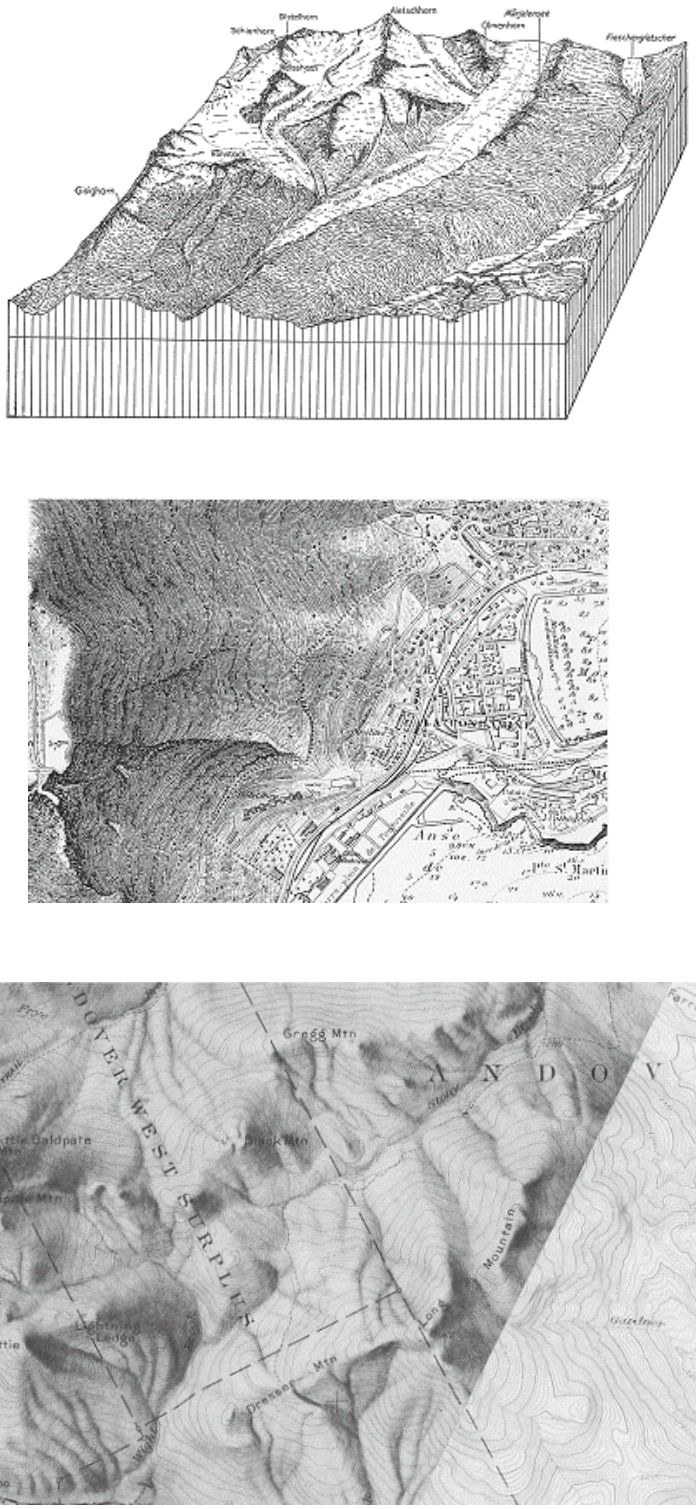

Figure 4.6 Examples of traditional surface representation techniques, including block diagrams (a; top), hachuring (b; middle) and relief shading/contours (c; bottom) (all after Campbell, 1984).

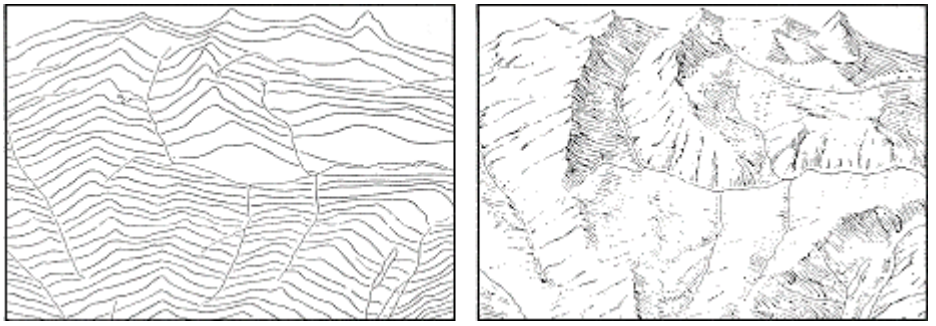

Figure 4.7 Examples of alternative surface representation techniques, illuminated contours (top), physiographic diagrams (middle) and inclined contours (all after Campbell, 1984).

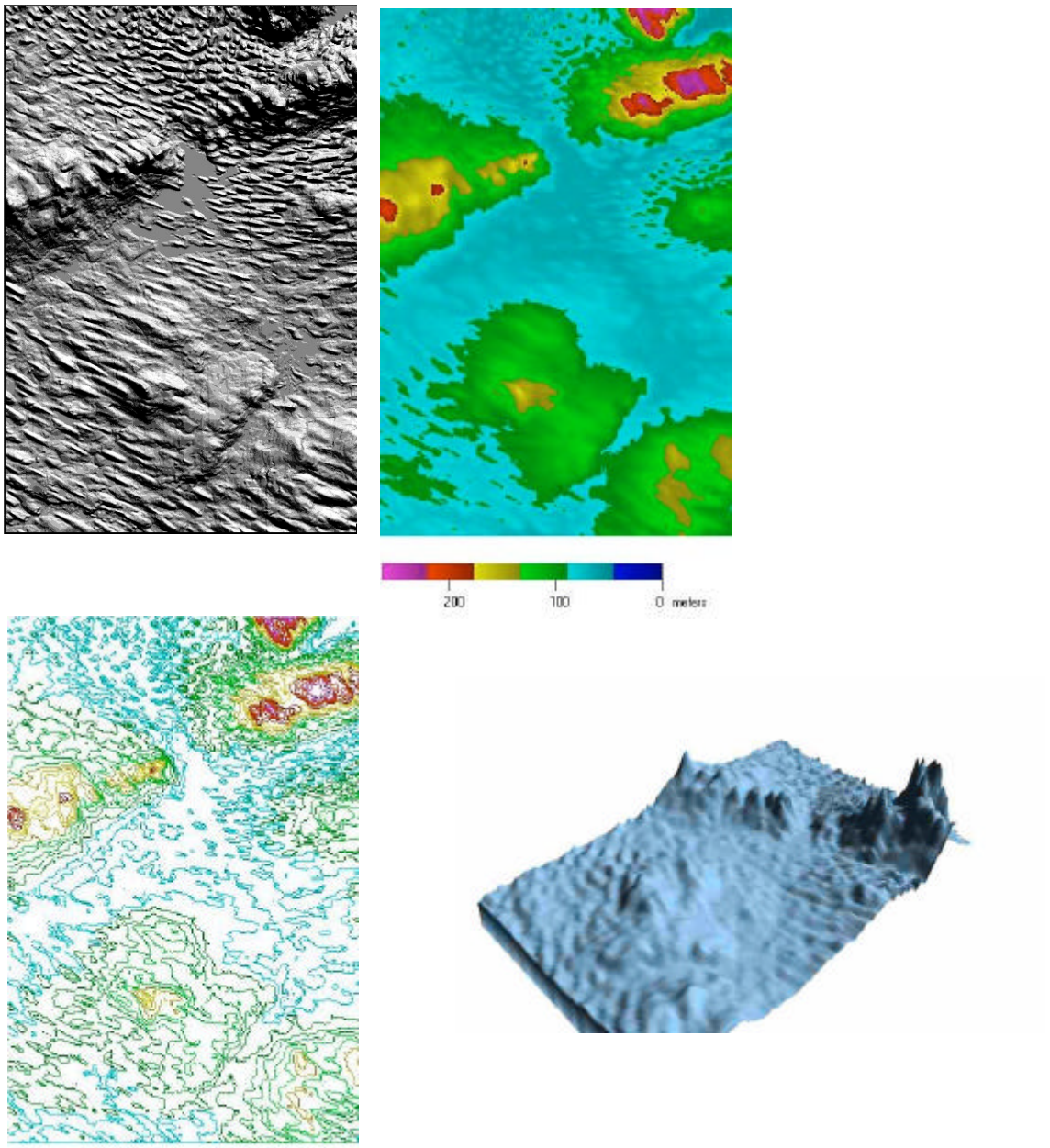

Figure 4.8 Examples of computer based mapping, including relief shading (top left), colour shading of elevation (top right), contouring (bottom left) and perspective viewing (bottom right). The area is 30km long by 20km wide.

the operator to distinguish relationships which may not be readily visible either from the ground or through using traditional aerial photography. Unfortunately it was not possible to digitise using a perspective view so that it was recorded correctly on an orthographic basemap, however there is no reason why this technology cannot be readily developed. Figure 4.8 shows examples of relief shading, colour shading, contouring and perspective viewing in computer based mapping.

4.3.2 Storage Techniques

Three dimensional spatial data have traditionally been stored in two ways; either vector based (commonly Triangulated Irregular Networks or TINs) or raster based (grids). These techniques need to satisfactorily model the following criteria of surfaces:

- continually varying
- space exhausting
- spatially autocorrelated

Early storage techniques needed to be efficient, as well as interoperate with contemporary datasets (typically contour data). TINs are vector polygon based surfaces that apply varying height data across their facets in order to map the surface they represent (Figure 4.9). Each polygon is constructed to accurately represent the surface beneath it and is size variable. This takes advantage of spatial autocorrelation in that “smooth” landscapes can be described by larger polygons and so involve less storage. In addition, due to their construction, each polygon includes slope and aspect attribute data, as well as location.

The raster grid storage technique is commonly called a DEM (for surfaces) or Digital Terrain Model (DTM for terrain). Each cell within the grid is assigned a height value for the location it represents. Given the nature of a grid, if cell dimensions and the co-ordinates of the origin are known, then each cell location can implicitly be calculated.

Although less efficient than TINs (they are essentially a regular sampling technique), DEMs are the storage medium of choice as storage is now relatively inexpensive and much earth science data (e.g. satellite imagery) is collected in this manner. DEM research dates to the late 1960s (Evans, 1972) with most work based upon contour data converted to raster grids. The launch of Landsat 1 by NASA in 1972 brought grid based data to the earth sciences. In addition to the abundance of remotely sensed data (and the processing techniques that have developed in tandem), DEM data is now becoming widely available. In Europe this began with the conversion of existing map data to DEMs. For example, in the UK the Ordnance Survey (OS) created 50m resolution DEMs based upon its 1:50000 map products. More recently they have generated 10m resolution data based upon their 1:10000 products.

The Irish Ordnance Survey (IOS) have generated a country wide DEM using digital photogrammetry, showing the move from traditional survey techniques to digital mapping. However it is the advent of satellite based techniques that are producing the greatest revolution. The UK now has the Landmap DEM (Kitmitto *et al*, 2000) based upon ERS-1 interferometric SAR (inSAR) data of the UK and Ireland. Of more interest is the Shuttle Radar Topography Mission (Rolando *et al*, 1996) or SRTM, which aims to deliver a near global DTM from 56°S to 60°N. This is also based upon inSAR, with data collected by the Space Shuttle. Data products will eventually include 90m resolution global data and 30m resolution data upon request.

This, however, still leaves large unmapped landmasses north of the 60°N latitude. Photogrammetry was previously the only technique for producing DEMs, however researchers have experimented with creating them from satellite imagery. Limited experimentation began with early Landsat imagery, however the advent of SPOT allowed this to become a reality through the use of their side-looking HRV sensor. This is expensive and currently has sporadic coverage. Much more success has been had with ERS SAR data (e.g. Landmap). The recent fully operational status of the ASTER sensor aboard NASA's Terra satellite has altered this now. This uses twin, nadir and aft

looking, visible and near infra-red, sensors to collect data for the creation of DEMs (30m resolution).

The preceding discussion has highlighted the different storage techniques available for three dimensional surface visualisation, showing that the availability of global high quality, inexpensive, DEM data is rapidly approaching. For landform mapping, the move away from the sole use of field mapping, aerial photography or satellite imagery has begun. Many researchers are unfamiliar with the use of DEMs and may not be aware of data accuracy issues and visualisation problems. The following section briefly discusses some of the methods commonly used in surface visualisation (focusing on DEMs) and highlights some of the problems in their use.

4.3.3 Surface representation: Relief shading

Relief shading is perhaps the most popular 3D visualisation technique used within computer mapping software as it is quick to render and readily recognisable by most operators. This method simulates the shadow thrown by an apparent light source shining from one (or more) directions across a three-dimensional landscape. The azimuth of the light source is variable, although it is usually fixed in the north-west as, visually, this provides the most desirable image (Lidmar-Bergström *et al*, 1991).

The similarities between the use of relief shaded and satellite images in visualisation is striking. It is even more so when you consider that both incorporate vertical viewing and a single illuminating light source. As a result DEMs suffer from exactly the same biases as satellite imagery (as described in §4.2.1). More specifically *relative size* is principally dependent upon the resolution of the DEM data. For most high resolution DEMs this is currently between 10m and 50m. *Azimuth biasing* is directly dependent upon the azimuth of the illuminating source, although with a DEM this can be set by the operator. Finally, real world (solar based) effects on *landform signal strength* are very sensitive to changes in illumination elevation. Although such changes can be made to the illumination source within a DEM, this generally has the effect of increasing or reducing the ambient light visible within the rendered image,

rather than producing the more complex atmospheric and surface interactions that take place within a real landscape.

4.4 Generalisation

4.4.1 Introduction

Chapter 2 introduced the main stages performed during an ice sheet reconstruction (Figure 2.1). Once landform data has been satisfactorily mapped, they are then required to be generalised. This is a data reduction stage that reduces the amount of overall data, whilst retaining the essential patterns of lineament orientations required to meaningfully interpret the data. It allows the interpreter to untangle the complexity of individual lineaments by representing them with broad lineament patterns. A good example of this is the Glacial Map of Canada (Prest *et al*, 1968) which is based upon mapping individual glacial landforms but has been very broadly generalised both for cartographic purposes, as well as to make its interpretation much easier.

Generalisation is a qualitative and subjective technique, relying upon the abilities of the observer. Given that the aim is to identify broad patterns, prior to interpretation, it is preferable that this stage should be as objective as possible. This would not only allow more objective generalisation, but also introduce consistency both by a single observer and between observers. In order to appreciate the complexity of the generalisation process, this section introduces its broad application within cartography and then reviews its use within satellite image based ice sheet reconstructions.

4.4.2 Cartographic Approaches

Generalisation involves the simplification or removal of detail. At a methodological level, generalisation is purely a data reduction (or data compression) stage as it involves going from more to less information. As a consequence of data reduction, the procedure also removes noise and random effects from the data set, so aiding interpretation. The original mapped data represent abstracted objects of reality (*simplification*) and the process of generalisation further abstracts these objects. It is the method of *selecting* mapped features for abstraction that is integral to the informational context of

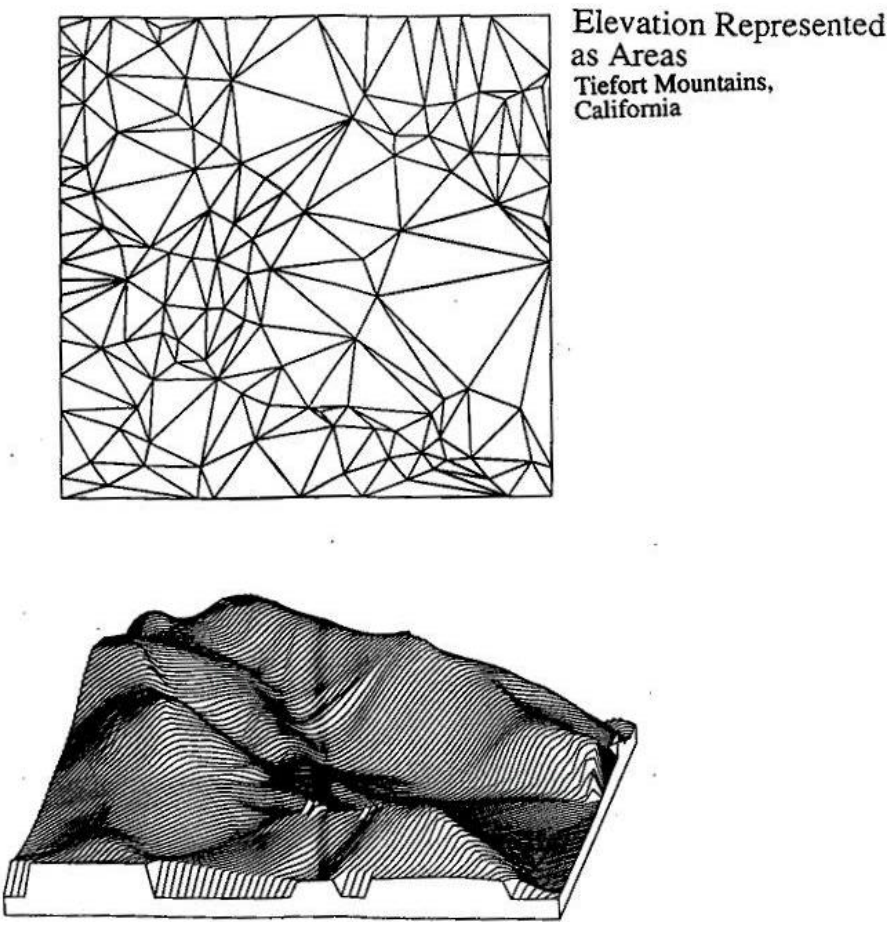

Figure 4.9 Example of a landscape stored as a TIN (top), with a wireframe perspective view of the same landscape (bottom; after Goodchild and Kemp, 1990).

the generalised map, at the desired scale, and the consequent *reduction* in the amount of information, such that the generalised map presented to the end user is clear and concise.

The process of generalisation has traditionally been performed by cartographers and uses their preconceptions, experience and knowledge of heuristics (object symbolisation). These factors, and their overall combination, produce the finished mapped product. Jones (1997) suggests generalisation involves two stages; *semantic* and *geometric* generalisation. *Semantic generalisation* is the selection of objects that are necessary to convey the theme of the map at the appropriate scale. *Geometric generalisation* is concerned with the processes by which those selected objects are informationally reduced, whilst retaining their essential characteristics, for their presentation in a mapped product. During the generalisation of mapped lineaments, it is *geometric generalisation* that is of interest.

The process of generalisation has been particularly difficult to automate due to the complex interplay of visual and attribute phenomena related to, and between, the mapped objects. Overall design heuristics, coupled with the map purpose and consequent relative importance of objects within that map, require the processing of much related information. As Jones (1997) states *"successful generalisation requires a holistic approach in which the interaction between cartographic objects can be monitored... at present this is usually achieved by the human eye."*

As spatial data are increasingly being collected with greater precision, generalisation becomes important both in terms of data reduction and the presentation of data for different purposes. Muller (1991) warns that higher precision could well lead to further errors in observations as there is a greater likelihood of perturbation by high frequency random errors. Generalisation is therefore a necessary step as, although it reduces resolution, it filters out error and emphasises trends within the data. This is precisely the purpose of generalising mapped lineament data for interpretation.

4.4.3 The use of generalisation in ice-sheet reconstructions

In general, researchers apply a manual, visually based, technique in order to group lineaments. By generalising they want to remove unnecessary detail, leaving a simplified representation of their original data set. Figure 4.10 shows summary lineaments mapped from aerial photography by Kleman *et al* (1997). Generalisation is designed to remove the detail apparent in 4.10a and allow the observer to move on to group flow patterns into meaningful flow sets, as shown in Figure 4.10b. Generalisation therefore needs to group "similar" lineaments together, whilst retaining much of the essential information. Phrases such as "coherent lineament pattern", "parallel conformity", "spatially coherent" and "internally homogenous" attempt to describe the visual techniques applied. These imply a dependence upon a similarity in orientation, although covers other factors such as length and density, however their descriptive nature is vague and implies a lack of procedures for generalisation. Scale is integral to the process of generalisation, yet these phrases imply different techniques at different scales. Published research has tended to concentrate on the glacial implications of mapped data or the techniques used to either acquire the satellite imagery or interpret the results, rather than the methods of generalisation. This section briefly reviews the use of generalisation in previous research work, broadly ordered by the same research groups discussed in Chapter 3.

Punkari (1982) almost certainly needed to generalise his data but did not discuss the issue. Punkari (1985, 1993, 1996) later mentions generalisation in relation to mapping presentation, but does not discuss it. In Punkari (1995) he intimates that "trend lines" are produced by using principal lineament orientations from rose diagrams for 50 x 50 km^2 grid squares (Figure 3.3). To help with his grouping into flowsets he also used cross-sectional histograms of different landforms (Figure 3.4). Dongelmans (1996) suggests that lineaments should have *"corresponding trends and spatial continuity*", however his method goes from observation data to fully interpreted flow sets

Boulton and Clark (1990) *"simplified by summarising parallel flow patterns by a few more continuous 'ice flow' lines.*" They combined flow lines to create flow

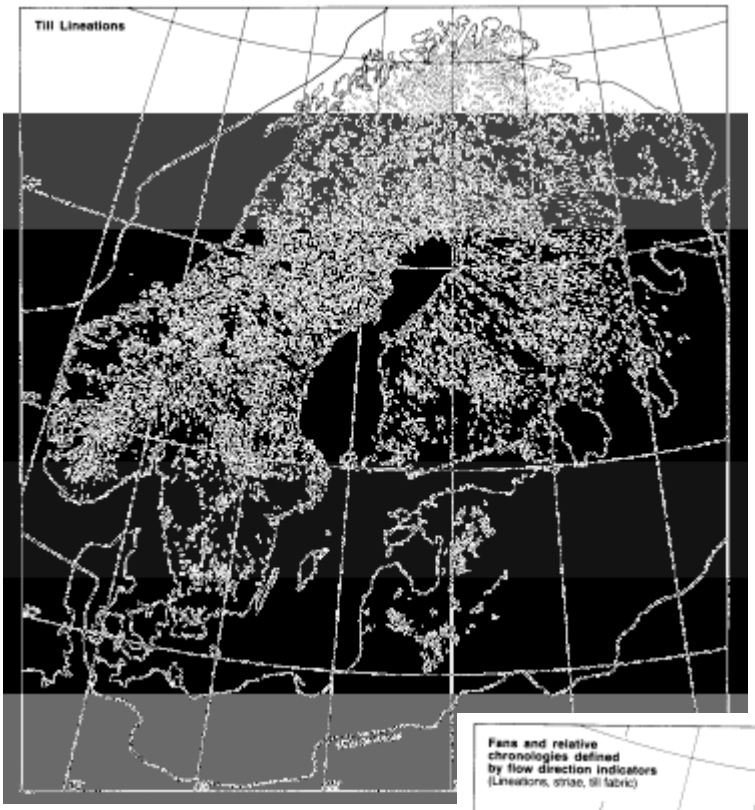

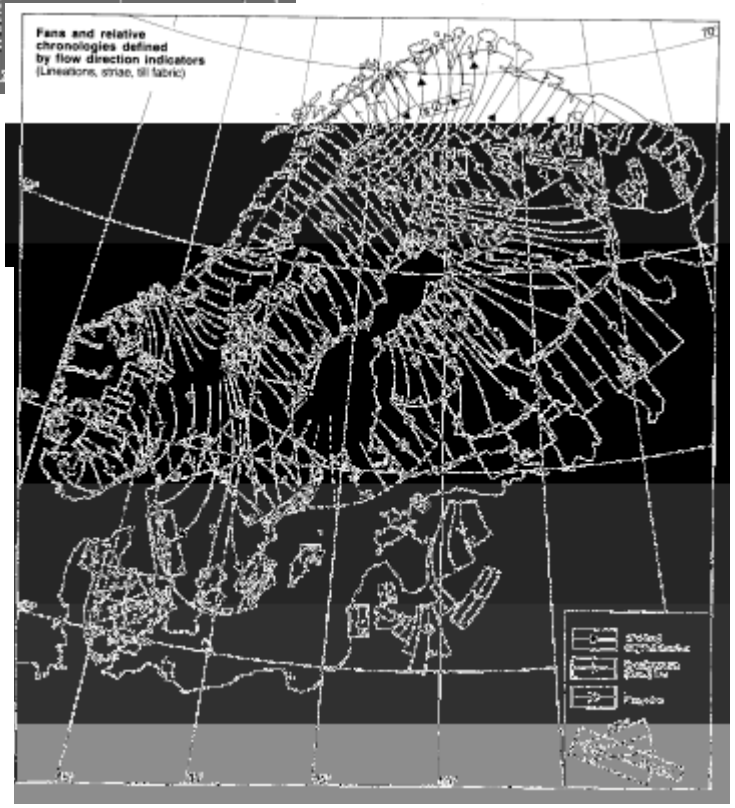

Figure 4.10 Summary lineaments mapped from aerial photography and collated from various sources (top) are generalised and organised into a set of coherent flow sets that can then be interpreted into a rational glacial history.(Kleman *at al,* 1997).

sets. They valued the degree of "lineament alignment" as an important attribute, but only briefly addressed the issue. Knight (1996) states that the formation of flow sets requires an intermediate (generalisation) stage where *ice flow trend lines* are formed (Figure 3.12). Clark (1997) suggests grouping into "*sub-parallel sets whose topology and extent is glaciologically plausible*."

Kleman (1990) advises "*regionalisation based on ... internal homogeneity*" and Kleman *et al* (1996) suggest that any generalisation should require lineaments to be "*spatially coherent*." In applying the *Inversion Model* of Kleman *et al* (1996), Kleman *et al* (1997) define their generalised lineaments as "*temporary tools"* designed to "*simplify and spatially delineate map representations of glacial landform swarms*." They are defined "*on the basis of spatial continuity and the resemblance to a glaciologically plausible pattern, i.e. a minimum-complexity assumption*."

McCabe *et al* (1998) combine the processes of generalisation and interpretation. They go on to suggest that alignment, location, morphological attributes and cross-cutting relationships are important factors in the formation of flow sets. However, combining these procedures is inappropriate as it is not possible to derive unique flow sets from complex and cross-cutting lineament patterns (Clark, 1997) and consequently any results obtained using this method should be viewed as the authors preferred interpretation, rather than an objective evaluation of all the landform evidence.

Clark (1999) stresses that grouping landforms into similar sets requires recognition of three criteria; *parallel conformity*, *proximity* and *morphometry*. As with other workers, similarity of orientation is important. Clark also suggests that close proximity is a useful criteria; this is dependent upon the size of landform and, ultimately, the scale of processes operating at the ice sheet base, although Clark *et al* (2000) state that this will be of the order of up to 2-3 times the dimension of the landform. Density might be a more appropriate criteria. The final criteria, morphometry, is very general and could refer to many individual and shape related measurements, although landforms should display similarity.

All of the above work address generalisation, however the degree and scope of discussion is varied. Figure 4.11 clearly illustrates how one set of mapped lineaments can be alternately interpreted. An objective understanding of the characteristics of the data would make generalising them easier and more objective. The following paragraphs (see Figure 4.12) provide an example from the Storkerson Peninsular, Canada, using a simple set of lineament data (after Stokes, 2001). The lineaments can all be intuitively grouped together primarily using similarity in orientation (or “parallel conformity”). This attribute is universally accepted by all researchers, provided that any grouping based upon it is within a plausible glacial scenario. The lineaments are not all of a similar orientation, but rather show a gradual change from north to south. Lineament length is also considered useful. In this example the eye is drawn to the relatively large number of large lineaments, however upon closer inspection there are also a large number of medium and small sized forms which are equally spaced between the larger forms. This is to be expected and lends to the overall visual impression that this group of lineaments share a common form of origin. Further visual inspection suggests that mean lineament length may decrease from north to south. This is perhaps influenced by the impression of a decrease in lineament density from north to south. These last two points are both glacially plausible and highlight the further point that lineament groupings are dynamic forms and would be expected to change.

Other attributes, such as plan-form/cross-sectional morphometry and cross-cutting are often neglected or only briefly touched upon. Indeed the admission that the same data can provide a variety of glaciologically plausible scenarios suggests that generalisation is subjective, based upon a variety of criteria that vary between researchers and which operate at different scales. At the very least these alternative scenarios should be investigated.

4.4.4 Conclusions

Generalisation is an essential stage of data reduction, performed in order to highlight trends within datasets used for glacial reconstruction. This section has described the general cartographic approaches to generalisation and then gone onto review how researchers have applied *geometric* generalisation techniques

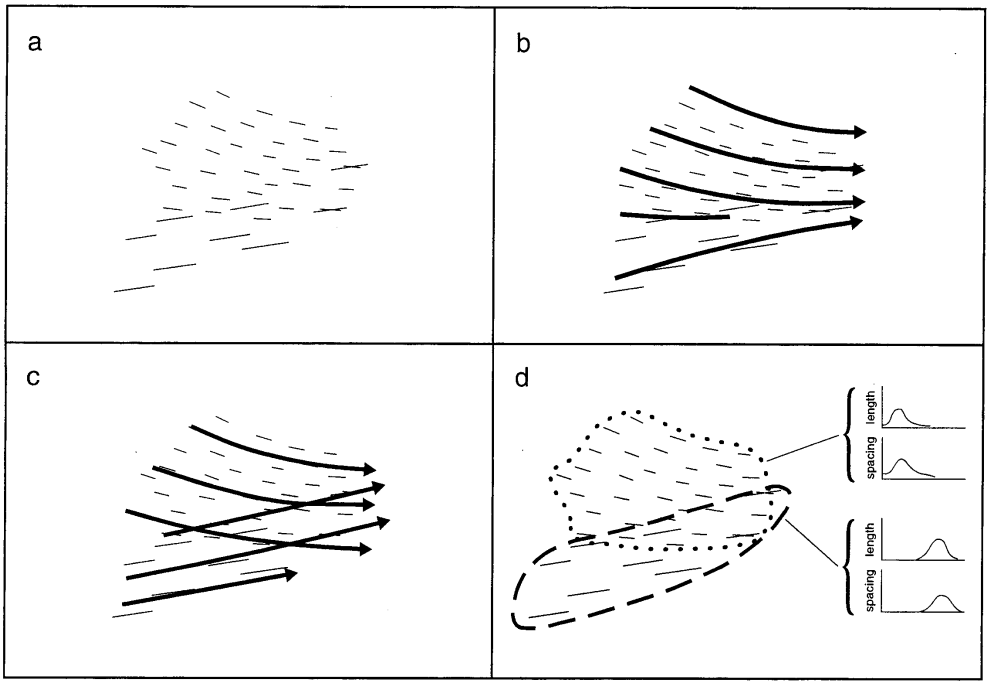

Figure 4.11 (a) shows individual mapped lineaments, whilst (b) and (c) show two alternative interpretations of their formation. (d) illustrates that by grouping lineaments and reviewing their characteristics (e.g. spacing and length), there can be a basis for interpretation (Clark, 1993).

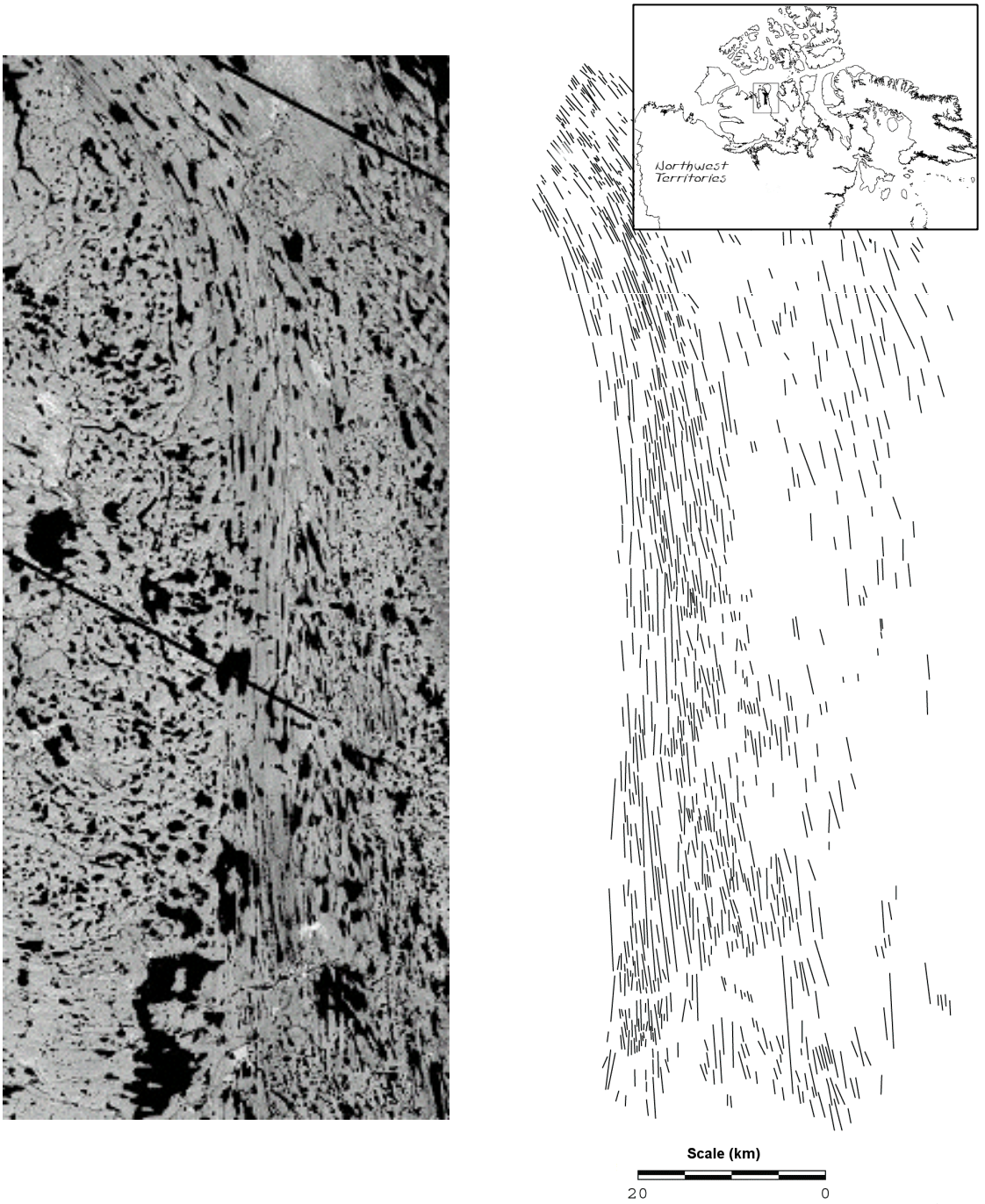

Figure 4.12 Landsat TM satellite imagery of Storkerson Peninsula, Canada (left) and the lineaments mapped from the main ice stream area (right). The area is 112km long by 56km wide (after Stokes, 2001).

prior to the interpretative stages of the reconstruction process. Although there has been the development of grid based statistics to help in the process, these have largely remained unused with reliance being placed upon the visual acuity of the observer.

With the development of new methodological techniques, researchers have become increasingly aware that landform assemblages are a complex mix of landforms created during different periods of time and contextually located at different positions under and around an ice sheet. The land surface simply represents the dynamic intermixing of different processes, in different contexts, at different times. In order to interpret these data, a reduction in their complexity and the development of trends is essential. Not only is generalisation an essential stage, but it needs to be as objective as possible in order to allow reproducibility.

4.5 Conclusions

This chapter has presented the three key research areas within ice sheet reconstruction research that require addressing. Initial exploratory lineament mapping in Ireland suggested that landform representation varied between different types of satellite imagery. This chapter has outlined the basis for variability in landform mapping which include *landform representation* and *operator variability*. Although such variability can never be entirely removed, it should be possible to minimise their effects within a study and, given suitable mapping methods, even between studies. Of more concern is the variability in landform representation between satellite imagery due to relative size, azimuth biasing and landform signal strength. It is important for an interpreter to know if the available imagery is representing all or some lineaments within a study area. If some lineaments are not being represented, are these errors systematic or random? Chapter 5 provides a review of landform representation errors within satellite imagery. In addition to giving measures of the effects of each of the variables discussed in this chapter, it concludes with a summary of the main problems and gives detailed advice on the most appropriate methods and sensors with which to acquire imagery.

DEMs have traditionally been viewed using relief shading, however this suffers from the same azimuth biasing that effects satellite imagery. Although landform signal strength is not a problem (there are artificially high levels of light used in relief shading), relative size still is. It is therefore important to understand the different visualisation options that are available to interpreters and which ones provide the greatest levels of completeness. Chapter 6 reviews these problems and then provides a case study to show a practical use of the methods developed.

During the process of ice sheet reconstruction, once landform data have been mapped, it is necessary to generalise this data before any interpretation can begin. §4.4 showed past approaches to generalisation within the reconstruction literature. It is essential that generalisation is as quantitative as possible, such that it can be verified and reproduced by other researchers. This requires either a fully automated approach or a manual approach which provides quantitative information about mapped data to aid generalisation and goes onto give statistical feedback. Chapter 7 develops these techniques and provides a summary of “best practice” for interpreters.

Chapters 5, 6 and 7 are complementary work and provide a holistic view of ice sheet reconstruction techniques. This is reviewed by investigating satellite imagery and DEM based mapping methods and the techniques used to take this “raw” data to make it ready for interpretation.

5 Mapping glacial lineaments from satellite imagery: an assessment of the problems and development of best procedure

5.1 Introduction

The ability to detect and map landforms on satellite imagery is comprised of two elements:

- the mapping ability and specialist experience of the observer.
- the spectral and physical characteristics of the sensor and their interaction with the imaged surface.

The first element has been shown in limited scenarios to be highly variable *between* different observers. Although this variability can never be entirely removed, it can be mitigated against by well defined and meticulous mapping procedures. It is the former element that this chapter now addresses, providing an assessment of problems through a series of experiments using multiple images of a series of test areas, and a Digital Elevation Model (DEM). A procedure for best practice is then developed. The impetus for this research came from initial glacial landform mapping in Ireland using radar imagery and a review of this work is provided as an example of the problems in landform detectability.

The representation of a landform on an image is controlled by the size of the landform in relation to the resolution of the image (*relative size*), the orientation of the landform with respect to the incident solar illumination azimuth (*azimuth biasing*) and the tonal and textural definition of the landform on an image (*landform signal strength*). These three variables interact, producing a complex "surface" of landform representation. That is, they each effect landform representation in different ways in different parts of the image. This chapter attempts to highlight the propagation of these biases and provide guidelines for

minimising their effects. An earlier version of this work has been published (Smith *et al*, 2001).

5.2 Methodology

In order to assess the impact of the above variables on landform representation, suitable images from a range of earth resources satellites are required. A study area that contained enough lineaments to be statistically viable needed to be selected. The region around Lough Gara, County Roscommon, Ireland (1539km^2), bounded by the Ox Mountains on the west and the town of Sligo to the north, was selected (Figure 5.1). There is complete coverage from four of the five main earth resources sensors; Landsat MSS, Landsat TM, SPOT Panchromatic and ERS-1 Synthetic Aperture Radar (SAR). Unfortunately there were no suitable cloud free scenes for Landsat ETM+ available for this study area, so a second test area on the Kola Peninsula (1183km^2), Russia, has been used to supplement the results.

The above images, and the lineaments mapped from them, are initially visually assessed through descriptive inter-image comparisons (§5.3.1). They are then analysed through the experimentation described in §5.2.3.

Given the differences between the SAR and VIR sensors a case study (§5.4) is used to illustrate the complementary nature of SAR imagery, in addition to the inter-image comparisons. The SAR case study area (2150km^2) lies west of Strangford Lough, County Down, Ireland, bordered on the south by Dundrum Bay (Figure 5.1). A discussion of inter-image comparisons from the Lough Gara region (§5.5) is also presented, providing a case study showing the effects of representation biases in this area.

The chapter concludes with a summary of the results and the main issues resulting from them. Recommendations for the most appropriate satellite imagery to acquire in order to map glacial lineaments, with respect to relative size, azimuth biasing and landform signal strength, are presented. This includes a discussion about calculating the most appropriate dates for image acquisition.

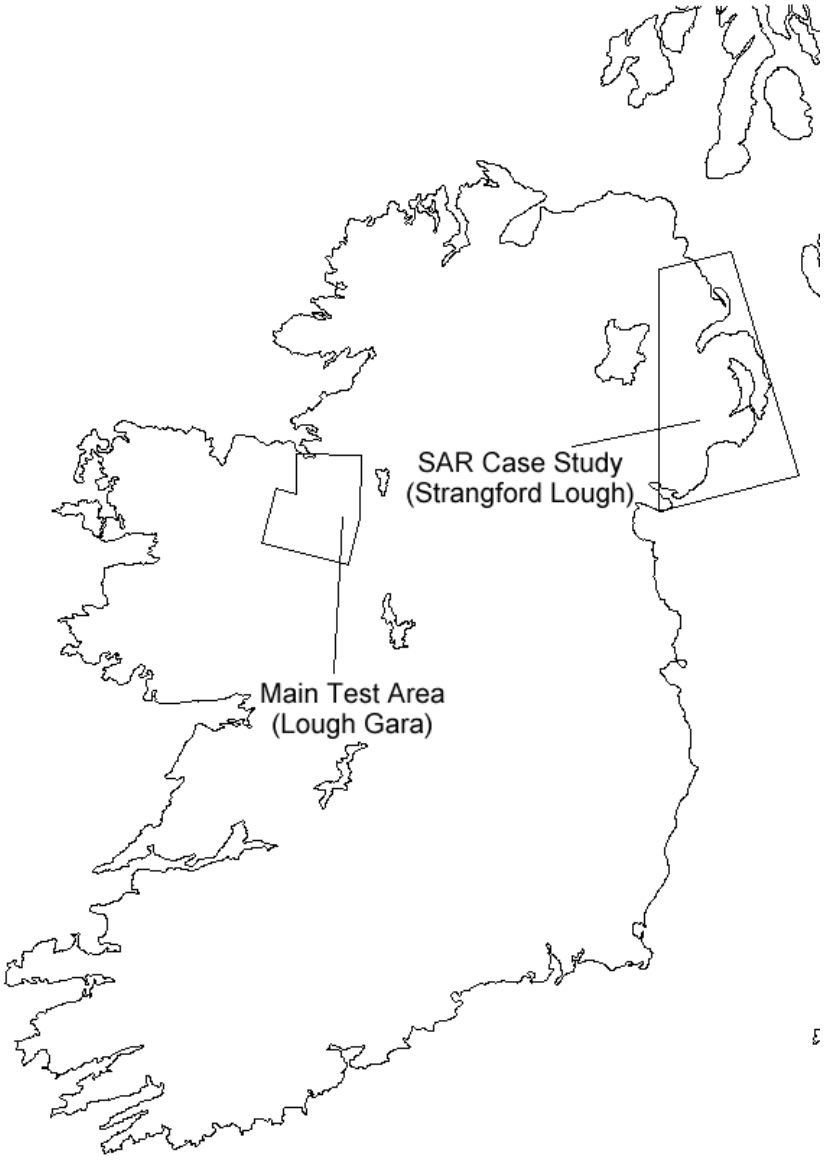

Figure 5.1 Location of the main test area (Lough Gara) and SAR case study area (Strangford Lough) in Ireland.

5.2.1 Accuracy Assessment

Appendix 3 broadly discusses spatial data accuracy with reference to the different elements of accuracy, the general schemes used to assess accuracy and methods to mitigate against error. In order to assess the accuracy with which landforms can be mapped from each type of imagery it is necessary to have good information on the landforms which are known to be present in the test area. However, as it is not possible to completely know which landforms are actually present, accuracy assessment can only be accomplished by comparison with the most accurate measurement available (i.e. "truth").

For this purpose a high resolution DEM (Figure 5.2a) was used to create a morphological map (now simply referred to as *truth*) for a subset of the area (587km^2). Computer aided relief shading is an effective method for visualising a DEM and mapping landforms (see §5.2.2). This suffers from the same azimuth biasing as satellite imagery. Therefore the morphological map was produced through full break-of-slope mapping using multiple illumination azimuths (Figure 5.2). A comparison of truth with a selection of the original stereoscopic aerial photography and topographic mapping confirmed its accuracy.

The DEM was created by the Irish Ordnance Survey from 1:40000 stereoscopic aerial photography at a spatial resolution of 50m, using a digital analytical plotter (O'Reilly, pers. comm 2003). The spatial resolution of the DEM is similar to that of the imagery, but because the landform mapping is based upon stereoscopy rather than photo interpretation, and because the original photographs are at a higher resolution than the satellite imagery, the morphological map produced from the DEM will be at a higher level of accuracy than is possible using satellite imagery.

In addition, relief shading (§5.2.2) assumes an homogenous, specular, surface. The relief shaded scene therefore visualises high reflectance from all surfaces. Although this does not accurately simulate the diversity of real world surface reflectance, it has the effect of highlighting subtle topographic variations.

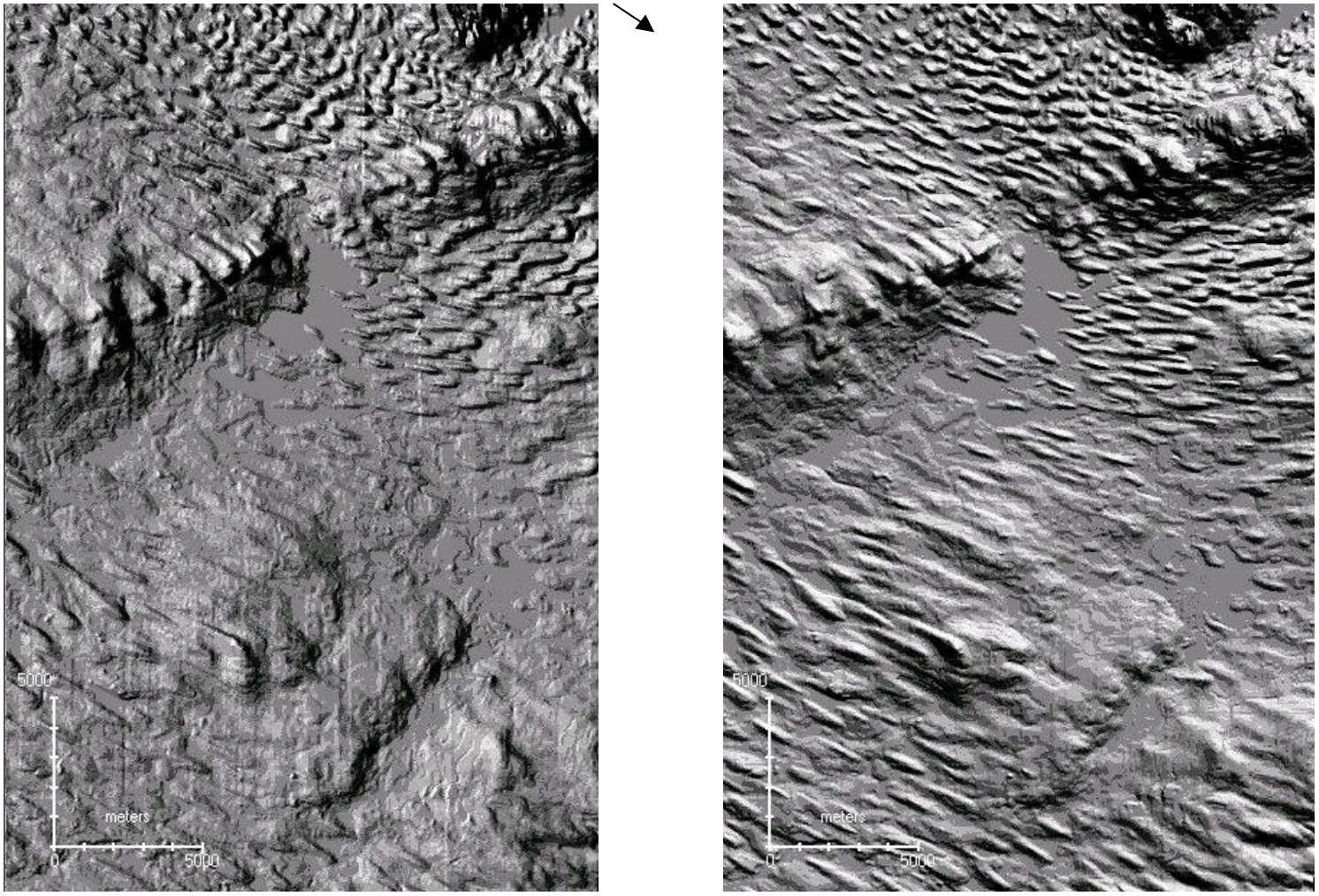

Figure 5.2a and b Hillshaded DEM of Lough Gara, Ireland, using an illumination azimuth parallel (left) and orthogonal (right) to the principal lineament orientation. Note the dramatic changes in lineament morphology, particularly above the centre of the image. Arrows indicate the azimuth angle.

5.2.2 Computer Rendering Techniques

Computer rendering is the graphical recreation of a real word scene through numerical modelling and visualisation on a computer monitor. There are a number of techniques used to perform rendering, either predominantly physically or visually based. Relief shading by fixed azimuth (i.e. solar illumination) is one of several computer rendering techniques that is commonly used within 3D visualisation environments, including GIS (e.g. Figure 5.2). Generally, it is less effective than other methods at producing realistic images (see Appendix 1), however it is fast and efficient, making it suitable for many environmental science applications. Other rendering techniques were explored (e.g. ray shading), however these results were not satisfactory and so were not pursued any further. Appendix 1 provides a brief introduction to the main rendering techniques currently employed.

5.2.3 Orientation Data

Within geology and geomorphology, orientation data are used extensively to refer to attributes of spatial phenomena (e.g. lineaments, faults). These are usually recorded as compass bearings relative to north and can be analysed and visually presented in a number of ways. For example, rose diagrams and Corona plots can be used to display orientation data. However, fundamental to orientation data is that 0°=360° and therefore many standard statistical summaries are not appropriate (e.g. the mean of 1° and 359° cannot be 180°). An appropriate approach to analysing orientation data is to treat them as vectors (Cox, 2001). If the phenomena are recorded simply as an orientation then, each vector can be given unit weight. However other orientation data may well have a magnitude that can be applied as well (e.g. wind speed and direction). This chapter is concerned with lineaments of a certain orientation and so the former case is applicable. It is therefore appropriate to calculate the vector mean as:

$$S = \sum \sin q$$

$$C = \sum \cos q$$

$$\bar{q} = \arctan(S / C)$$

where *?* is the orientation (in degrees) and $\bar{q}$ is the vector mean. The strength ('parallelness') of the resultant vector (mean resultant length) can be calculated as:

$$\bar{R} = \sqrt{S^2 + C^2} / n$$

where *n* is the number of observations. $\bar{R}$ varies between 0 and 1, with 1 representing orientation in the same direction and 0 in multiple directions. The latter can occur from a variety of situations, such as a uniform distribution or evenly distributed clusters. Vector strength can also be used as a surrogate for the standard deviation. Chapters 5, 6 and 7 discuss orientation of lineaments in detail and therefore analysis using vectors is used extensively.

5.2.4 Experiments

1) **Landform Signal Strength** – In order to assess the effect of varying solar elevations on landform representation, imagery would have ideally been obtained from the same sensor over a range of solar elevation angles. The difficulty in obtaining cloud free scenes, and because the azimuth angle also varies with elevation angle meant that this was not practical. Therefore a visual comparison was performed between two images broadly categorised as having low and high solar elevation angles.

It was also hoped to use a DEM to model the effects of landform signal strength by simulating different solar elevations through the use of relief shading, however the results were not satisfactory (see Appendix 1) and, after pursuing alternative rendering techniques (see §5.2.2), this line of inquiry was dropped.

2) **Azimuth Biasing Effect** – In order to assess the biasing effect, an image with a single illumination azimuth but varying lineament orientations was used. A relative comparison was then performed between the image and truth.

A further experiment was also performed using the DEM to investigate azimuth biasing more objectively by simulating different azimuth angles through the use of relief shading. All lineaments were mapped and then compared with truth.

3) **Relative size** – In order to assess the effect of image spatial resolution on landform representation a Landsat ETM+ image was obtained, which is ideally suited to this task, as the high resolution panchromatic band (15m) and lower resolution multispectral bands (30m) are acquired at the same time and hence solar illumination is the same. Band 2 was selected to compare against the Panchromatic band, as a greyscale image was appropriate and they both record an overlapping part of the EM spectrum.

SPOT Panchromatic, Landsat TM Band 5 and Landsat MSS Band 4 were used for all lineament mapping (Table 5.1). The Landsat TM and MSS bands were chosen as the near-IR enhances any moisture variations (Clark, 1997), whilst tonal variations are more efficiently detected by the human eye from a greyscale image (Estes *et al*, 1983). Where appropriate all images had pre-processing techniques applied to them following the guidelines of Clark (1997). All mapping was performed by one observer and observer variability is assumed to be minimal through consistency produced by this.

Satellite Images	**Spatial Resolution (m)**	**Date**	**Lat/Long (°) of Image Centre**	**Illum Elev (°)**	**Illum Az (°)**
Lough Gara					
ERS-1 SAR	25	04/08/92	54:14N 8:53W	23.1	104D
ERS-1 SAR	25	02/03/93	54:19N 8:51W	23.1	104D
Landsat TM	30	10/12/	53:39N 7:43W	11.2	160
Landsat TM	30	06/05/89	54:51N 7:58W	48.3	147
Landsat MSS	80	06/01/83	54:51N 7:45W	10.1	157
SPOT Panchromatic	10	28/11/92	53:39N 8:20W	14.3	167
SPOT Panchromatic	10	28/11/92	54:07N 8:10W	13.9	168
Strangford Lough					
ERS-1 SAR Landsat TM	25 30	30/06/93 03/11/90	54:28N 6:00W 54:31N 4:28W	23.1 18.1	256A 158
Kola Peninsula					
Landsat ETM+	15/30	17/07/99	66:57N 32:24E	43.8	166

Table 5.1 Meta-data for satellite imagery used in this study (D=descending, A=Ascending).

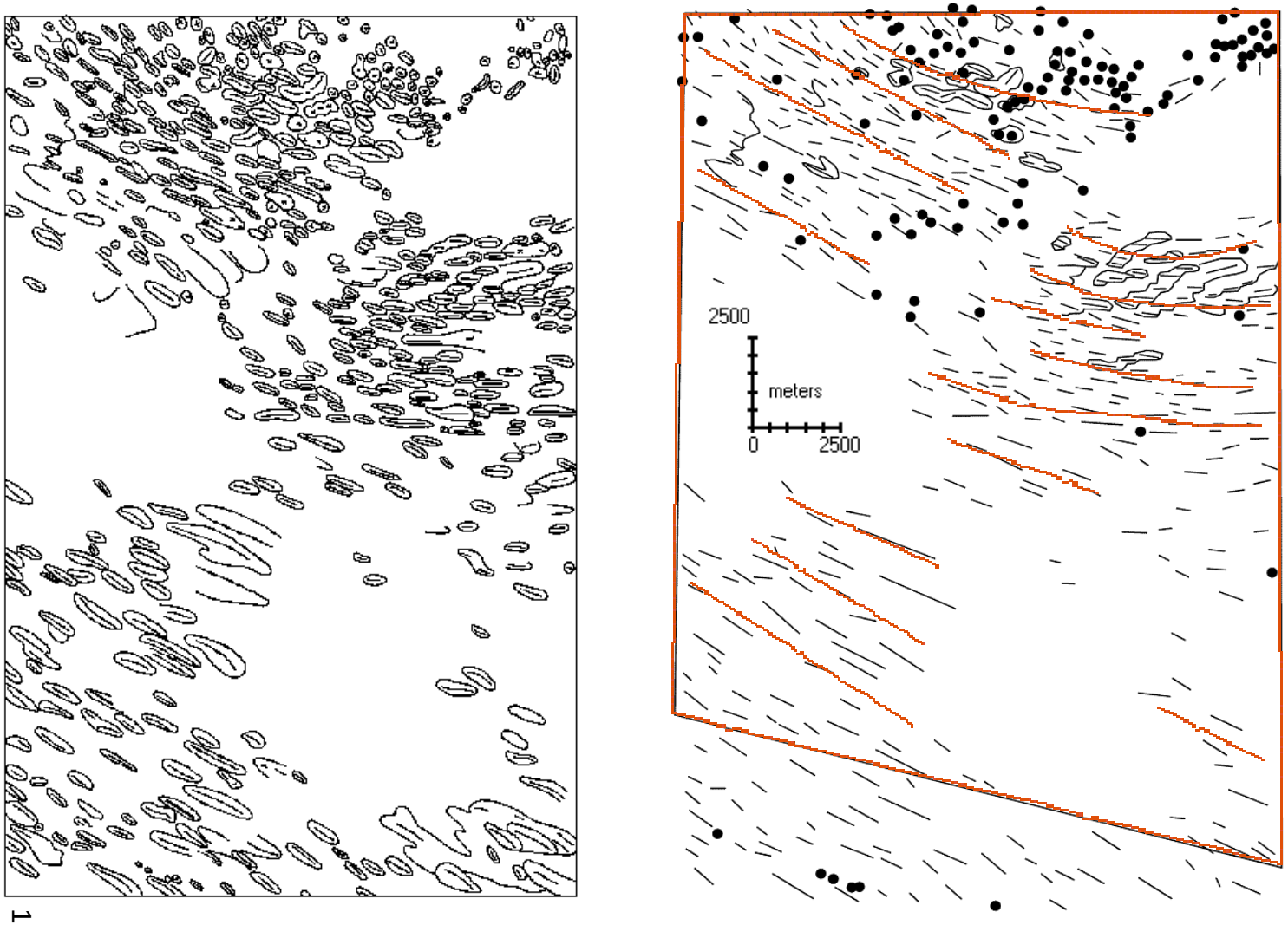

Figure 5.3 (a) Morphological map (truth) created from a high resolution DEM using break-of-slope mapping for Lough Gara, Ireland. (b) Data from (a) were then generalised. Lines represent lineaments, points represent hillocks and polygons represent transverse ridges. The box outline shows the area of overlap with the satellite imagery. The red outlined overlay shows generalised flow patterns.

5.3 Results

These sections present the results of inter-image comparisons and analysis of the controls on detectability. The first section provides a description both of the images and of the landforms mapped from them, whilst the second section presents summary statistics for each experiment. The figures are further illustrated with zoomed sections of the Landsat MSS, Landsat TM, SPOT and SAR images.

5.3.1 Inter-image Comparisons

Truth

Figure 5.3b shows a map of all detectable lineaments produced from truth (Figure 5.3a) for a subset of the Lough Gara study area (this is outlined on all subsequent satellite images). There is a strong trend of lineaments oriented NW-SE, with longer lineaments in the southern area. A spread of lineaments oriented E-W is also noticeable. There is a strong concentration of hummocky terrain in the northerly part of the map, with few hummocky forms elsewhere.

The northern half of the map also contains transverse ridges, often with lineaments overlying them. This map is taken to be the most accurate representation of the landforms present (i.e. “truth”) against which the other images are tested.

Landsat MSS Image

The low contrast and spatial resolution (80m) within the image leads to poor lineament detection (Figure 5.4b and zoomed section in Figure 5.5). Although the southern portion of the image depicts E-W trending lineaments, curving to the NE, this is not clear and is barely detectable in many parts. The presence of hummocky terrain in the central portion is clearer, whilst the northern area depicts clearly detectable lineaments although their trend is not so obvious. The forms in the south, whilst less detectable, appear wider and longer. The overall impression is one of an ability to see lineaments, but not identify and map them precisely.

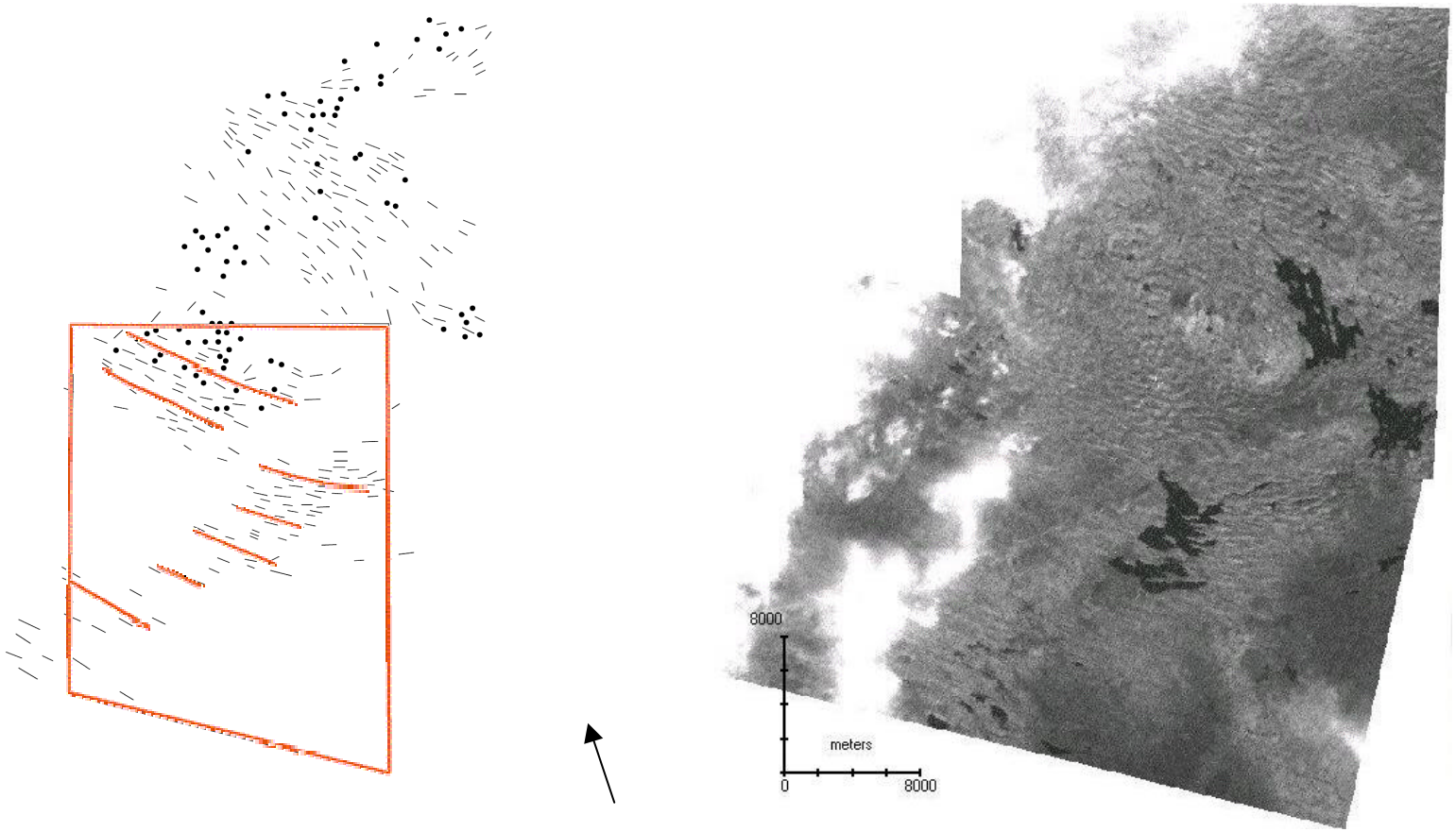

Figure 5.4a and b Landsat MSS glacial lineament map (left) and image (right) for Lough Gara, Ireland. Arrow indicates azimuth angle. The red outlined overlay shows generalised flow patterns.

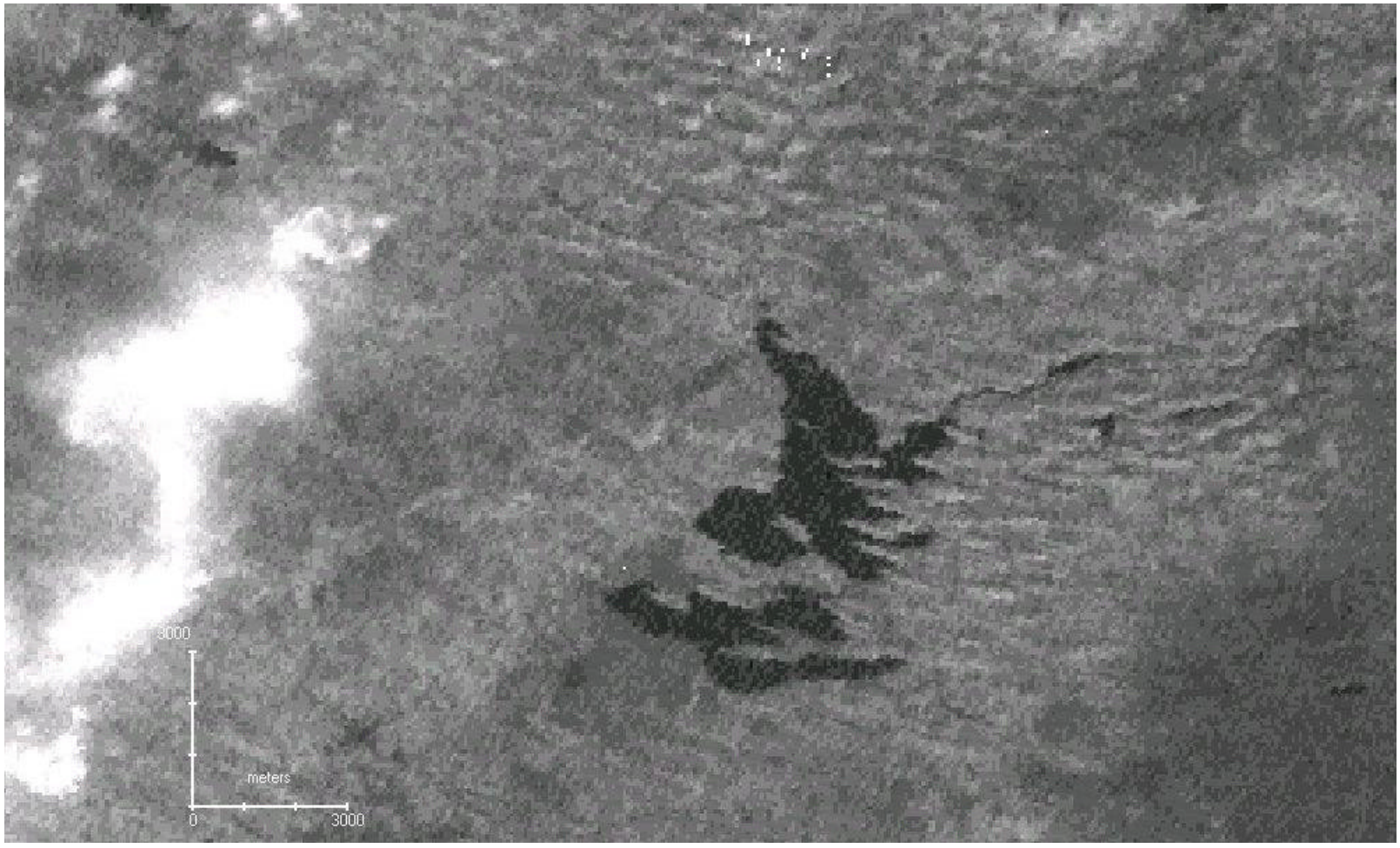

Figure 5.5 Zoomed portion of the Landsat MSS image for Lough Gara.

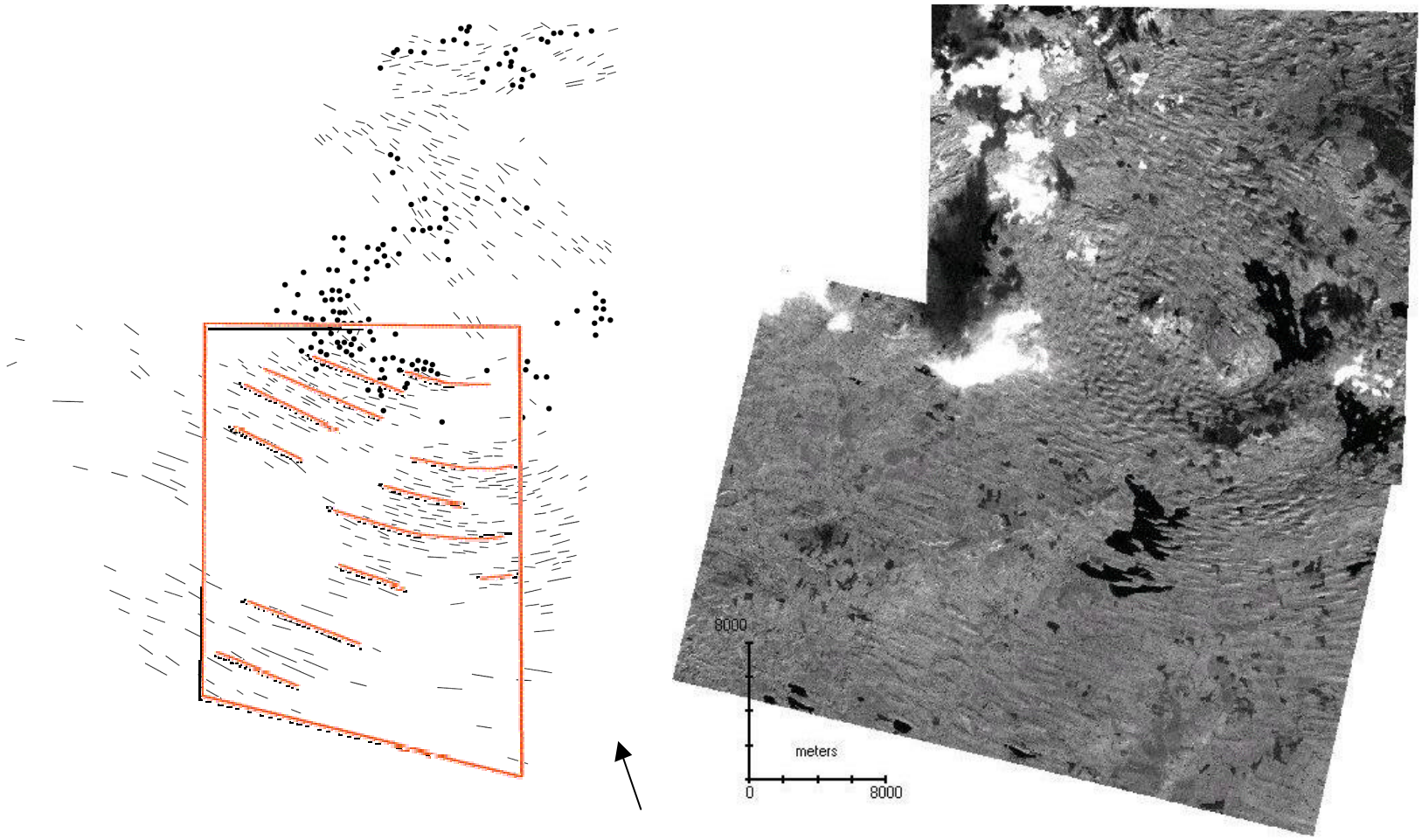

Figure 5.6a and b Landsat TM glacial lineament map (left) and image (right) for Lough Gara, Ireland. Arrow indicates azimuth angle. The red outlined overlay shows generalised flow patterns.

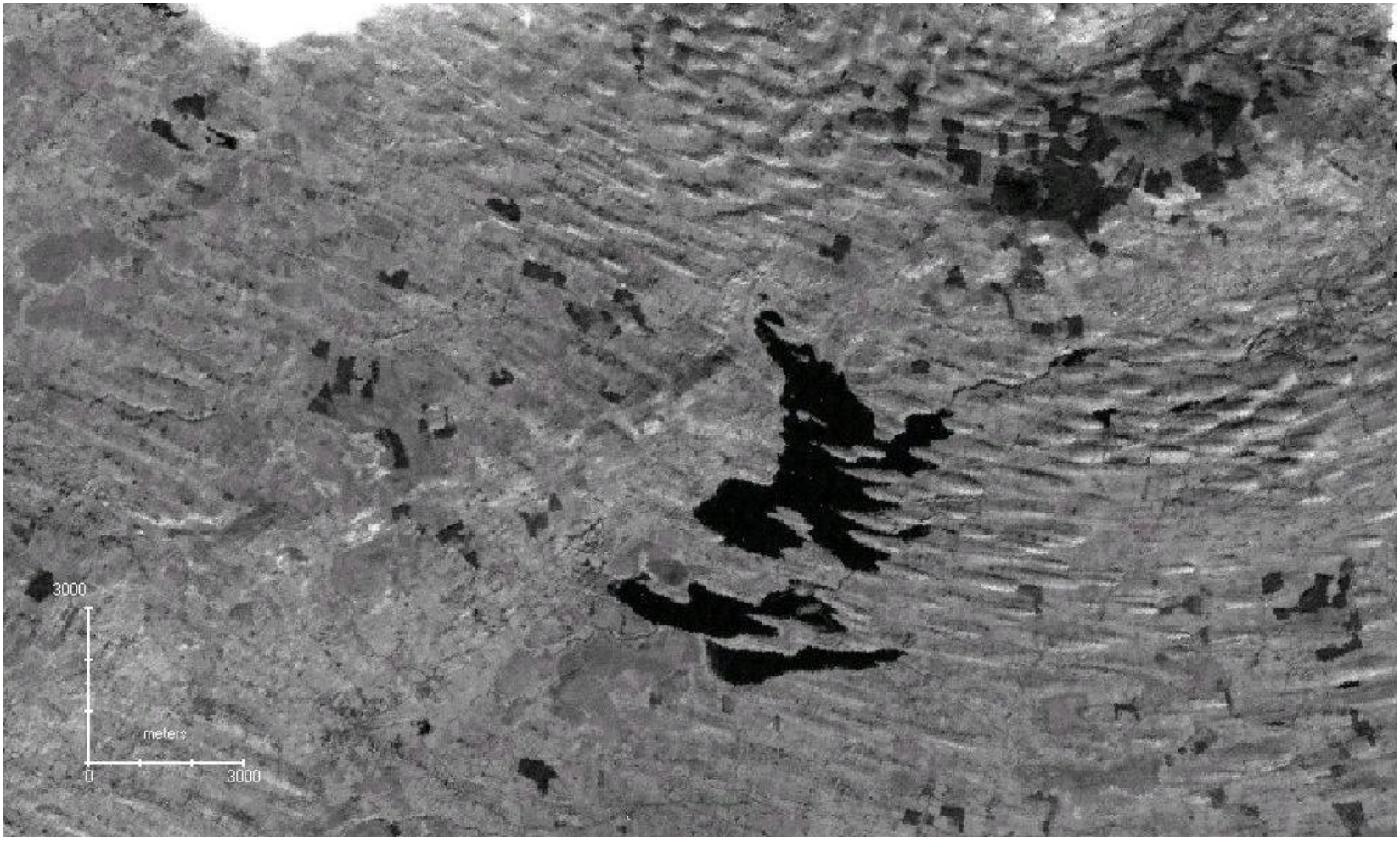

Figure 5.7 Zoomed portion of the Landsat TM image for Lough Gara.

Figure 5.4a shows the lineaments that have been mapped from this image. There is a strong lineament orientation of NW-SE, with some lineaments in the east trending W-E and some in the north trending SW-NE. The central area has a greater abundance of hummocky terrain, with further hummocks in the northern area. In general there are far fewer lineaments mapped in comparison to truth, however the main trends are readily apparent, although no transverse ridges have been identified.

Landsat TM Image

The topographic shadows increase the amount of contrast present, which, in addition to the increase in spatial resolution (30m), in comparison to Landsat MSS, produces a high quality image (Figure 5.6b and zoomed section in Figure 5.7) allowing the straightforward recognition of landforms.

In the southern portion of the image long, broad lineaments are visible in the west (trending east-west), becoming more apparent in the east whilst curving towards the NE. The central region shows hummocky terrain, comprised of many small circular hills. In the northern part of the image there is a clear orientation NW-SE, although in the extreme NE corner lineaments are again trending E-W.

In contrast to the MSS mapped data, Figure 5.6a shows a greater number of lineaments mapped, although still less than for truth. The same general pattern is visible between all three maps. In comparison to the MSS mapped data, the eastern area shows a clear transition in lineament orientation from NW-SE to NE-SW. In addition, the northern area shows some lineaments cross-cutting one another.

SPOT Panchromatic Image

Simple contrast enhancements were necessary in order to make the best use of this high resolution (nominal 10m pixel size) image (Figure 5.8b and zoomed section in Figure 5.9). Initial assessment of the amount of contrast available for lineament mapping suggests a high quality image, although closer inspection reveals that the contrasts are more subdued and, although landforms are

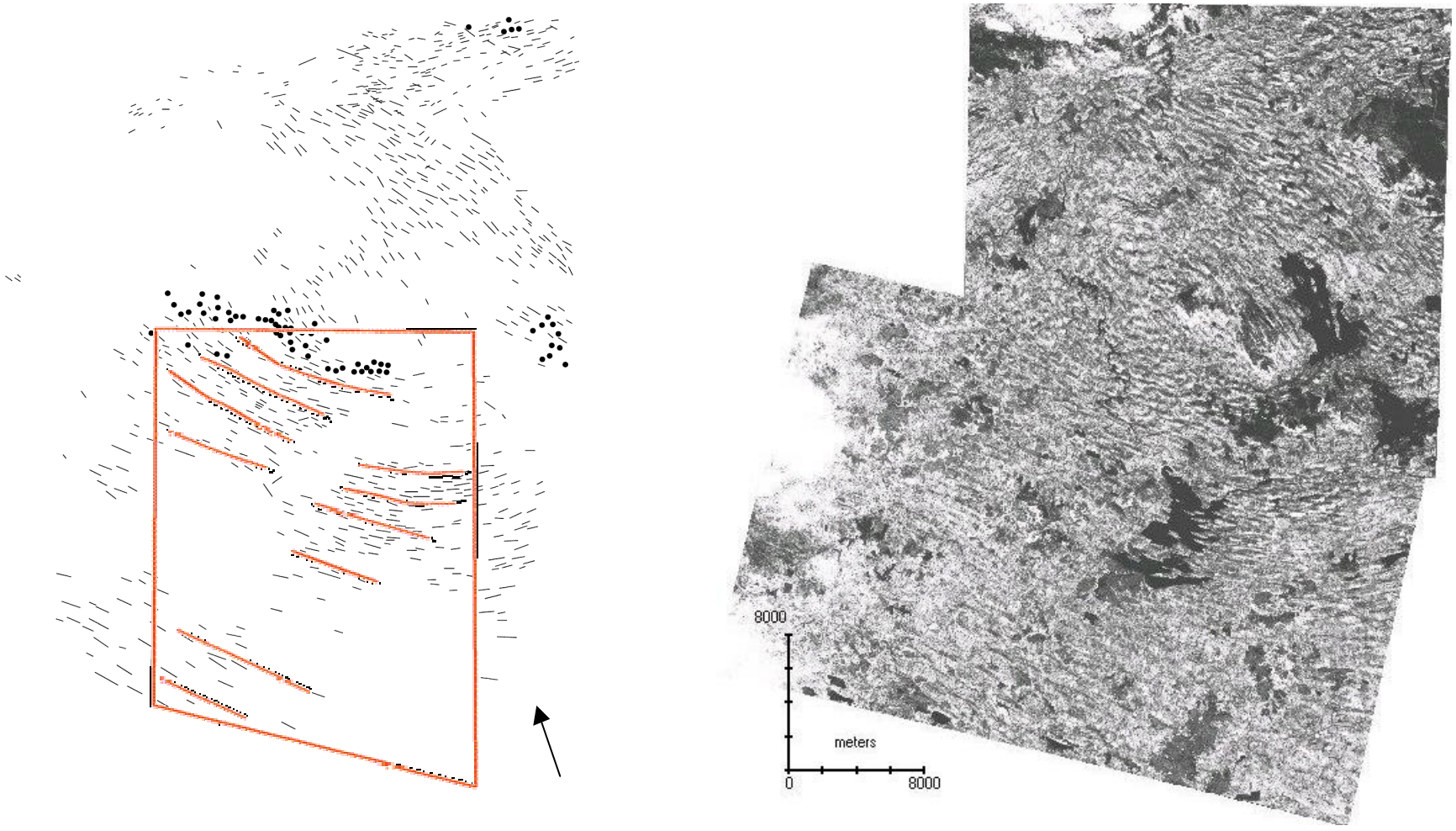

Figure 5.8a and b SPOT glacial lineament map (left) and image (right) for Lough Gara, Ireland. Arrow indicates azimuth angle. The red outlined overlay shows generalised flow patterns.

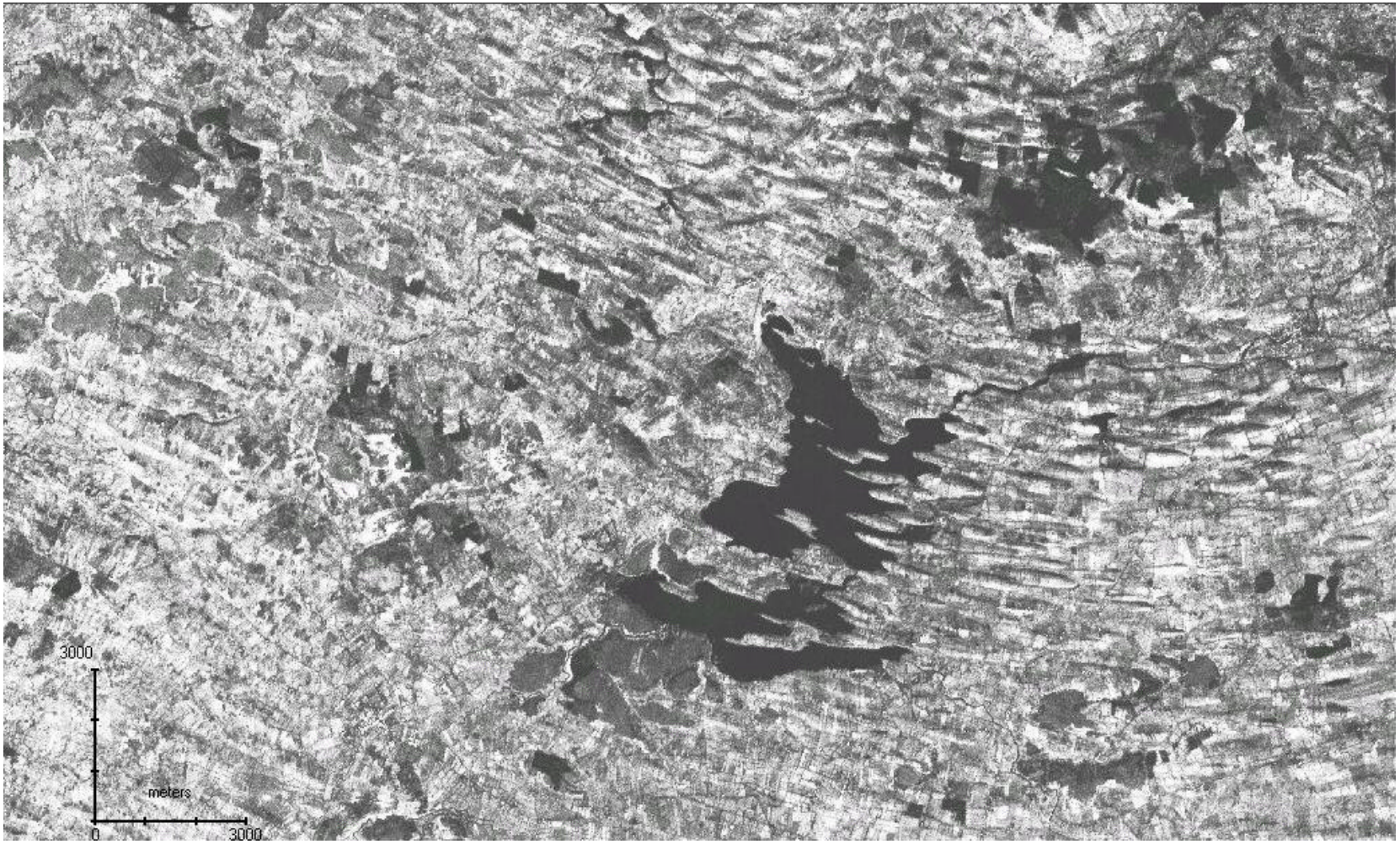

Figure 5.9 Zoomed portion of the SPOT image for Lough Gara.

clearly visible, their representation is not as good as with the TM image. However the high spatial resolution allows detailed landform mapping, clearly showing areas of intersection between E-W and NW-SE trending lineaments in the northern region. The southern region shows longer lineaments in the W trending NW-SE, curving towards NE-SW in the eastern area. The central region appears as a more complicated area of “hummocky” terrain, with elongate and ovoid forms present. Like the truth, TM and MSS mapped data, the SPOT data again shows the same general trends (Figure 5.8a). There are even more lineaments mapped than in any of the previous images (Table 5.2), although less than the truth. There are noticeably fewer hummocks than the Landsat MSS and TM images and a greater incidence of crossing lineaments in the northern portion of the image.

ERS-1 SAR Image

The SAR image (Figure 5.10b) is initially very striking simply because it is visually different from the other VIR imagery (zoomed section in Figure 5.11). Close inspection, and familiarity with working with SAR imagery, shows the presence of NW-SE oriented lineaments in the northern region. In the NE corner there are also lineaments oriented NE-SW. The northern western area also has several lineaments oriented NE-SW. This area grades into hummocky terrain in the central region. In comparison to the VIR imagery, Lough Gara is difficult to locate and, once found, there are very few lineaments visible. Indeed the whole of the southern portion of the image shows very few lineaments.

This inspection is born out by the lineament mapping (Figure 5.10a), generally showing far fewer lineaments mapped than in any other image with almost a complete absence of the central area of curving flow. However the lineaments oriented on the eastern and western sides of the north of the image are better defined and more numerous than on the VIR imagery.

Landsat ETM+ Image

Panchromatic

Simple contrast enhancements were again employed to prepare the image. The high contrast within the image is mainly manifested through spectral

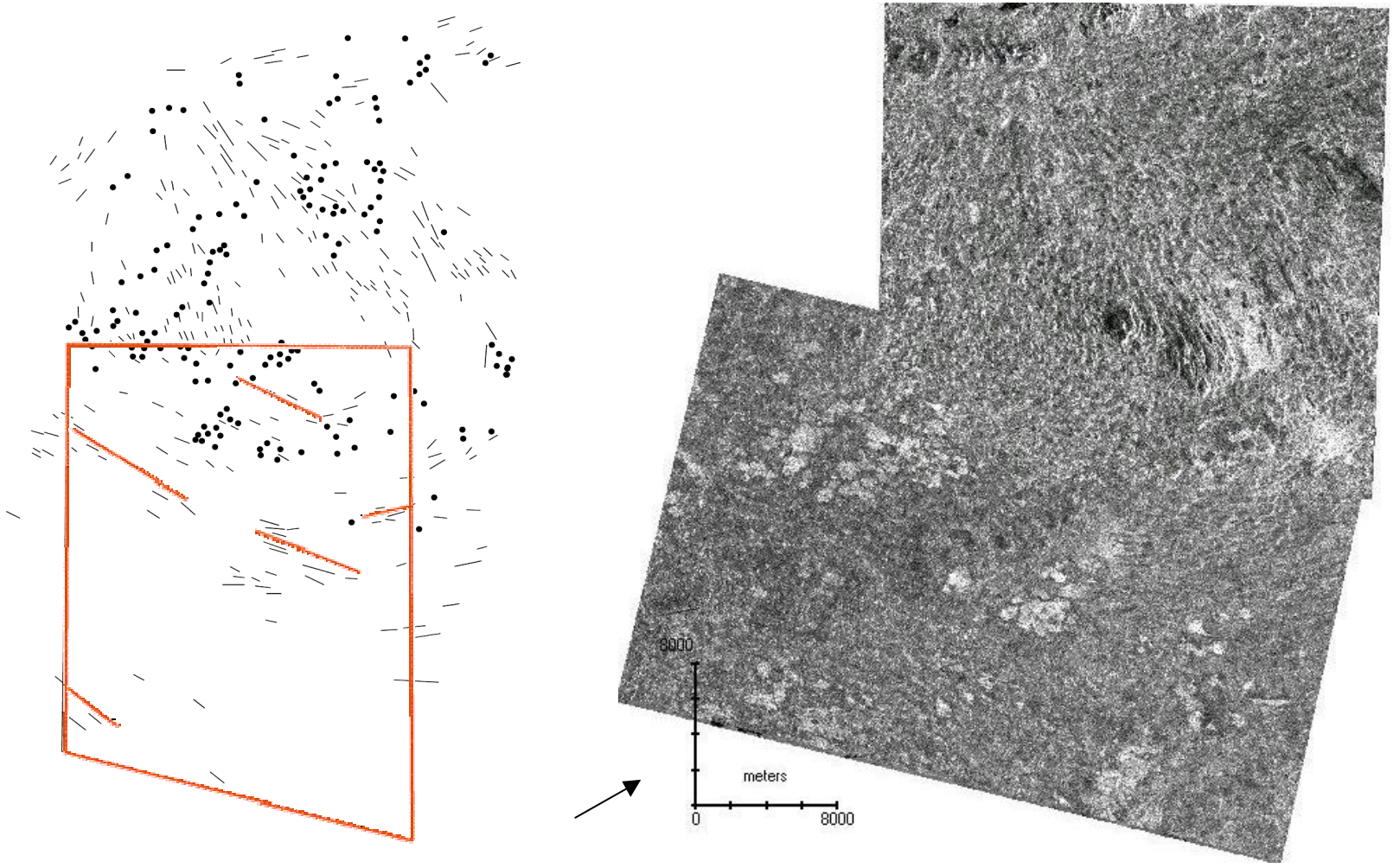

Figure 5.10a and b ERS-1 SAR glacial lineament map (left) and image (right) for Lough Gara, Ireland. Arrow indicates azimuth angle. The red outlined overlay shows generalised flow patterns.

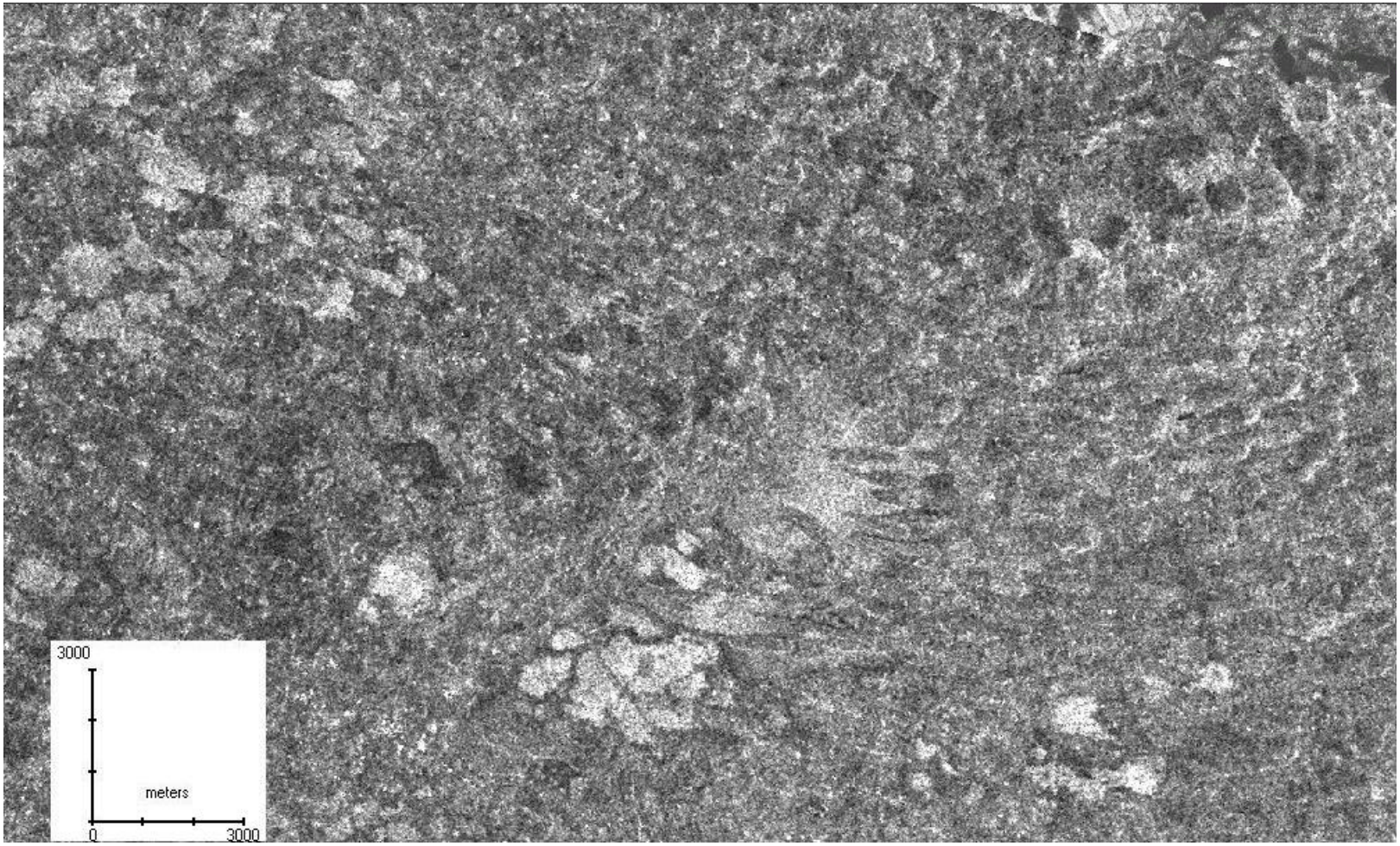

Figure 5.11 Zoomed portion of the ERS-1 SAR image for Lough Gara.

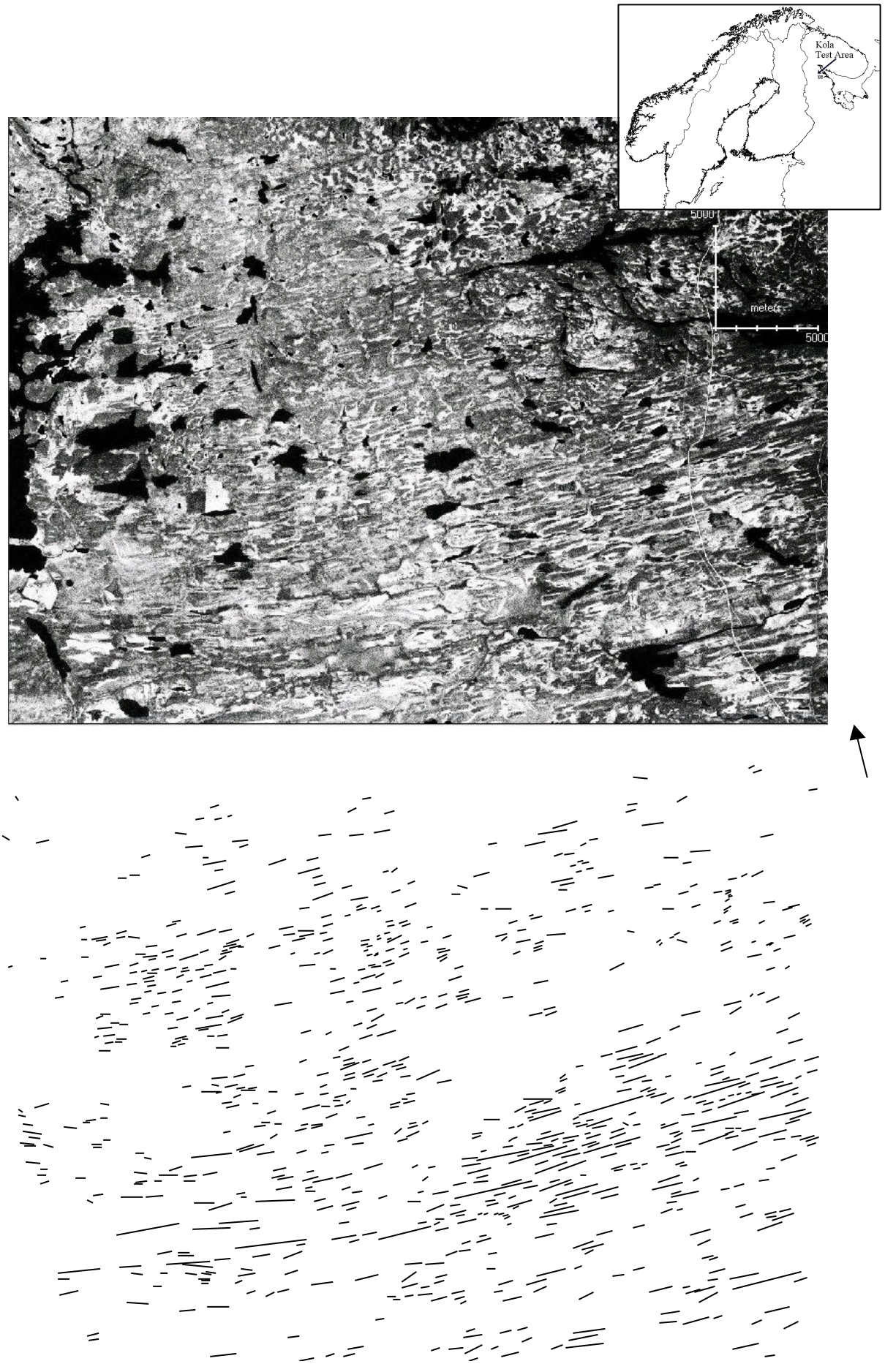

Figure 5.12a and b Landsat ETM+ Panchromatic (15m spatial resolution) image (top), and glacial lineaments mapped from it (bottom), for the Kola Peninsula, Russia. Arrow indicates azimuth angle.

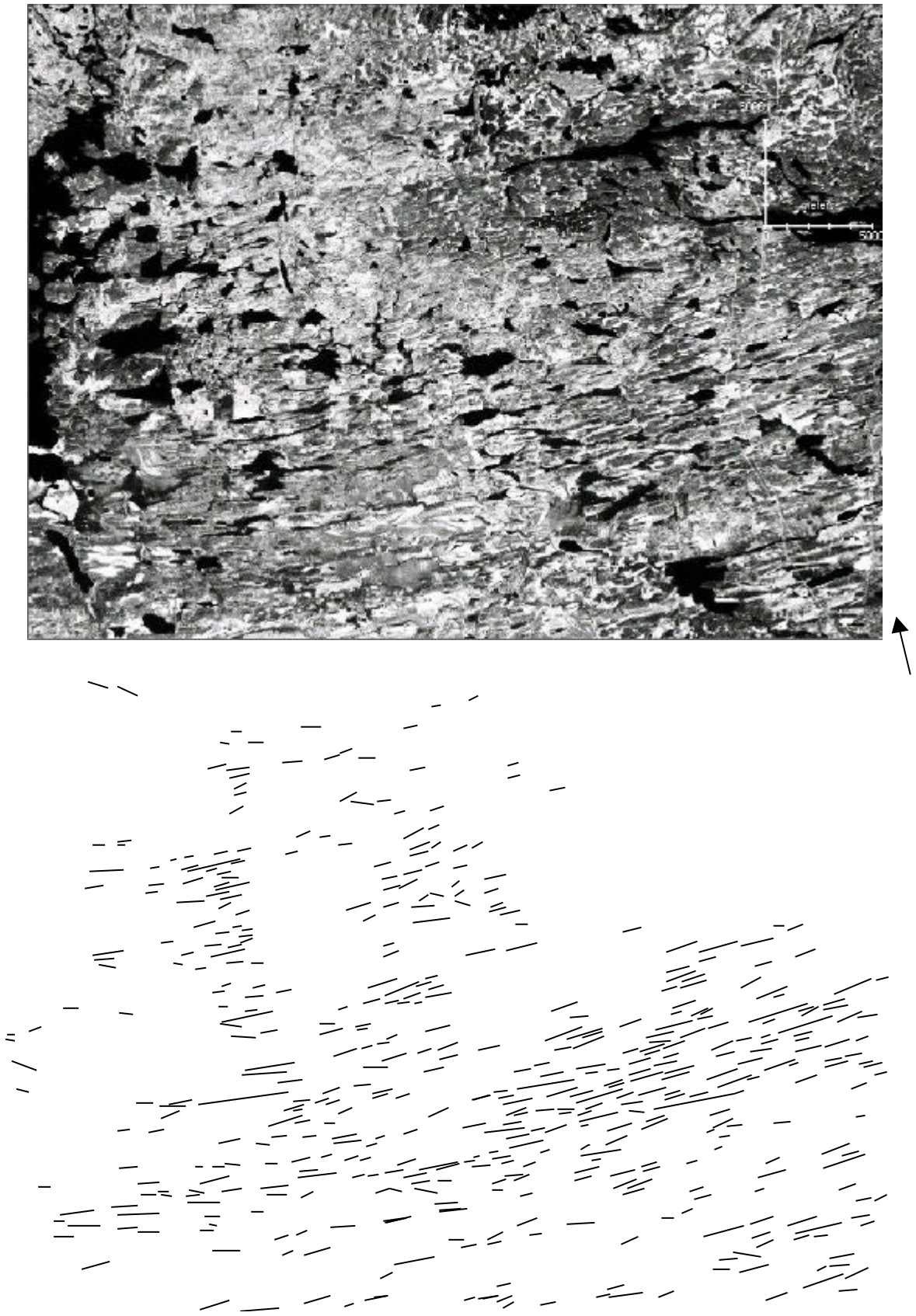

Figure 5.13a and b Landsat ETM+ Multispectral (Band 2; 30m spatial resolution) image (top), and glacial lineaments mapped from it (bottom), for the Kola Peninsula, Russia. Arrow indicates azimuth angle.

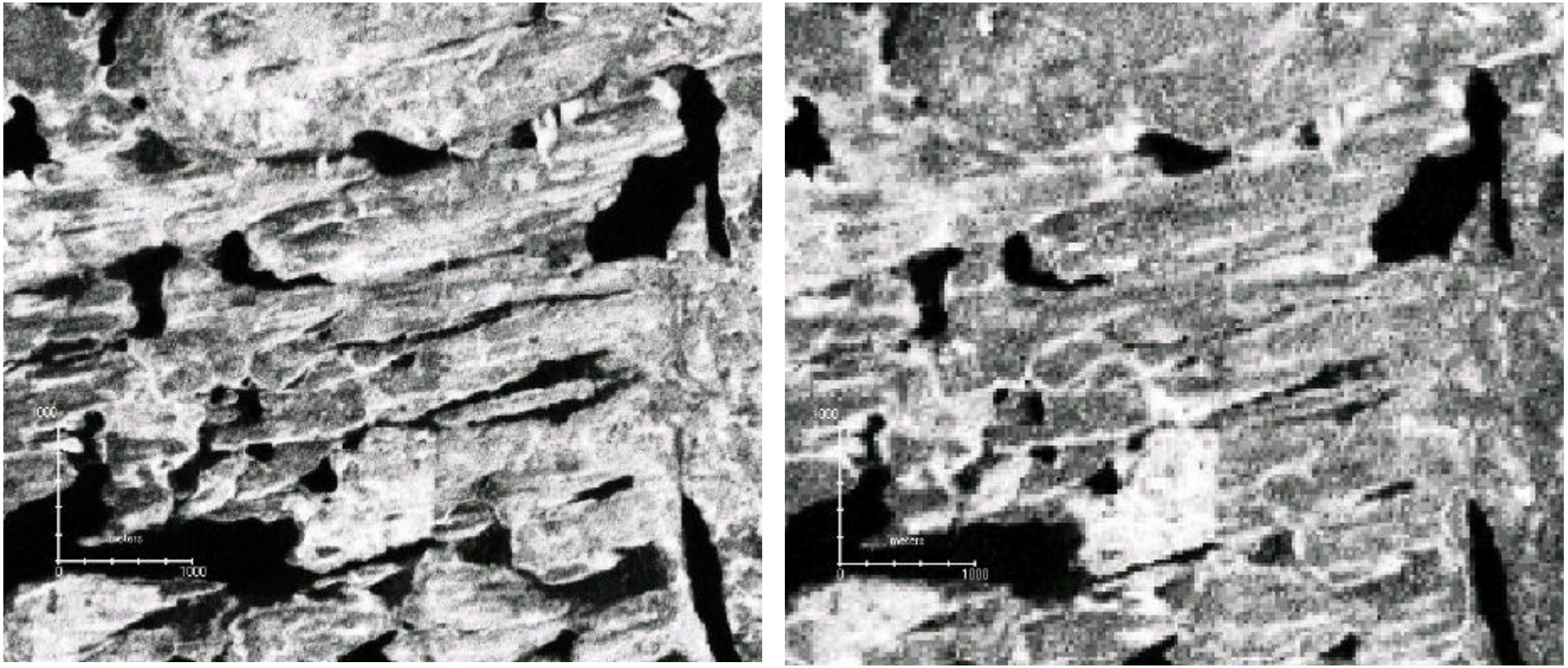

Figure 5.14a and b Zoomed sections of Landsat ETM+ Panchromatic (left) and Multispectral (right) images (Kola Peninsula, Russia) showing the effect of sensor spatial resolution (15m and 30m respectively) on lineament detection

differentiation (Figure 5.12a and zoomed image Figure 5.14a). Non-vegetated regions appear as dark areas and typically mark lineament ridges, which are often offset from elongated lakes. The high spatial resolution of the image (15m) allows clear identification of lineaments as short as 80m in length.

The mapped lineaments (Figure 5.12b) show a strong orientation of SW to NE, ranging up to 4km in length. The larger lineaments are clearly detectable, although they are sometimes composed of several, smaller, lineaments.

Multi-spectral (Band 2)

The multi-spectral image (Figure 5.13a and zoomed image Figure 5.14b) also allows lineament detection through spectral differentiation. The effect of decreased resolution (30m) is clearly apparent through the higher proportion of longer lineaments mapped. For example, where many individual lineaments might have been mapped on the panchromatic image, the multi-spectral image often shows a single, larger, lineament. The mapped lineaments (Figure 5.13b) range from 280m to 4km in length, with a strong SW to NE orientation.

5.3.2 Analysis of Controls on Detectability

In this section the lineament maps are used to infer what the main controls on lineament detectability are.

1) Landform Signal Strength

Low (11.2º) and high (48.3º) solar elevation images were acquired for the test areas (Figure 5.15a/b). These show the dramatic impact solar elevation has on lineament representation. The high solar elevation provides little tonal and textural variation, whilst the lack of surface cover variation means that the lineaments are very difficult to identify. Conversely low solar elevation selectively enhances landforms.

2) Azimuth Biasing Effect

Although it is possible for the azimuth angle to vary from due east to due west, testing its effect on landform detectability is difficult as it is not possible to hold other factors, such as solar elevation, constant. As a result it is not possible to

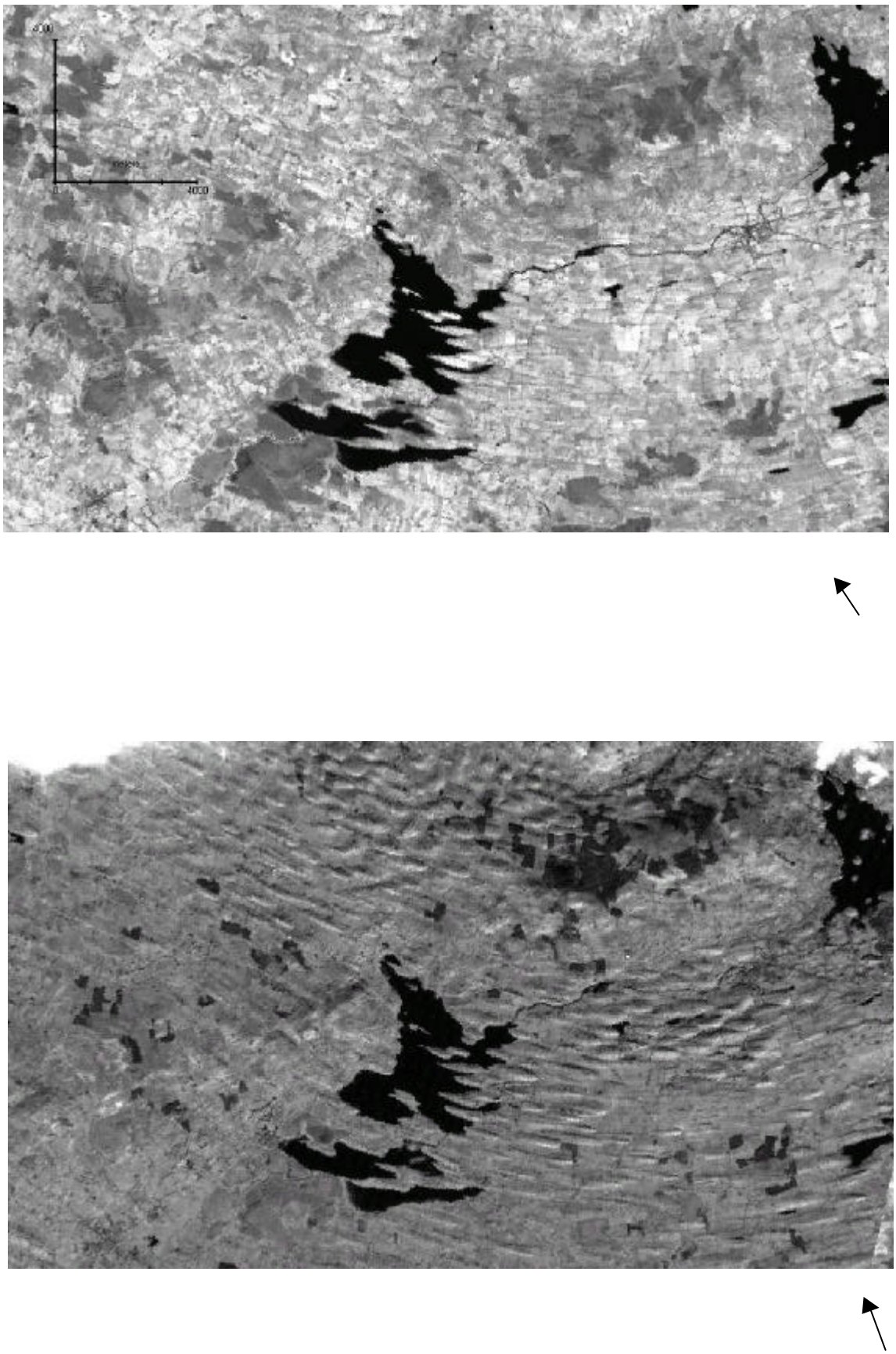

Figure 5.15a and b Landsat TM images of Lough Gara, Ireland, with a high solar elevation angle of 48.3º (top) and a low solar elevation angle of 11.2º (bottom). This illustrates the poor representation of lineaments as a result of the high solar elevation. Arrows indicate azimuth angle.

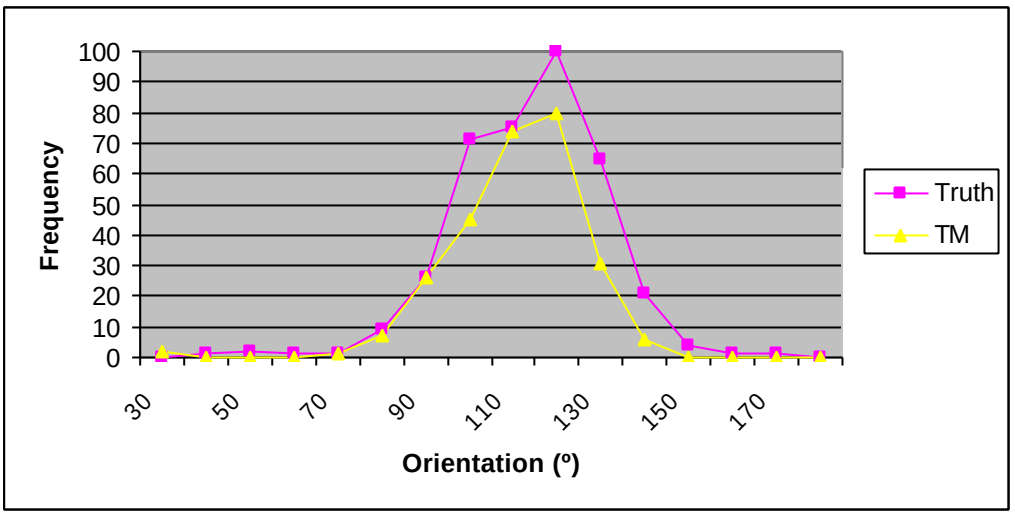

Figure 5.16 Frequency polygon of lineament orientation for Landsat TM and the truth data. Azimuth biasing is not readily apparent due to the restricted zone of lineament orientations.

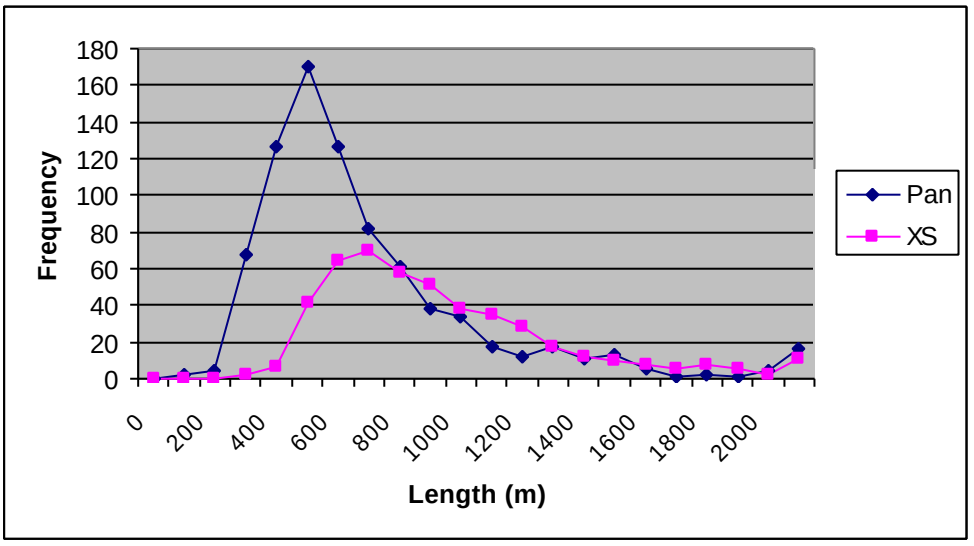

Figure 5.17 Frequency polygon of lineament length for Landsat ETM+ Panchromatic (15m; Pan) and Multispectral (30m; XS) data, Kola Peninsula, Russia. These illustrate the increased number of smaller lineaments that were mapped from the panchromatic image.

test variations in the azimuth angle using different imagery. Consequently, the effect of varying lineament orientations was used to test the azimuth biasing effect. This was achieved through the use of one image (Landsat TM) with a variety of oriented lineaments. This was then compared to truth. The Landsat TM image has an azimuth angle of 159.7º; so lineaments oriented in this direction should be selectively "hidden." Although the Landsat TM has a lower maximum lineament orientation in comparison to the truth (Table 5.2), the frequency polygon shown in Figure 5.16 shows little difference between the two data sets. This is a result of the dominant lineament direction of 110º. The mean lineament orientation for both data sets (Table 5.2) also support this.

Lineament Orientation	***Truth***	***Landsat TM***
Vector Mean *(°)*	109	107
Min *(°)*	40	24
Max *(°)*	161	135
Number	377	271

Table 5.2 Descriptive statistics of lineament orientation for truth and Landsat TM data. The higher maximum for truth data suggests the selective "hiding" of lineaments oriented parallel to the illumination azimuth.

In order to explore this effect more fully, the DEM of the Lough Gara region was relief shaded with illumination orientations parallel, orthogonal and intermediate to the principal lineament direction. Figures 5.2a and b show the DEM relief shaded using an illumination orientation parallel and orthogonal to the principal lineament direction. The difference between the two images is striking, showing not only the complete disappearance of lineaments (not visible in *parallel* that are visible in *orthogonal*), but also a change in the shape of other forms. This includes the appearance in *parallel* of transverse ridges (in the north), which have lineaments superimposed on to them.

The above description is supported by the statistics in Table 5.3. These show a dramatic reduction in the total number of lineaments mapped using a *parallel* illumination, when compared to the *orthogonal* and *intermediate* illuminations. It is also important to note that the *parallel* image identifies transverse ridges within the image and an increased number of hillocks. The transverse ridges

were identified on the aerial photography, although their morphology is subdued due to their reorientation by the overlying lineaments. As a result the *parallel* image selectively enhances these, whilst the *orthogonal* image degrades them. The increase in the number of hillocks is probably due to the misrepresentation of lineaments as hillocks and consequently their misidentification.

Landform	*Orthogonal*	*Parallel*	*Intermediate*	*Truth*
Lineament	371	176	330	442
Hillock	101	120	75	109
Transverse Ridge	0	20	0	25

Table 5.3 Total number of lineaments, hillocks and ridges mapped from the DEM for alternately relief shaded azimuth angles, illustrating the selective "hiding" of lineaments and enhancement of transverse ridges for those mapped from the *parallel* image.

3) Relative Size

Intuitively it would be expected that, as resolution increases, smaller lineaments become detectable and so more lineaments are mapped. As a result the modal lineament length (histogram peak) will gradually decrease.

Using the Landsat ETM+ Panchromatic (15m) image of the Kola Peninsula, 813 lineaments were mapped, compared to 473 lineaments for the multi-spectral (30m) image. This significant increase (170%) in lineaments can be attributed solely to the resolution of the sensor, as all other variables are constant (e.g. solar elevation, azimuth angle). Table 5.4 presents descriptive statistics for these data. This shows that in addition to more lineaments being mapped, the panchromatic image represents not only shorter lineaments, but a greater number of them. This has the overall effect of reducing the mean (from 892m to 647m) and consequently shifting the histogram peak towards the origin (Figure 5.17). In addition the total length of all lineaments on the panchromatic image have increased by 125%. This supports the above evidence, showing that there are an increased number of shorter lineaments.

Lineament Length	*Panchromatic*	*Multispectral*
Mean *(m)*	647	892
Min *(m)*	81	282
Max *(m)*	3951	4040
Total Lineament Length (km)	526	422
Number	811	472

Table 5.4 Descriptive statistics of lineament length for the Landsat ETM+ high resolution (Panchromatic: 15m) and low resolution (Multispectral: 30m) data. These highlight the greater number of smaller lineaments mapped on the panchromatic image, arising from its better spatial resolution.

5.4 Use of SAR Data

5.4.1 Introduction

This section introduces and presents details concerning the use of SAR data for landform mapping. The first section introduces some of the characteristics of radar data pertinent to mapping landforms, whilst the second section presents a case study for the area around Strangford Lough (NE Ireland), comparing and contrasting an ERS-1 SAR image with a Landsat TM image. The third section goes on to make the reader familiar with a significant amount of landform mapping that was performed over a large part of Ireland at the beginning of this research. This was begun in order to produce a glacial reconstruction of the region, however serious deficiencies were noted in the landforms visible on the imagery and the mapping was later abandoned. The final section concludes with some general comments on the use of radar imagery for landform mapping.

5.4.2 Characteristics of Radar Data

In order to understand the benefits and difficulties in using radar data, I will briefly introduce some of the main concepts involved in radar remote sensing. This research had access to an archive of satellite based ERS-1 radar data and so the discussion is based around this sensor, although the concepts can equally be applied to other radar systems. The backscatter recorded on a radar image is predominantly controlled by the following:

- wavelength
- polarization
- look angle
- signal-to-noise ratio
- dielectric coefficients

Radar (or **ra**dio **d**etection **a**nd **r**anging) is located in the microwave part of the electromagnetic spectrum. This operates over wavelengths from approximately 1mm to 1m (compared to visible light which operates between 0.4 and 0.7µm) and, because of this, has the ability to continuously record data regardless of cloud cover or night-time conditions. Although it is possible to record microwaves *emitted* by the Earth (passive sensing), emission levels are typically low and therefore active sensors (radar) are the most common. The active microwave instrumentation (AMI) aboard the ERS-1 satellite operates in the 3.75-7.5cm part of the EM spectrum (called the C band). Although this sensor can “see through” cloud cover, the wavelength can be attenuated (weakening of the signal due to absorption and scattering), particularly during heavy rain events. In these situations the rain (or shadow) may well be recorded on the image.

Polarization refers to the way the electric radar signal is filtered in relation to the direction of wave propagation. The signal can be either vertical (V) or horizontal (H) when it is either transmitted or received. This gives rise to differences in the way objects appear on imagery as they interact with V or H polarized signals differently. ERS-1 SAR imagery is VV polarization (transmitted and received with vertical polarization).

The look angle is the angle from the point directly beneath the sensor to the point of interest. As noted in §4.2, this “side looking” capability specifically highlights topography and so makes SAR particularly effective at imaging lineaments.

The signal-to-noise ratio refers to the amount of actual genuine backscatter that is recorded on an image, in comparison to areas where no return signal is received.

The intensity of radar return signals is strongly affected by the electrical characteristics of the surface being imaged. The *dielectric coefficient* is a measure of an object's reflectivity and conductivity and, for natural materials, typically varies between 3 and 8. Of importance for natural environments is that the presence of moisture significantly increases the reflectivity of a surface. Therefore the weather conditions at the time of image acquisition *and* prior to it will influence the moisture content of natural surfaces (e.g. vegetation) and so the reflectivity of objects.

Chapter 4 introduced the main controls of landform detectability. These included relative size, azimuth biasing and landform signal strength. These will now be discussed in relation to radar. Relative size is predominantly concerned with the resolution of the sensor. For ERS-1 this is nominally 25mx25m and is close to the resolution of Landsat TM data. Azimuth biasing occurs in a similar way to VIR imagery, except that illumination for the image is provided by the sensor itself so that the illumination angle is perpendicular to the flight of the spacecraft. Finally, the landform signal strength is predominantly controlled by the look angle of the sensor. This is fixed (for ERS-1), so any variability in surface reflectivity will be controlled by the surface being imaged.

In summary, the type of image recorded is controlled by the wavelength, polarization and look angle of the sensor employed. The dielectric coefficient of the surface being imaged is important and, for natural environments, will be particularly sensitive to changes in moisture content. The signal-to-noise ratio can inform us of quality of an image that is recorded.

The AMI aboard ERS-1 is designed slightly differently to other satellite based radar systems. It operates at a slightly shorter wavelength, has a relatively steep look angle and employs VV polarization. The shorter wavelength means that surface vegetation will reflect radar signals and that heavy rain events may

produce interference, whilst the steeper look angle produces less geometric distortion as a result of the side-looking sensor. Finally, the choice of polarization was taken in order to enhance oceanic reflectivity, rather than HH or HV systems which are typically employed for enhancing land based radar return signals.

5.4.3 SAR Case Study

To illustrate the complementary nature of SAR and VIR imagery, a case study using a Landsat TM and ERS-1 SAR image was performed. In order to accomplish a similar experiment to those performed for the VIR imagery it would be necessary to control 2 of the 3 variables affecting landform detectability (i.e. relative size, azimuth biasing and landform signal strength). As Landsat TM and ERS-1 SAR have very similar spatial resolutions (30m and 25m respectively), the effect of relative size (relationship between spatial resolution and lineament length) can be controlled. However it is not possible to control for the differences in landform signal strength or azimuth biasing. As a result I cannot perform the same experimentation that was used earlier in this chapter. Rather this case study is designed to highlight the benefits in using SAR imagery to detect landforms, as well as the differences with VIR imagery.

The case study was located in the Strangford Lough region of north-eastern Ireland where a descending ERS-1 SAR image and a cloud free, winter (low sun angle), Landsat TM image were acquired (meta-data are presented in Table 5.1). The images were geocorrected and then any detectable lineaments mapped.

Figures 5.18 and 5.19 depict a selected region from the SAR and TM images respectively; the dominant lineament directions for SAR (north-south) and TM (east-west) are striking, and are further illustrated by the frequency histograms of lineament orientation (Figure 5.20). Table 5.5 also supports these results showing a much higher mean lineament orientation for the ERS-1 SAR data.

These results are principally explained by the difference in azimuth angle between SAR and VIR imagery. SAR imagery is obtained by active detection

using a sensor angled obliquely, orthogonal to the satellite track. As the satellite is polar-orbiting, this means that all images are sensed in an easterly or westerly direction depending on whether the satellite is in an ascending or descending orbit. Consequently all lineaments oriented approximately north-south are selectively enhanced, whilst those oriented approximately east-west are selectively degraded (Graham *et al*, 1991).

Lineament Orientation	*SAR*	***Landsat TM***
Vector Mean *(°)*	145	105
Min *(°)*	0	3
Max *(°)*	179	167
Number	289	349

Table 5.5 Descriptive statistics of lineament orientation for ERS-1 SAR and Landsat TM data for the Strangford Lough region, highlighting the different populations of lineaments (with different orientations) mapped.

5.4.4 Landform Mapping of Ireland

The research for this thesis was initially concerned with producing a glacial reconstruction of the United Kingdom and Ireland. Project feasibility was to be tested through a pilot study involving a large proportion of Ireland for which ERS-1 SAR satellite imagery had previously been acquired specifically for this purpose. Ireland contains one of the largest drumlin swarms in Europe and, as a result, is an important area for lineament research. Given the good preservation of glacial bedforms in the landscape, there should be plenty of evidence on which to base a geomorphological glacial reconstruction. In addition, the fact that the Irish ice sheet is thought to have been almost entirely separate from the British mainland (although there is evidence of marginal influence from the Scottish Uplands) means that it can be studied as a small, self-contained, unit.

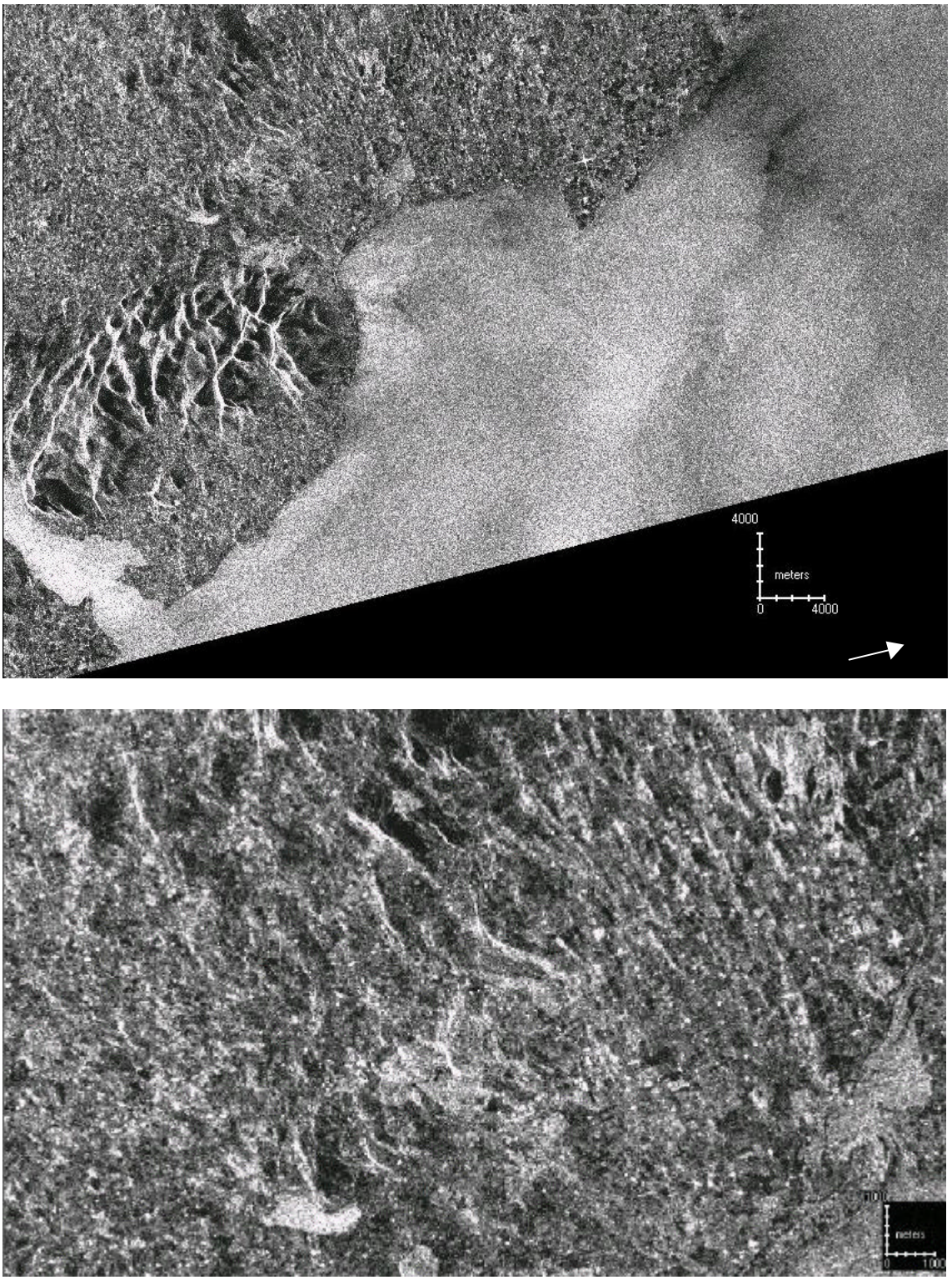

Figure 5.18a and b ERS-1 SAR image (top) of Strangford Lough, Ireland. In conjunction with Figure 5.19, note the dramatic effect of the azimuth angle on lineament representation. Image b is a zoomed region. Note that the E-W trending lineaments on the Landsat TM (Figure 5.19) image are not visible on the ERS-1 SAR image. Arrow indicates the azimuth angle.

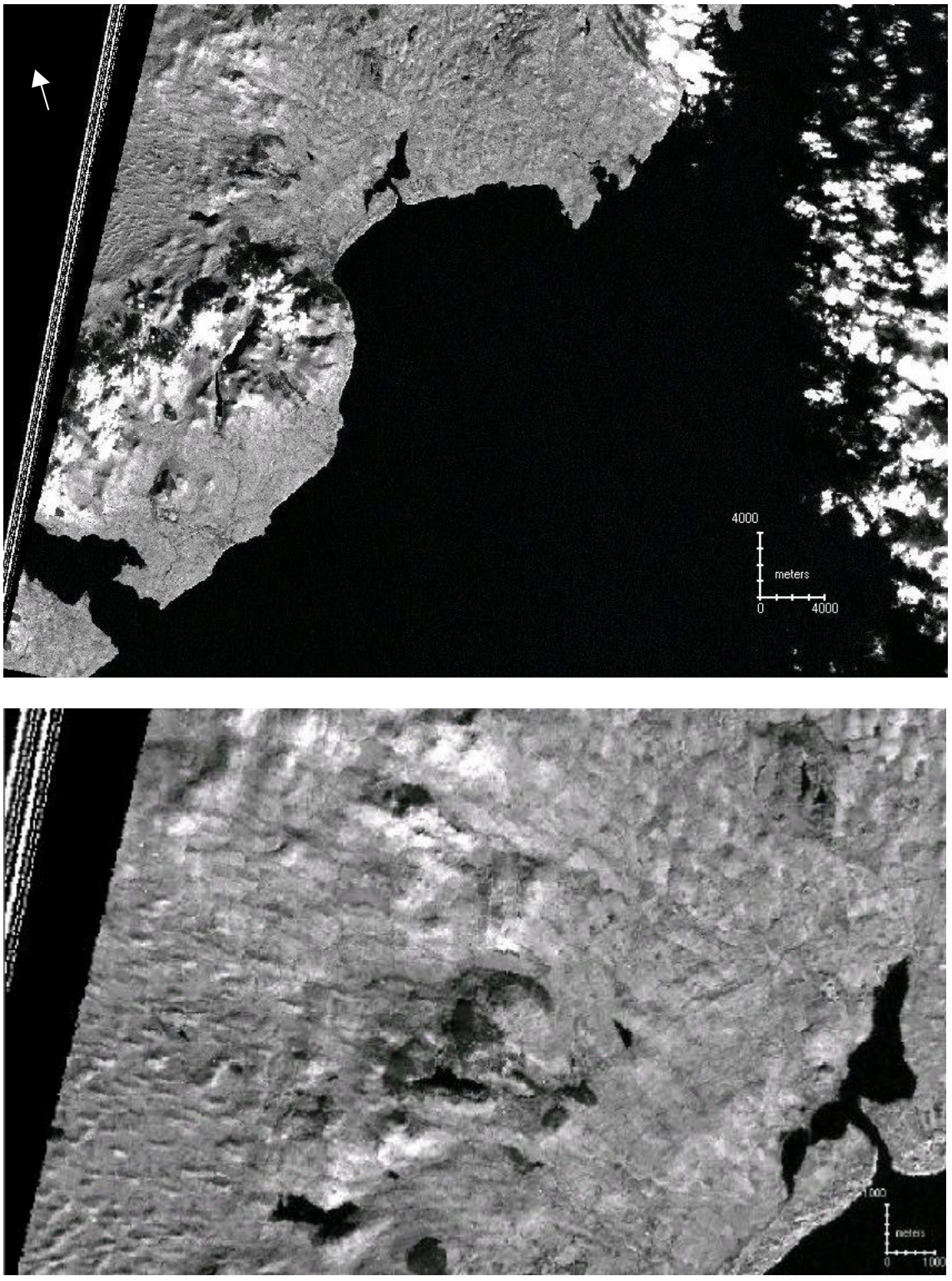

Figure 5.19a and b Landsat TM image of Strangford Lough, Ireland. In conjunction with Figure 5.18, note the dramatic effect of the azimuth angle on lineament representation. Image b is a zoomed region. Note that the E-W trending lineaments on the Landsat TM (Figure 5.18) image are not visible on the ERS-1 SAR image. Arrow indicates the azimuth angle.

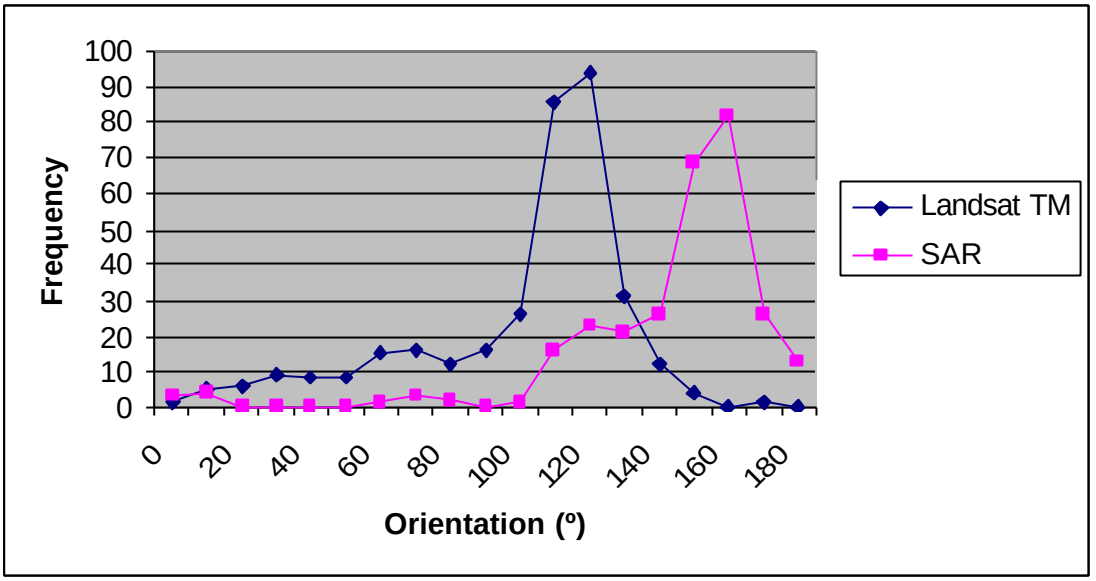

Figure 5.20 Frequency polygon of lineament orientation for Landsat TM and ERS-1 SAR data, illustrating the completely different populations of lineaments (with different orientations) mapped for Strangford Lough, Ireland.

Having acquired the relevant SAR imagery and applied the pre-processing techniques outlined by Clark (1997), mapping was performed using the same methods employed earlier in this chapter. Figure 5.21 depicts all the lineaments mapped for this part of the project. These patterns have been outlined, in parts, by various authors but never mapped in their entirety. Figure 5.22 provides an example of the type of summary mapping that has been performed. This is a generalised view of the authors review of data from various field and aerial photography mapped sources, as well as personal experience. Much of the published evidence for lineaments fails to recognise the presence of cross-cutting in the landscape and therefore this summary highlights dominant lineament patterns around the country. Many of these patterns will have occurred at different times and trying to synthesise this information is virtually impossible.

In Chapter 1 I outlined the impetus for the research in this thesis and this included the generally poor landform representation of ERS-1 SAR imagery in Ireland. The remainder of this section reviews the lineament mapping performed in Ireland and summarises the reasons for its poor performance.

In reviewing Figure 5.21, the first point to note is that ERS-1 SAR coverage of Ireland is **not** complete. Imagery was not obtained for southern Ireland, although few drumlins are known to exist in this region (Warren, 1992). However in the remainder of the country a variety of small areas were missed due to lack of coverage. For example, the rectangular band running across the middle of the country lies *between* two images. Likewise, small areas in the west, north-west, north-east and east also remain uncovered. The area in the east turns out to be quite critical as a significant number of bedforms can be found in this area (Clark and Meehan, 2001).

Figure 5.21 depicts several areas that are noticeable due to the parallel conformity of the mapped landforms. An example of this is Donegal Bay (outlined on Figure 5.21); Figure 5.23 shows a zoomed section (a) of this area, with the lineaments mapped from it (b). The lineaments are clearly defined on

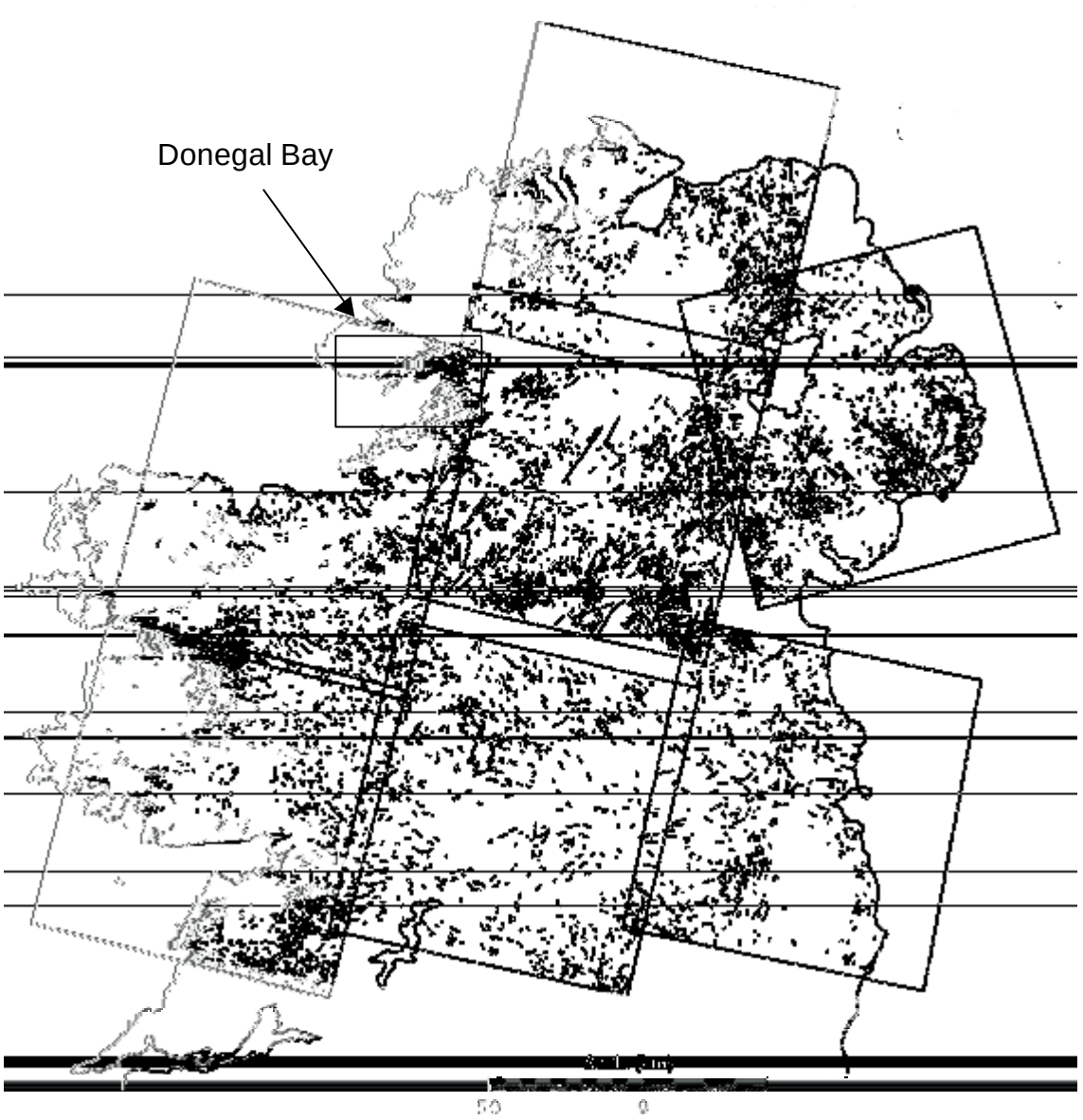

Figure 5.21 Lineament mapping from ERS-1 SAR satellite imagery (including an outline of the SAR image coverage and locations noted in the text). Whilst good quality mapping can be verified (e.g. around Clew Bay), there are many areas where lineament mapping is poor.

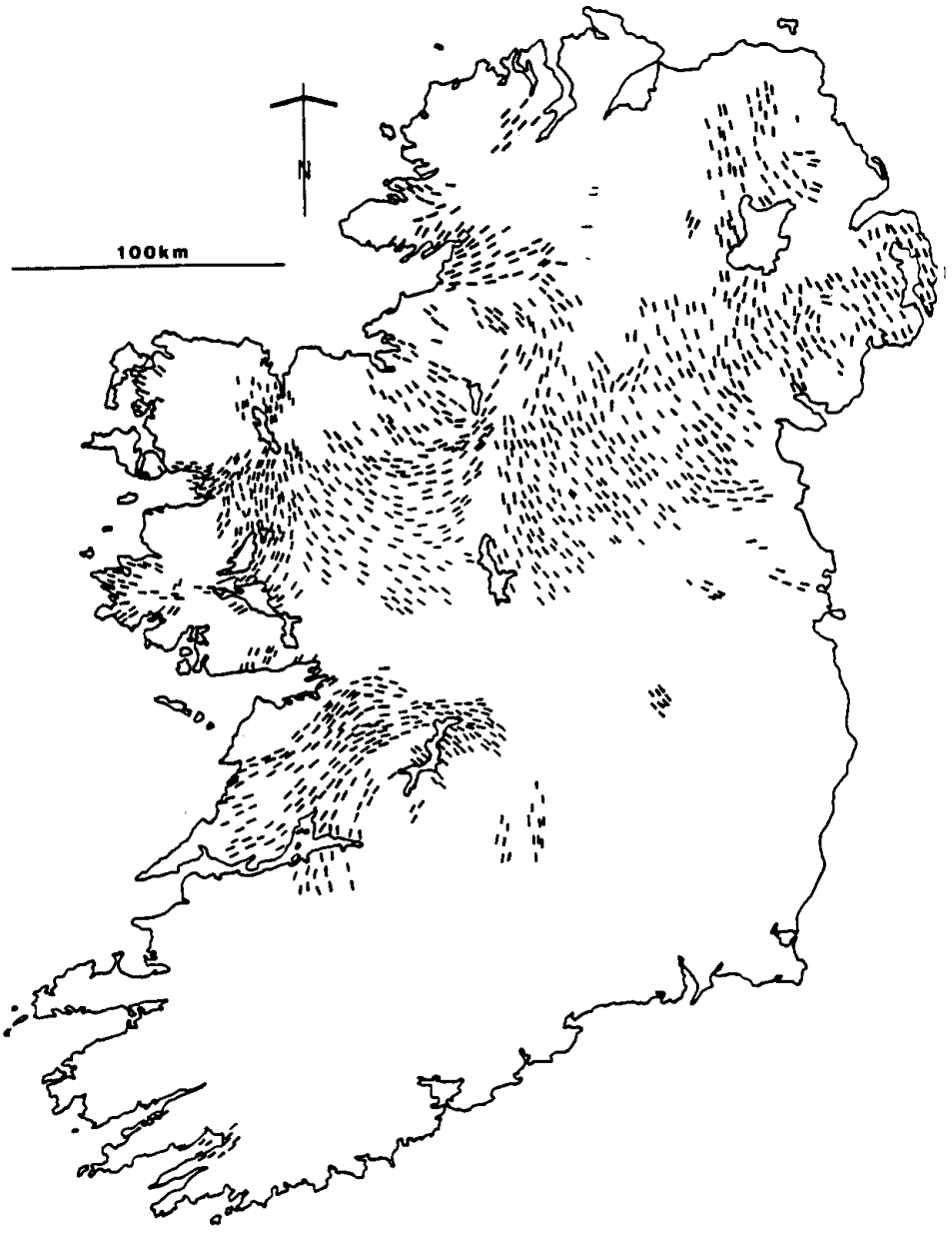

Figure 5.22 Generalised distribution and alignment of drumlins in Ireland, as after Warren (1992).

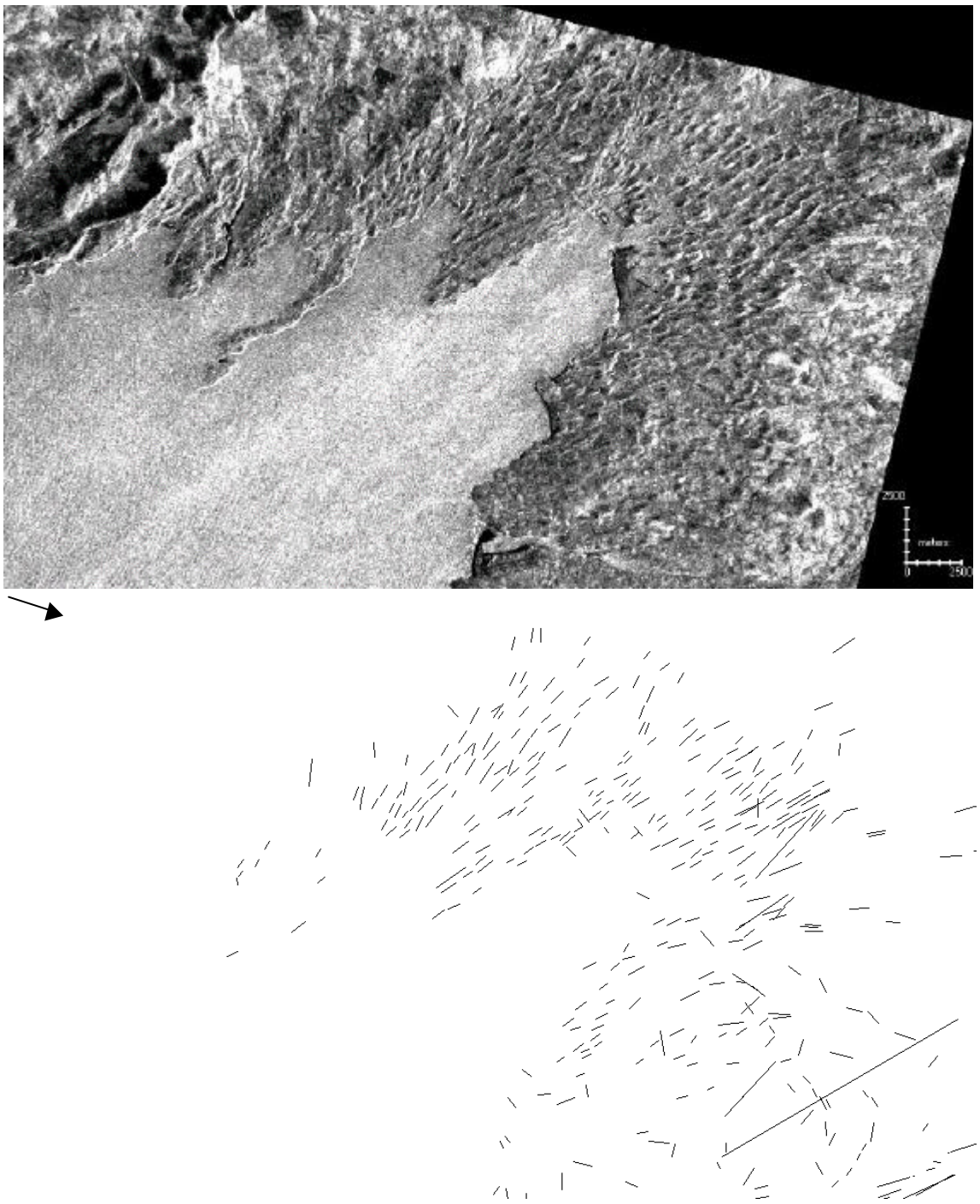

Figure 5.23 a and b ERS-1 SAR image (top), and glacial lineaments mapped from it (bottom), for Donegal Bay, Ireland. Arrow indicates azimuth angle.

the image and easy to map. This is in contrast to other areas that show no preferred orientation (e.g. central regions). Figure 5.24 shows an area around Lough Sheelin, County Cavan. This again demonstrates the *complementary* nature of SAR imagery. In the north of the ERS-1 SAR image, lineaments are strongly defined, whilst in the south they are poorly defined. The opposite is true of the Landsat TM image.

In comparison to Figure 5.22 the differences are very distinctive. The areas of high parallel conformity are similarly matched in Figure 5.21, however much of the remaining areas are very different. The SAR mapping shows lineaments that are well represented, whilst failing to identify lineaments which have been mapped on Figure 5.22. In addition, particularly in the midlands, there appear to be a large number of “spurious” lineaments.

There is undoubtedly reasonable lineament representation on parts of the SAR imagery acquired for Ireland, yet many questions remain about the overall quality of the product. This has to be placed within the context of successful use of SAR by other researchers. Knight (1996) successfully applied ERS-1 SAR mapping to the glacial landforms of the Ungava Sector of the former Laurentide Ice Sheet, whilst Ford (1981) showed high quality imagery from SEASAT-1. Although not detailed, Punkari (1985) described the utility in using Soviet airborne radar.

5.4.5 Conclusions

It is appropriate to explore some of the reasons why ERS-1 SAR data has proved so unreliable in Ireland. It is also worth commenting on the same factors that effect the VIR imagery: relative size, azimuth biasing and landform signal strength. The resolution of ERS-1 SAR data is relatively good and so moderate size lineaments should be easily distinguishable, however cross-cutting relationships will almost certainly **not** be visible. Azimuth biasing, as discussed in the previous section, strongly influences the representation of landforms on an image and is probably the main cause of differences between ERS-1 SAR and Landsat TM images. Landform signal strength, for SAR sensors, is linked to the look angle of the sensor. This is fixed for ERS-1 SAR, being relatively steep.

Although this reduces geometric distortion, it is less likely to highlight subtle topographic features.

Other factors that will effect the SAR image include the sensor wavelength, sensor polarization and surface characteristics. The wavelength of ERS-1 SAR will interact with both surface vegetation and severe rain events. If a region is heavily forested then the signal return will record the reflectance of the vegetation canopy **not** the terrain surface. Likewise, the VV polarization is designed to enhance oceanic, rather than land surface, reflectivity (Lillesand and Kiefer, 2000). The final area that is likely to affect the SAR image are the surface characteristics. These are principally the dielectric coefficient and geometric arrangement of the surface. An increase in the moisture content will increase the reflectivity of an object, particularly vegetation. The roughness of the surface will also affect reflectivity. In general, smooth, or *specular*, surfaces reflect incident radiation directly *away* from the sensor and so there is minimal backscatter. Conversely rough objects (and this will include urbanised areas) will have a much higher degree of backscatter.

These general comments provide some insight into the specific case for Ireland, however, as noted above, researchers have demonstrated that radar imagery is a good tool for mapping glacial landforms. Ford worked in limited parts of Ireland, whilst Knight acquired imagery for parts of the former Laurentide ice sheet. Clearly azimuth biasing is a major problem for SAR, but this is also the case for the other VIR imagery reviewed in this chapter. The most likely explanation is the combination of surface cover, moisture content and sensor design of ERS-1. Humankind has had a long residence time in Ireland and, over that period, the landscape has been cultivated and urbanised. In rural areas, the vegetation cover will dominate the way backscatter is returned subordinating topographic variation. Ireland also has relatively large amounts of precipitation and so high moisture content, and hence reflectivity. The wavelength used by ERS-1 SAR is designed to interact with this type of surface cover. Likewise, in urban areas there will be high backscatter. Both of these areas will tend to over-ride the subtle underlying topographic signal that is recorded as a result of the look angle of the sensor (i.e. subtle lineaments are less likely to be visible).

In comparison to Knight's (1996) study area (sub-Arctic Canada), most of the landscape has no urbanisation or agriculture and so there is still a strong association between surface cover and landforms. In addition, inter-drumlin areas in this cratonic region are likely to act as collection areas for moisture, further helping the delineation of the lineaments.

Overall SAR imagery was found to be inappropriate for mapping glacial landforms for large parts of Ireland. It is unfortunate that a large amount of mapping was required in order to highlight this effect. However, globally, other regions may have greater success. The side-looking geometry of the sensor is still able to detect subtle topographic variations and it is possible that an alternative satellite sensor may well produce imagery better suited to detecting lineaments. For example, JERS-1 operates in the L-band (23cm) and would therefore be more likely to record the actual topographic surface rather than vegetation.

With practice, good results can be obtained using SAR imagery for glacial landform mapping (e.g. Knight, 1996). This was not the case for our test area (see also §5.6) around Lough Gara where azimuth biasing and a degraded topographic signal reduced the representations of landforms on the image. However an awareness of these issues has allowed the successful use of radar imagery, utilising the benefits of consistent, "any weather", data acquisition.

For poleward latitudes, the ascending and descending paths of near polar orbiting satellites cross at high angles. This is illustrated in Ireland with ascending paths having a sensor azimuth ~104º, whilst descending paths have ~256º. By obtaining both sets of imagery for an area, azimuth biasing can be reduced, however two sets of mapping would be required.

5.5 Case Study: Lough Gara Satellite Imagery

The lineaments mapped from the Landsat MSS, Landsat TM, SPOT and SAR imagery for Lough Gara are now used to supplement the inter-image comparisons with quantitative data and so highlight the errors and bias often

present within imagery acquired for landform mapping. These are illustrated through discussion of landform signal strength, azimuth biasing and relative size, including a review of the flow patterns generated from the mapped data. The SAR image is necessarily discussed separately within each section as a result of the different inherent characteristics of the sensor. In addition, discussion of coincidence between lineaments mapped from each image type is also provided.

5.5.1 Landform Representation

The landforms mapped from the different satellite imagery are subject to the three main controls on landform representation. The effect of each of these variables is discussed in turn in order to highlight, for this series of images, the main control on representation.

Landform signal strength has an important impact on lineament representation (§4.2), however the solar elevation angles for the VIR images of Lough Gara are all similar (Table 5.1) and so can be assumed to make little difference to landform representation.

The effect of *azimuth biasing* can be significant, as illustrated by the SAR case study (§5.5). For the Lough Gara area, the lineaments are predominantly oriented in an east-west direction (as illustrated in truth). As the VIR imagery are predominantly illuminated from the south they are effectively able to display the landforms. As the images were acquired at a similar time of year, the illumination azimuths are similar and so there is little variation in landform representation as a result of azimuth biasing.

The SAR imagery is very different to the VIR imagery, with a very small number of lineaments mapped as illustrated by Figure 5.6a (and described in the inter-image comparisons). Inspection of lineament orientations shows that they have a comparable mode and range to those mapped from truth (Figure 5.25). Intuitively I would expect azimuth biasing to occur as the illumination orientation of 104º is close to the histogram peak of 120º. This appears not to be the case,

although with a relatively small sample size it is possible that such an effect is hidden.

The main difference in landform detectability between the VIR images relates to *relative size* (i.e. spatial resolution), given the minimal effects of landform signal strength and azimuth biasing. Table 5.6 shows an increase in the number of mapped lineaments as spatial resolution increases; this is demonstrated by the low number of landforms mapped from Landsat MSS (128) and the higher numbers mapped from Landsat TM (275) and SPOT (284), when compared to truth (398). Figure 5.26 presents a frequency polygon of the total number of lineaments mapped from each image. This demonstrates that as sensor resolution increases, so the number of lineaments mapped increases and their size decreases. This may disguise the fact that, although higher resolution imagery resolves more, shorter, lineaments, lower resolution imagery may still be able to resolve (although less well) these same lineaments as fewer, contiguous, lines. Table 5.2 also presents total lineament length for each image, a measure designed to remove the effect of fragmentation of mapped lineaments. This highlights the poor ability of SAR and Landsat MSS to satisfactorily resolve lineaments, whilst Landsat TM and SPOT are clearly better. Interestingly Landsat TM has the longest total lineament length of all the imagery suggesting that it is able to resolve all the lineaments visible on SPOT, although more fragmentation occurs on the latter. As a result Landsat TM appears to be satisfactory for lineament mapping, but higher resolution imagery may be necessary in order to resolve cross-cutting relationships.

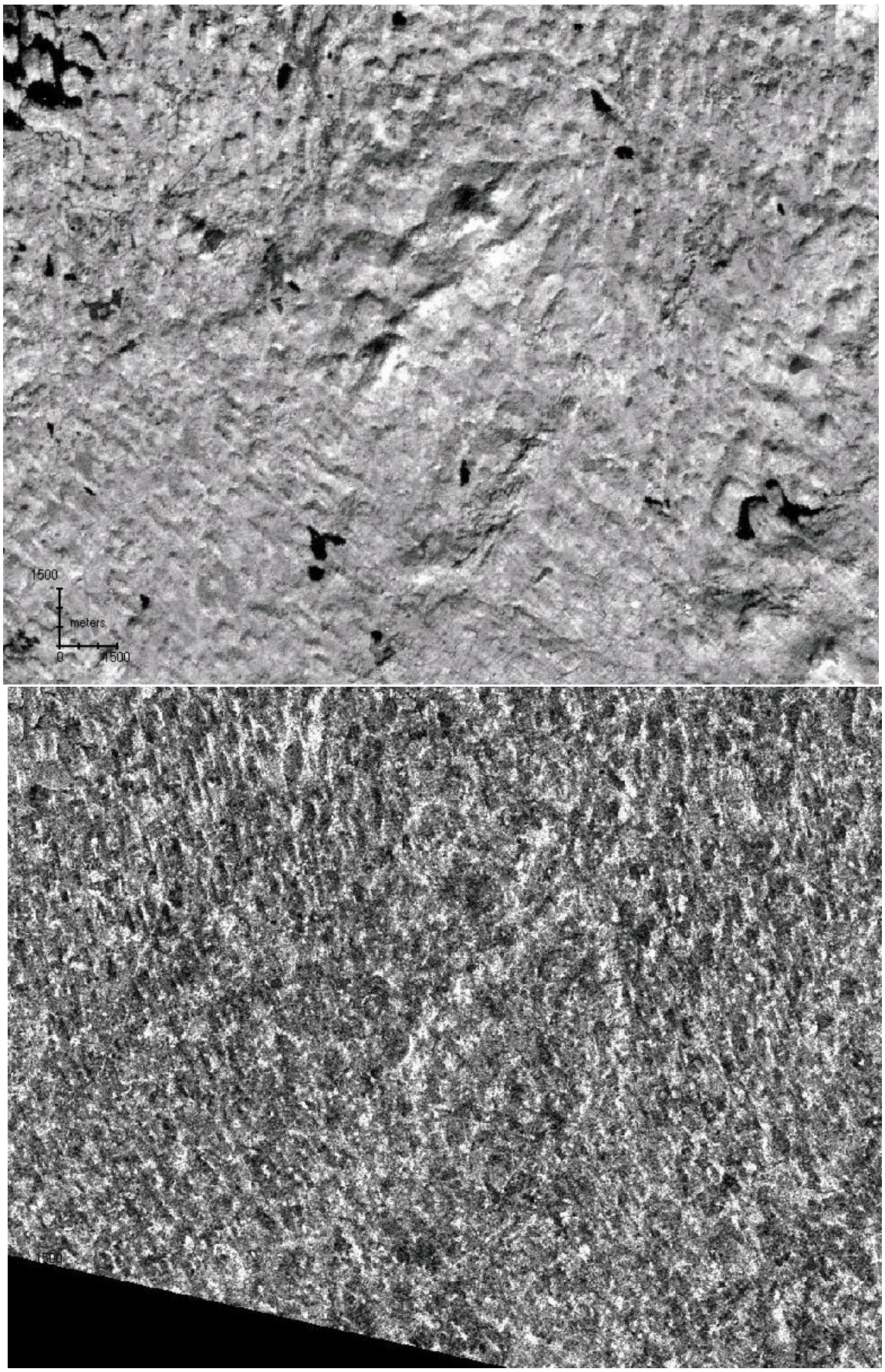

Figure 5.24 a and b Landsat TM image (top) and ERS-1 SAR (bottom) around Lough Sheelin, County Cavan, Ireland. Note the strong representation of lineaments in the north of the SAR image *absent* on the TM image and vice versa.

Region	Image (resolution)	Total Number of Lineaments	Total Number of Hillocks	Total Lineament Length (km)
Ireland	Landsat MSS (80m)	128	30	93
	Landsat TM (30m)	275	47	194
	SPOT (10m)	284	27	166
	ERS-1 SAR (25m)	75	49	58
	Truth (50m)	398	101	230
Russia	Landsat ETM+ Pan (15m)	813	-	526
	Landsat ETM+ XS (30m)	473	-	422

Table 5.6 Total number of lineaments and total lineament length mapped from each of the image types.

Finally, in terms of an ice sheet reconstruction, flow patterns, generalised from individual lineaments (Chapter 2), are the most important elements as they are the *non-interpreted* building blocks used to interpret the morphological data and guide ice sheet reconstruction. Any differences between datasets is unimportant as long as the flow patterns are consistent and correct. Figures 5.2, 5.3, 5.5, 5.7 and 5.9 include overlays of flow patterns for the respective imagery. All overlays are shown comparatively in Figure 5.27. Not surprisingly, the greater the number of mapped lineaments, the easier it is to generalise them into flow patterns. In addition there is more detail in the orientation of flow patterns, as well as the presence of cross-cutting. Therefore the SPOT imagery is able to highlight the curving flow in the southern portion of the image, as well as the detailed cross-cutting in the northern section. Although this level of detail is missing from the Landsat MSS imagery, similar flow patterns are still able to be drawn. The flow patterns from the SPOT and Landsat TM imagery are very similar to those from truth, however the SPOT image additionally has the presence of transverse ridges which were not identified on the Landsat TM. The poorest results were obtained from the SAR imagery. Flow patterns for the northern area are similar to those from the VIR imagery, however the southern area is poorly represented.

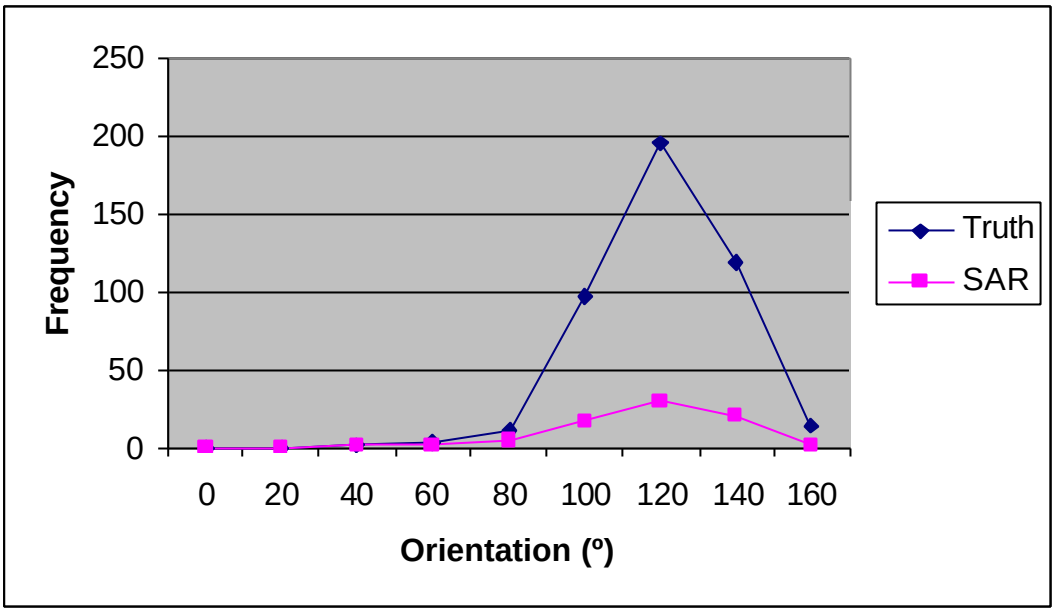

Figure 5.25 Frequency polygon of lineament orientation for ERS-1 SAR and the truth data. Although far fewer lineaments have been mapped from the SAR image, lineaments have a similar mode and range of orientation.

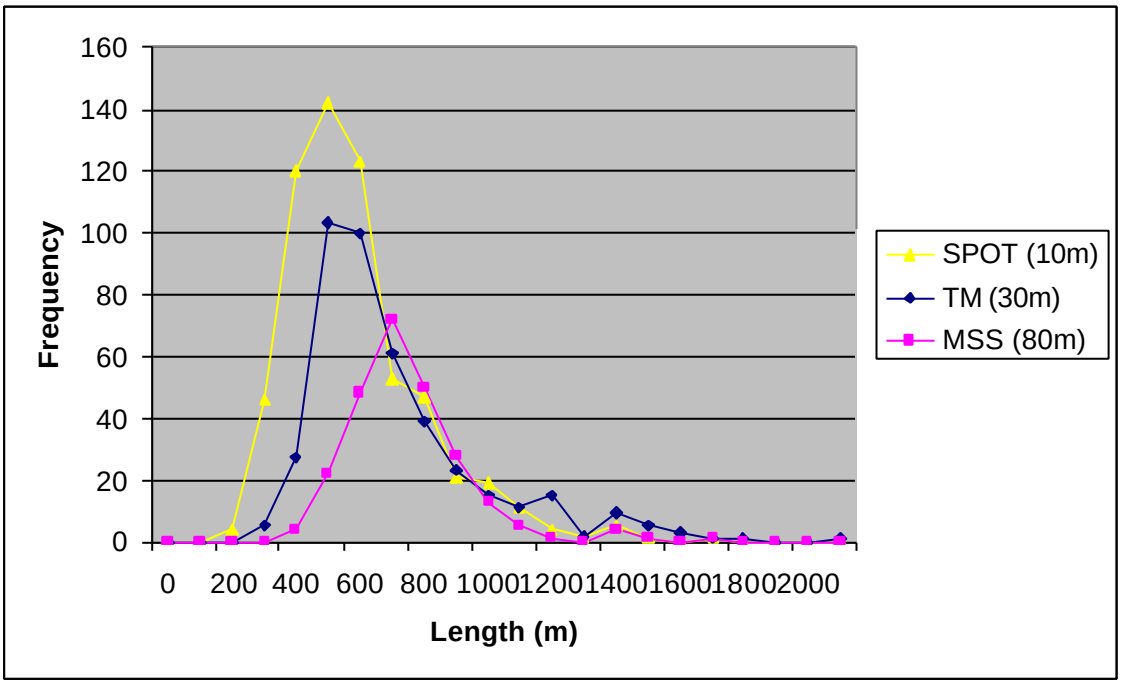

Figure 5.26 Illustration of the effect of sensor spatial resolution on the total number and distribution of lineaments mapped from satellite imagery. The frequency polygon shows that as resolution increases, so the number of lineaments mapped increases, the size of lineaments decrease and the population peak shifts towards the origin.

5.5.2 Lineament Coincidence

In addition to reviewing the different spatial bias effects on VIR imagery, it is also appropriate to consider the degree of coincidence in lineament mapping between the different imagery and the truth. Coincidence was assessed visually with lineaments required to be within approximately 200m of each other and not deviate by more than 15º. Visual assessment was selected as the optimum method as consideration could be given to any deviations a result of poor digitising or varying geocorrection. Mapped lineament overlays are visually presented in Figures 5.28-5.33.

Each VIR image is overlaid on to truth (Figures 5.28-30), with relevant statistics provided in Table 5.7. These show the number of lineaments coincident with lineaments on truth, hillocks coincident with lineaments, the total coincident lineament length and the percentage of lineaments (on truth) coincident with each image. In general there is an increase in the number of coincident lineaments (column 1) as the spatial resolution of the sensor increases. The number of coincident hillocks (column 2) remains fairly constant, showing similar azimuth biasing between image types, irrespective of resolution. Total coincident lineament length (column 3) also increases with sensor resolution. Finally the percentage coincidence (taking into account hillock/lineament coincidence; column 4) increases with spatial resolution. As a final note the SAR imagery can be seen to perform very badly with only 9% coincidence and a small 19km total coincident lineament length.

Image	Number of Coincident Lineaments	Number of Coincident Hillocks	Total Lineament Length (km)	Lineament Coincidence (%)
Landsat MSS	69	23	47	22
Landsat TM	178	11	134	47
SPOT	197	14	117	51
ERS-1 SAR	23	13	19	9

Table 5.7 Number of coincident lineaments, number of coincident hillocks and total lineament length, with the truth, for each image type. The final column shows the percentage of lineaments on *truth* that are coincident with each image type.

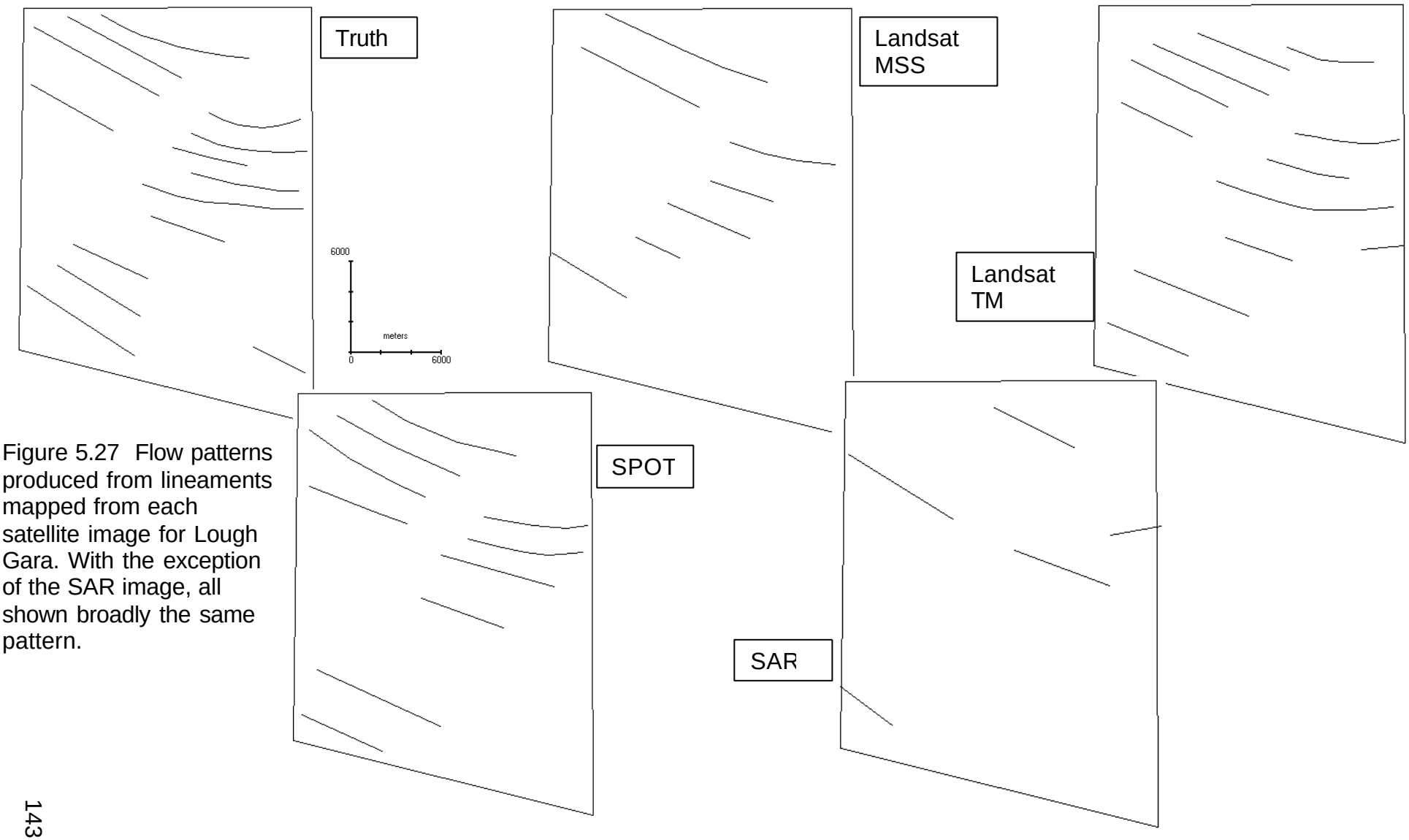

Figure 5.27 Flow patterns produced from lineaments mapped from each satellite image for Lough Gara. With the exception of the SAR image, all shown broadly the same pattern.

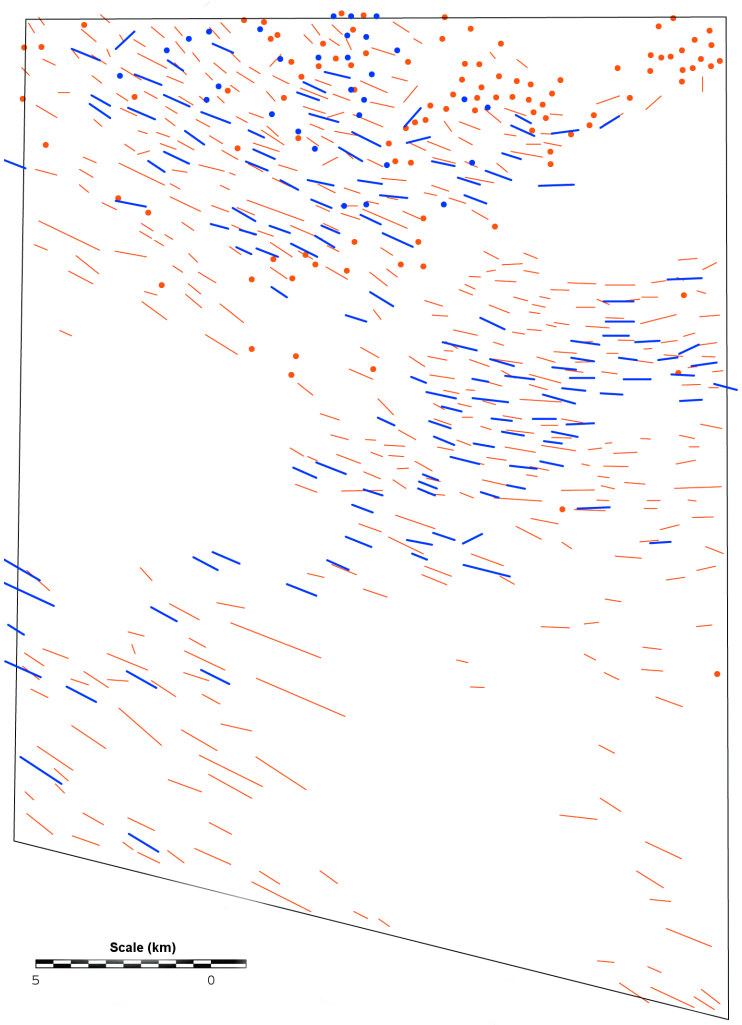

Figure 5.28 Overlay of lineaments and hillocks mapped from Truth (red) and Landsat MSS (blue) imagery.

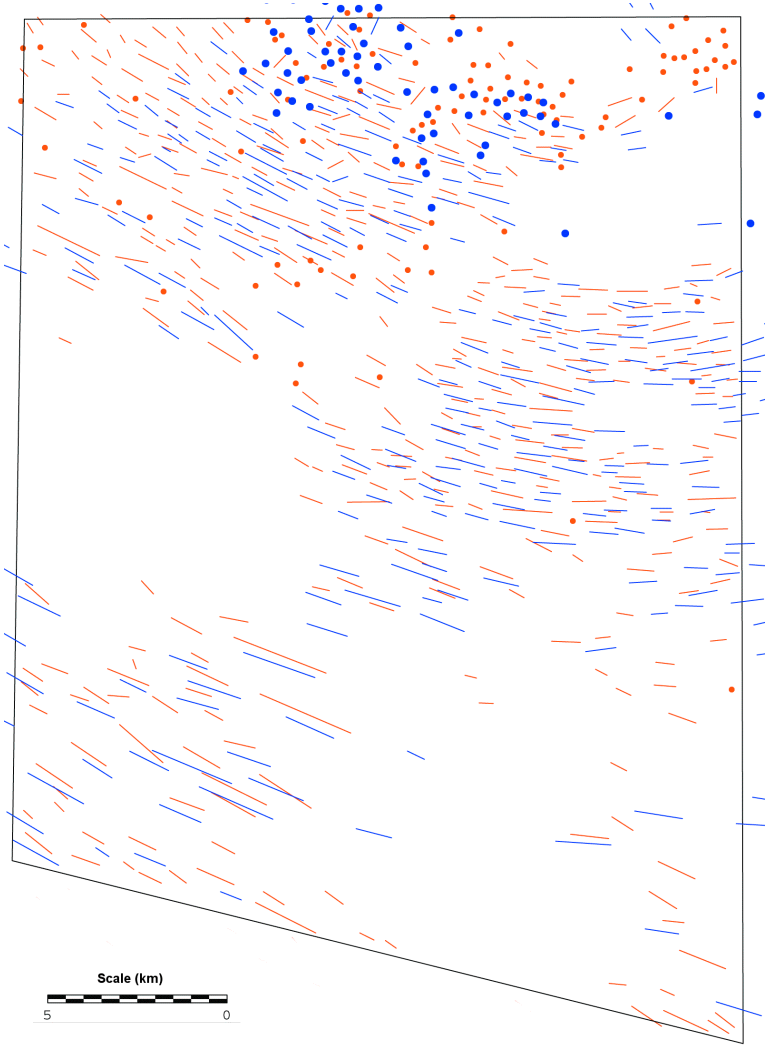

Figure 5.29 Overlay of lineaments and hillocks mapped from Truth (red) and Landsat TM (blue) imagery.

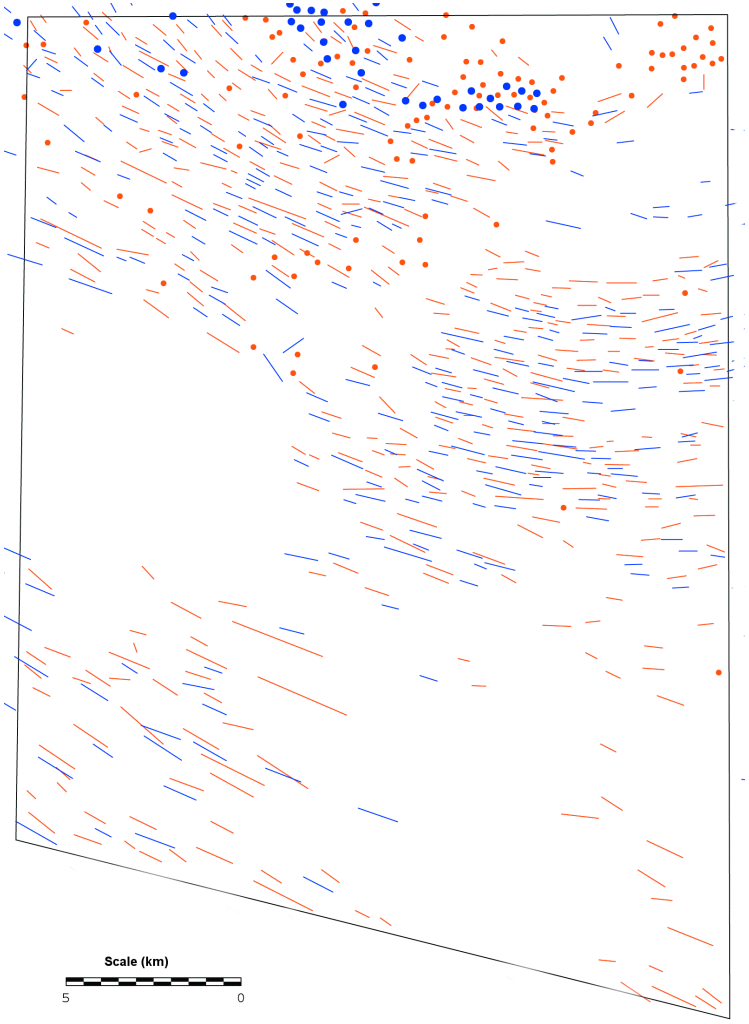

Figure 5.30 Overlay of lineaments and hillocks mapped from Truth (red) and SPOT (blue) imagery.

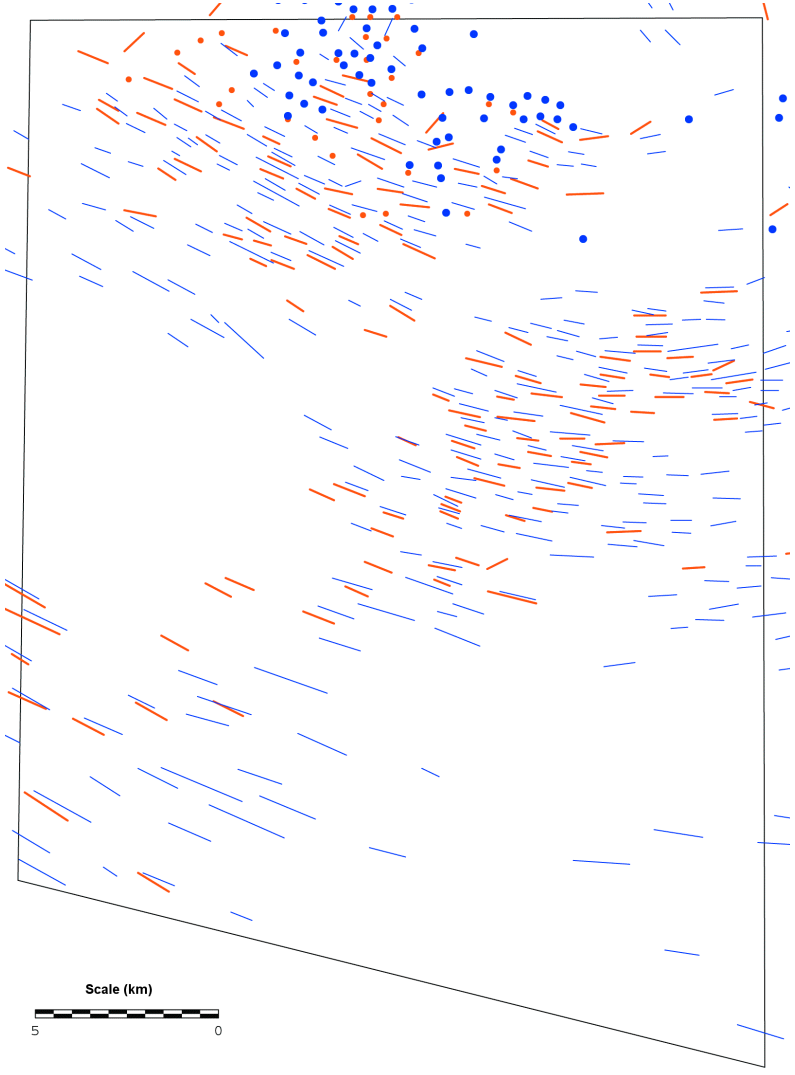

Figure 5.31 Overlay of lineaments and hillocks mapped from Landsat MSS (red) and Landsat TM (blue) imagery.

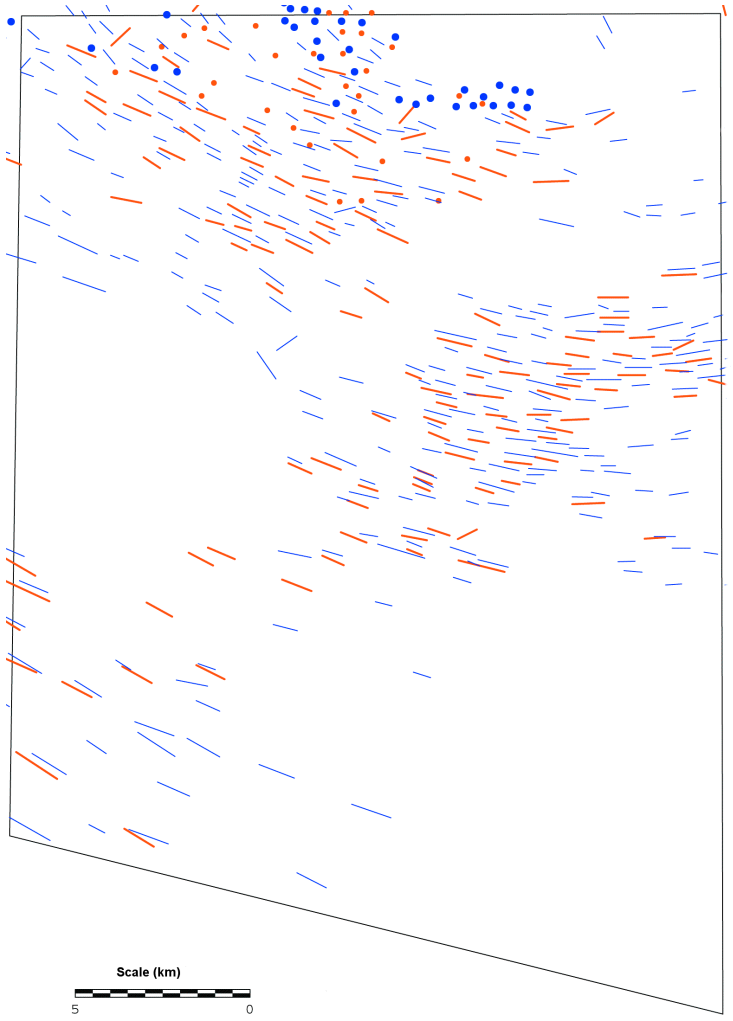

Figure 5.32 Overlay of lineaments and hillocks mapped from Landsat MSS (red) and SPOT (blue) imagery.

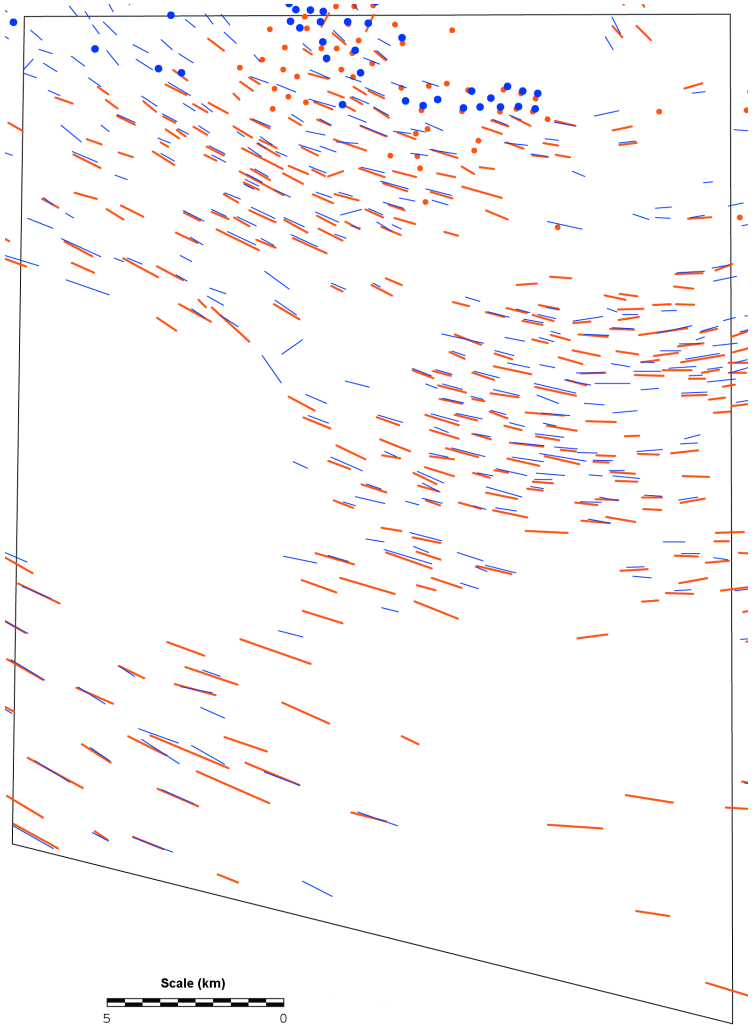

Figure 5.33 Overlay of lineaments and hillocks mapped Landsat TM (red) and from SPOT (blue) imagery.

Individual inter-image comparisons were performed and summarised for the VIR imagery in Figures 5.31-5.33, with summary statistics in Table 5.8. The results are not surprising in that over 70% of lineaments on Landsat MSS are coincident with those on SPOT and Landsat TM. SPOT and Landsat TM are also highly coincident, a product of their high spatial resolution. Again however, there are 20-30% of lineaments that are generally not coincident (e.g. 30% of lineaments on Landsat MSS are not coincident with those on Landsat TM), comprised of varying orientation, length and location. This can only be accounted for by geocorrection, mapping and comparison errors.

	Landsat MSS	Landsat TM	SPOT
Landsat MSS		50	40
LandsatTM	70		73
SPOT	78	82	

Table 5.8 Percentage spatial coincidence of lineaments between the VIR satellite images. For example, 70% of lineaments on Landsat MSS are coincident with those on Landsat TM

In summary, for this particular area, azimuth biasing and landform signal strength do not contribute major elements of bias for VIR imagery. Relative size has the single largest affect on mapped lineaments, whilst geocorrection, mapping and comparison errors probably account for the remaining variability. The SAR imagery is strongly affected by azimuth bias and is a poor data source for lineament mapping in this instance.

5.6 SummaryandRecommendations

This chapter has described the benefits in using satellite imagery for glacial landform mapping. However these benefits have to weighed against weaknesses in its use. There are two main areas where error can be incorporated into a landform map (where there is a primary focus on lineament mapping). These are inherent bias within the imagery acquired and the ability of the observer to map the landforms. The latter has been touched upon by several authors whilst the former is the topic of this chapter.

Image bias can occur from relative size, azimuth biasing and landform signal strength. The effect of each of these variables on lineament mapping has been

investigated for study areas in the Lough Gara region of western Ireland and the Kola Peninsula, Russia.

The results suggest that low solar elevation is required (for VIR imagery) in order to selectively highlight landforms (e.g. see Figures 5.5b and 5.6). From experience it is advised to obtain imagery with a solar elevation below ~20º, although <15º is desirable. Depending on latitude, solar elevations as low as 5º are possible. For Landsat ETM+, daylight imaging is not performed for solar elevations below 5º. Above 20º there is a gradual decrease in the relief effect and tonal variation to a point where lineaments are only detectable by surface cover variation. The availability of appropriate imagery from archive is variable, depending upon the latitude of the study area and the sensor desired. In mid-latitudes, winter scenes are necessary in order to acquire a low solar elevation and, coupled with the requirements for scenes to be snow and cloud free, makes suitable imagery difficult to obtain. In high latitudes, summer imagery is required in order acquire snow free scenes, although this is not necessarily ideal as solar elevation can be quite high (Table 5.1). Aber *et al* (1993) suggest that light snow cover, in association with a high relief effect, can increase detectability as tonal variation due to surface cover is effectively masked. This has to be weighed against the possible reduction in the relief effect with increased snow depth. Subtle landforms can quickly become “hidden” making mapping of features such as cross-cutting landforms difficult.

Perhaps the single greatest bias, over which the observer has little control, is the azimuth biasing effect. Both the SAR case study and the DEM experiments suggest that large omissions and misidentification can occur as a result of azimuth biasing. More particularly, the above constraints on acquisition dates for VIR imagery produce a small solar azimuth window through which images are available. As a consequence, lineaments oriented parallel to the azimuth are selectively diminished, such that they may change shape, appear as hillocks or completely disappear. It is important to be familiar with a study area in order to be aware of this problem; for some areas no action may be necessary as lineaments may not be oriented in this direction. However other areas may require the acquisition of alternative data sources in order to mitigate

against this error. These sources include local mapping in the form of topographic maps, digital elevation models or field mapping. Where these are not available SAR imagery can be usefully used. Its alternative viewing geometry satisfactorily supplements VIR imagery, although mappers should not underestimate the experience required in its use (see Vencatasawmy *et al,* 1998 for further discussion).

The final bias, relative size, is familiar to most researchers. The higher the resolution of the satellite imagery, the greater the ability to map smaller landforms. The above results show a 170% increase in mapped lineaments by moving from 30m resolution data to 15m data. However higher precision data does not necessarily mean better quality results and it is important that researchers select imagery to match the requirements of their project. For ice sheet reconstruction, overall lineament trend is the single most important element. As a result, azimuth effects are the most serious problem since they can introduce a selective bias into the mapping. In contrast, relative size and solar elevation are less important than azimuth bias here, since the errors produced should be distributed randomly across lineaments of all orientations. From a more practical perspective, it is useful if the image coverage is as large (and cheap!) as possible. High resolution data are desirable if detailed or cross-cutting mapping are intended. Equally, multi-spectral data are very useful as they can be used to delimit lineaments through surface cover changes. These requirements point to Landsat ETM+ as the optimal images, given the near-global coverage, large scene area (180x180km), high resolution (15m panchromatic) and multi-spectral facilities. In addition, the open access policy of NASA make the data very cheap. The disadvantage, in the short-term, is the short mission run-time which means, for mid-latitude regions, that suitable imagery may not yet be available.

If Landsat ETM+ data are not available for a particular region, then the choice of imagery becomes more difficult. SPOT are available in both high resolution panchromatic and multi-spectral formats, but the scene coverage is small (60x60km) and relatively expensive. Landsat TM has had a longer mission time and so suitable imagery may be available that takes advantage of the larger

areal coverage and multi-spectral format. Although cheaper than SPOT, Landsat TM is considerably more expensive than Landsat ETM+ and has a lower resolution (in equivalent panchromatic mode). Finally, Landsat MSS has had a very long mission time (and consequently large archive) and benefits from the areal coverage and multi-spectral format of the other Landsat missions. However it suffers from relatively poor spatial resolution.

As a result, it is recommended that Landsat ETM+ is used wherever suitable imagery is available. Otherwise, SPOT is desirable for geomorphological or cross-cutting mapping over small areas. If mapping glacial landforms over larger areas then Landsat TM is the best alternative, particularly where more detailed information on cross-cutting is required. Finally, Landsat MSS has great utility in the large archives and low cost that make it appropriate for small-scale mapping within tight budget constraints, or as a reconnaissance tool.

The acquisition of appropriate imagery requires identifying the desired sensor and selecting cloud free imagery that has low solar elevation and little snow cover, as well as being aware of the solar azimuth and any biasing that might occur.

The most suitable dates for image acquisition are dependent upon latitude, satellite overpass time and the satellite repeat cycle. Ideally it would be good to pinpoint an approximate date when viewing conditions are optimum and then search for cloud free imagery. The accompanying CDROM contains two Microsoft Excel ™ spreadsheets which allow the user to do just that. They contain complete overpass time and latitude/longitude data for Landsat ETM+.

The first spreadsheet presents solar azimuth and elevation angles (accurate to 0.5°) for every Landsat ETM+ grid cell (termed World Reference System or WRS) on the first day of every month. Appendix 2 explains the calculation of solar elevation and azimuth in more detail, with a worked example.

The overpass times use a sample set of data from the year 2000, however they can vary by ±5mins due to the degradation of orbit the satellite suffers through

the year. This degradation is corrected on an annual basis. The overall affect on the calculation accuracy is minimal for the purposes of identifying the most suitable acquisition dates. Given this data, the user can locate which month is the most appropriate to obtain data.

The second spreadsheet contains the overpass time and latitude/longitude data, along with the necessary equations to calculate solar azimuth and elevation, allowing the user to make their own calculations if necessary.

Figure 5.33 presents a graphical illustration of the variation in solar elevation and azimuth for the Landsat ETM+ scene of Lough Gara, Ireland (WRS 207.23). January and December are clearly the best months to obtain imagery with low solar elevation, however days in these months are often cloud covered. The solar elevation then rises to a peak of ~60º in June and July. Solar azimuth also varies from ~145º to ~165º.

In addition to the use of satellite imagery, this chapter has shown that DEM data can be effectively used to map landforms. Researchers should be aware of the impending arrival of a variety of different, satellite based, DEMs. SRTM data is now partially available at 90m and 30m spatial resolutions. The 90m data will be publicly available, whilst limited non-USA 30m data will be available to researchers upon application. Data from a second sensor (owned by the German and Italian space agencies) was also used to produce a further DEM and this will be available for commercial purchase. Researchers will find, however, that there will still be large regions that lie outside the SRTM coverage area. In addition, the use of C-band radar by SRTM means that the true ground elevation may not be calculated in vegetated areas due to interference. With the launch and operational status of NASA's Terra satellite, in particular the ASTER sensor, high spatial resolution data (nominal 15m pixels) is available for purchase. Although not as cost effective as Landsat ETM+, ASTER includes an extra aft-looking infrared sensor that is designed to collect stereo satellite imagery. The ground receiving station then processes this data creating a relative or absolute DEM (30m resolution) to order. Not only will ASTER provide

virtually global coverage, but, as it is polar-orbiting stereo data will be continually collected.

DEM data will clearly be a valuable resource for future glacial landform mapping, whilst placing new demands upon researchers in its use. This chapter has demonstrated that, for landform mapping, they can be superior to satellite imagery. Chapter 6 goes on to explore how best they may be visualised so that they can be utilised in a broad mapping programme. This is illustrated through the application of the techniques developed, to a case study. However the partial global coverage of SRTM and the currently small archives of ASTER means that the continued use of satellite imagery will be necessary.

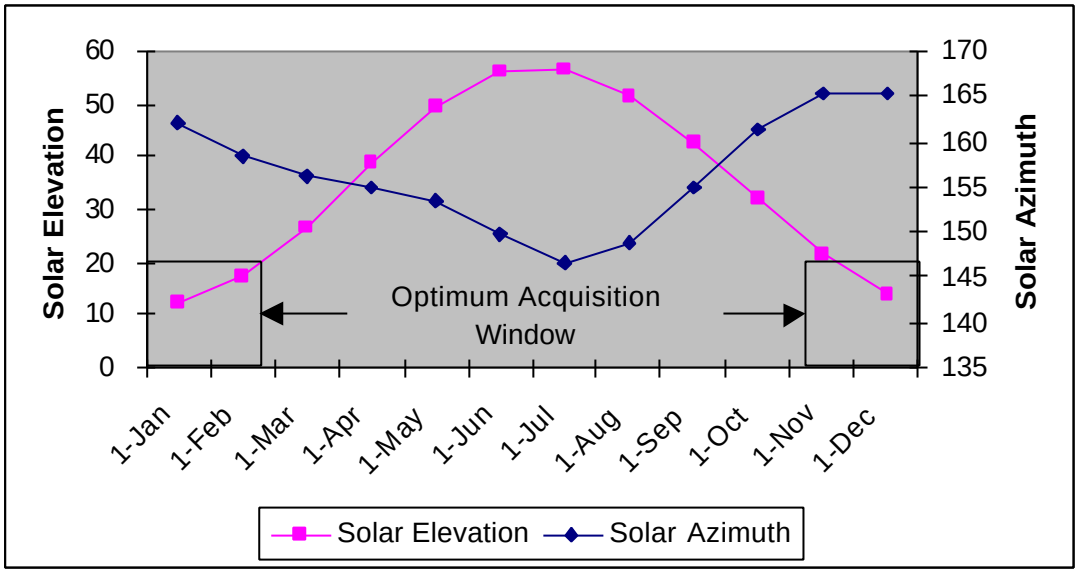

Figure 5.34 Illustration of the variation in solar elevation and azimuth for the Landsat ETM+ scene of Ireland (WRS 207.23). Note the rise in solar elevation from ~10º to ~60º, whilst solar azimuth varies from ~145º to ~165º.

6 Visualisation of High Resolution DEMs for Landform Mapping

6.1 Introduction

With the increased availability of digital elevation models (DEM) in areas with detailed topographic maps and the promise of SRTM data, DEMs are set to become a valuable source of topographic data for the glacial researcher. National mapping programmes are producing DEMs, often with a pixel resolution of 10m and height accuracy of ±1.0m. These have been created from either surveyed contour data or directly from aerial photography using digital analytical plotters. Air and space borne SAR systems are another major data source for the creation of DEMs, with, for example, the Landmap project (Kitmitto *et al*, 2000) providing complete DEM coverage of the United Kingdom and Ireland.

Glacial mapping from DEMs has been briefly touched upon by Lidmar-Bergström *et al* (1991) who used relief shading to visually display landforms, whilst Chapter 5 utilised them for providing control data for the production of a morphological map of "truth". For linear landforms Lidmar-Bergström *et al* (1991) state that they can be less visible when shaded from a limited sector, although they become more visible through a small change in light source azimuth. They created two, broadly orthogonal shaded DEMs for viewing glacial landforms, but only used one for mapping. They did not discuss the implications of how relief shading could be implemented within a broad mapping programme without the bias they had mentioned or how shape can change for those landforms that are not purely linear when viewed under different light source azimuths.

Through the production of the morphological map for this research, the same azimuth biasing as illustrated for the satellite imagery, was encountered. The morphological map was created by break of slope mapping from two illumination azimuths, however this is time consuming and not a viable option

for regional scale landform mapping. Consequently this chapter explores a variety of methods for visualising DEM data with the aim of reducing bias', and quantitatively assesses their suitability.

6.2 Mapping Approaches

The human eye is particularly good at perceiving subtle greyscale changes in an image (Estes *et al*, 1983) and therefore the creation of an image through the use of shading to highlight topographic variation has been a popular method to map landforms from DEMs (also see §5.2.2 and Appendix 1). The main variables controlling visualisation include the illumination azimuth, illumination elevation and vertical scale. Linear landforms are particularly sensitive to variations in the first of these, such that systematic bias may be introduced in the representation of landforms. Different methods for visualising DEM data have therefore been explored.

The different approaches explored are listed and discussed below:

1. RELIEF SHADING

a. Orthogonal Illumination Directions (Figures 6.1a and 6.2a)

This method requires the creation of at least two relief shaded images from a DEM, parallel and orthogonal to the principal lineament direction. This arrangement should allow the visualisation of all landforms on the image.

2. Combined Viewing

a. False Colour Composite (Figure 6.3)

Remote sensing software typically allow the colour co-visualisation of up to three images through the use of the red, green and blue colours on a computer monitor. In this method two relief shaded images were created as in method (1), and assigned to a different monitor colour (i.e. image 1 is viewed as blue and image 2 as green). This has the effect of colouring areas of the image that appear in only one, or both, images.

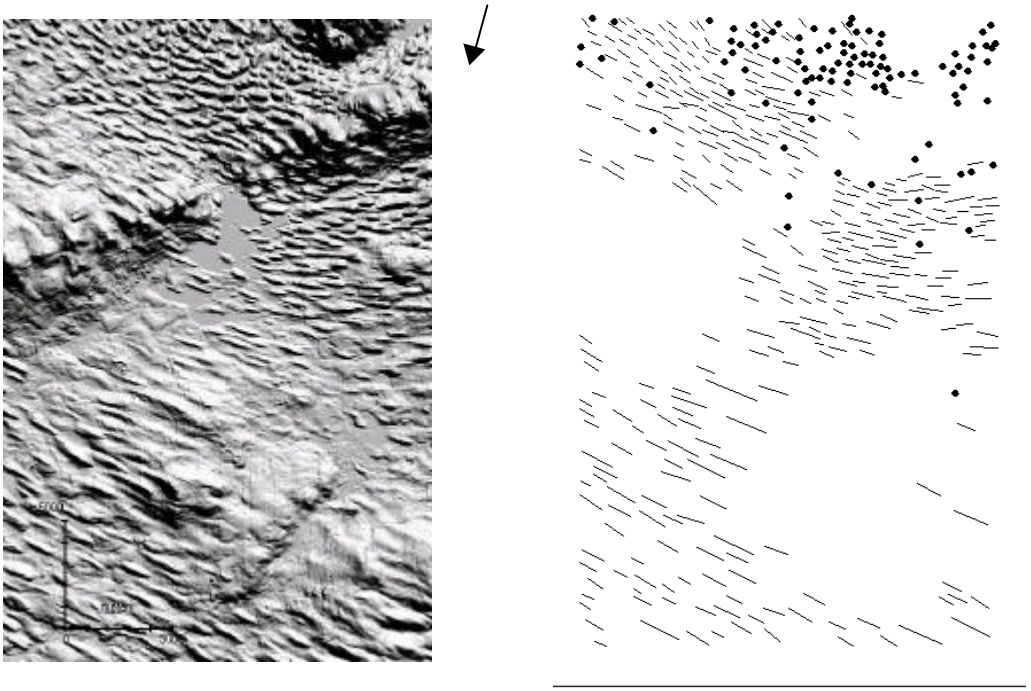

Figure 6.1 a and b Relief shaded DEM of Lough Gara, Ireland, (left) using an illumination azimuth orthogonal to the principal lineament orientation and glacial landforms mapped (right) from this image (lineaments represented as lines and hillocks points). Illuminated from 20º (© Irish Ordnance Survey).

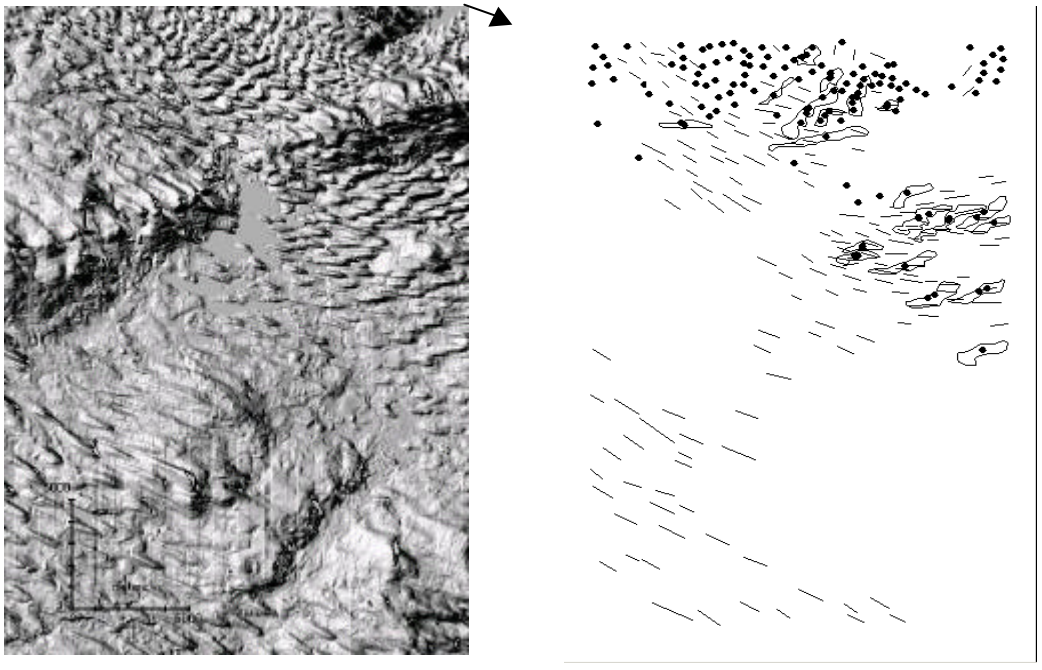

Figure 6.2a and b Relief shaded DEM of Lough Gara, Ireland, (left) using an illumination azimuth parallel to the principal lineament orientation and glacial landforms mapped (right) from this image (lineaments represented as lines and hillocks points). Illuminated from 290º (© Irish Ordnance Survey).

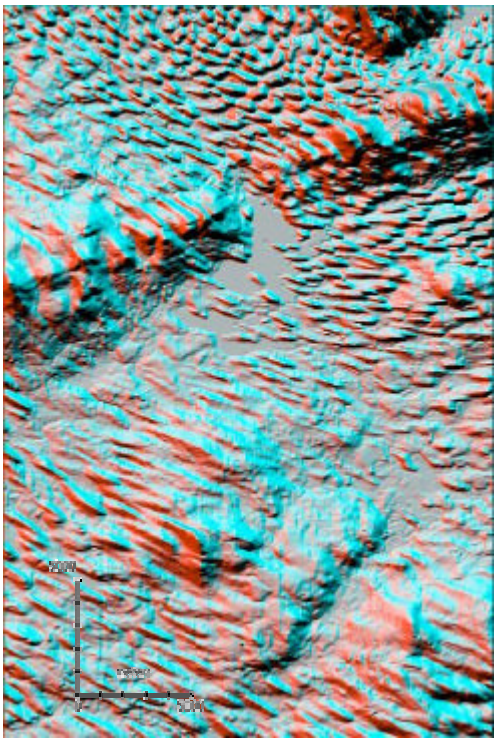

Figure 6.3 False colour composite co-visualisation of Lough Gara, Ireland, from a DEM, relief shaded parallel and orthogonal to the dominant lineament direction. The parallel image is coloured in green/blue and the orthogonal image in red (© Irish Ordnance Survey).

b. Statistical Analysis (Figure 6.4)

Geographic Information Systems (GIS) allow the exploration of differences and similarities between images using a variety of statistical methods. These can be used to isolate and emphasise traits or features from 2 or more input images. Methods include addition, subtraction, minimum, maximum and mean between different images. A log transform can also be used to emphasise low elevation detail (e.g. Guzzetti and Reichenbach, 1994), however this is relative within the study area (i.e. a global operator) and does not highlight smaller, localised, elevation variations (i.e. lineaments).

A common method applied in remote sensing is Principal Components Analysis, or PCA, which aims to describe the different image bands with new orthogonal axes. Essentially it compresses the multiple components (images) of the original data and creates a new set of axes along the line of maximum data variance. Once the pixels have been resampled onto their new co-ordinate system, they then contain more information that any other single band in the original data (Figure 6.5).

c. Combination Viewing (Figure 6.5)

Remote sensing software can load several images, *layered* on top of each other. It is possible to fade or flicker between these layers to facilitate a visual comparison; this technique can be used to jointly map two alternatively shaded DEMs as described in point (1).

d. Dynamic Illumination Variability (accompanying animated GIF file)

The orthogonal and parallel images introduced above illustrate two discrete views of the variability in landform representation within the continuous range from 0°-360°. Disc 1 provides an example of Dynamic Illumination Variability whereby the terrain is viewed using a constantly changing illumination azimuth. This provides a full, visual, depiction of landform representation change with azimuth.

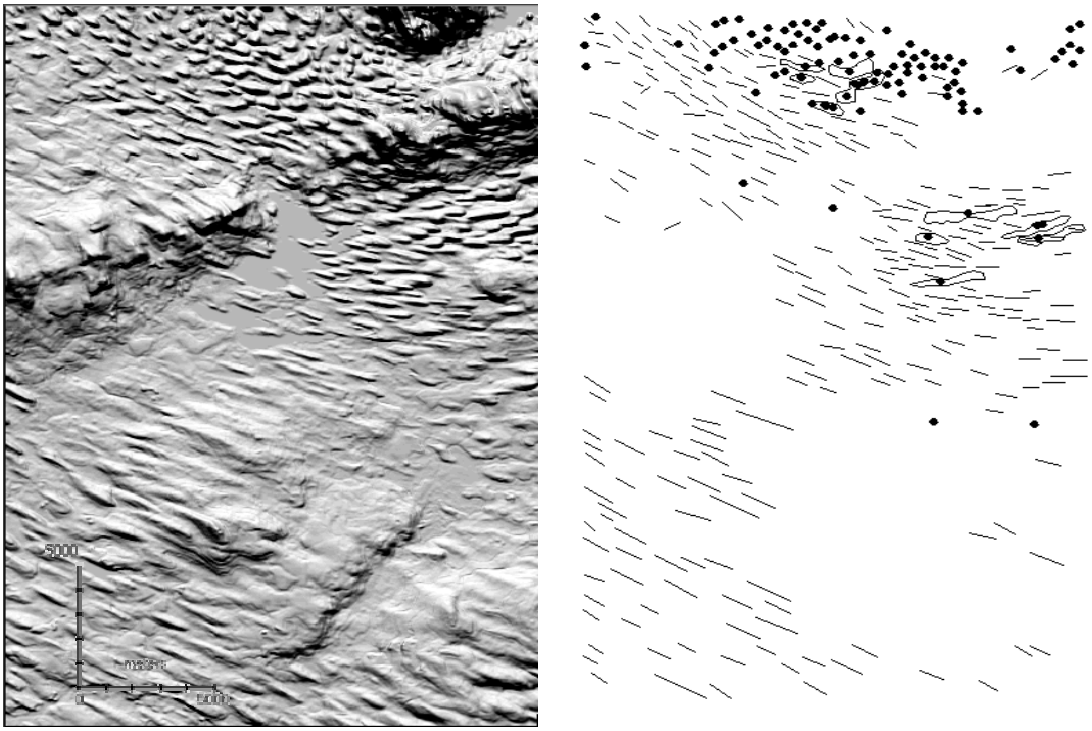

Figure 6.4 a and b Principal Component 1 of Lough Gara, Ireland, (left) produced from a DEM relief shaded parallel and orthogonal to the dominant lineament direction and glacial landforms mapped (right) from this image (lineaments are lines and hillocks points; © Irish Ordnance Survey).

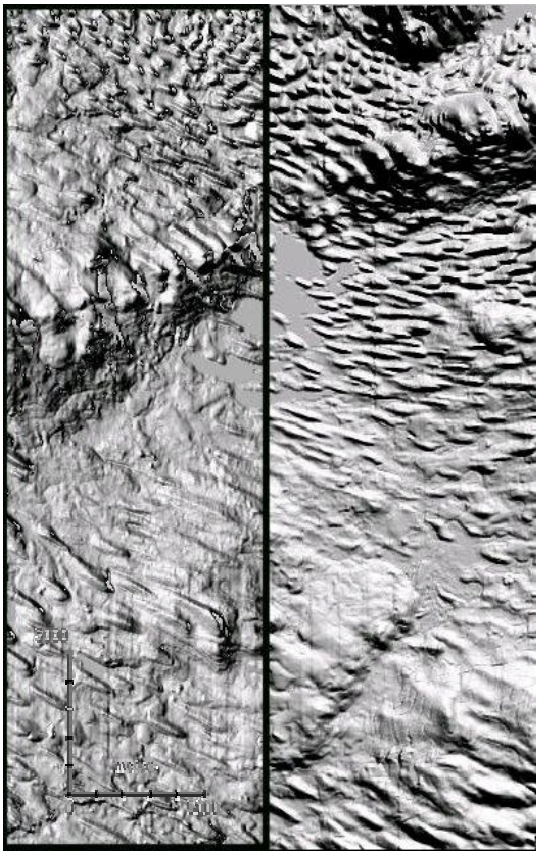

Figure 6.5 Combination Viewing of Lough Gara, Ireland, (left) produced from a DEM relief shaded parallel and orthogonal to the dominant lineament direction. The rectangle outlines the border between the combined images. In this approach it is possible for software to repetitively flip between the two image types whilst on-screen mapping is performed (© Irish Ordnance Survey).

3. Surface Derivatives

a. Gradient (Figure 6.6a)

Lineaments are topographically distinct as a result of their elevation difference from the surrounding terrain, which is a function of changes in surface gradient. Lineaments can therefore be highlighted by calculating gradient across a whole image. The brightness of each pixel is directly related to slope angle so that bright areas are flat and dark areas are steep.

b. Slope Curvature (Figure 6.7a)

Gradient alone cannot be developed to identify lineaments. Rather it is the change in gradient (i.e. curvature) that makes lineaments topographically distinctive, particularly in cross-section. Gradient changes from flat at the base, moderate up its sides and flat again on the top. Consequently curvature shows rapid changes at the base and the top (i.e. the concave slope at the base and the convex slope at the summit). Figure 6.7a shows that when this is calculated across a region, outlines and ridges are clearly discernible and not only are they highlighted but they are also normalised for elevation and, as the image is not illuminated, there is no azimuth bias. This is a major advantage.

4. 3D Viewing

a. Perspective Viewing (Figure 6.8b)

As a DEM provides elevation data, it is possible to overlay it with thematic information (e.g. map or satellite image) which can then be distorted with respect to elevation. This is typically used to view a landscape obliquely and generate “fly-bys”. This system is essentially the same as flight simulator software and allows a detailed examination of the landscape. Software is being developed that allows direct digitising from such imagery as a 2D or 3D GIS layer, however at present, this is not possible. In addition the process is time consuming and so does not lend itself to rapid mapping.

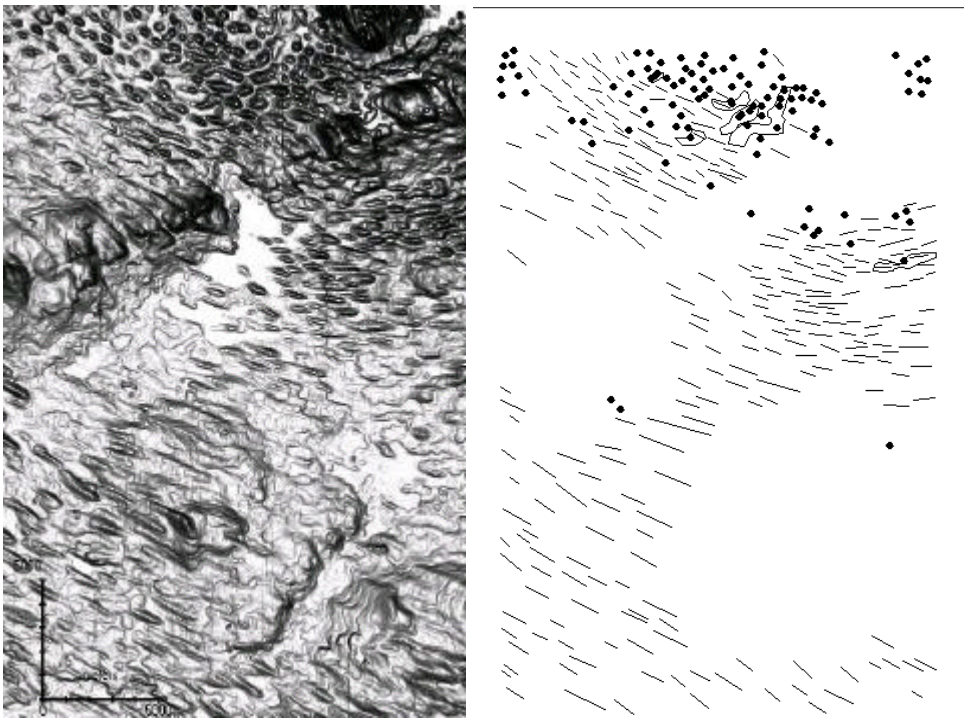

Fig 6.6 a and b An image showing gradient of Lough Gara, Ireland, (left) and glacial landforms mapped (right) from this image (lineaments represented as lines and hillocks points; © Irish Ordnance Survey).

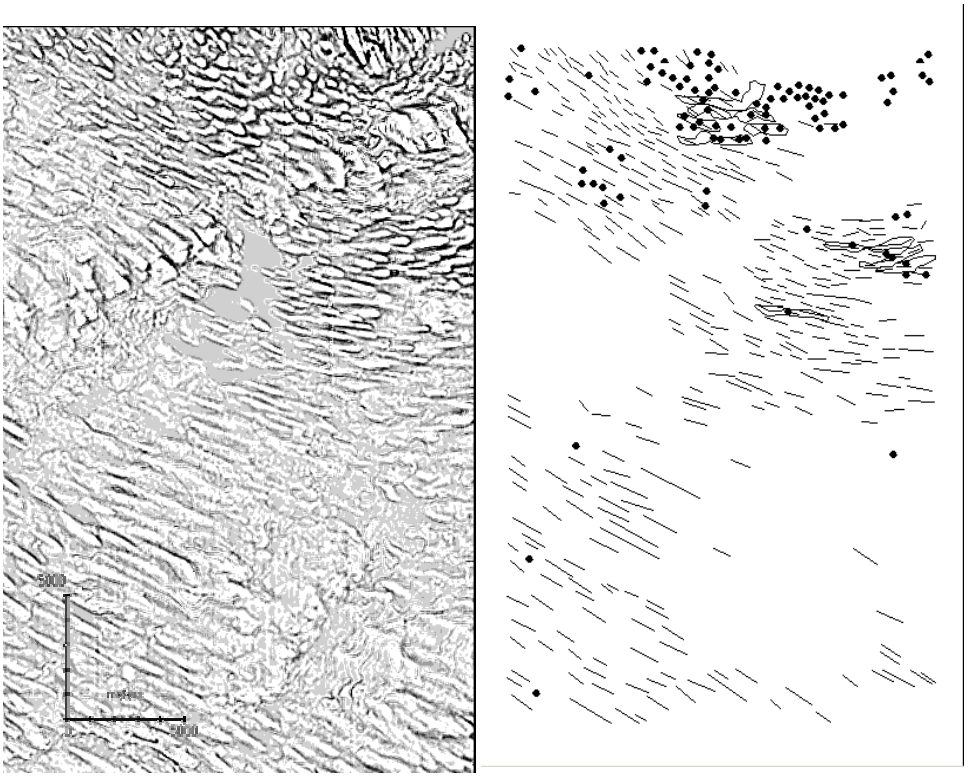

Figure 6.7 a and b An image showing Profile Curvature of Lough Gara, Ireland, (left) and glacial landforms mapped (right) from this image (lineaments are lines and hillocks points; © Irish Ordnance Survey).

b. Stereo Viewing (Figure 6.8a)

An anaglyph or stereo-pair image can be created from a DEM or stereo aerial photos and then overlaid with thematic data (as above). The DEM or aerial photo data is used to introduce parallax effects into the resultant image making it viewable as a 3-dimensional scene either as an anaglyph image (Figure 6.8a) or by using 3D viewing goggles. This system is essentially an entirely digital photogrammetry workstation. Like photogrammetry, digitising is possible. It is also possible to perform stereo perspective viewing and “fly-bys”, with the same caveats noted above.

5. Localised Spatial Enhancement

Traditional image contrast techniques are applied to a whole image and so operate globally. As a result many lineaments remain hidden as, although they are *locally* distinct, globally they are not. The following techniques are designed to apply locally based contrast enhancements to an image.

a. Adaptive Filtering (Figure 6.9a)

Adaptive filtering uses locally derived linear stretches to provide contrast enhancements. The input image is partitioned into windows, and the transformation parameters are calculated for each pixel as a linear interpolation of the stretch parameters for adjoining blocks. Fahnestock and Schowengerdt (1983) discuss this in more detail.

In this method (termed *local contrast stretch*) a simple, locally based, contrast enhancement is applied to each individual pixel, over a 3 by 3 window. Local topographic variations are selectively enhanced, using the following method, which is based upon 8bit data and therefore scaled to 256 data values:

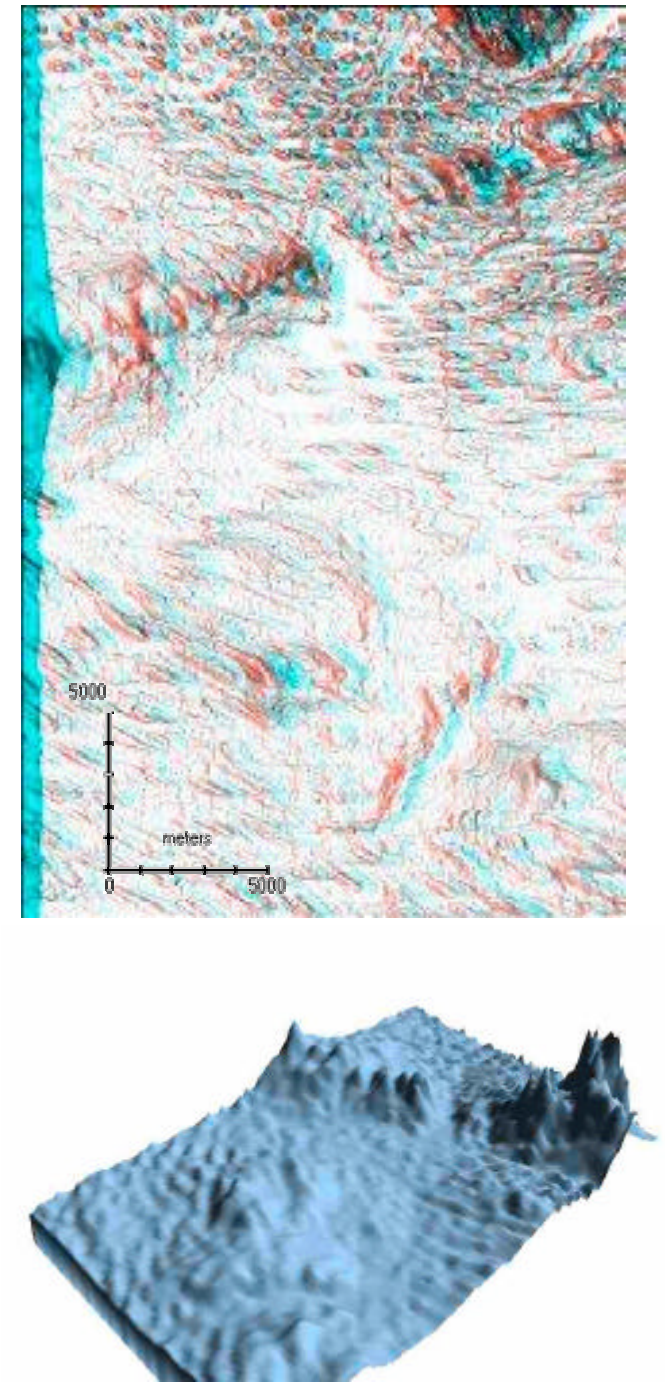

Figure 6.8a and b a. Anaglyph image created from a gradient map (please use attached glasses). b. Perspective view of Lough Gara, Ireland (© Irish Ordnance Survey).

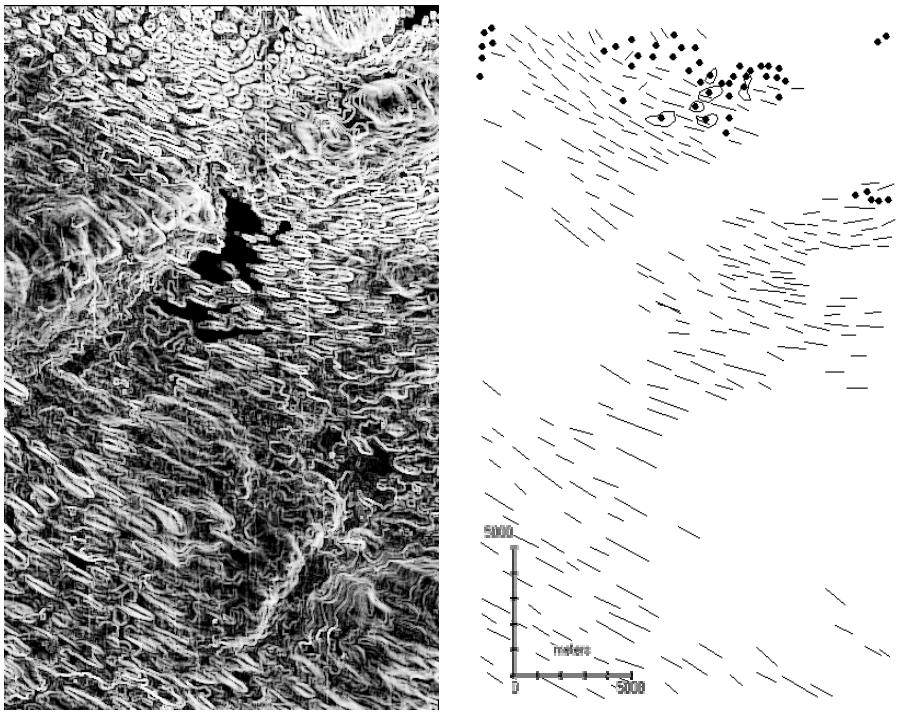

Figure 6.9 a and b Local contrast enhancements applied to the image of Lough Gara, Ireland, (left) and glacial landforms mapped (right) from this image (lineaments are lines and hillocks points; © Irish Ordnance Survey).

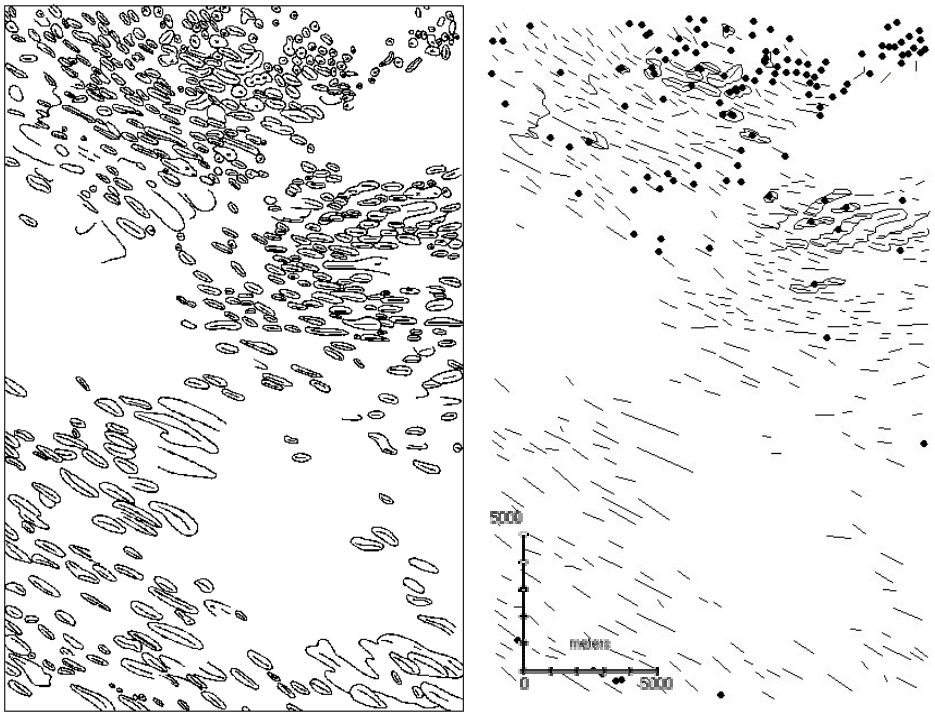

Figure 6.10 a and b Morphological map (truth) of all resolvable lineaments produced from the DEM of Lough Gara, Ireland (left) and the generalised lineament map derived from it (right).

$$x_{out} = y_{\min} - x_{in} . \frac{y_{\max} - y_{\min}}{256}$$

where

x_{out} is the output pixel value

x_{in} is the input pixel value

y_{min} is the minimum pixel value within the moving window

y_{max} is the maximum pixel value within the moving window

Figure 6.9a illustrates this approach using a 401x601 window.

b. Texture Filter

Texture filtering has traditionally been used to selectively highlight textural elements within VIR/IR imagery, although low pass, high pass and edge detection filters are more commonly used. These techniques have become prominent with the popularity of radar data. Textural information within gridded elevation data is typified by small, apparently random, changes in elevation. For lineaments these are spatially correlated so that texture filtering can highlight them. Irons and Peterson (1981) discuss optimised texture filters for a variety of different applications.

6.3 Method

In order to provide a comparative analysis of different DEM visualisation methods, a drumlinised area from the Lough Gara region of the Republic of Ireland was selected. This is the same region that was used in Chapter 5 for assessing the problems in mapping glacial lineaments from satellite imagery. The DEM was created by the Irish Ordnance Survey using high resolution (1:40,000) stereo aerial photography at a spatial resolution of 50m. They used *direct terrain extraction* to generate the DEM data values. In this method the aerial photography is scanned into the system and a stereo model generated. This is then used to calculate elevation using regularly spaced grid sampling. This moderate resolution DEM is able to resolve individual drumlins, although

cross-cutting patterns and smaller forms are difficult to distinguish. A brief discussion of this data can be found in §5.2.2.

The above 9 methods were initially assessed in order to disregard any that were unsuitable. The *False Colour Composite* method was unsatisfactory as the variation in colour distracted the eye from the underlying terrain making mapping difficult. *Combination Viewing* and *Dynamic Illumination Variability* were useful as interpretative tools and as a means of highlighting the azimuth bias, however there is currently no easy method by which mapping can take place using these techniques. The *3D Viewing* techniques allowed viewing in stereo, however the technical requirements and mapping difficulties are such that it is currently inappropriate for widespread landform mapping. Finally, of the local contrast enhancements the *texture filter* produced results similar to *slope curvature* and was therefore not considered. All processing, unless otherwise specified, was performed using Erdas Imagine™.

The remaining 5 methods were selected for testing:

1. **Relief shading** - in order to reproduce the variability introduced by alternate relief shading azimuths, three new images were created, relief shaded *orthogonal* (20º), *parallel* (290º) and *intermediate* (335º) to the principal lineament direction (290º). Increasing the amount of vertical exaggeration helped better visualise the landforms, however individual results will depend upon the method of relief shading implemented by the software in use.
2. **Overhead Illumination** - this was created in the same way as *relief shading*, except using a solar elevation of 90º.
3. **Principal Components Analysis (PCA)** – a standard PCA method was used, utilising the *parallel* and *orthogonal* relief shaded images.
4. **Slope Curvature** – this was calculated in ARC/INFO, which has been implemented using the method of Zevenbergen and Thorne (1987). A 3 by 3 low pass filter, followed by a histogram stretch using a low number of bins (less than 10 in this instance) was effective for visual highlighting. A standard deviation stretch using a value of 0.2 was also useful. The low pass has the effect of softening the contrast within the image which makes viewing easier. Both the standard deviation and histogram stretches

essentially highlight the extreme values within the image, providing good delineation of lineament outline or crest.

5. **Local Contrast Stretching** – the local contrast stretch performs a standard linear contrast stretch over a localised region as described above. The region (or locale) is pre-defined using a set window size and is dependent upon the resolution of the DEM and the dimensions of landforms that are being studied. A variety of different window sizes were explored and a 3 by 3 window was found to give the best results.

To allow absolute inter-comparison (see below) a measure of the landforms that are actually present within the terrain is needed. The morphological map (simply referred to as *truth*) created for the satellite image comparisons in Chapter 5 was used for this purpose (Figure 6.10a; see §5.2.1). This was compiled from break of slope mapping using multiple illumination azimuths and checked using stereo aerial photography (see §5.3.2 for further discussion).

The investigation then involved mapping all landforms present within the images produced by the five selected visualisation methods. Mapping was performed by one observer and observer variability is assumed to be minimal through consistency produced by this. To check for this, the orthogonal relief shaded image was mapped again at a later date and used as a set of control data. The results in §6.4 discuss this further. Simple line geometry was used for digitising lineaments, with polygons for spatially larger landforms and points for local summits in hummocky terrain.

The above images, and the lineaments mapped from them, are initially visually assessed through descriptive inter-image comparisons (§6.4.1). A comparison of the number of lineaments mapped, their orientation, length and coincidence is also provided (§6.4.2). Coincidence was assessed visually to account for errors by observer mis-digitisation.

6.4 Results

This section presents the qualitative and quantitative results of the image comparisons. The qualitative section provides a description of both the images

and the landforms mapped from them for each mapping approach, whilst the quantitative section presents summary statistics for mapped landforms.

6.4.1 Visual Image Inter-Comparisons

1. Truth Data (Figure 6.10a/b)

The morphological map shows a strong trend of lineaments oriented NW-SE, with longer lineaments in the southern area. A spread of lineaments oriented E-W is also noticeable. There is a strong concentration of hummocky terrain in the northern part of the map, with a few hummocky forms elsewhere. The northern half of the map also contains transverse ridges, often with lineaments overlying them. This map is taken to be the most accurate representation of the landforms present (i.e. “truth”) against which the other images are tested.

2. Orthogonal Illumination (Figure 6.1a/b)

The orthogonal illumination azimuth produces a detailed representation of the longer lineaments in the southern half of the image. It also revealed a large number of smaller, densely packed, lineaments in the northern and eastern parts of the image. The eastern area shows a change in lineament orientation from broadly SE to ENE, with these latter forms having a lower elongation ratio (i.e. fatter). The northern area also exhibits some of these “fatter” forms, including some circular hill forms generically termed “hillocks”. The topographic maps for the area suggest a thin drape of till over the southern area, a conclusion supported by the dominant bedrock ridge running NE to SW and in the extreme NE area. Note the irregular looking ridge in the SW corner which is actually a river terrace.

Mapping confirmed the existence of the dominant set of NW-SE orientated lineaments, with shorter forms in the northern and eastern areas. The ENE-SSW oriented lineaments in the eastern area and “hillocks” in the northern area were also identifiable and therefore mapped.

3. Parallel Illumination (Figure 6.2a/b)

The parallel illumination azimuth dramatically dampens the effect of all lineaments that were strongly represented in Figure 6.1a. This effect is particularly well demonstrated in the southern part of the image; many landforms are still visible, but their outline is indistinct and often represented as cuspate forms. Similar effects are apparent in eastern and northern parts of the image. However it is the “fatter” forms from the previous image that have dramatically changed shape and orientation. The eastern part of the image depicts composite lineaments making up larger, transverse, NE-SW trending landforms, termed transverse ridges. This effect is repeated in the northern part of the image, although the circular “hillocks” are still evident.

The mapping confirmed the visual appraisal. There were far fewer lineaments mapped, however there are a greater number of “hillocks” in the northern area and the addition of transverse ridges in the northern and eastern areas.

4. Intermediate Illumination (Figure 6.11a/b)

The intermediate illumination azimuth looks very similar to Figure 6.1a, although strongly represented landforms from that image are now less distinct. The transverse ridges in the eastern area (Figure 6.2a) are not evident, although their presence can be hinted at when compared to Figure 6.2a.

Mapping results appear very similar to those for Figure 6.1b, with a large number of lineaments oriented NW-SE. Again there are a number of “hillocks” in the northern area and an arc of lineaments in the eastern area.

5. Principal Components Analysis (PCA) (Figure 6.5a/b)

The PCA image would be expected to contain the essential elements of both input image (i.e. *parallel* and *orthogonal* relief shaded images), however the transverse ridges shown in Figure 6.5a are subtle such that an inexperienced observer would not identify them. Strongly represented landforms from Figure 6.1a are subdued and, in some cases, omitted, however the transverse ridges in the northern and eastern areas are visible although not as distinct as in Figure 6.2a.

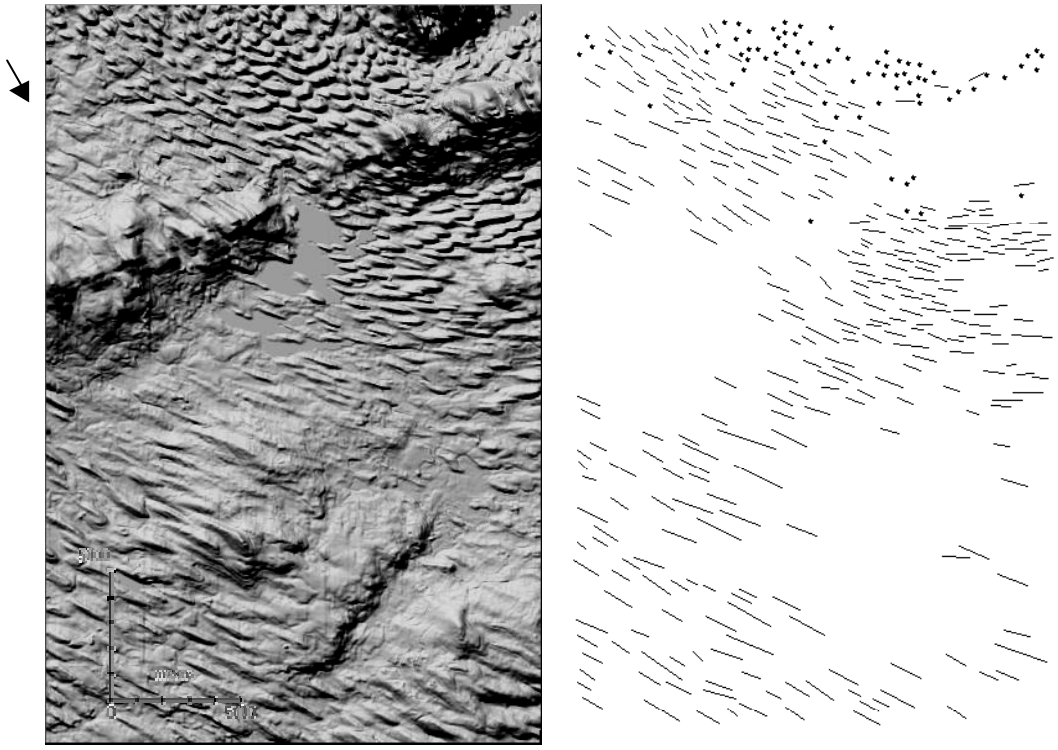

Figure 6.11a and b Relief shaded DEM of Lough Gara, Ireland, (left) using an illumination azimuth at 45º to the principal lineament orientation and glacial landforms mapped (right) from this image (lineaments represented as lines and hillocks points; © Irish Ordnance Survey).

Mapping clearly identified the strong NE-SW alignment of lineaments and the presence of some of the transverse ridges. There are also a large number of “hillocks” mapped in the northern area.

6. Gradient (Figure 6.6a/b)

Using overhead relief shading, initial viewing is favourable with distinctive shading of the landforms produced. Lineaments are clearly delimited and easy to map, again showing the predominance of fewer, longer, lineaments in the southern portion of the image, with smaller, narrower landforms in the NW. However the transverse landforms in the eastern area are less distinct, although, as with the *Intermediate Illumination*, their presence can be discerned when compared to the *Parallel Illumination*.

Mapping results are similar to both the *Parallel* and *Intermediate* illuminations showing the main NW-SE lineament trend, the arc of lineaments in the east and hillocks in the north.

7. Slope Curvature (Figure 6.7a/b)

The lack of azimuth bias in calculating curvature is clear and was therefore a good approach for mapping lineaments. There are hints of transverse ridges in the eastern and northern areas, however this is not visually strong and might be considered noise. The mapping results largely bear out the description above; there are fewer lineaments mapped when compared to other methods, however the same basic trends are still visible.

8. Local Contrast Stretch (Figure 6.9a/b)

Initial viewing appears confused, but close inspection of the image shows that many lineaments are clearly outlined, again highlighting the dominance of NE-SW oriented lineaments, as well as many hillocks in the north. Transverse landforms are not clearly outlined although a small number have been mapped in the north of the image.

6.4.2 Analysis of Landform Detectability

The quantitative results were gathered from image inter-comparisons carried out in the method described above. These results fall into three main sections discussing mapped landform totals, lineament length and orientation and inter-image lineament coincidence. The control data are discussed separately in §6.4.2.4.

Landform totals and lineament length/orientation are broad global measures that can be usefully used to compare and contrast the landforms mapped from the different visualisation methods. The former assesses completeness in terms of number of landforms, whist the second assesses the degree of similarity through descriptive statistics. It is also appropriate to consider locational similarity of mapped landforms and this is achieved by considering the degree of coincidence in lineament mapping between the different mapped data and truth.

Landform Totals (Table 6.1)

The simplest descriptive term is the total number of landforms mapped when compared to the total number of landforms present, so providing a measure of completeness for the lineaments mapped from a specific dataset. The *truth* shows a total of 442 lineaments mapped, with only *Slope Curvature* (361) and *Orthogonal Illumination* (374) having similar landform totals. *Intermediate Illumination* has a slightly lower mapped lineament total (338), whilst the *PCA* (271), *Parallel Illumination* (203), *Local Contrast Stretch* (267) and *Overhead Illumination* (273) are significantly lower. Total lineament length also provides a surrogate measure for number of lineaments, however it also normalises for segmentation of lineaments. This highlights that *truth* has a greater number of shorter lineaments. In this instance *Slope Curvature* and *Orthogonal* and *Intermediate Illumination* have greater total lengths. However it also highlights the low values of *Overhead Illumination*, *PCA* and *Parallel Illumination*.

Landform	Lineament	Hillock	Ridge	Total Lineament Length (km)
Slope Curvature	361	84	10	297
PCA	271	89	10	218
Orthogonal Illumination	371	101	0	289
Parallel Illumination	176	120	20	146
Intermediate Illumination	330	75	0	146
Local Contrast Stretch	267	45	0	234
Overhead Illumination	273	102	0	218
Truth	**442**	**109**	**25**	**263**
Control (Orthogonal Illumination)	382	117	0	260

Table 6.1 Total number of lineaments, hillocks and ridges mapped from the different visualisation methods. Total lineament length is also included.

The number of hillocks mapped are similar between all the visualisation methods, except *Local Contrast Stretch* which is substantially lower, whilst *Slope Curvature*, *PCA* and *Intermediate Illumination*, have slightly lower numbers mapped than for the other methods.

Finally, totals for number of transverse ridges mapped is variable with the *Intermediate Illumination*, *Orthogonal Illumination*, *Local Contrast Stretch* and *Overhead Illumination* having had none mapped. Some ridges were mapped on *Parallel Illumination, Slope Curvature* and *PCA*, with *Parallel Illumination* mapping nearly as many ridges as *Truth*.

In summary, *Orthogonal*, *Parallel* and *Overhead* are the best methods to identify lineaments, ridges and hillocks, respectively. However, *Curvature* data performs very well at identifying lineaments and satisfactorily for hillocks and ridges. The *Parallel Illumination* data performs well at identifying hillocks and ridges, but poorly for lineaments. The remaining images have different strengths and weaknesses but are unable to match the performance of the above two.

Lineament Length and Orientation

In addition to mapped landform totals, which provide an overview of the completeness of different visualisation methods, it is also appropriate to review lineament length (Table 6.2) and orientation (Table 6.3). These allow us to assess any differences in the characteristics of the landforms being mapped between approaches.

	Min	Max	Mean	Standard Deviation
Orthogonal Illumination	307	2604	780	352
Parallel Illumination	354	2136	829	292
Intermediate Illumination	317	2602	843	363
Local Contrast Stretch	381	2760	887	382
Overhead Illumination	326	3026	851	350
PCA	332	2340	806	323
Slope Curvature	285	3063	827	381
Truth	**172**	**2758**	**595**	**331**
Control (Orthogonal Illumination)	347	2584	798	338

Table 6.2 Minimum, Maximum, Mean and Standard Deviation calculations for **lineament length** (in metres) from the different visualisation methods.

The results for lineament length show consistency between visualisation methods with the minimum and maximum values similar. In comparison to truth, Overhead Illumination and Slope Curvature have slightly higher maximum values, whilst Parallel Illumination has a slightly lower value. The mean is consistently higher for all methods. The previous section has already demonstrated that there are more lineaments mapped in Truth and, generally these tend to be shorter (and hence the smaller minimum value).

The results for lineament orientation are more varied, a reflection of the azimuth bias present in the relief shaded images. The greatest variation in the northmost value comes from Parallel Illumination and Overhead Illumination, with relatively north and south values respectively. The southmost values are similar, although

truth has the most northerly value. The vector mean and vector strength are all similar, bar the vector strength for Parallel Illumination and Truth which tend to be lower, a reflection of their extreme values.

	Min	Max	Vector Mean	Vector Strength
Orthogonal Illumination	51.3	142.8	111.7	0.974
Parallel Illumination	13.4	147.5	109.0	0.948
Intermediate Illumination	61.0	149.8	111.0	0.976
Local Contrast Stretch	45.0	149.9	111.6	0.971
Overhead Illumination	71.6	147.5	111.3	0.970
PCA	50.7	145.3	111.1	0.971
Slope Curvature	34.7	147.0	113.3	0.972
Truth	**39.6**	**160.6**	**115.7**	**0.954**
Control (Orthogonal Illumination)	22.3	155.0	112.0	0.973

Table 6.3 Minimum, Maximum, Vector Mean and Standard Deviation calculations for **lineament orientation** (in º) from the different visualisation methods.

Inter-image Lineament Coincidence (Table 6.4)

Coincidence was assessed visually with lineaments required to be within approximately 200m of each other and not deviate by more than 15º, although consideration was given to a greater deviation due to azimuth biasing if the lineaments were crossing. Visual assessment was selected as the optimum method as consideration could be given to any deviations as a result of poor digitising. The results for coincidence between all the different visualisation methods is given in Table 6.4. The table also includes a comparison with the control data set.

To help visualise these comparisons, Figures 6.12 and 6.13 provide overlays of the four main methods (Slope Curvature, Gradient, PCA and Local Contrast Stretch) with truth. As each individually relief shaded image (parallel, intermediate and orthogonal) suffers from azimuth biasing, it is not necessary to visually appraise lineament coincidence between these.

	Slope Curvature	*PCA*	*Orthogonal Illumination*	*Parallel Illumination*	*Intermediate Illumination*	*LocalContrast Stretch*	*Overhead Illumination*	*Truth*	*Control (Orthogonal Illumination*
Slope Curvature		63	60	64	60	81	81	45	
PCA	74		71	68	71	68	71	53	
Orthogonal Illumination	87	85		66	81	84	86	64	87
Parallel Illumination	52	45	40		40	52	52	33	
Intermediate Illumination	87	87	84	72		80	81	61	
LocalContrast Stretch	64	70	60	69	64		78	53	
Overhead Illumination	61	72	63	70	65	80		50	
Truth	79	83	88	80	81	82	81		
Control (Orthogonal Illumination)			79						

Table 6.4 Coincidence of landforms using different visualisation methods, expressed as a percentage of the total number of lineaments mapped. For example, 85% of lineaments mapped from the PCA image were coincident with those mapped from the Orthogonal Illumination image.

Figure 6.12
a Overlay of lineaments and hillocks mapped from Local Contrast Stretch (blue) and Truth imagery (red).

b Overlay of lineaments and hillocks mapped from Curvature (blue) and Truth imagery (red).

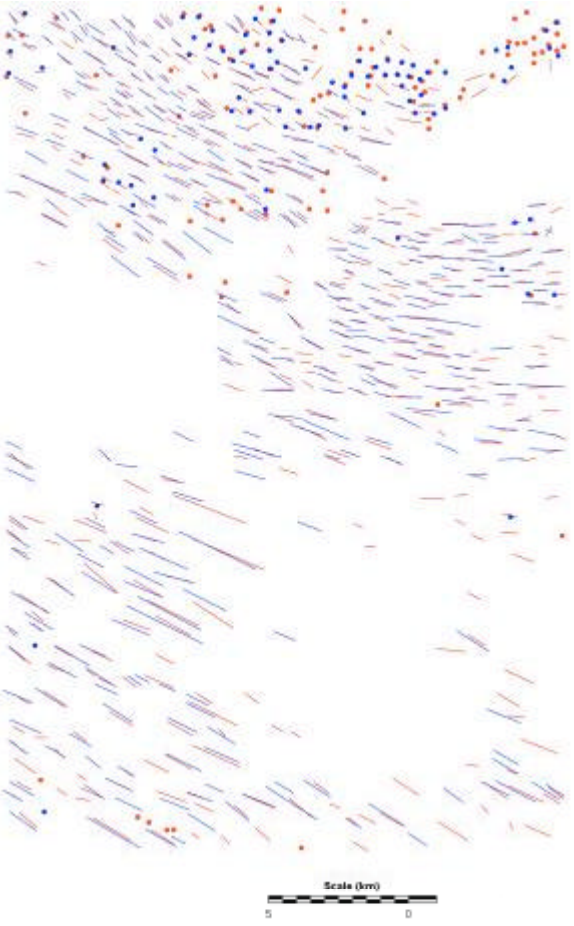

Figure 6.13
a Overlay of lineaments and hillocks mapped from PCA and Truth imagery.

b Overlay of lineaments and hillocks mapped from Gradient and Truth imagery.

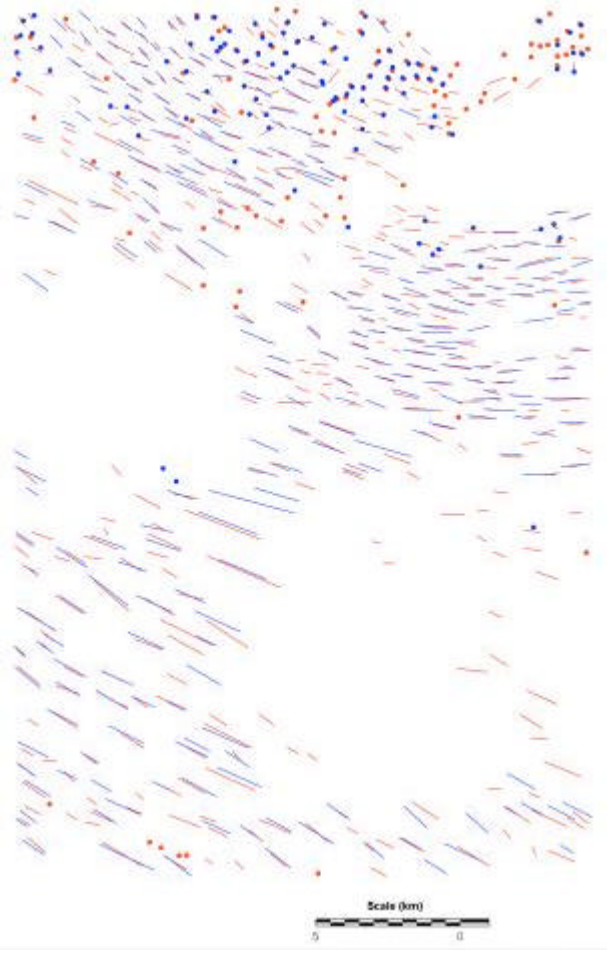

In assessing the results displayed in Table 6.4 it is most appropriate to review coincidence with truth (greyed). The penultimate column shows the degree of *locational completeness*. This depicts the lineaments mapped by truth which are locationally coincident with the different mapping methods. The Orthogonal and Intermediate Illumination perform better than the other methods and Parallel Illumination performs noticeably worse.

The penultimate row highlights what can be considered an *error rate*. This depicts the lineaments mapped by the different methods which are locationally coincident with truth. Given truth is considered our complete dataset we would expect these values to be high and, indeed, all of them are approximately 80%. The following section further discusses mapping error by considering the control data set.

Control Data

In order to test for variations in the ability and consistency of the operator a control dataset was created. This involved re-mapping landforms represented on the *Orthogonal Illumination*. Chapter 4 highlighted the poor results that have been obtained in assessing the reproducibility of lineament mapping *between* individual operators, however the emphasis is on reproducibility by a single individual. This is important in terms of assessing the results and conclusions drawn from them, as well as showing that individuals can consistently map over large areas.

A qualitative comparison of the control data shows a strong visual consistency (Figure 6.14), with a small number of localised inconsistencies. In terms of landform totals (Table 6.1) there is very close agreement between the two datasets. The control dataset has 2% more lineaments and 17% more hillocks. The close agreement between lineament totals shows strong consistency between mapping sessions, although the number of hillocks mapped increased in the control dataset. The results for lineament orientation and length are again very similar, although the values for northmost and southmost orientation are

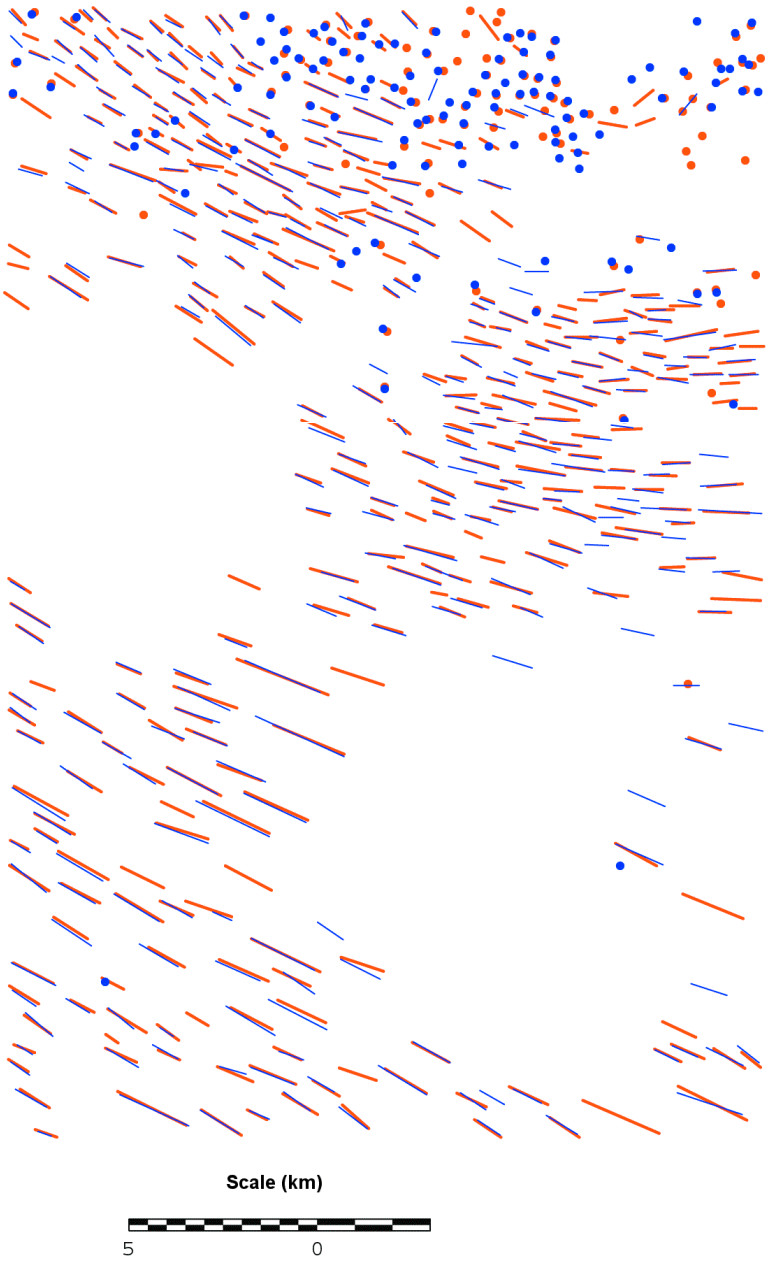

Figure 6.14 Overlay of lineaments and hillocks mapped from Orthogonal and Control imagery.

different due to several lineaments digitised differently between interpretations. The coincidence between mapped lineaments (Table 6.4) also shows good consistency with an average 83% coincidence.

Consistent mapping requires a fixed and rigorous method in identifying and delimiting individual features. This usually requires several different iterations in the mapping process, as well as much concentration. If the mapping process is divided between several operators then it is important that they can identify individual landforms and that they are consistent in this through the use of specific definitions of these landforms and the methods used to identify them.

It is probable that general mapping programmes will have lower rates of coincidence by individual operators. Such inconsistencies are unfortunately inherent to visual mapping and require that a rigorous approach to the mapping process is taken. However it must be born in mind that, for glacial reconstructions, general lineament trends are the most important result and inconsistencies can be accepted as long as they are randomly distributed across the image rather than systematically.

This section has attempted to show that operator variability is minimal, however even when larger variations are evident they should be randomly distributed. In contrast, many of the relief shaded visualisation methods implicitly incorporate selective bias which has a more drastic result on the interpretation of mapped glacial landforms and it is therefore more important to select an appropriate method of mapping.

6.5 Recommendations

The single most important conclusion to draw from the above results is that, although the data used for geomorphological mapping can generally be considered consistent (i.e. DEMs), the methods by which they are used to perform such mapping are not. It is therefore possible to introduce bias' into these maps that make them inconsistent. Strong landform assemblages will be readily apparent regardless of the method used to visualise them. However it is subdued landforms that are of particular importance to the glacial researcher as

they can be informative about the previous state of the landscape in relation to prior glaciations and, as a result, provide information about landscape change through time. *Observation* is the key to environmental understanding, and we are obliged to observe in an impartial, appropriate and consistent manner.

More generally, there are a variety of methods that can be used to visualise landforms from a DEM, each with their own advantages and disadvantages. Relief shading is the most common method by which this is achieved. Most general texts suggest illuminating from the NW as this provides a more "natural" means to view the data. However it is when illuminated from an orientation normal to the dominant lineament direction that the most visually pleasing results are obtained. Several authors have commented on the bias that *may* be introduced by single azimuth illumination (e.g. Graham and Grant, 1991 and Lidmar-Bergström *et al*, 1991) and as such it is suggested that two illumination angles, orthogonal to one another, and parallel and normal to the dominant lineament orientation, are used.

The results indicate differences in the landforms mapped from the different visualisation methods, such that this is an important consideration in any future mapping exercise. All datasets pick out the strong NW-SE lineament trend, however it is the more subtle ENE-SSW transverse ridges that are difficult to detect.

From a methodological viewpoint, Gradient, Slope *Curvature* and *Local Contrast Stretching* are the most preferable methods as they provide an unbiased representation of the surface. *Slope Curvature* performs very well, although it is unable to fully represent the variety of orientations of the transverse ridges. *Gradient* provides a visually appealing image, however it is unable to provide a satisfactory level of mapping. Although the *Local Contrast Stretching* is a good idea the resulting imagery is unsatisfactory.

Given that the *Parallel* and *Orthogonal Illuminations* are used to compile the landforms mapped in *Truth*, a combination of these images (the *PCA* image) should have great utility. Unfortunately the transverse ridges depicted in *PCA*

are sufficiently subtle as to prove difficult to map. Therefore this method has proved unsatisfactory and the individual *Parallel* and *Orthogonal Illuminations* are incomplete. The *Intermediate Illumination* is simply a compromise between these two illumination azimuths and is subsequently unsuitable.

In conclusion, all the single image methodological approaches are unsatisfactory and provide an incomplete visualisation of the actual terrain being mapped. This work has been unable to find a single image type that offers both no azimuth bias and yet portrays the landscape optimally. The advent of cheap, high resolution, readily available global DEM data is rapidly approaching and methods to make best use of this resource are needed. Given the good representation of the dominant lineament direction by *all* methods, the most useful results will be obtained by illuminating the DEM *parallel* to the dominant lineament orientation. This should have the effect of visualising these lineaments, as well as more subtle landform remnants within the environ, so providing a means to a more complete and rapid mapping of the desired region. This can be aided by dramatically increasing the vertical exaggeration of the DEM such that small elevation changes are readily apparent. Clearly if an accurate geomorphological map is required this will not suffice. It is therefore preferable to begin mapping with a bias free visualisation and *Slope Curvature* is best suited to this task. This can then be supplemented with further mapping from *Parallel* and *Orthogonal Illuminations*. The following section goes on to apply the visualisation methods, developed above, to a case study in order to learn the best compromise.

6.6 Case Study – Demonstration of landform mapping from a high resolution DEM of the Lake District

6.6.1 Introduction

The above sections have outlined the different methods used to visualise DEM data. This section aims to provide a demonstration of this methodology applied to the mapping of landforms from a high resolution DEM.

In selecting an area to apply the methods developed in this chapter, it was decided that this should incorporate the most difficult elements that are likely to be encountered during mapping. These include:

- a large area
- lineaments of a wide variety of sizes
- a mixture of different bedform shapes
- intermixing at the surface with geological structure
- high, variable, relief
- multiple ice flow directions incorporating cross-cutting

A large area (8,900km^2) of previously glaciated terrain located around the Lake District, United Kingdom, was selected (Figure 6.15) as it incorporates all of the elements noted above. In addition, there has been some field mapping performed within this area (e.g. Mitchell, 1994, Riley, 1987) and these are discussed later. The DEM used was the Ordnance Survey Panorama© dataset. This is 1:50,000 scale DEM that has a spatial resolution of 50m and was produced from original contour data (height accuracy of ±3.0m; Ordnance Survey, 1995). The Panorama© data is freely available to the British academic community for research and teaching purposes and its resolution is representative of the type of DEM data that will shortly be available globally. It has been discontinued as a commercial product and there is currently no direct replacement. Using the visualisation techniques outlined above, landform mapping was performed. The mapping process follows the same techniques used earlier in this chapter and outlined in §6.3. The landforms mapped during this exercise have been used to produce a subglacial bedform map of the Lake District (located on the inside cover). This represents the most complete glacial landform mapping covering the entire Lake District. Although partially covering areas that have already been field mapped, it identifies a considerable amount of previously unmapped landforms.

6.6.2 Visualisation Methods

Given the demanding nature of the terrain that was being mapped, a variety of visualisations and mapping methods were reviewed in order to achieve the best results. These were based upon the recommendations developed in §6.5. After

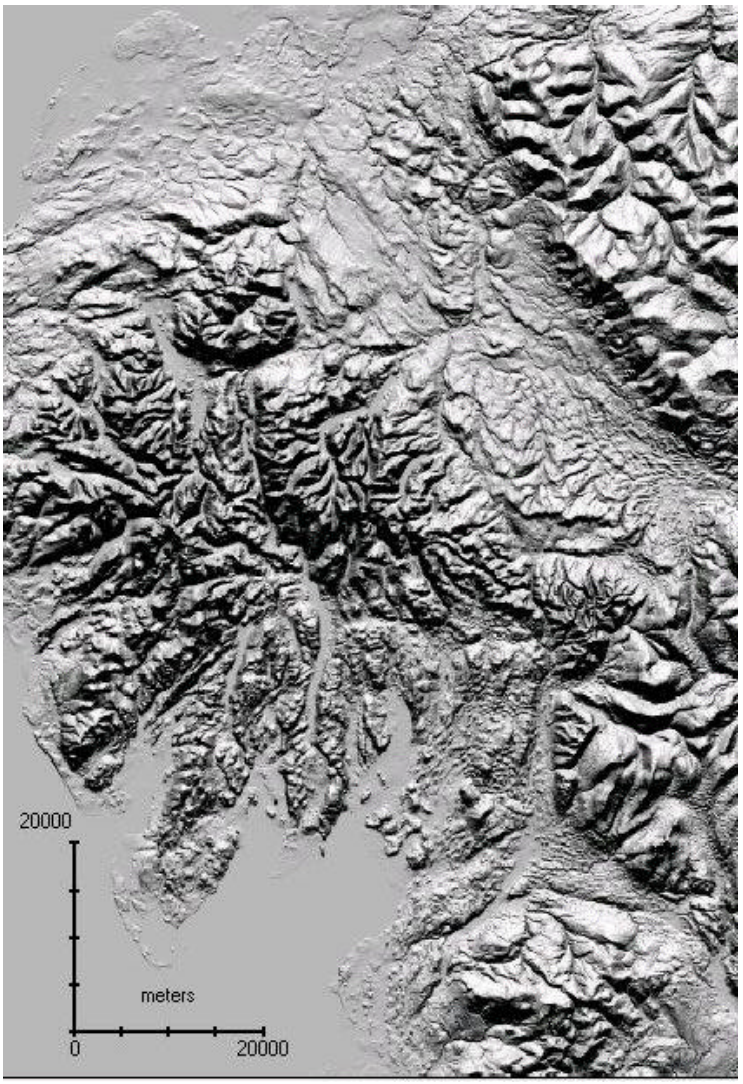

Figure 6.15 a (top) Relief shaded DEM data of the Lake District, United Kingdom. Relief shading is from the north, parallel to southerly dominant lineament direction (©Ordnance Survey).

b (bottom) Zoomed section of figure a. In the north central region are broadly SW trending lineaments, whilst the east central region contains a mixture of irregular bedforms and hummocky terrain.

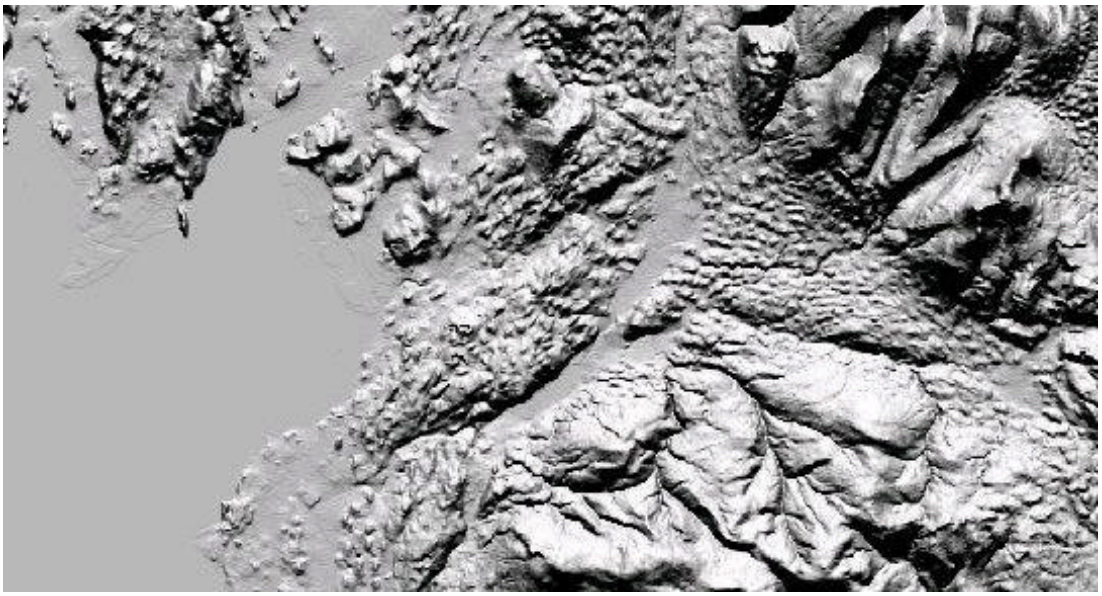

initial exploration of the terrain, it was ascertained that the dominant lineament direction was southerly, although there were areas where there were easterly and south-easterly elements. Parallel (Figure 6.15) and orthogonal (Figure 6.16) relief shaded images were generated. These were the principal images used for mapping and were excellent at identifying the predominant lineaments in the image, as well as other, less common, bedforms. Depending upon the principal orientation of the bedforms being mapped, either the parallel or orthogonal images were used. After the first-pass of mapping, the latter image was used to check for other bedforms not readily apparent on the first image. Additionally, gradient and profile curvature images (Figure 6.17) were generated to aid the overall mapping process.

Selecting images with appropriate relief shading becomes difficult when there are multiple lineament orientations, however the above approach works well. Of more concern to consistency in the mapping process is the presence of geological structure and high relief. The former can be mitigated against through the aid of geological maps to avoid mapping structure as lineaments. The high relief of the Lake District was more problematic when mapping from relief shaded images due to the shadows cast into valley areas (Figure 6.18a). Although an obvious problem, it is difficult to remove. One solution is to increase the illumination elevation angle (Figure 6.18b) such that it comes closer to overhead illumination, however this reduces the benefit of emphasis of less-well delineated forms within the landscape. A second solution is to change illumination azimuth by 180º to illuminate areas that were previously in shadow (Figure 6.18c). This worked well, however it adds a further two images that then require viewing. In addition, some observers may find it difficult to map as it may have the optical illusion of inverting the landscape, although this can be mitigated against by turning the image upside down.

One of the limitations of relief shading noted in Chapter 5 was the assumption of an homogenous, specular, surface. The relief shaded scene therefore visualises high reflectance from all surfaces. This has the effect of removing shadow from areas of high reflectance and therefore making bedforms difficult to map, an inverse to the problem noted above (Figure 6.18a). Lowering the

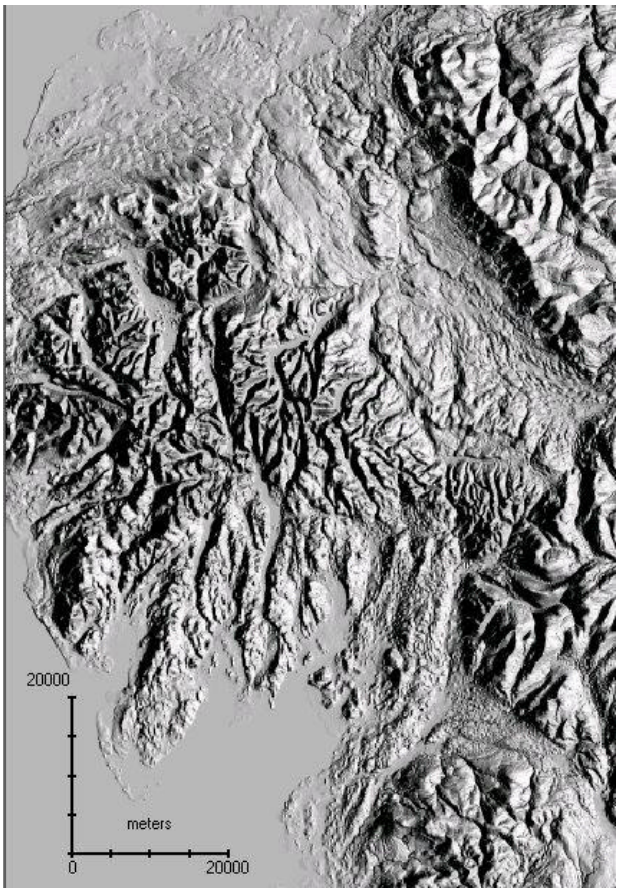

Figure 6.16 a. (top) Relief shaded DEM data of the Lake District, United Kingdom. Relief shading is from the east, orthogonal to dominant lineament direction (©Ordnance Survey).

b (bottom) Zoomed section of figure a. In comparison to 6.15b the lineaments in the north central region are strongly defined, whilst the bedforms in the east central region appear to composed almost entirely of hummocky terrain.

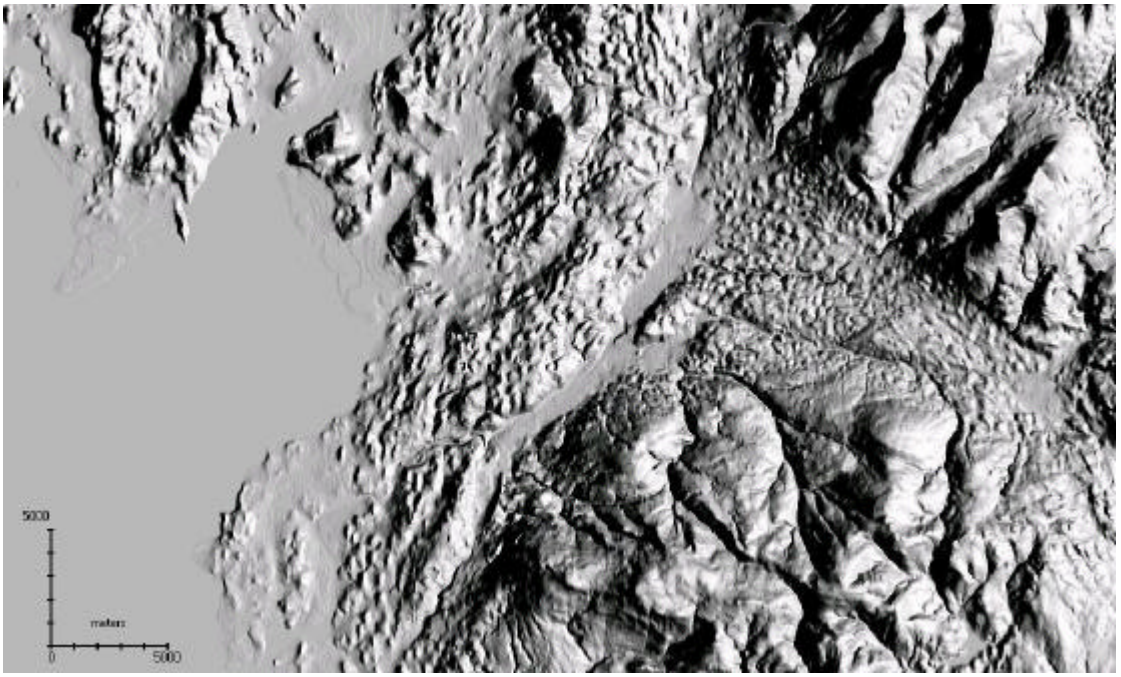

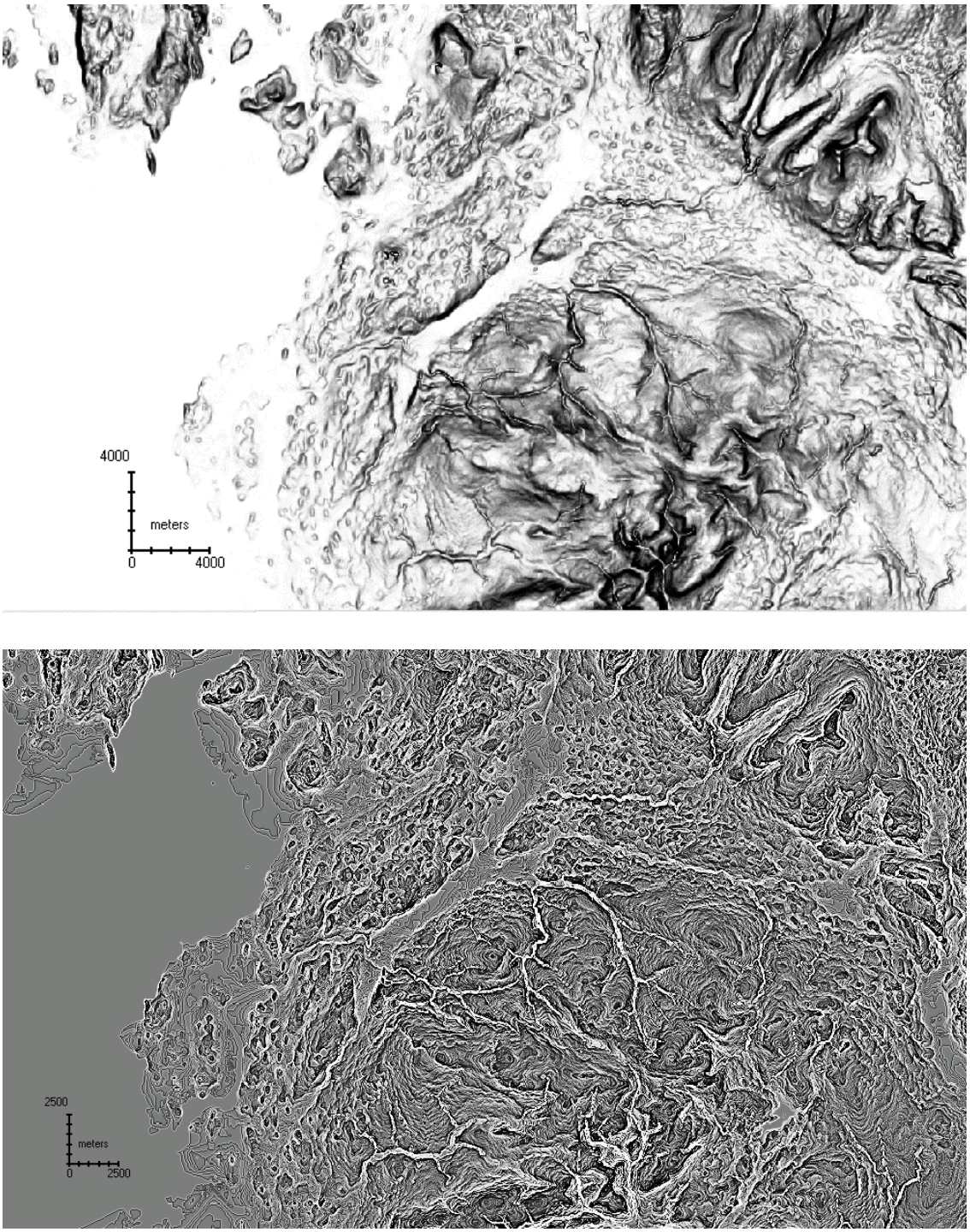

Figure 6.17 a. Gradient calculated from the Lake District DEM data (top). The principal landform elements appear similar to those using orthogonal shading. b. Profile curvature calculated from the Lake District DEM data (bottom). Although more difficult to interpret there is a lot of detail present.

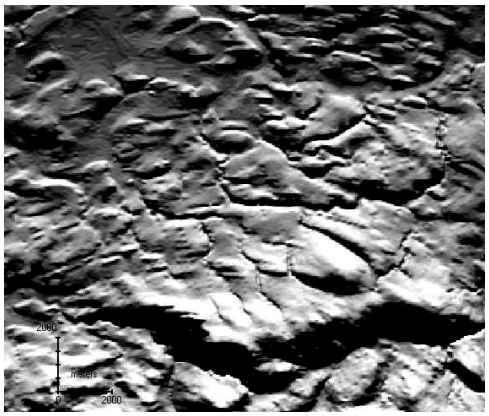

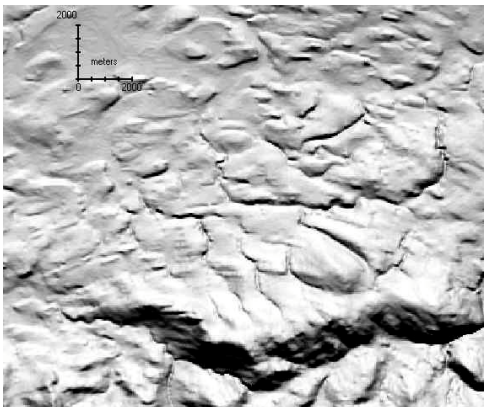

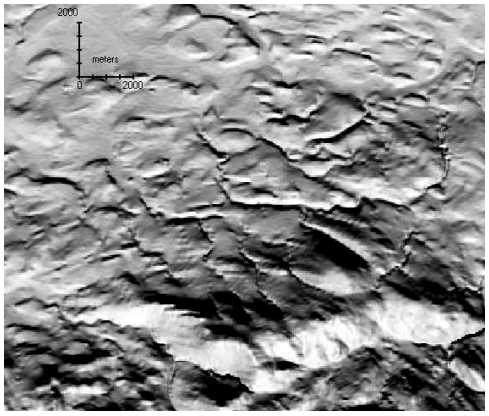

Figure 6.18 a,b,c Relief shaded DEM's of the Lake District, illustrating the problem of shadow. A standard relief shaded image (illumination from the north with mid-illumination elevation; top left) has landforms hidden in the shadow on the south side of the main bedrock ridge. High illumination elevation (top right) solves this problem, but then obscures bedforms on the north side of the ridge through high reflectance. Relief shading from the south (bottom) can also mitigate this problem, however some observers may need to invert the image (©Ordnance Survey).

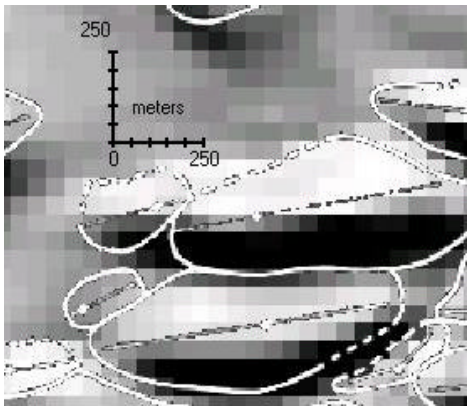

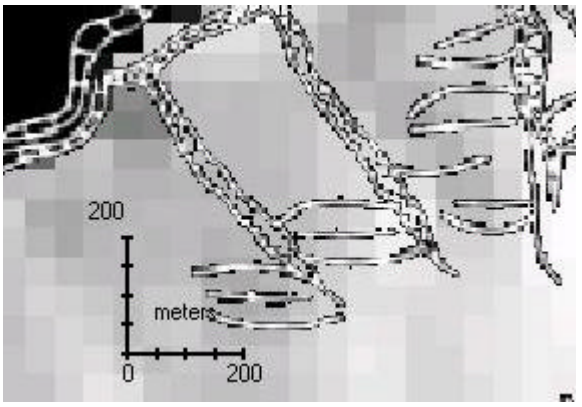

Figure 6.19 Relief shaded DEM (left; shaded from the north) overlaid with field mapped data (Riley, 1987). Large lineaments are clearly visible, whilst smaller ones are not. A second relief shaded DEM (right; shaded from the north) overlaid with field mapped data (Mitchell, 1994) showing that spatially large lineaments may not be visible. In this case the relief of lineaments is too small to be detected by the DEM. (©Ordnance Survey).

illumination elevation angle helps mitigate against this, but then puts other areas of the image in shadow such that they cannot be mapped from (Figure 6.18b).

One final area of difficulty is concerned with the resolution of the DEM. Horizontally, the OS DEM has a pixel size of 50m. In practise, mapping landforms less than ~200m in length is difficult (Figure 6.19a). The vertical resolution of the OS DEM is based upon contours from the original 1:50,000 map series which have an interval of 10m. Clearly this will not be sufficient for lineaments with a low height as they will not be delineated (Figure 6.19b), even if they are spatially extensive.

6.6.3 Mapping Results

This section briefly presents the mapping results of the case study for the Lake District, using the DEM and mapping techniques described above. The pullout map (back cover) displays the lineaments, transverse and circular/ovoid bedforms that were mapped during this process. Immediately noticeable are the lineaments in the north that tightly curve around the northern extent of the Lake District mountains. They display parallel conformity such that they appear to make up one contiguous set of lineaments. This continues south-east towards the eastern edge of the area. The density of lineaments, in comparison with the rest of the area, is relatively low. There are few hillocks, other than on the outer northern fringe. There is also a small set of lineaments oriented towards the north-east.

The eastern fringe of the area is a region of very dense bedforms, including lineaments intermixed with hillocks and irregular shapes. Initially it might appear that the lineaments oriented N-S join with these, however closer inspection shows that some lineaments are oriented at up to 90° to one another. The irregular make up of bedforms in this area suggests that there is a mixing of different bedforms from different flow events and this is supported by the presence of cross-cutting lineaments. Indeed, lineament orientations suggest three main sets broadly oriented south-east, south and east.

The southern portion of the image is composed of a mixture of easterly and northerly oriented lineaments, intermixed with many hillocks and irregular shaped forms. Unlike other parts of the area, lineaments encroach upon and traverse across areas of relatively high relief. This is particularly apparent in the areas previously field mapped by Mitchell (1994; Figure 6.19b). It also shows that in these upland regions, at least, there are many smaller bedforms that are unresolvable by the OS Panorama© DEM data (the following section discusses this in more detail).

Given that lineaments were actively being formed at high elevations, it is surprising that there is a band where no landforms have been mapped separating the north and south. This apparent absence of lineaments is possibly due to them being undetectable by the DEM at the current resolution. Further investigation would be required to confirm this.

Closer inspection of the easterly oriented lineaments suggest that these can further be split into two separate groups. The eastern and central areas of the south, have lineaments oriented in a south-easterly direction that, in at least one location, cross-cut with easterly oriented lineaments. The easterly oriented lineaments continue into the central region and intermix with the southerly oriented lineaments. This latter group appear consistent with those from the northern region. The south central and easterly areas are composed of heavily deformed transverse ridges and hillocks which are indicative of re-orientation of landforms within this area by later ice flow events.

This section has described the basic patterns evident from the landform mapping presented earlier. It also highlights interesting features within the dataset that can indicate different flow stages and later be used to interpret the ice flow evidence. Chapter 7 goes on to provide techniques to aid in the preparation of lineament data for interpretation. This case study is explored further in that chapter.

6.6.4 Comparison with Field Mapping

Due the abundance and quality of lineaments, in comparison to other areas within the UK, the Lake District has been the focus for several mapping exercises. These include Hollingworth (1931), Raistrick (1933), Burgess (1979), Vincent (1985), Riley (1987), Arthurton (1981, 1988), Boardman (1981), Whiteman (1981), Mitchell (1994) and Brandon (1998). Riley, Mitchell, Whiteman and Boardman produced detailed morphological maps, whilst British Geological Survey (BGS) memoirs produced by Burgess, Arthurton and Brandon all contain maps of drumlin location and orientation. In addition, these data have been incorporated into a *generalised* glacial landform map of the UK through the BRITICE project (Clark, 2002). It is therefore appropriate to compare the mapping performed in this thesis, with those of previous exercises. This will focus on a comparison of field mapping with the DEM and the data mapped from it.

Moderately detailed mapping was performed by Hollingworth (1931), who covered the Eden Valley and Solway Basin, and Raistrick (1933), who reviewed the area around Settle. Vincent (1985) provided a general description of the area immediately around Morecambe Bay. In all cases the broad orientation of lineaments is matched by that of the DEM mapping.

Burgess (1979), Arthurton (1981, 1988) and Brandon (1998) all produced summary drumlin location maps in the geological memoirs accompanying BGS 1:50,000 map sheets. Drumlin mapping is not within the direct remit of the BGS and therefore the quality and methods employed is dependent upon the individual members of the survey. The above authors could have used satellite imagery, topographic maps or aerial photography, referenced to a field based overview, to perform their mapping. Detailed morphological mapping is unlikely given the time consuming nature of the process. Only Brandon (1998) provided detailed mapping (covering the Lancaster region), whilst all the remaining authors performed drumlin crest mapping.

Burgess covered the Brough region. The mapping is very general and could well have been performed directly from topographic maps. It covers the same

region as Riley (1987; see below), with the latter providing detailed morphological mapping. Arthurton covered both the Settle and Penrith regions. Penrith occupies the lower Eden valley, close to the Solway Firth. The general location and orientation of drumlins is matched by the mapping performed here, although more forms are included. The Settle region covers broadly the same area as Raistrick (1933); only the western area mapped by Arthurton is covered in this research. Again the broad distribution and orientation of drumlins is similar. Detailed mapping by Brandon (1998) shows very close agreement with the relief shaded DEM (Figure 6.20a), however Figure 6.20b is dominated by small, ovoid, bedforms with no preferred orientation. This borders a region tentatively interpreted as ribbed moraine and are possibly representative of highly dissected transverse bedforms. Overall the similarity between the two datasets is very good.

The detailed morphological maps of Boardman, Whiteman, Riley and Mitchell are now discussed. Boardman (1991) mapped drumlins immediately around Keswick and further west at Troutbeck Station, just bordering the Eden Valley. Both sets of drumlins are moderately small (~300-500m long) and, although just resolvable on the DEM, were not mapped due to their isolated nature and uncertainty over their origin.

Figure 6.21 shows the field mapping of Riley (1987) overlaid on a relief shaded DEM. On reviewing the mapping of Riley it is immediately apparent that there is strong correlation between the two datasets. Although some lineaments are not visible on the DEM, these are the exception and are probably below the resolution capabilities of the DEM data. The fit of the remaining data is excellent, even matching changes in the shape of individual lineaments. It should be noted that this area is generally flat, having well defined lineaments which are up to 950m long and 50m high. The mean lineament length is 325m, with a standard deviation of 175m. They are consequently large, well defined landforms. Riley does go on to discuss cross-cutting drumlins. These have been heavily modified by subsequent ice-flow and are visible on the DEM. Similar mapping was performed by Whiteman (1981) just to the north-west (surrounding Appleby) with a close match to the underlying DEM also good.

Field mapping performed by Mitchell (1994) is depicted in Figure 6.22. This bears almost no relation to the DEM. Although there are some lineaments which align well, there are many lineaments for which there is no direct comparison, whilst others have a vague representation on the DEM. Lineaments are oriented in many directions in this complex area and changing the illumination azimuth helps further mapping. However many of the lineaments mapped by Mitchell are at, or below, the resolvable threshold. This is confirmed by the statistics for the area, which show a mean length of 220m and a standard deviation of 90m. The maximum lineament length is 640m. This highlights the resolution limitations of mapping from this DEM, although there will also be accuracy limitations in both the mapping and plotting of the original fieldwork. One further explanation for the discrepancies is the low relief of the lineaments (Mitchell, pers comm). Inspection of 1:10,000 and 1:25,000 maps shows no lineaments. Both these series have a 10m contour interval and are unable to define these landforms. More detailed mapping is unavailable due to the remote, upland nature, of the terrain. As the OS DEM is created from original 1:50,000 mapping with 10m contours, it is not possible to extract the lineaments from the surrounding terrain. Indeed DEM interpolation from the contours will have smoothed the slope so that they are not visible. Further examination of 1:10,000 aerial photography reveals *some* of the lineaments. The high resolution, in comparison to the DEM data, allows better interpretation of the landscape, however there are many lineaments which are not clearly identifiable. Mitchell (pers comm) states that the relief of the lineaments is small and that field mapping is the best method for their identification.

Finally, Figure 6.23 shows the lineament mapping overlaid onto those of the BRITICE project. The BRITICE project used photocopies or scanned images of the original, published, mapped data from which lineaments were generalised into a single data source. By its nature, this is not an accurate procedure. The original sources for compilation may well have inaccuracies or inconsistencies in both the mapping and coordinate system. Indeed, many “maps” do not use a coordinate system and require “eyeballing” into an approximate location.

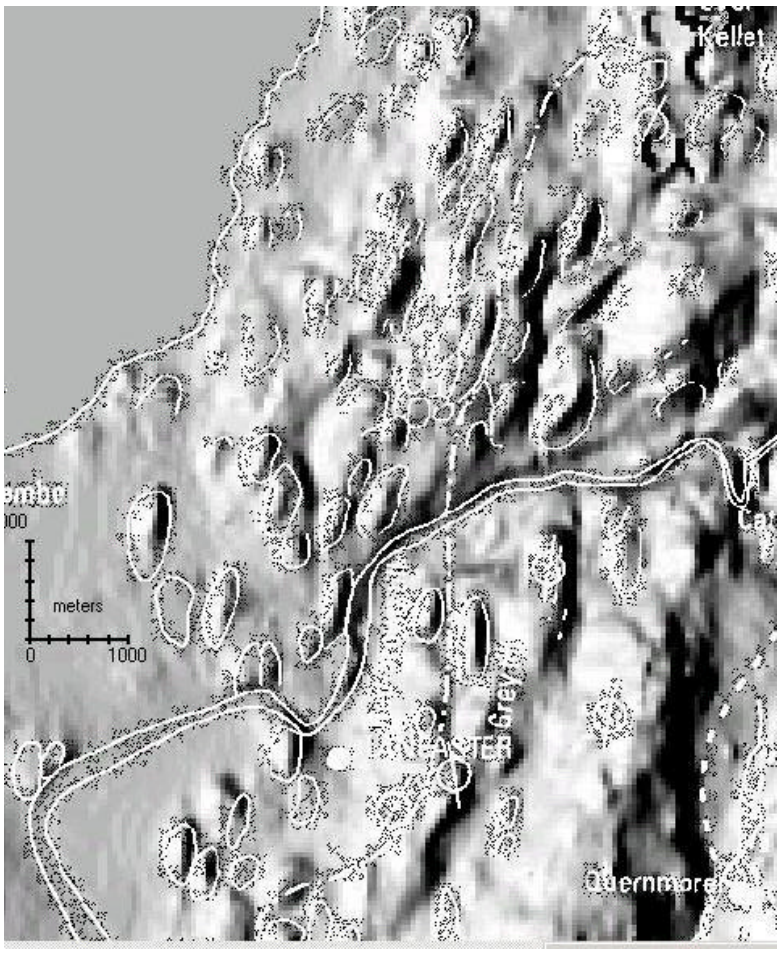

Figure 6.20a Relief shaded DEM (shaded from the west) of the Lake District overlaid with field mapping data from Brandon (1998). Note the close correspondence between the DEM and the field mapping (©Ordnance Survey).

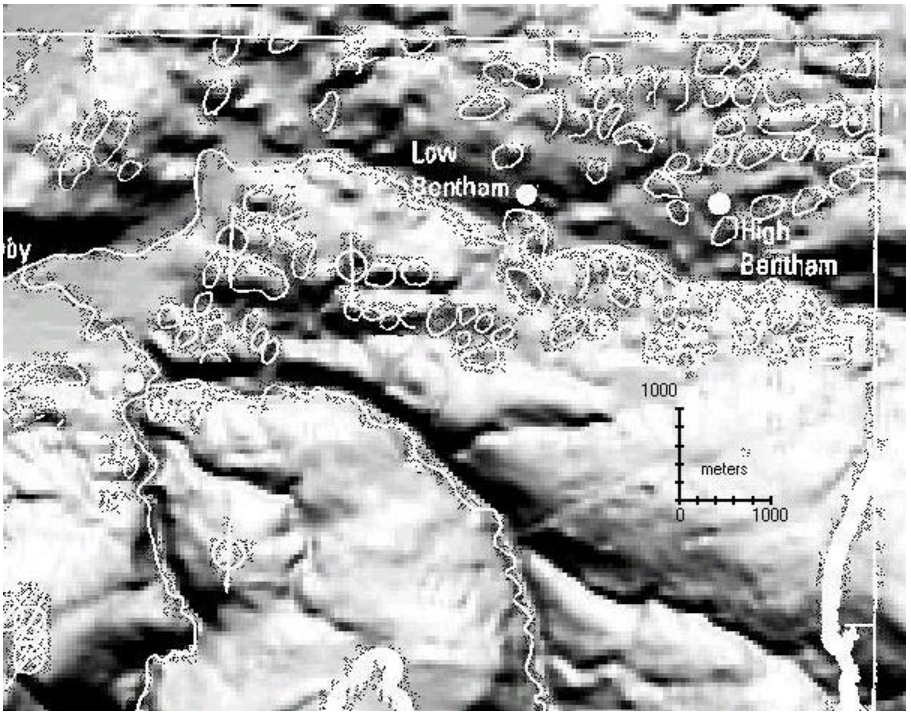

Figure 6.20b Relief shaded DEM (shaded from the north) of the Lake District overlaid with field mapping data from Brandon (1998). Note small, ovoid, bedforms with no preferred orientation in the top right corner (©Ordnance Survey).

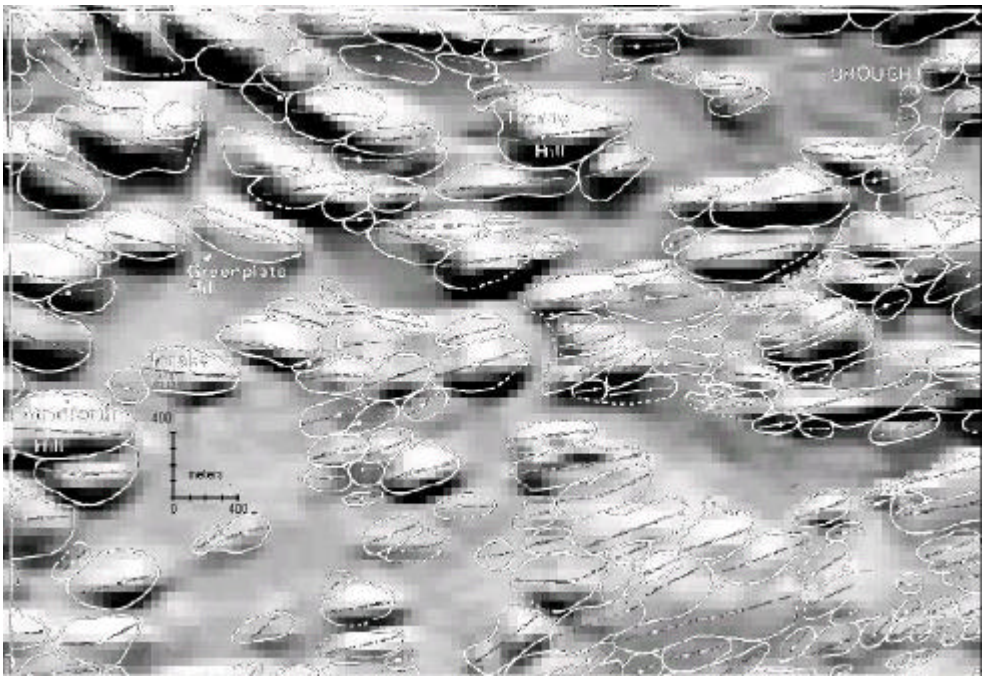

Figure 6.21 Relief shaded DEM (shaded from the north) of the Lake District overlaid with field mapping data from Riley (1987). Note the close correspondence between the DEM and the field mapping, although smaller lineaments are not visible on the DEM (©Ordnance Survey).

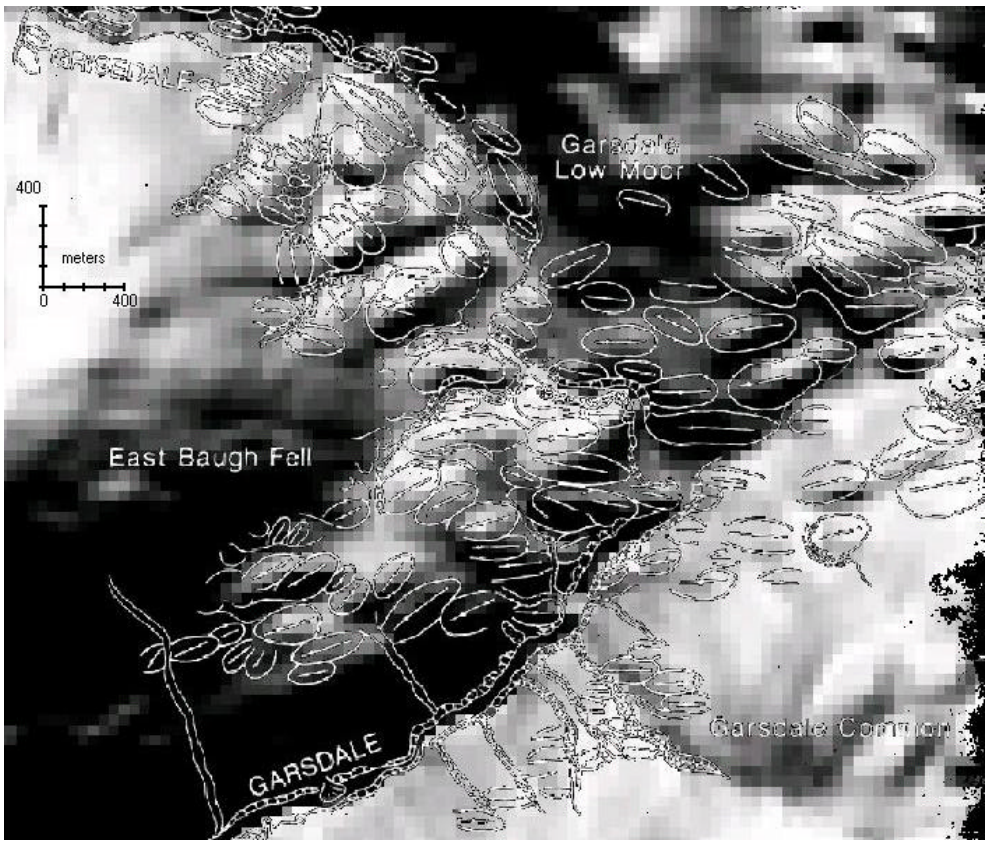

Figure 6.22 Relief shaded DEM (shaded from the north) of the Lake District overlaid with field mapping data from Mitchell (1994). Note the poor correspondence between the DEM and field mapping. Some larger lineaments (middle left) are visible, whilst others are not.

In general there is good correspondence between the two data sets, although the DEM mapped data is generally more numerous. However both sources have small, localised, regions of mapping where there is not coverage by the other. In the north both data sets show the tightly curving lineaments around the north of the Lake District, with the suggestion of a further flow direction towards the north-east. The eastern region again shows two or three main flow components, although the BRITICE data show no cross-cutting landforms. This is unexpected as Riley specifically discusses cross-cutting in this area. In the southern portion of the Lake District, the BRITICE data is sparse. In the mountainous area in the east there are some lineaments which generally confirm the mapping from the DEM, whilst in the central region there are virtually no landforms mapped. This area is perhaps one of the most interesting areas as the bedforms are heavily deformed and record multiple flow directions. Indeed nearly all the mapping here represents new data.

This section has compared the DEM mapped data with those performed by field mapping. These publications have essentially been used as verification through being used as a higher resolution data source. In general the DEM data have performed very well, however issues of completeness as a result of both horizontal and vertical resolution need to be born in mind. Given the coverage of DEM data and the speed of mapping, these limitations are fairly minor. Further investigation could be appropriately directed at higher resolution DEM data to assess the potential benefits and to see if the above issues can be resolved.

6.6.5 DEM Datasets

Although §6.3-6.5 outlined, tested and reviewed a variety of different methods for visualising DEMs, this has been performed using data supplied by the Irish Ordnance Survey (IOS) based upon direct terrain extraction (DTE) from stereo aerial photography. The above case study used Ordnance Survey (OS) data based upon DEMs interpolated from contours created using stereo aerial photography. The products clearly have different derivations and this section addresses some of the issues that arise from this.

Chapter 4 introduced some of the different methods used to create DEMs. These are principally the conversion from contour data, satellite stereo imagery and radar interferometry. Contour based DEMs have traditionally been the most popular, but with the rapid collection of remotely sensed terrain data the other types are becoming more common. The IOS and OS DEMs used in this chapter have been produced using different methods and, although the visualisation techniques apply equally, the two DEMs are not directly comparable. It is worth noting the following points about these DEMs:

- DTE measures the exact surface height and so will incorporate the elevation of vegetation and buildings into the DEM.
- Contours typically attempt to represent the actual, bald earth, surface. The landscape is smoothed during the generation of contours, with further smoothing sometimes taking place during interpolation, although there will also be the introduction of noise.
- There is less contour information available for interpolating DEMs in flat areas and ”stepping” is often noticeable.

These three main points affect the methods used to visualise the DEMs. The “rougher” surface produced by the DTE DEMs should produce a lower level of specular reflection under relief shading, adding a “fuzzy” texture. This feature is not apparent on the Irish DEM, perhaps a result of the low levels of urbanisation and a rugged upland landscape (i.e. little surface cover). The Irish DEM was also initially produced at 10m resolution and then re-interpolated down to 50m (O’Reilly, pers. comm 2003). This will undoubtedly have smoothed the landscape.

Relief shading is therefore not seriously affected by the differences between DTE and contour based DEMs, however the same is not true of the shape related (non-directional) terrain visualisation methods (i.e. curvature, gradient and local contrast stretch). These rely on terrain shape and it is not surprising that they perform less well when based upon contour generated DEMs. Figure 6.17b shows curvature for the Lake District, depicting the strong influence of contours on the image, particularly in the flatter coastal areas (e.g. north-west part of the figure). There is still a lot of very useful information in the image

making it worthwhile to use during the mapping process, however interpretation is much harder in comparison to the one created from the Irish Ordnance Survey DEM. Similar observations can be made concerning the local contrast stretch and gradient images.

Overall, this highlights the differences between DEMs generated using different methods. Further investigation could be usefully applied to describing the broad parameters effecting the different types of DEM and how these affect the uses to which the DEM is put. In this context, the visualisation techniques that have been assessed will all broadly operate in the same manner, however some are better suited to certain types of DEM. The generation of a better quality curvature image is strongly beneficial for the use of DTE data. Further investigation of SAR interferometry (both space and airborne based) and satellite stereo imagery will highlight the benefits and deficiences in using this data.

6.7 **DiscussionandConclusions**

Satellite imagery is likely to be replaced by DEM data and this has been used as a data source for landform mapping by several researchers. Again comments have been made concerning the best use of relief shaded DEMs, however no one has faced the central issue of how best to visualise 3D data. Stereoscopic mapping is perhaps the most preferable. Even where suitable small scale photography is available (~1:150,000), the process is time consuming and, if geometric accuracy is desired, difficult. Workstation based methods are slowly arriving and will hopefully provide a more integrated visualisation and mapping based approach. However the high cost of proprietary software and hardware mean that this will not become a ubiquitous method for some time.

The advent of near-global DEM data provides an economic and quick alternative. Three dimensional viewing of digital DEM data has been available on commercial grade photogrammetry workstations for some years. This technology is beginning to filter down to mid-range computer mapping solutions, however it is still expensive and often requires proprietary software and

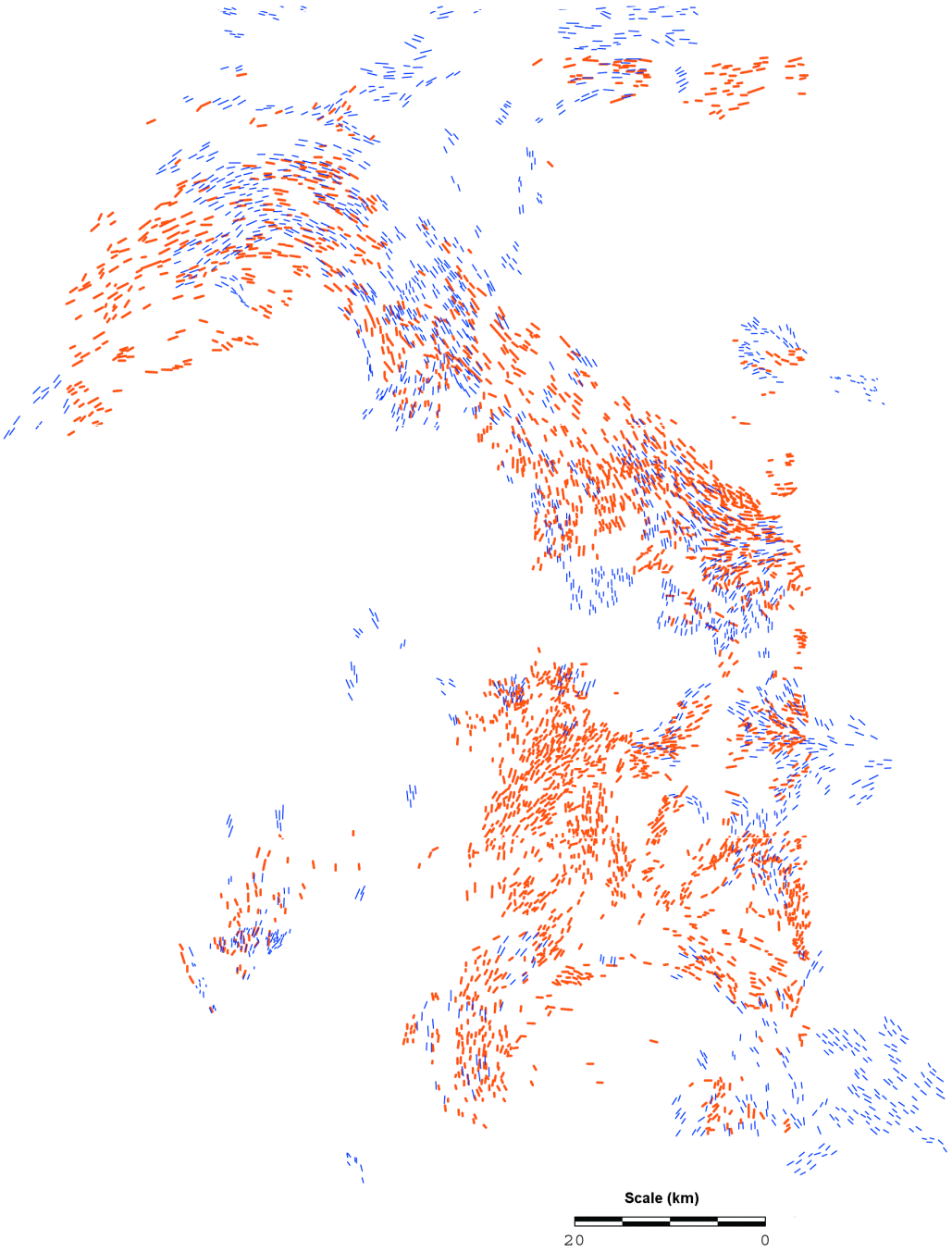

Figure 6.23 Lineaments mapped for the BRITICE project (blue) overlaid on those mapped and from the DEM data (red). In general there are far fewer lineaments in BRITICE, although the general trends match well. BRITICE has far less data for the southern region, although there are small localised clusters throughout the area which are not present on the data mapped from the DEM.

hardware. In addition, to be of use, it must allow the observer to digitise orthographically, even when viewing perspectively. This technology is not accessible, or cost-effective, for many researchers and therefore appropriate methods of viewing 3D terrain in two dimensions are needed. Section 6.2 presented a variety of different visualisation techniques, including relief shading, image processing of textures and analysis of curvature. These techniques all provide different ways of interpreting the terrain; some introduce bias' which may disguise certain landforms or enhance them to make interpretation easier. They are all designed to help the observer explore their data further so that appropriate mapping can then take place. Five of these techniques were tested in their ability to represent glacial landforms. Section 6.4 presented the results of these inter-comparisons, with §6.5 making recommendations for the use of DEM data in a systematic mapping exercise. Finally, §6.6 used these recommendations in providing a case study for glacial landform mapping from DEM data. The Lake District was selected for the case study as it provides a complex array of landforms and relief that make mapping difficult. It is clear that no single visualisation method is able to provide a source for consistent, complete, mapping. Rather, one or two methods are required to map the majority of landforms and these need to be supplemented with a variety of other visualisations in order to cross-check and complete the mapping exercise. It is preferable to begin mapping with a bias free visualisation (i.e. gradient or slope curvature) and, once first pass mapping has been completed, move on to supplementing this data with mapping from parallel and orthogonal relief shaded imagery. This sequence is important as it places more emphasis upon the use of bias free visualisations during the initial mapping phase.

This chapter has been concerned with the methods used to visualise DEMs for landform mapping, so that consistent data can be acquired. However DEMs are created from a variety of different sources and it is important for the observer to be aware of the implications of using different datasets. DEMs were originally developed from contour maps produced using field and aerial survey data. The resultant digital DEM data products have therefore been interpolated, with the exact methods used determining the quality of the final data set. For example, the Panorama© data were originally produced for military applications and so

individual grid cells contained maximum height values to make sure that aerial guidance systems could guarantee they were “above surface”. However, alternative acquisition methods are now driving the production of modern DEMs and with them come different data quality issues.

Digital aerial photography, digital photogrammetry and SAR interferometry are the most popular methods currently in use. The type of sensor, and whether they are spaceborne or airborne, will determine the specific type of dataset that is eventually acquired. Chapter 5 briefly introduced some of the DEM alternatives to using satellite imagery for landform mapping, including ASTER and SRTM. The availability of data for the UK is particularly illustrative of the recent interest and explosion in DEM data sets.

The original Ordnance Survey Panorama™ 50m and, higher resolution Profile™10m, data are currently available. CHEST has recently released the Landmap dataset (25m resolution) which was created using spaceborne SAR interferometry (ERS Tandem strip data). The SRTM C-band (30m and 90m resolutions) and X-band (25m resolution) data will shortly be available. Finally, Intermap has recently completed airborne SAR interferometry with the intention of producing a high resolution product (3m resolution) of the whole country and an ultra-high resolution product (0.3m resolution) of urban areas.

Before any mapping begins, it is important to appreciate the characteristics of the source data set, including any limitations in its use. For example, the Landmap DEM is a *surface* model, in that it provides height values for the visible surface. It does not provide height values for the bare earth or basic terrain. Therefore it may be unsuitable for landform mapping in a heavily forested landscape.

With appropriate visualisation methods and an understanding of the constraints imposed by different DEM datasets, an observer can be confident that, within these constraints, an accurate and complete mapping exercise has been performed. Chapter 7 now goes on to review the methods by which this mapped

data is incorporated into a glacial reconstruction and implements techniques by which this can be performed in an objective and quantitative manner.

7 Lineament Spatial Variability and Classification into Flow-Patterns

7.1 Introduction

Aerial photo and satellite image mapping has revealed complexity within glacial landform assemblages that had previously been unrecognised (Clark, 1993). An increase in the amount of data has forced a re-evaluation of interpretive methods that has resulted in a shift away from a tendency to “clump” lineaments together into single generalised flow patterns, to “splitting” them into components of distinctive patterns that record flow configurations at different times (e.g. Figure 7.1). This process allows the development of alternative interpretations from which realistic flow configurations can be devised. Lineament generalisation and interpretation is concerned with how complex patterns of individually mapped lineaments can be coherently organised into feasible glaciological scenarios.

This chapter reviews the manual approaches used in generalisation and how these are applied to glacial reconstructions. Technical and methodological advances in mapping and understanding glacial assemblages mean that new demands are being placed on the interpretation of mapped data. With the complexity of the processes that create landforms being unravelled, it is vital that both mapping and generalisation are performed as objectively as possible, such that they are reproducible by other researchers. This chapter explores and presents a set of techniques to allow researchers to do this, concluding with a discussion of best practice.

7.2 Generalisation: A Visual Methodology

7.2.1 Introduction

Although chapters 2 and 4 introduced the concepts behind the generalisation of raw lineament data into recognisable flow patterns so that they could then be interpreted, it is hard to appreciate the difficulty that this task presents. Figure 7.2a shows nearly 12,000 lineaments mapped from a part of Canada (after Stokes, 2001). The patterns displayed by this data are both complex and

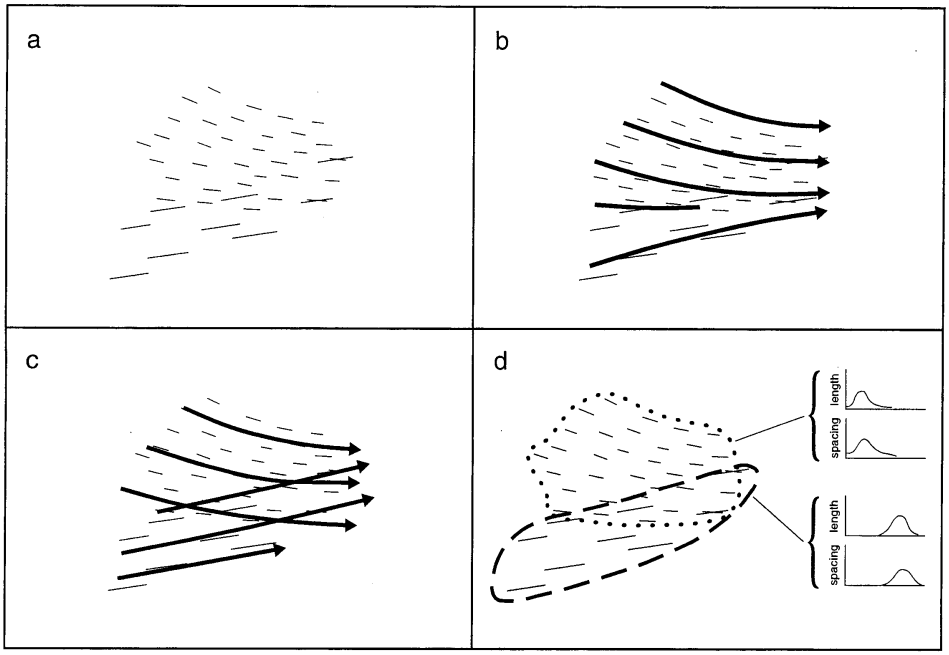

Figure 7.1 (a) shows individual mapped lineaments. These would traditionally have been interpreted as representative of a single ice flow event (b), however cross-cutting evidence means that they must have formed from two events (c). In the absence of cross-cutting indicators, interpreters visually discriminate between flow patterns, however flow pattern characteristics can potentially provide quantitative methods to validate such groupings (Clark, 1993).

confusing. Trying to order the data so that a concise set of flow patterns can be produced allowing interpretation and explanation is a time consuming task. This has traditionally been performed using manually based, visual, techniques. They are strongly dependent upon the ability and experience of the interpreter and it would be easy for this qualitative assessment to include an element of interpretation. Figure 7.1 illustrates a scenario which could be generalised into one converging flow pattern or two cross-cutting patterns. Clearly the presence of cross-cutting is important here, however the characteristics of each flow pattern can equally be used to verify that such a division exists. Ideally generalisation should form a semi-quantitative stage that can then go on to produce flow sets which can be interpreted. Figure 7.2b shows the flow sets that were generated from the raw lineament data presented in Figure 7.2a. Generalisation is therefore a stage which goes from “more” data to “less” information. It is this process that identifies broad trends within the data set and allows them to be highlighted for later interpretation. The following section introduces the visual heuristics used by researchers to perform such a task, before going on to suggest how better techniques may be used to implement this.

7.2.2 Identification

Within the context of glacial lineaments, generalisation involves the simplification of detailed landform patterns (recognition of the main trends) by removing potential noise and random effects. This initial stage provides a reduction in the complexity of lineament patterns. The reduced data set is then classified into component flow sets (see §2.3).

A visual approach to generalisation begins with the premise that *a similarity of form indicates a similarity of formation* (see below for a full discussion of the different variables this includes). Given that flow sets can vary in time and space depending on whether they are identified as synchronous or time-transgressive, it holds that flow patterns can also vary in time and space. This extra layer of complexity in interpretation, produces a similar increase in complexity of the original mapped lineaments. However simply because

Figure 7.2 (a) Example of ‘raw’ lineaments mapped from satellite imagery for the Dubawnt region, Canada (Stokes, 2001). There are nearly 12,000 lineaments that need to be generalised into a simpler dataset ready for interpretation.

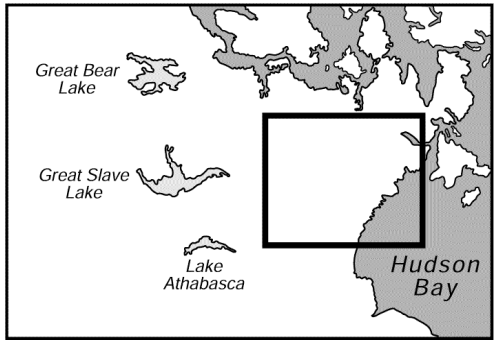

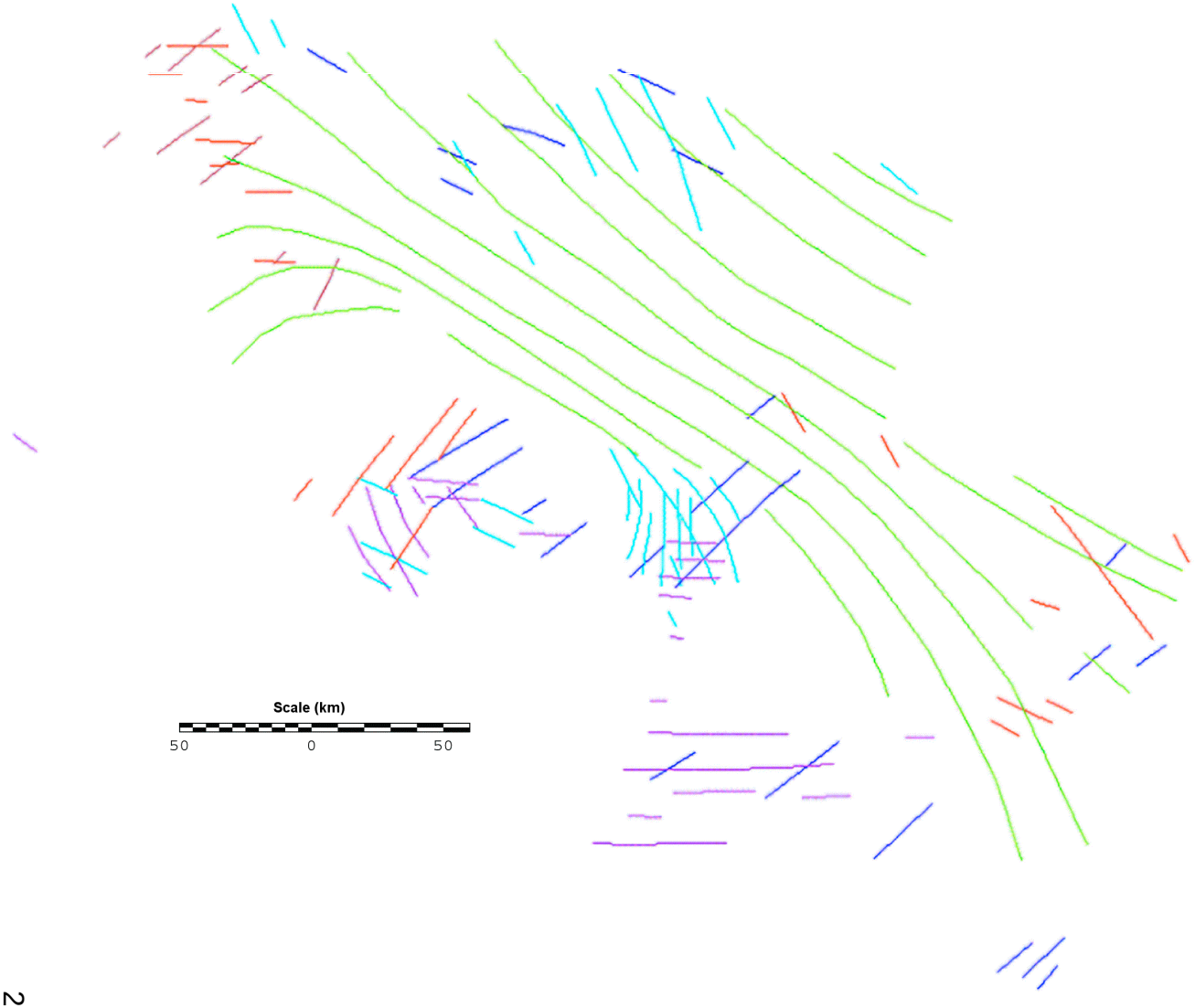

Figure 7.2 (b) Flow sets produced from Figure 7.2a have reduced the amount and complexity of the raw data allowing an interpretation of the main flow patterns (Stokes, 2001).

lineaments do not display consistent spatial trend in morphometry and orientation does not mean they do not have a similarity of formation. The identification of lineament similarity needs to address these complexities and as a result needs to be performed at the local scale, identifying gradual changes in form, in order to reveal patterns at the regional scale. This distinction is important as visual identification requires devolving a complex pattern at large scales (to produce flow patterns) and then combining these results to reveal a global arrangement (flow sets). Methodologically, this involves the non-interpretative generalisation at the local scale (e.g. flow patterns), before interpretative generalisation occurs at the regional scale (e.g. flow sets).

As similarity of form controls whether a lineament is included within flow pattern or flow set membership, it is important to understand which morphological variables are visually useful and the manner in which they are used. These include:

- Orientation
- Orientation conformity (or parallel conformity)
- Length
- Length conformity
- Spacing (density)
- Spatial Continuity

- *Elongation ratio (and other shape factors)*
- *Height*
- *Material composition*

The availability of data depends upon the method in which lineaments have been surveyed; if this has involved digitising from satellite imagery, height and composition data will not be available. Historically, satellite imagery has not been detailed enough to map beyond crestlines (i.e. outlines or break-of-slope), although the availability of economic, and high resolution, Landsat ETM+ data is changing this. Crestline mapping also allows large areas to be covered rapidly. The advent of high resolution, widely available, DEM data means that, for many areas height *and* shape information will be available. Although height varies

within groups of lineaments, this is usually related to length, width and volume. In terms of understanding lineament flow patterns, it is less useful.

Lineament morphometry has been studied in detail to help decipher the glaciological context of sediment emplacement, with the elongation ratio a popular shape factor (Menzies, 1987). The value of this information is debatable as lineament length can be considered a good proxy. Indeed, variation in lineament shape can be due to cross-cutting through superimposition and re-orientation. Within these contexts, the elongation ratio is meaningless. For these reasons, and because lineaments are most commonly mapped, the remaining discussion will focus solely on mapping lineament crest lines.

A crestline is composed of a single line and its attributes are therefore length and orientation. As generalisation is concerned with similarity *between* forms, conformity of orientation and length can also be considered, in addition to the density and spatial continuity of lineaments. These six variables (highlighted above) form the basis of any generalisation procedures.

Orientation conformity, or *similarity in orientation*, is probably the most influential variable as an observer will be visually drawn to this feature. If a lineament is surrounded by like oriented lineaments, the strength of similarity is high. As this check is performed at the local sale, gradual changes in orientation, whilst maintaining parallel conformity, are allowed (e.g. Figure 4.11).

Equally, similarity in length is expected, with gradual changes in length (within an individual event) allowed. This is related to the speed of ice flow, sediment supply and residence time. However, there may be groups of lineaments whose length are very similar or (as in Figure 4.11) groups of long lineaments surrounded and intermixed with lineaments of a variety of sizes. This is not a random mix but a structured intermixing.

Finally, density and spatial continuity need to be considered. Lineament density should be consistent throughout a group of lineaments. Again this can be expected to change gradually, however it is common for “gaps” to appear within

groups of lineaments. This is due to topographic (i.e. relief) or glaciological factors. Groups of lineaments should still appear continuous, as large gaps could well signify a separate ice flow event.

This section has outlined the importance of grouping lineaments locally and has identified the main variables that are used to do this. However nature is far more complex, and makes generalisation difficult. For example, Figure 7.3 shows two hypothesised splaying lineation patterns. Although initially similar in appearance, the first shows high orientation conformity (Figure 7.3a) and no cross-cutting, whilst the latter has low orientation conformity (Figure 7.3b) and cross-cutting. The latter pattern can easily be mis-interpreted which leads the interpreter to a different set of contextual assumptions concerning the process of formation. This would then be interpreted into flow sets incorrectly. To complicate this record of a single event, it would be possible for the pattern to be further intermixed with a later, superimposed, set of cross-cutting lineations. Deciphering this record of landform assemblages requires an understanding of how they were formed with as an objective generalisation of the original mapped data as possible.

7.2.3 Quantitatively Based Solutions

The above sections have outlined the scope of the problems involved when generalising and how current manual methods attempt to solve them. The methodologies developed to interpret complex ice flow patterns place new demands upon the data (and consequently the techniques and processes by which they are collected and collated) which they are based. Although a whole variety of landform data are collected, lineaments are the most common, widespread and prolific. For these reasons, generalisation is necessary. At its most basic, the data is simply composed of lineament crestlines which allow the use of length and orientation, and their associated variables, to be use for generalising. Above all else, generalisation needs to be locally based and adaptive. Therefore any solution to providing objective-based generalisation needs to consider the above factors. Two broad approaches can be devised:

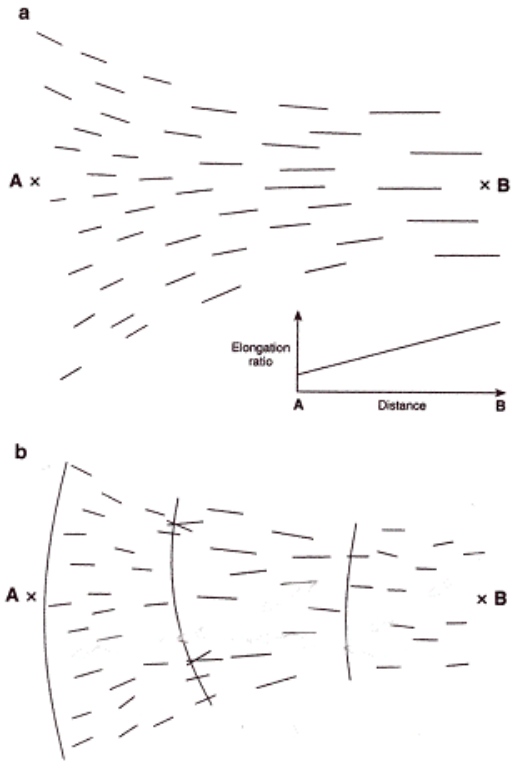

Figure 7.3 Lineament generalisation needs to correctly identify flow patterns. In this scenario, (a) depicts clearly defined lineaments that are generated isochronously. Cross-cutting and low orientation conformity occur in (b). A single, time-transgressive, flow pattern is depicted, rather than two cross-cutting flow patterns (modified from Clark, 1999).

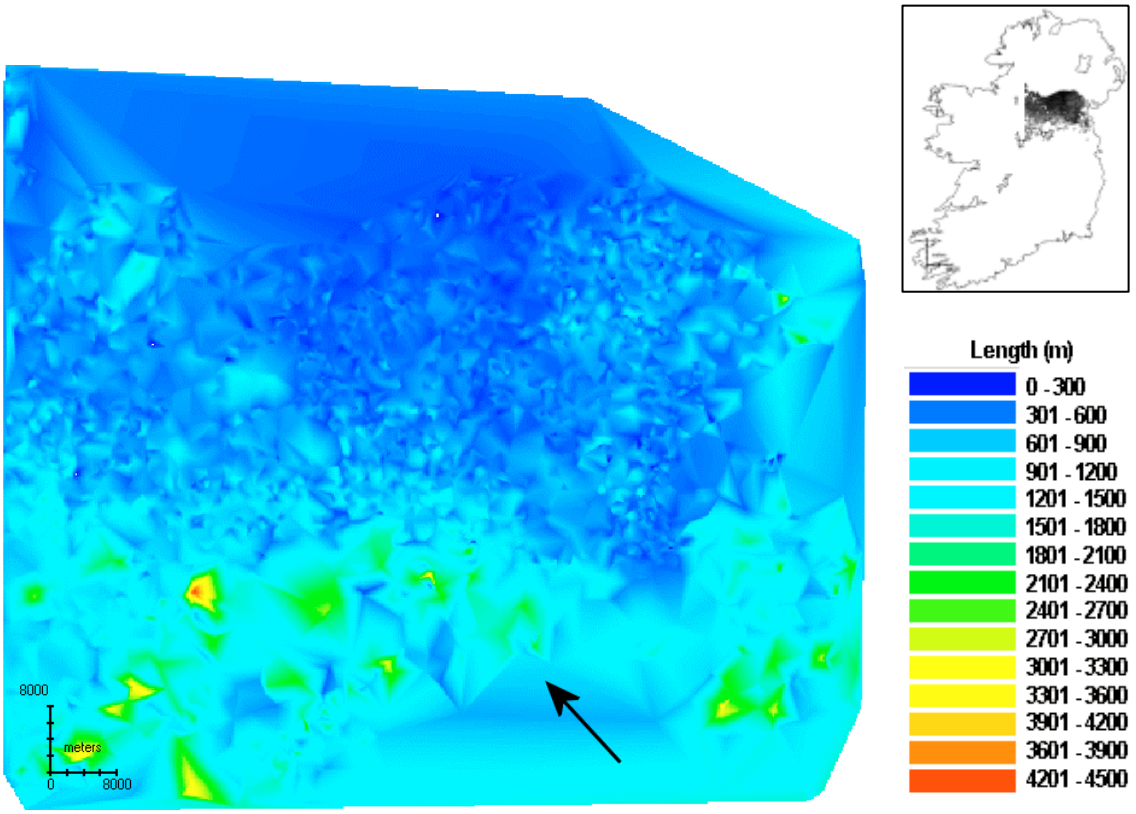

Figure 7.4 Interpolated surface of lineament length generated using a Triangular Irregular Network (TIN) for the Irish Midlands. Note the “gap” effects (arrow) that occur as a result of interpolating across large areas with no data values (data from Clark and Meehan, 2001).

1. **Manual Flow Set Classification** - a fully iterative, interactive, approach that provides quantitative checks on the generalisation procedure. This approach uses visualisation techniques to aid the identification of flow patterns. Mapped lineaments can be difficult to interpret, therefore "surface" maps of orientation and length are suggested to help guide the observer into separating lineaments into flow patterns. Once complete, statistics and graphics on each flow pattern (e.g. orientation, density) are provided to allow an assessment of the component flow patterns. This iterative approach provides the observer with a set of tools to converge upon a solution or set of solutions, and so give a quantitative check on a qualitative procedure. It is essentially a manual procedure that is validated by the use of exploratory statistics.
2. **Automated Flow Set Classification** - an algorithmic based approach (that could potentially be automated) to group lineaments together. This would be locally adaptive and developed from the visual heuristics used by interpreters.

Methodologically the second approach is the most desirable and should provide an objective approach to generalisation. However it is not easily possible to automate within current GIS and requires thorough testing in a variety of glaciological scenarios. The first approach is therefore appropriate as it is can be performed without proprietary software and allows the interpreters own expert knowledge to be used in the generalisation process. In addition, the use of exploratory statistics allows interactive back-checking.

The remaining sections develop and appraise these two approaches and then apply them to an actual case study. The chapter is then concluded with recommendations for best practice.

7.3 Development of Manual Flow Set Classification and Verification Techniques

7.3.1 Introduction

This approach outlined above aims to provide the interpreter with graphical data to help identify areas where there may be multiple flow patterns. Following the manual assignment of lineaments to flow patterns, iterative exploratory statistics are then used to provide quantitative checks. This section develops these two components to provide a method that can be used by the researcher.

7.3.2 Spatial Data Visualisation

Although the human eye uses complex visual heuristics to assign lineaments to flow patterns, it is difficult and prone to variation. Providing clear graphical representations of lineament data, within a methodological framework, should allow a more quantitative approach to developing flow patterns.

Lineaments have two main characteristics; length and orientation. If a lineament is reduced to point data, then these attributes can be interpolated (separately) as a surface and so provide clear and concise detail concerning the variation of attribute values within an area. Given the circular scale used for orientation data, it is not appropriate to directly interpolate orientation (i.e. the average of 358° and 2° is **not** 180°). Rather, it is required that the sine and cosine of orientation is interpolated and then, using the tangent, these values are recombined to give an interpolated orientation.

The type of interpolation used also requires consideration. It is not necessary to use an exact interpolator (i.e. the fitted surface is not required to honour the exact values of the attributes as the plot is purely illustrative), however it is important that interpolation is restricted to areas where data is available (i.e. only interpolate across small “gaps”). The use of Triangular Irregular Network (TIN) is not appropriate as it interpolates an entire area (i.e. it is space exhausting; Figure 7.4). Grid based methods however allow the restriction of interpolation of individual grid cells to areas where there is data nearby. It is important to realise that all interpolators suffer from problems at “edges”. If there is no data beyond a certain point, the algorithm is extrapolating rather than

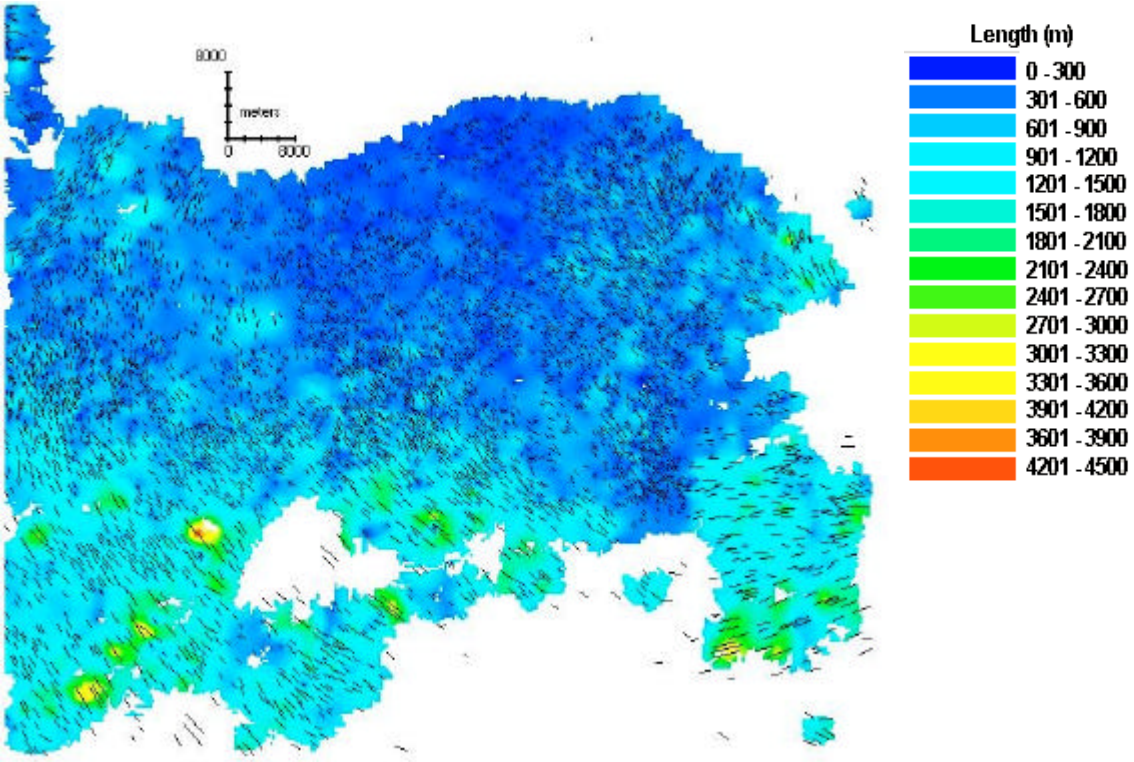

Figure 7.5 Interpolated surface of lineament length generated using the lineament midpoint. A grid based Kriging interpolator, restricted to interpolation within 3km of at least three data points for the Irish Midlands. This grid based interpolator demonstrates how they can be configured to remove edge effects and only interpolate where there is sufficient data available. Mapped lineaments are overlaid to show correspondence to the original data (data from Clark and Meehan, 2001).

interpolating. If there really is no data, then strange “edge effects” will become apparent (displayed in Figure 7.4). For this application, a “patchy” surface is desired so that “holes” are left with no data interpolated across them (Figure 7.5). However it should be noted that there will be small edge effects around all of these holes. The software used for this purpose was Golden Software’s Surfer™ which has a diverse selection of interpolators that allow detailed control over which lineaments are used for interpolation.

The main interpolation methods include *nearest neighbour*, *inverse distance*, *kriging* and *radial basis functions* (which includes the popular splines method). Kriging and splines are generally considered the best interpolators, although they can be slower than methods such as inverse distance and nearest neighbour. Radial based functions use data within a local radius to fit a user selected quadratic applying optimal weights. Kriging uses weighted values from data in the surrounding region to estimate the current point, however its weightings are derived from an understanding of the spatial structure (autocorrelation) of the data. Several different methods were tested, however for the visualisation purposes required, they were all fairly similar and took the same amount of time to produce. Kriging was selected for all interpolation.

For my purposes, two main options are available which control the final interpolated surface. The first is the density, or resolution, of grid cells. The greater the number of cells the smoother the surface, but the longer the interpolator takes. In addition, the coarser the surface, by definition, a greater amount of generalising will take place thereby highlighting trends within the dataset. The grid density value selected will depend on the distribution of lineament lengths that have been mapped.

The second option relates to the number of points used to interpolate each grid cell and the radii from which points can contribute. If input points are sparse then reducing the number of points that are required to contribute to a pixel value will increase the number of interpolated pixels. Reducing the radii will ensure that only *local* points are used in interpolation. This value may vary by up to an order of magnitude depending on the resolution of the original source

data and the size and density of lineaments being mapped. In general a value between 1 km and 5 km sufficed.

With the selection of a grid based surfacing technique and interpolation method complete, it was necessary to reduce the lineaments to data points in order to perform the actual surfacing. There are three options available:

1. Lineament midpoint
2. Lineament endpoints
3. Lineament segmentation (into points)

All three options were explored to see which best represented the data. The first solution provides a very good representation of the data, however the lineament attribute is now simply a single point. The original mapped lineament may well have been long and so appeared important to the interpreter, however its spatial extent is not spatially represented on the surface plot (e.g. Figure 7.5). Grid based algorithms use points closest to a grid cell in order to calculate its value. Therefore a long lineament exerts proportionately greater influence over pixel values close by and clearly identifies an “island” of long length. The longer the lineament the taller the island appears, rather than appearing as a spatially larger entity.

The second solution initially looks appealing, however by selecting endpoints artificial islands are incorporated into the plot (Figure 7.6). These are unsatisfactory and not appropriate. The final solution appears to solve these problems by segmenting the lineament into several points, all with the same attribute. However the pixel value of the surface is simply a combination of the surrounding points and with many points in a segmented line, a series of line like shapes appears on the plot. This can be avoided by increasing the area of inclusion for points making up the pixel value, but this simply reintroduces the edge effects noted earlier (Figure 7.7).

The original solution of using lineament midpoints provides the most graphically pleasing plot, each lineament simply has one value. Locally, longer lineaments

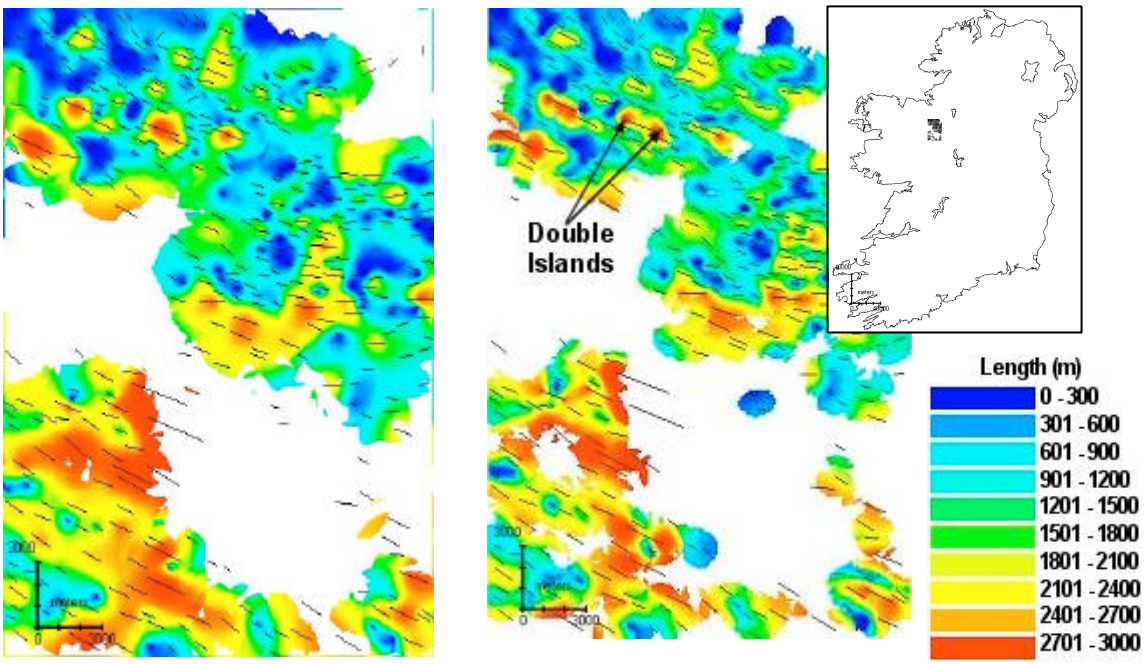

Figure 7.6 a and b Interpolated surface of lineament length generated using the lineament midpoint (a) and end points (b) for Lough Gara, Ireland. Note the appearance of double islands as of result of using end points. A grid based Kriging interpolator, restricted to interpolation within 3km of at least three data points is used.

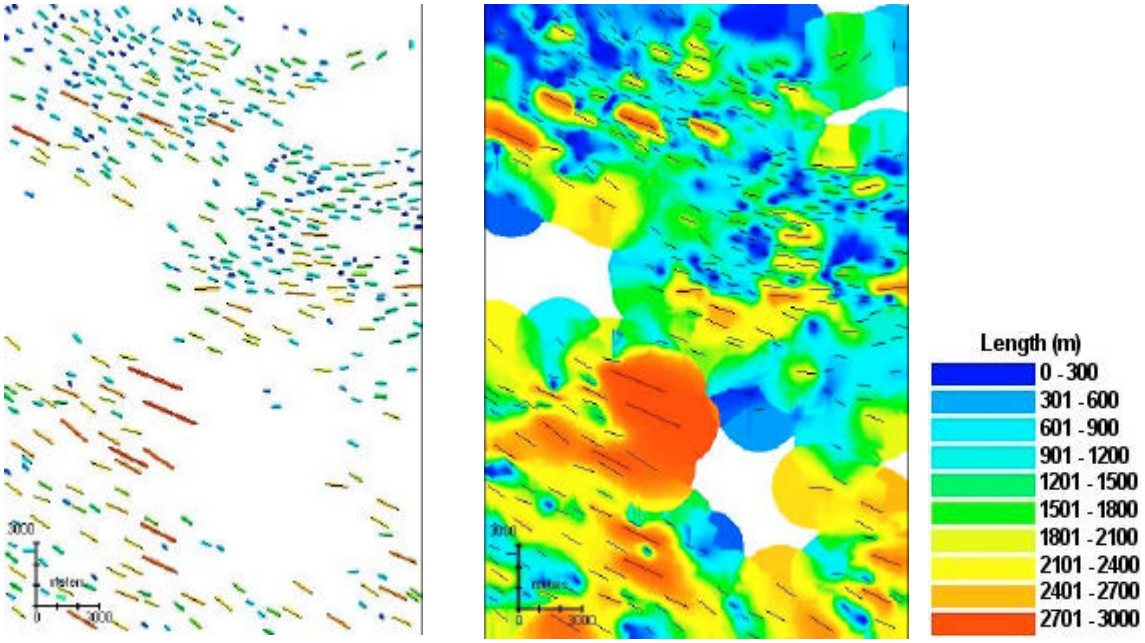

Figure 7.7 a and b Interpolated surface of relative lineament length generated using the lineament segmentation for Lough Gara, Ireland. Note the use of a restricted radii of interpolation (a) results in very little interpolation, whilst increasing the radii (b) produces very poor, overlapping, edge effects.

can influence the region immediately surrounding them and this shows up well on the plot. Over large areas, the small number of long lineaments is unimportant. Rather the overall trend of changes in length and orientation is vital in order to decipher the validity of an individual flow pattern and its glaciological context.

7.3.3 Visualisation Examples

As a demonstration, some real and simulated datasets are used to produce surface plots for each of the different variables. The previous section presented surface plots of lineament length, with the surface presented by a colour gradient from blue (short lineaments) to red (long lineaments). This is perfectly satisfactory for continuous variables, however the display of (aspatial) orientation is typically performed using rose diagrams or corona plots. With respect to spatial data, it would be feasible to use these plots on grid sampled data, however this is not appropriate as each grid cell contains orientation data. An option that was explored, was the use of vector plots (i.e. each grid cell containing an oriented arrow), however the presence of “halos” (see below) and the number of grid cells (well over 100,000 for a 100 km by 100 km area) made them difficult to interpret. The exploration of colour gradients was again pursued through the use of the colour circle used in computer graphics for the display of colours by hue, saturation and luminescence. This is an accepted colour gradient based upon circular visualisation and is appropriate for the display of orientation data.

Visual generalisation is strongly determined by lineament orientation and orientation conformity and this is an appropriate place to begin. Figure 7.8a shows a surface plot of orientation, overlaid with the original lineament data. The lineaments are simulated, being idealised into a highly conformant, cross-cutting, pattern. The different sets of lineaments are clearly picked out by the strong variegated pattern in the centre. In addition, a slight curvature from NW-SE can also be noted.

What is immediately apparent is that *three* directions are implied by the surface plot when only two are present. Because kriging essentially performs averaging

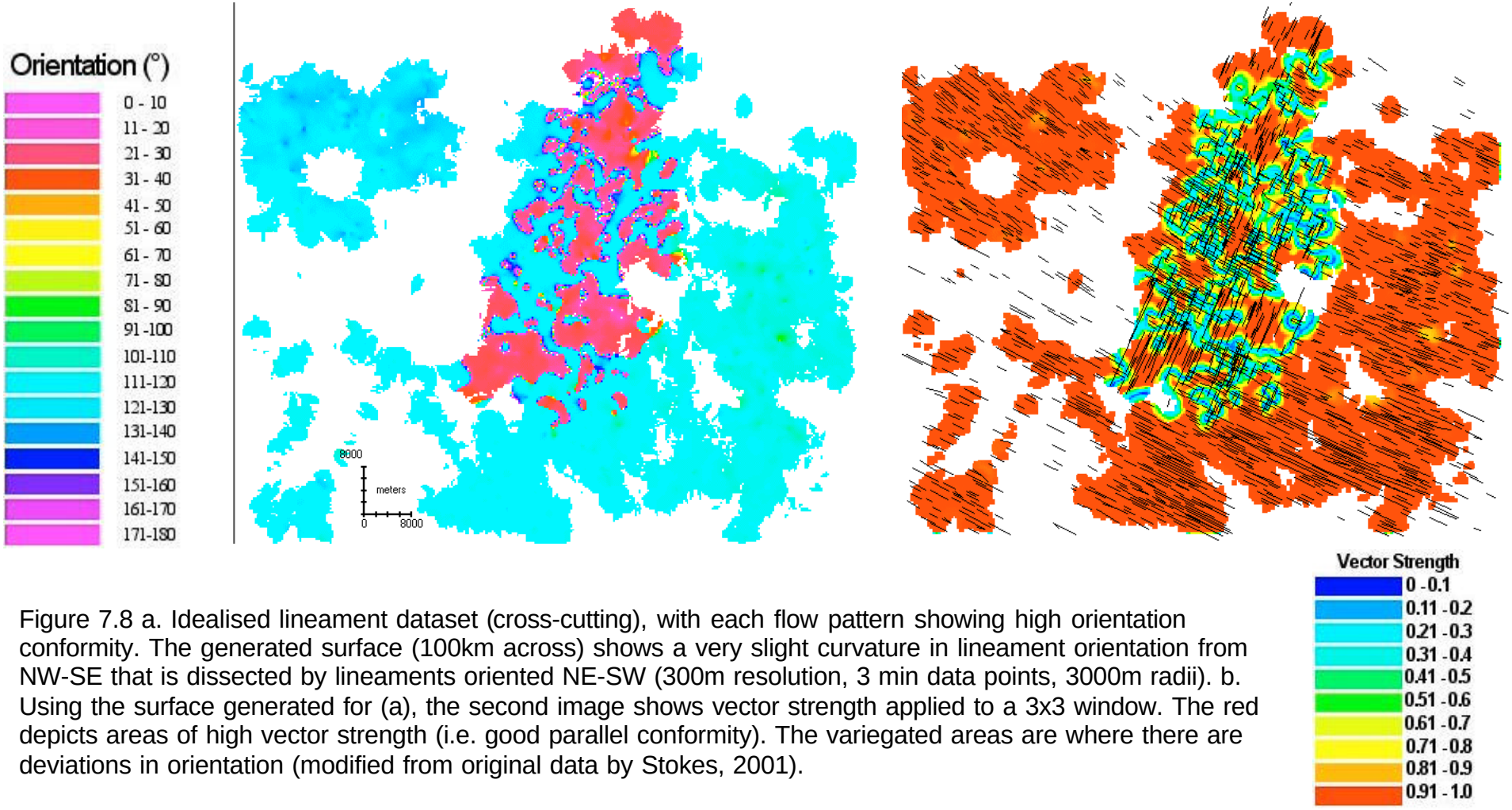

Figure 7.8 a. Idealised lineament dataset (cross-cutting), with each flow pattern showing high orientation conformity. The generated surface (100km across) shows a very slight curvature in lineament orientation from NW-SE that is dissected by lineaments oriented NE-SW (300m resolution, 3 min data points, 3000m radii). b. Using the surface generated for (a), the second image shows vector strength applied to a 3x3 window. The red depicts areas of high vector strength (i.e. good parallel conformity). The variegated areas are where there are deviations in orientation (modified from original data by Stokes, 2001).

over pixels, they can contain the orientation of *either* flow pattern or an average of *both* flow patterns. This is the reason for the “halos” surrounding the variegated region in the centre. Although not strictly “correct” it is a diagnostic feature that can be used to locate and verify cross-cutting. The previous sections have outlined the importance of *localised* lineament conformity. Therefore, an appropriate solution to visualising orientation conformity is to use a filter to calculate vector strength over an area (or window). This provides a measure of how parallel local landforms are. The best window size is partly dependent on the size of lineaments being studied, as well as the resolution of the surface plot. Different window sizes were applied and a 3x3 window was found to work effectively (Figure 7.8b). It is important to remember that this shows local *variation* in orientation (orientation conformity) and not orientation. Therefore high variability (variegated areas) denote areas where there are sudden changes in orientation. High vector strength (red) denote areas with low variability. In this example, high variability occurs where the two flow patterns intersect.

This above scenario is fairly simply and designed to highlight the interpretation of surface plots. Real lineament patterns are often more complex, such as those shown in Figure 7.5 for Ireland. This dataset is now used to compile the same orientation and orientation conformity plots (Figure 7.9a and b). There are two main glaciological scenarios where multiple flow patterns can occur: *separate* and *cross-cutting*. Figure 7.9b highlights the second of these. As seen in the previous scenario, cross-cutting results in a variegated pattern. Spatially delimited flow patterns will usually lead to a band of high variability where the two groups meet. If they are separated by a large distance, then orientation conformity will not delimit them and the original orientation plot should be reviewed.

Lineament orientation and orientation conformity are very valuable tools in distinguishing flow patterns, however other strands of evidence can help in identification as well as providing further glaciological information to help with interpretation. A further measure of orientation conformity is vector strength (based upon the original lineament data) , as described in §5.2.3. This is a

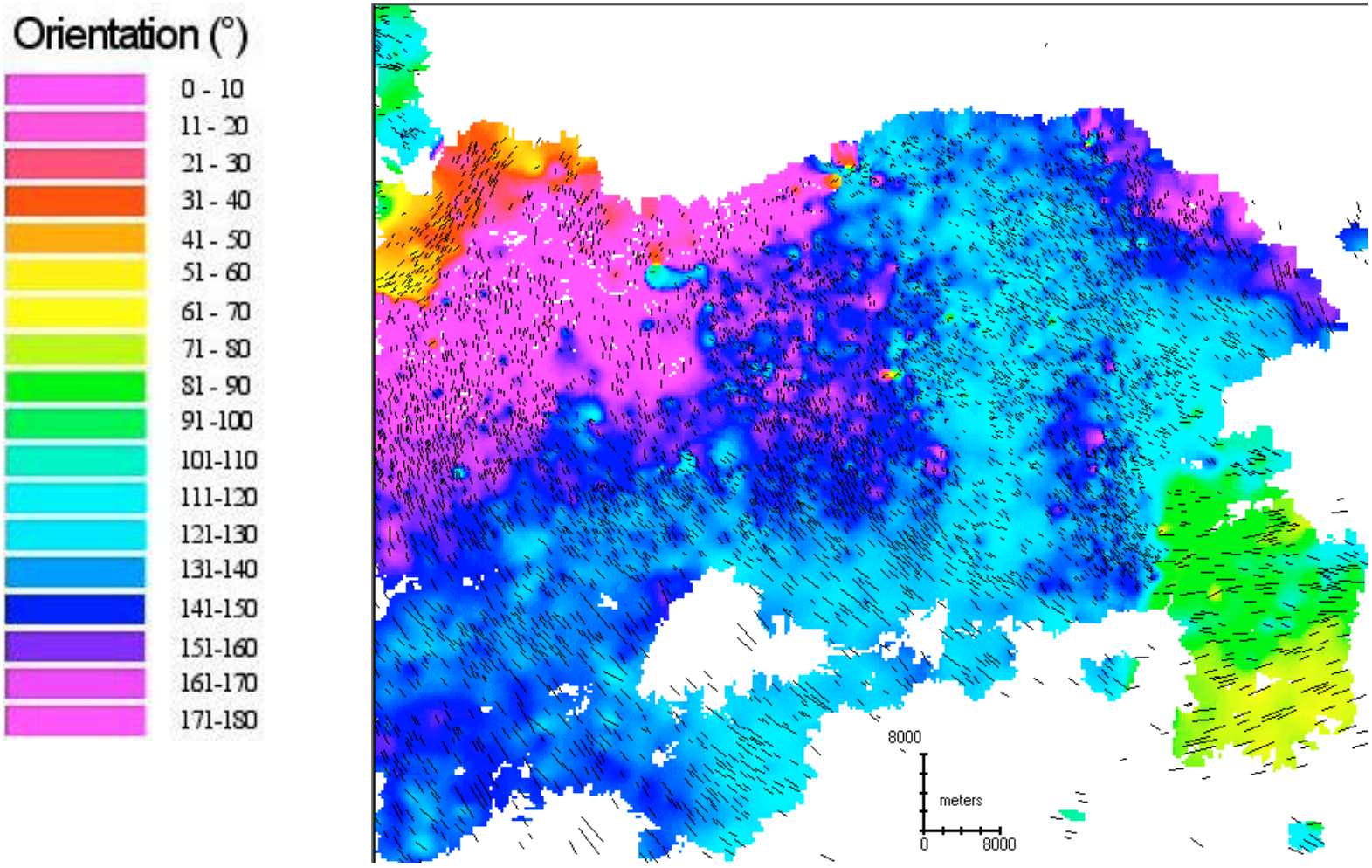

Figure 7.9 a. Vector Mean of lineament orientation for the Irish Midlands (300m resolution, 3 min data points, 3000m radii) (data from Clark and Meehan, 2001).

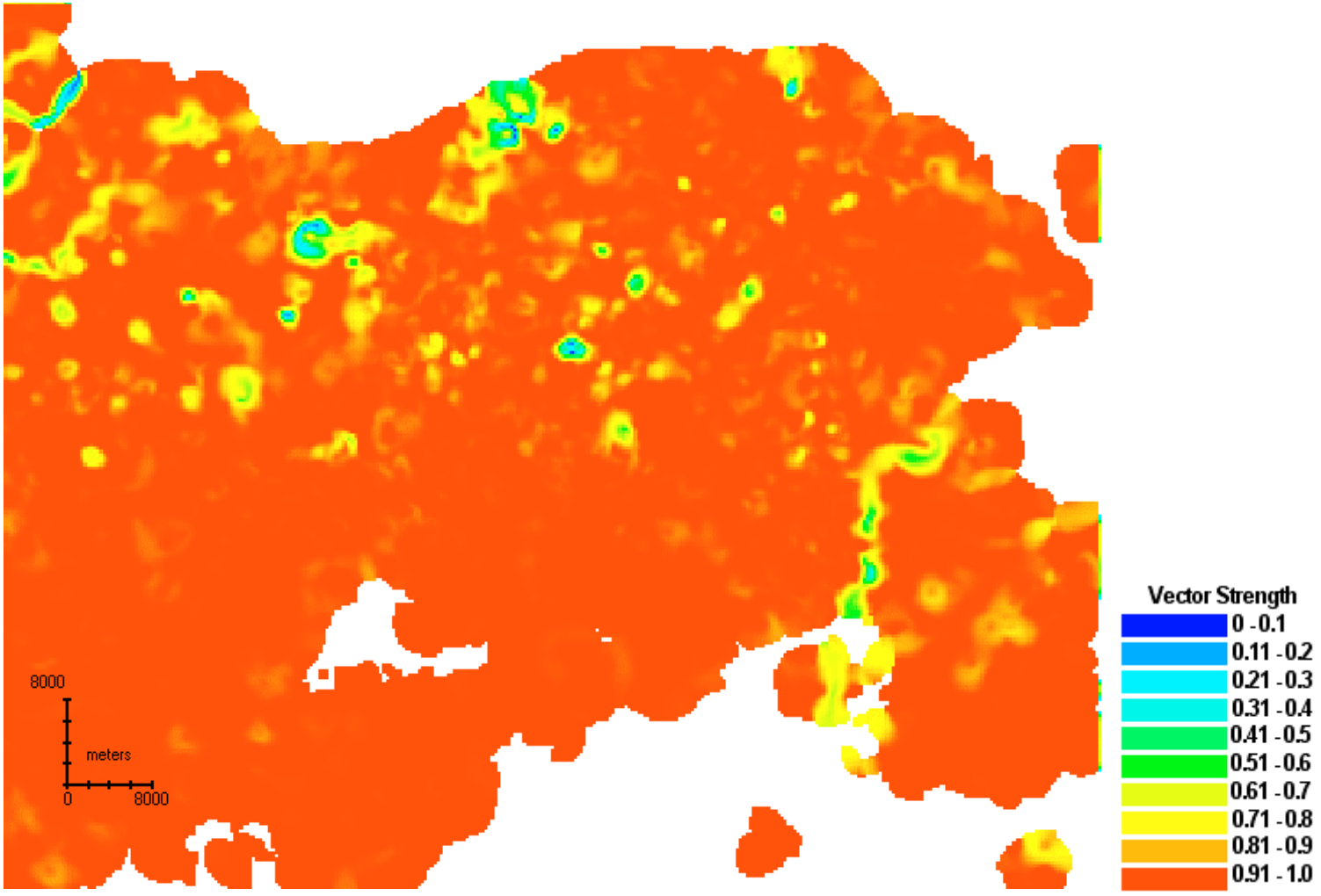

Figure 7.9 b. Vector strength for the Irish Midlands applied to a 3x3 window. The yellow depicts areas of high vector strength (i.e. good parallel conformity). The variegated areas are where there are deviations in orientation (data from Clark and Meehan, 2001).

region based measure and therefore it is necessary to apply sampling in order to apply it to spatial data. After lineament orientations and mid-points had been calculated, a grid was generated. Again, it is necessary to choose an appropriate grid size such that there will be enough data within each grid to make the results meaningful. Grid cells between 5 km and 20 km were appropriate. Lineaments falling within each grid cell were noted and the vector strength calculated on a cell by cell basis (Figure 7.10a). Cells that included less than three lineaments were excluded as they tended to occur around the edges of mapped areas and gave artificially high vector strength values. The figure clearly shows a dominance of high vector strength values, supporting the other evidence for high orientation conformity in the main NW-SE flow pattern. This is a useful indicator that shows if lineaments correctly belong to a single flow set and that they therefore likely represent a single event formed isochronously. In this particular scenario there is one dominant pattern, inter-mixed with several weaker ones. The figure particularly highlights orientation variation in the NW corner, as well as areas of mixed orientations across the N of the area. The NE and SE corners also show small amounts of variation in orientation. Vector strength clearly shows areas with good parallel conformity and provides good information on areas with potential multiple ice-flow directions.

Lineament length and length conformity can also be useful. As noted earlier, lineament attenuation is controlled by ice sheet *velocity*, *residence time* and *sediment supply*. Information on the variability of length can provide further information on glacial dynamics, as depicted in Figure 7.5. This shows a large region of short lineaments in the central north, which is bordered on the east and west by lineaments of varying sizes (variegated). Further out they are ringed by much longer lineaments. In this instance length variation could also be due to different flow patterns.

The final variables used in generalisation are *spacing* and *spatial continuity*. One measure of spacing is the density of lineaments, which is closely related to

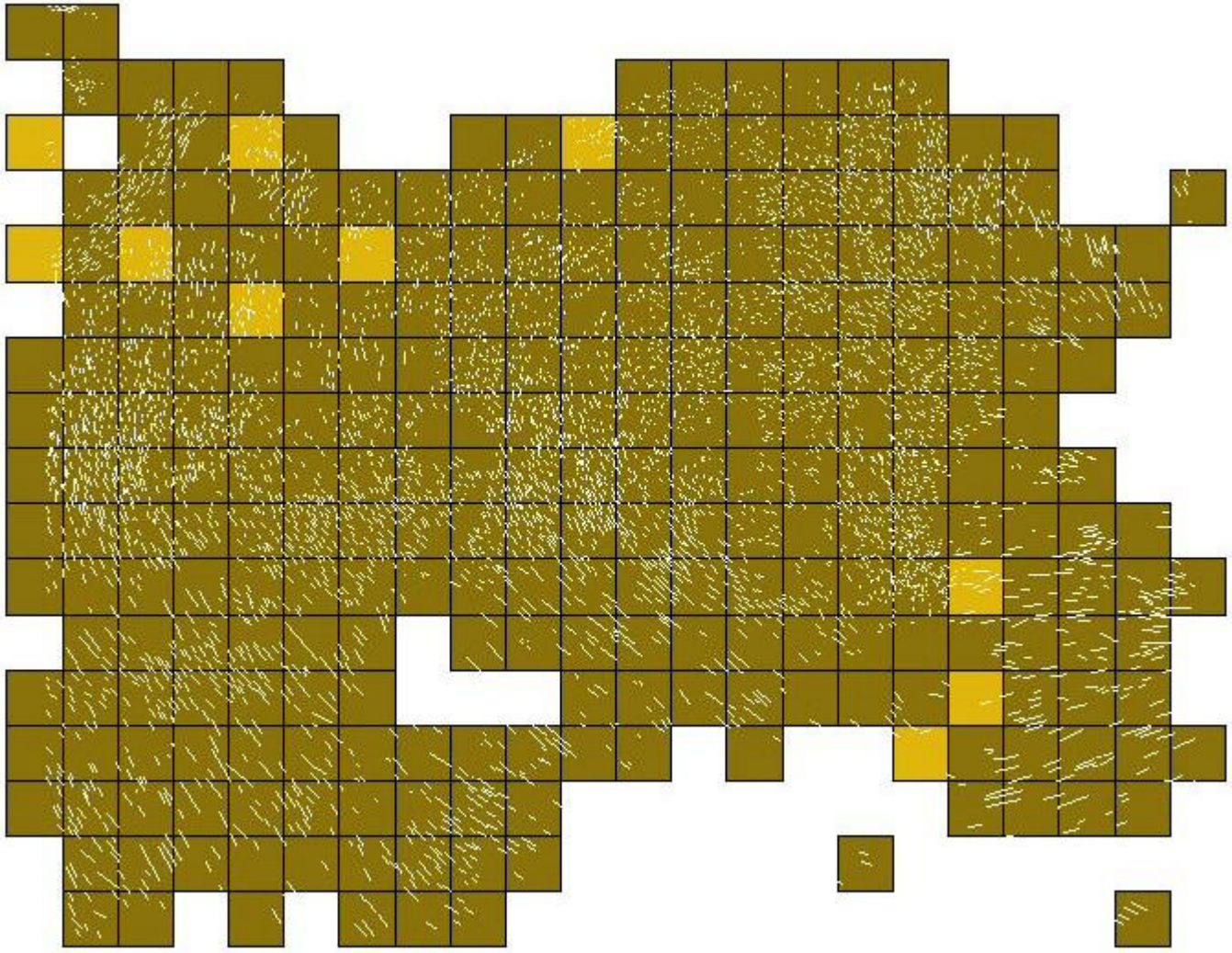

Figure 7.10 a. Vector strength using lineament orientation for the Irish Midlands based upon 5km grid squares (data from Clark and Meehan, 2001).

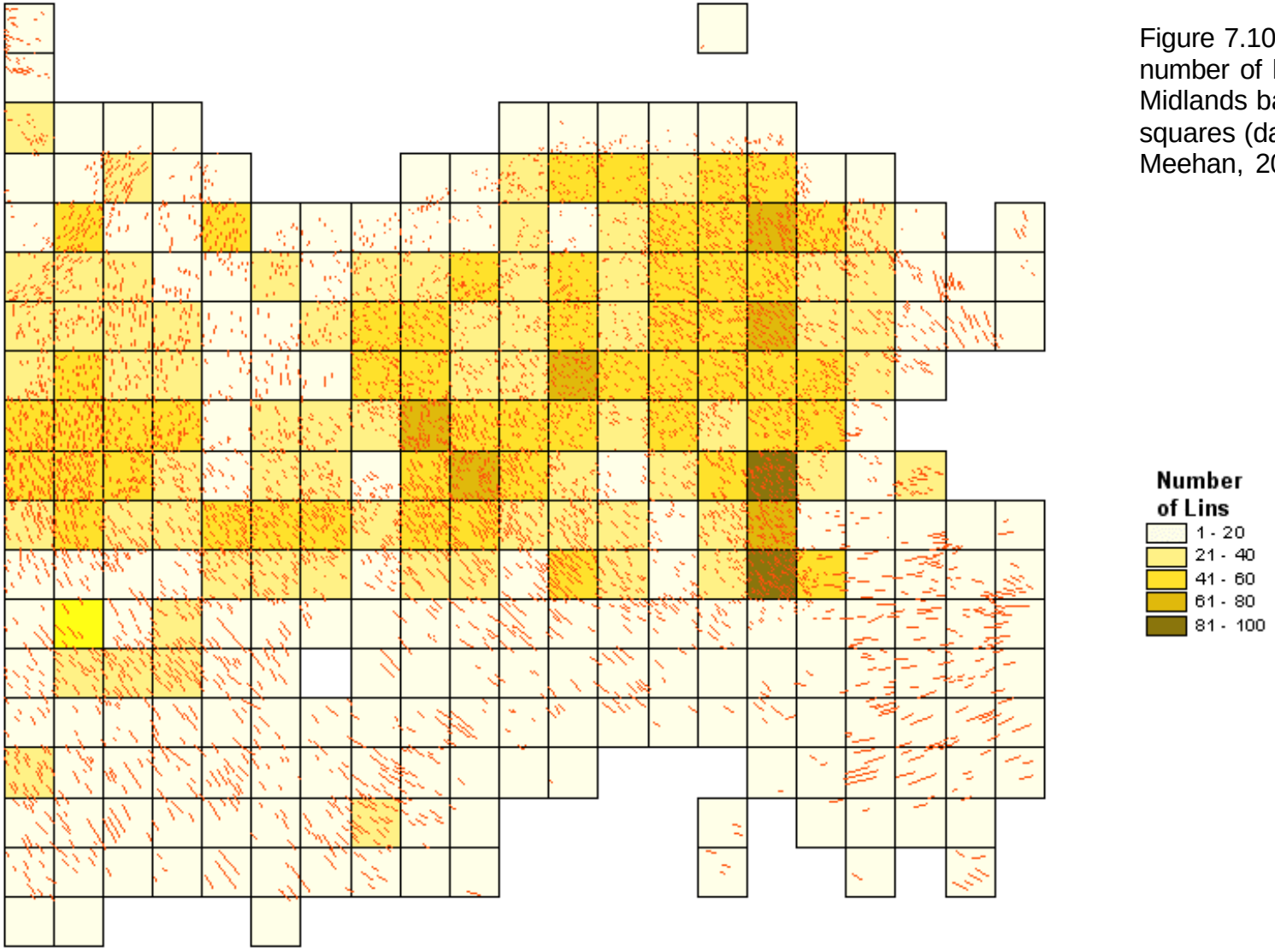

Figure 7.10 b. Density using the number of lineaments for the Irish Midlands based upon 5km grid squares (data from Clark and Meehan, 2001).

spatial continuity. Density can be measured on a region basis by counting the number of lineaments within a grid square. The number of lineaments within 5km grid squares were counted and these values directly plotted (Figure 7.10b). The plot clearly identifies areas of dense lineaments, as well as how continuous the patterns are.

7.3.4 Statistical Back Checking

Generalisation and the classification of lineaments into flow patterns has been a purely qualitative procedure relying on the ability and experience of the observer performing it. Although there are general ideas about the basic visual heuristics used, these are not firmly defined. As a result there are no objective checks that allow the procedure to be verified. This means that, using the same data, a different observer could yield different results. Ideally, flow set definitions should be openly verified such that others can validate them. In addition, comparisons of results using different source data will be more appropriate. This section provides simple statistical procedures to allow flow set definitions to be objectively verified.

As with the previous section, it is appropriate to use a simple, idealised, scenario to explore the basic techniques (as used in §7.3.3). Figure 7.8 clearly identified two main flow patterns based upon their orientation, which was then verified by looking at orientation conformity (i.e. vector strength). The lineaments were split into component flow patterns and, for each set, the orientation and length of lineaments extracted. Orientation data was then plotted on a rose diagram (Figure 7.11a) clearly depicting two distinct flow patterns. This is visualised in Figure 7.12 by creating surface plots for *each* flow pattern separately. These clearly demonstrate that each flow pattern appears as a distinct and valid unit, as they both show *internal* consistency and smooth gradients with high parallel conformity.

Frequency polygons depicting lineament length for each flow set were also plotted (Figure 7.11b). These show a strong similarity. In this example, length alone does not discriminate between the two flow patterns.

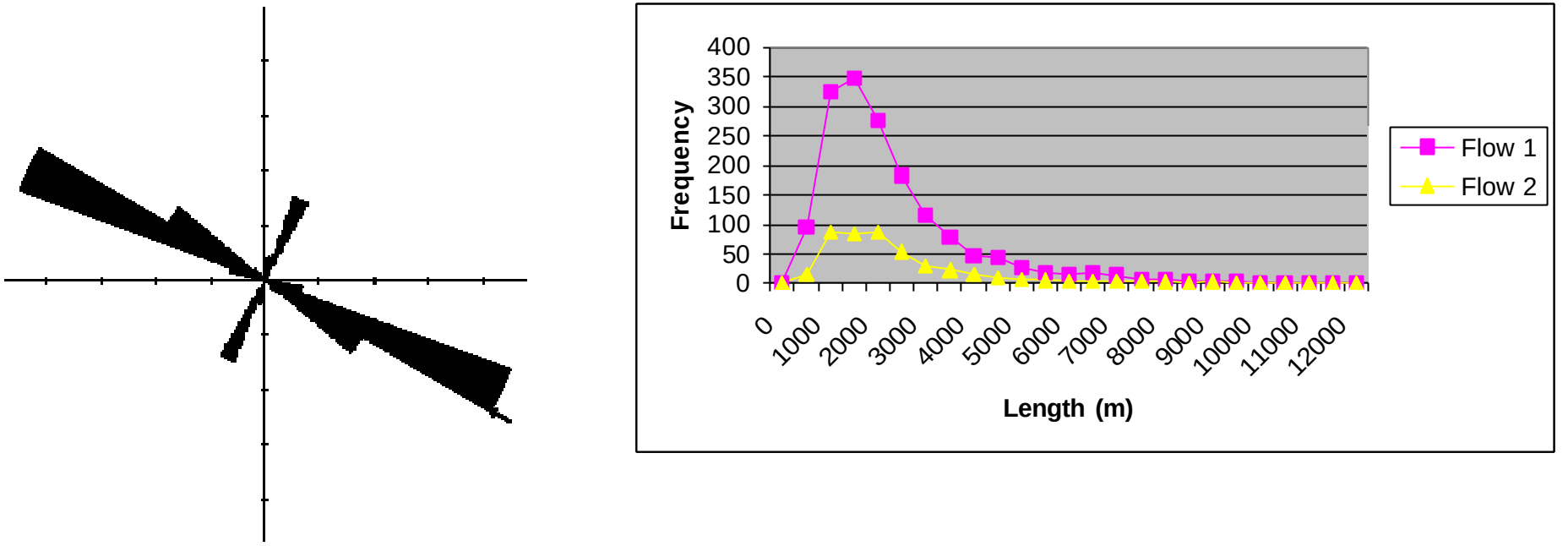

Figure 7.11 a. Rose diagram (frequency) showing the easily identifiable lineament orientations for two flow sets from the idealised data set. b. Frequency polygon of lineament length for the two flow sets. This shows a close similarity in the distribution of lineament length.

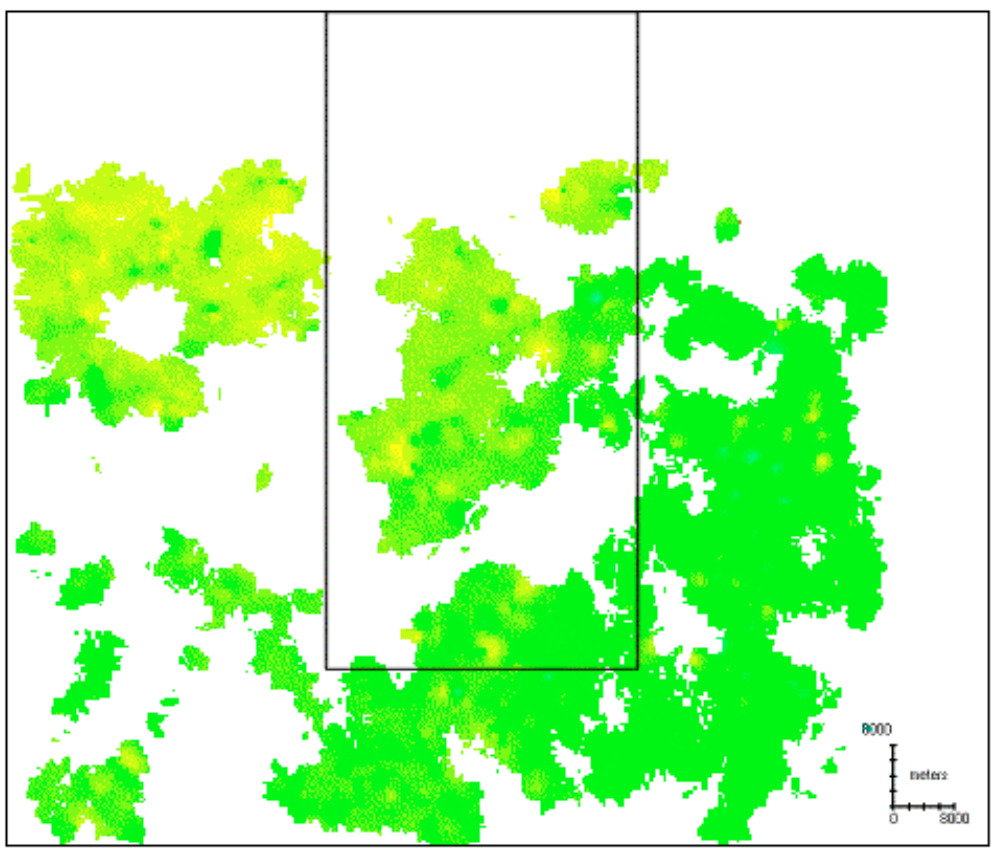

a

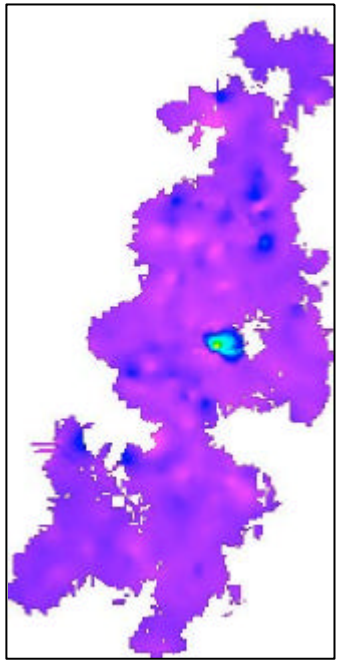

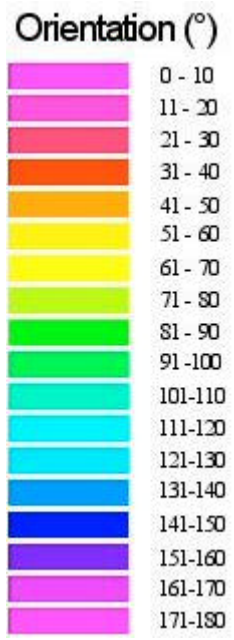

Figure 7.12 Variability of lineament orientation for the idealised data set (300m resolution, 3 min data points, 3000m radii). Dataset is 100km across. The two flow patterns have been separated and are visualised separately (see also box outline of a on b). This shows very strong parallel conformity, with a slight curvature for the first flow pattern (a). The second flow pattern (b) has a single lineament forming a small “island” oriented differently.

The above example is purposefully simple to highlight the basic ideas behind the verification of manually assigned flow pattern classifications. If a flow pattern is considered an individual *unit* then it should display consistency. Consistency is dependent upon whether a flow pattern is deemed to be time-transgressive or isochronous (as discussed in §7.2) and the glaciological context in which these patterns were generated (Clark, 1999 and Figure 3.20). Isochronous patterns are expected to display gradual changes in either (or both) lineament orientation or length (i.e. a smooth gradient of change). Time-transgressive patterns should be identified through cross-cutting, poor orientation conformity and abrupt changes in morphometry. Isochronous patterns are clearly easier to recognise, but careful study of both the surface plots and original lineament data should provide diagnostic features that allow the identification of either; and this can then be visualised and quantitatively verified through the use of the surface plots.

This approach is now applied to the lineaments mapped from the Irish Midlands, as used in the previous section. The lineaments mapped, and visualised in Figure 7.9, were separated into individual flow patterns. This required careful study of the surface plots, particularly orientation and orientation conformity, as well as the original lineament data. In addition, the regional topography must be considered as this can lead to the channelling of ice flow and so a convergence or divergence of localised lineament orientations. In general the Irish Midlands are relatively flat, however there are localised areas of moderate relief which could modify ice flow at a thinned ice sheet margin (i.e. during recession).

Figure 7.13 shows the four flow patterns (FP) that were developed. FP1 is both separate, and orientated transverse to, those in FP2. It is possible that FP1 also forms part of FP3, however this cannot be verified given their spatial separation. FP3 is composed of broadly S and SE oriented lineaments, which, in the south, lengthen the further south travelled (Figure 7.5). FP3 intersects with, but doesn't cross-cut, FP4. These two patterns are distinguished by differences in lineament orientation and length (Figure 7.5). Figure 7.14 shows rose diagrams for each flow pattern, highlighting their distinctive orientations. This also shows a greater spread in orientation for FP1. FP1 could be composed of two different

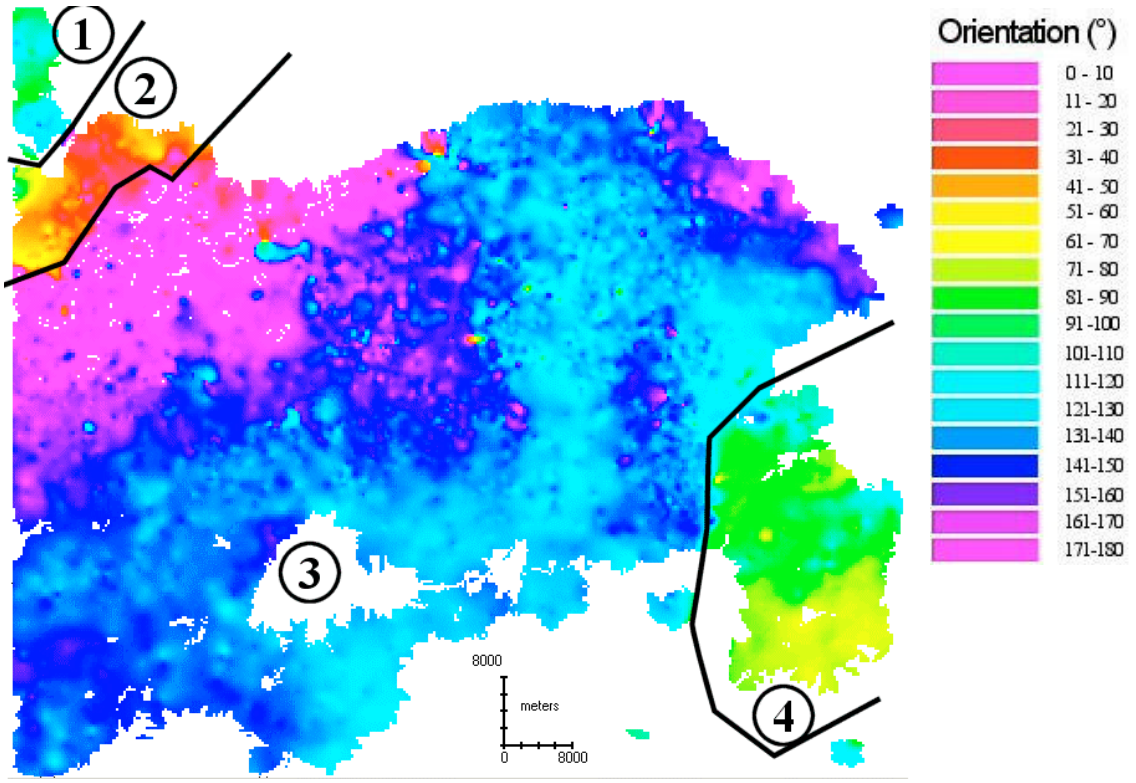

Figure 7.13 Surface plot of lineament orientation for the Irish Midlands (300m resolution, 3 min data points, 3000m radii). The region has four broad flow patterns which are marked. These are all spatially separate, except for a small overlap between 3 and 4. Although presented in a single diagram, they were all analysed separately.

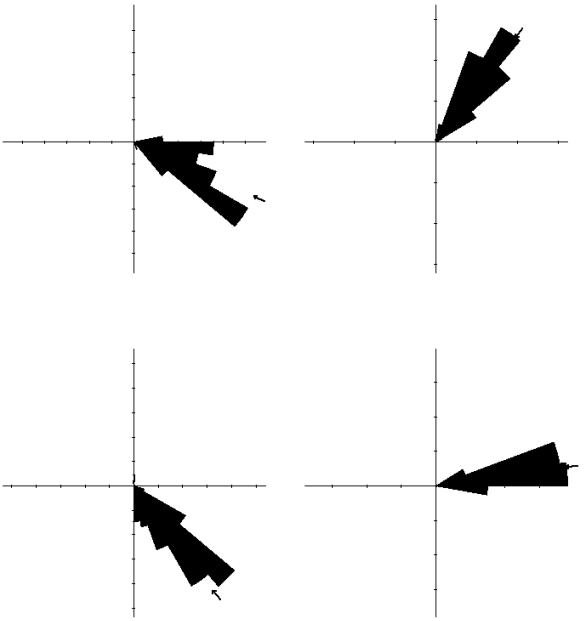

Figure 7.14 Rose diagram (frequency) of lineament orientation for flow patterns 1 (top left; 61), 2 (top right; 183), 3 (bottom left; 5156) and 4 (bottom right; 174) for the Irish Midlands. The four flow patterns are distinct. FP1 shows the widest variation and could be interpreted as two flow patterns, although there are not many data points.

patterns, however reference to elevation data shows moderate relief, which could have caused local divergence. FP3 is the largest flow pattern and covers the majority of the region. This shows a gradual change in orientation (Figure 7.9), although vector strength (Figure 7.15) suggests there is greater variability here. This could be, in part, due to the effects of topography, the presence of a second flow pattern or possibly a time-transgressive flow pattern. The first possibility requires the close scrutiny of topography to account for the effects of relief, whilst the second, although possible, should be more apparent throughout the whole area (rather than restricted to the NE) and additional features such as cross-cutting would be expected. The final suggestion is also possible, although again cross-cutting would be expected. Given the above options and the amount of information available, FP3 is retained as a single, isochronous, flow pattern due to the high orientation conformity.

7.4 Lake District Case Study

7.4.1 Introduction

This section is designed to use the techniques developed above and apply them to a real-world situation. Just as Chapter 6 used the Lake District as a study area for landform mapping, so this section will use those landforms mapped previously and separate them into flow patterns using these methods. In addition to the figures presented in this chapter, the map on the inside cover should also be consulted. It is important to note that this section provides no interpretation beyond that required to form flow patterns. It is a non-interpretative stage that is quantitatively verifiable and so re-usable by other researchers.

7.4.2 Flow Pattern Formation

The Lake District presents many difficulties both for landform mapping and the creation of flow patterns. For the latter, these difficulties include:

- Multiple flow sets
- Cross-cutting
- Different bedform shapes
- Interruption of bedform suites by relief.

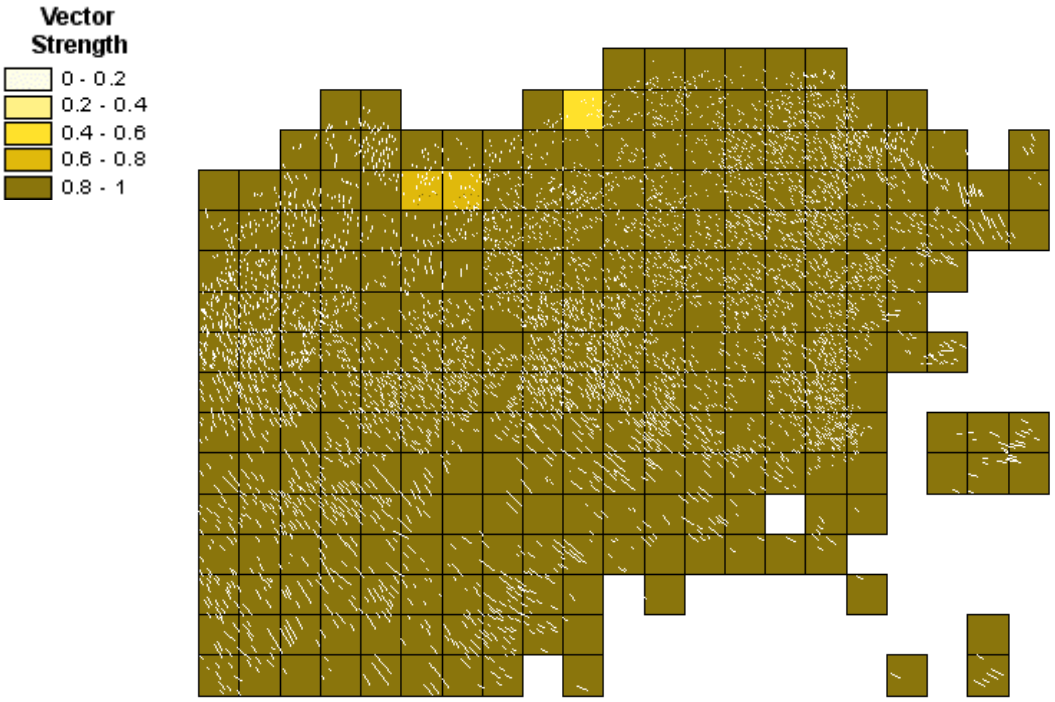

Figure 7.15 Vector strength using 5km grid squares for flow pattern 3 in the Irish Midlands. Note the lower vector strength values in the NW corner.

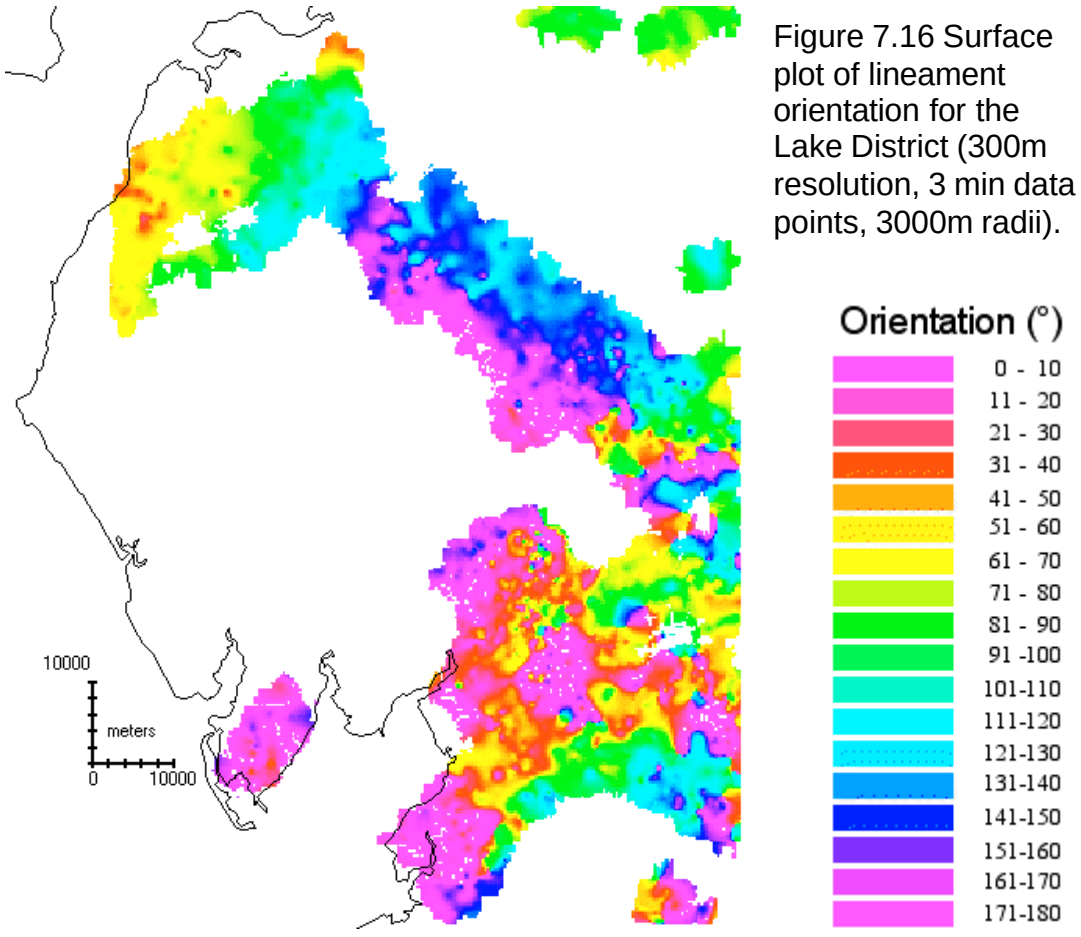

Figure 7.16 Surface plot of lineament orientation for the Lake District (300m resolution, 3 min data points, 3000m radii).

Initial exploration was performed by creating a surface plot of orientation for the Lake District (Figure 7.16). This highlights the complexity of lineament patterns within the study area. The northern region initially appears broadly straightforward. A curving pattern of lineaments is readily apparent (purple [0-20º], to red [21-50º] through yellow [51-70º], to green [71-100º] and blue [101-160º] then back to purple), however this is partially dissected by a variegated area on its southern edge (in the vicinity of Shap) indicating the possible presence of another flow pattern. On the eastern side (around Brough and Stainmore) there is a sudden change from lineaments trending to NW-SE (blue) with those trending W-E (green). This again has a variegated pattern suggesting cross-cutting. In the southern region the pattern becomes more complex. The western edge (from Kendal down to Lancaster) is strongly variegated showing one broadly dominant pattern trending N-S (purple) which is heavily dissected. The eastern region (incorporating the head of the Wensleydale valley and southwards into Ribbledale) has an intricate mix of lineaments of various orientations. This is partly due to the extensive relief in this region and requires careful investigation.

Further evidence for discriminating flow patterns is provided by vector strength applied to the original lineament data (Figures 7.17) and to the interpolated raster data (Figure 7.18). These plots both highlight high variability in orientation in the northern area, around Shap, of the dominant NW-SE flow and around Brough. In the southern region, the western and eastern edges are again highlighted. Figure 7.19 is a surface plot of lineament length and this further emphasises these zones of variability.

The manual development of flow patterns involved the use of the above figures, in conjunction with the original lineament mapping. Careful consideration was given to conformity in orientation and length and the patterns were iteratively developed to help converge upon consistent flow patterns. The broad outline of flow patterns is shown in Figure 7.20 and descriptive statistics shown in Table 7.1. It is important to note that these are developed as flow patterns and *not* flow sets. They are assessed in terms of orientation, length and spatial continuity and therefore it would be normal for some to link together to form flow

Flow Pattern	Number of lineaments	Mean		Min		Max		Data Spread	
		Length (m)	Orientation (º)	Length (m)	Orientation (º)	Length (m)	Orientation (º)	Standard Deviation Length (m)	Vector Strength Orientation (º)
L1	166	522	89	163		1626		225	0.839
L2	101	489	80	261		863		141	0.946
L3	643	689	90	180		2256		265	0.807
L4	152	460	81	162		1723		207	0.705
L5	576	448	5	103		1229		169	0.827
L6	181	472	89	134		1360		184	0.885
L7	237	469	42	130		1204		169	0.522
L8	27	582	37	269		1025		157	0.878
L9	71	690	85	269		1691		288	0.930
L10	147	493	113	115		1170		181	0.920
L11	126	431	17	145		1308		163	0.886
L12	80	452	102	134		1360		226	0.935

Table 7.1 Descriptive statistics for flow patterns L1-L12. For the mean, min, max data spread, the first column shows lineament length (In metres) and the second orientation (in degrees). For orientation, the vector mean and vector strength have been calculated, whilst the minimum and maximum have been omitted as they are meaningless for undirected circular data.

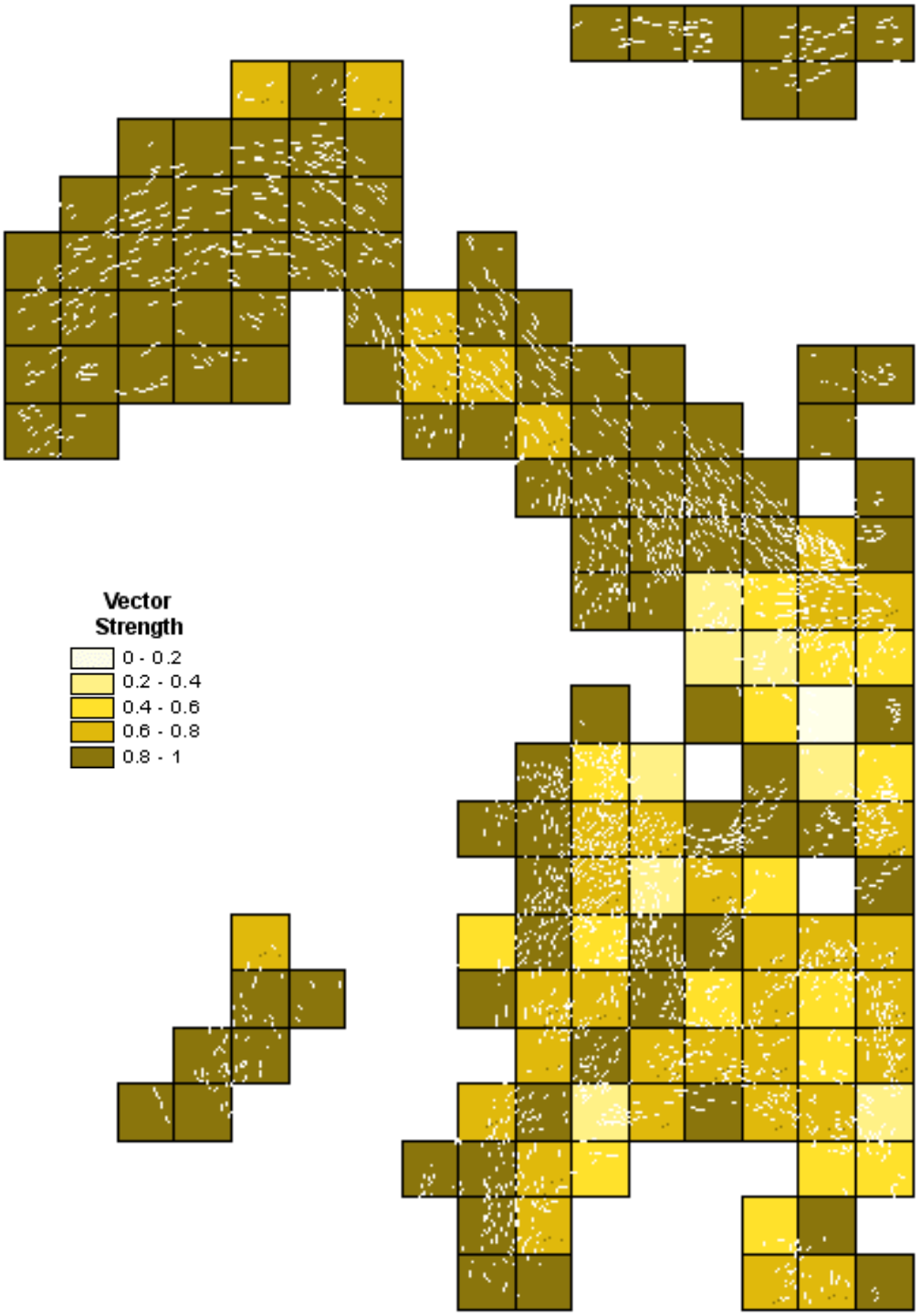

Figure 7.17 Vector strength using 5km grid squares for all lineaments mapped in the Lake District. Note that only parts of the north and central regions in the south have high vector strength values indicating a complex mix of multi-oriented lineaments elsewhere.

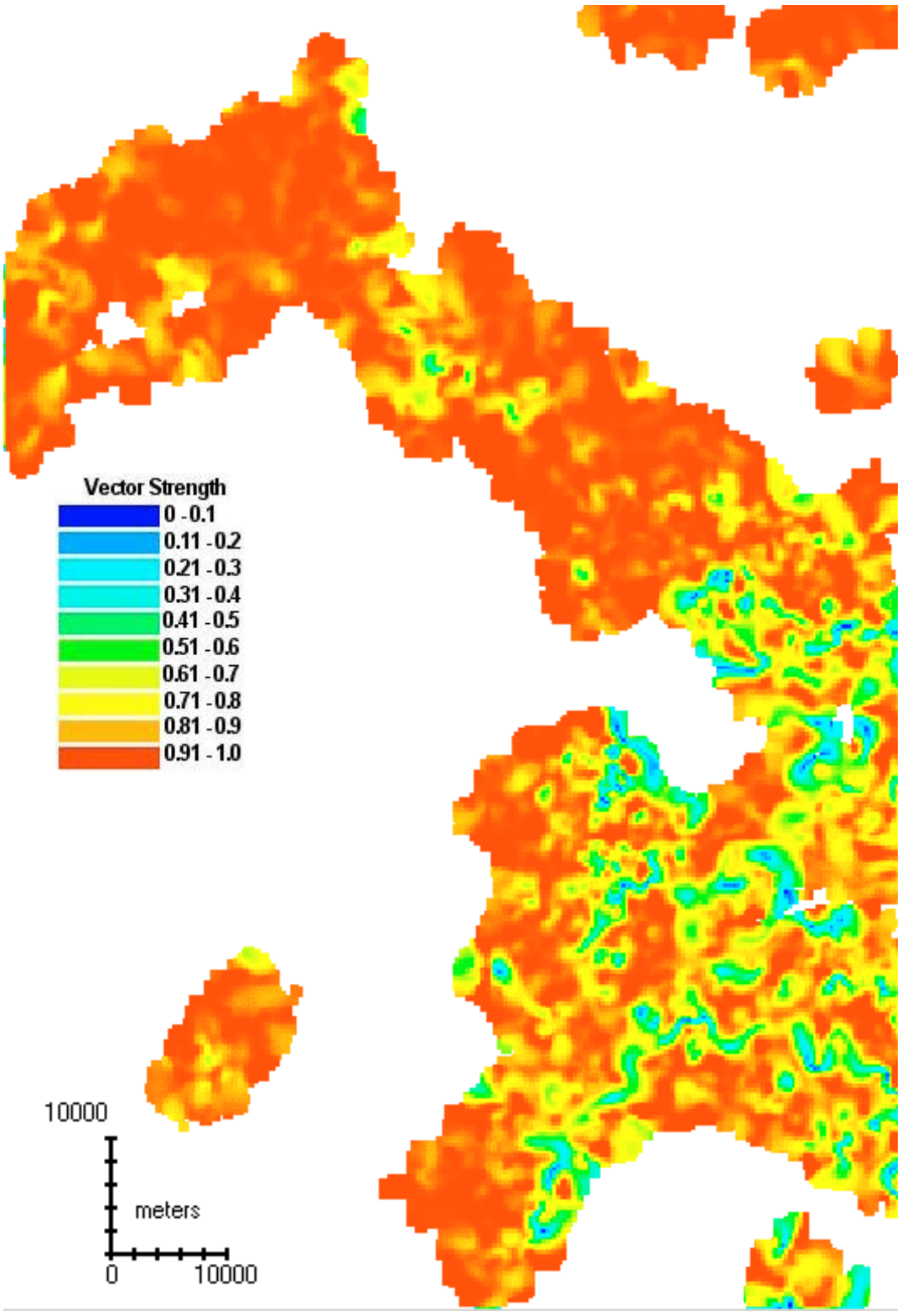

Figure 7.18 Using the surface generated for Figure 7.16 this image shows vector strength applied to a 3x3 window. Orientation conformity is generally good, although there are distinct areas of high variability in orientation. Red represents high vector strength (and so good orientation conformity), whilst variegated areas show lower vector strength values.

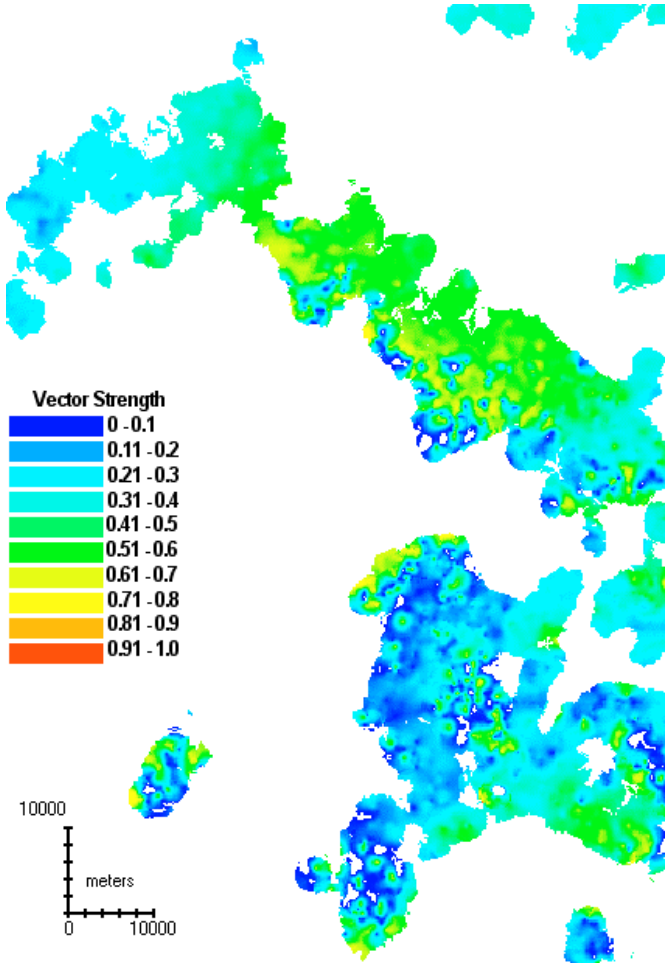

Figure 7.19 Interpolated surface of lineament length for the Lake District (300m resolution, 3 min data points, 3000m radii). Blue represent short lineaments and red, long.

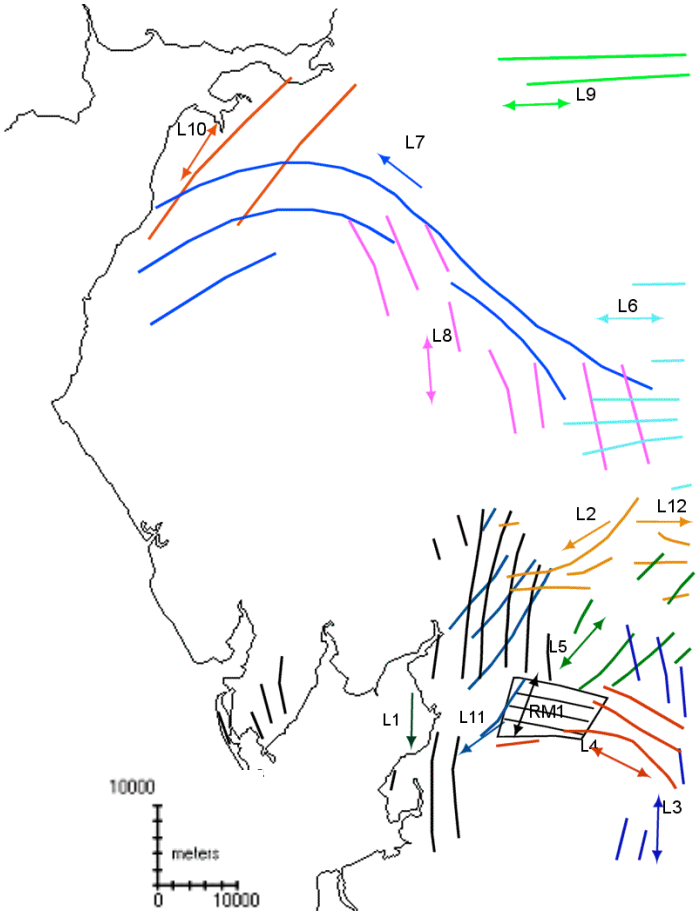

Figure 7.20 Generalised flow patterns developed from the individual landform data. Each flow pattern is numbered, with an arrow indicating the direction of flow. Colours are purely illustrative.

sets. However the Lake District is a fairly small region made up of many isolated flow patterns.

Although not strictly part of the generalisation process, it is also important, prior to the creation of flow sets, to collate pertinent glaciological information. These include ice thickness, ice flow direction and cross-cutting relationships (to infer relative age); this information can then be applied to individual flow patterns. *Ice thickness* can be determined by noting the maximum elevation that drumlinisation occurs at for a particular flow pattern. Field measurement of trim lines can also be used. *Ice flow direction* is determined by noting individual drumlin stoss-lee relationships (i.e. the steeper, fatter, stoss end typically points upstream). *Cross-cutting* relationships require evidence of the superimposition or re-modification of a drumlinised landscape (e.g. Figure 2.5a). Both cross-cutting and ice flow direction evidence requires detailed morphological information. As the discussion regarding satellite imagery recommends in §5.6, 30m or 10m resolution data are ideally needed. This advice is not directly transferable to DEM data; close scrutiny of the OS DEM data for the Lake District shows that it is not able to reliably provide this level of detailed information. In selected situations (e.g. Figure 7.25b) it is able to resolve necessary detail, however this is the exception rather than the rule. For ice flow direction, the traditional stoss-lee relationship may not be visible, particularly in areas that have been remoulded from different ice flow events. Whiteman (1981) specifically notes that, for his small study area in part of the Eden Valley (around Appleby), no preferred ice flow direction could be discerned. Therefore some regions may have no direction indicators available. In general, without clarification from the DEM, and in the absence of further corroboration from primary data sources (e.g. satellite imagery, aerial photography, field mapping), it is necessary to utilise published evidence. This is essential for comparative purposes and can provide additional directional information from erratic evidence. This supporting evidence is now collated using the DEM data and are discussed further in §7.4.4.

The entire area was split into northerly and southerly regions; each flow pattern is now discussed within this context. The northerly region is dominated by the

lineaments curving around the north of the Lake District (L7). This main ice flow was separated out from the surrounding lineaments and a surface plot of orientation created (Figure 7.21a). This shows a gradual change in orientation from SW-NE in the west, through to NW-SE in the east, with the overtopping of local relief up to 350m. Small variations in colour highlight localised changes in orientation with a pronounced region in the east trending N-S. Direction indicators from the DEM suggest ice flow was from SE to NW (Figure 7.25a).

L7 is intersected by two other main ice flow patterns, L8 and L6. L8 is predominantly trending NNW-SSE (Figure 7.21b), with ice flow tentatively ascribed as from SSE to NNW (a glaciologically plausible scenario) overtopping elevation of 300m. The NW part of this flow pattern shows good orientation conformity, whilst the SE section less so. L8 is cross-cut by L7 (i.e. L8 is older; Figure 7.25b). L6 is a predominantly W-E trending flow pattern (Figure 7.24a) that has good orientation conformity. There are no direction indicators in this area (see also the following section). Although cross-cutting is clearly evident with L7, it is not clear which flow pattern is older. The northern part of L6 occupies an upland region (around Stainmore) at ~500m and is associated with transverse forms located here.

The final two flow patterns in the northern region (L9 and L10) possibly form part of the same flow set. L9 forms a predominantly E-W flow which climbs elevation of 300m at the DEM edge (Figure 7.24b), whilst L10 is trending NE-SW. The latter has too few points (27) to be able to reliably create a surface plot for. No direction indicators are readily apparent.

In the southern region the dominant flow pattern is L1, which is trending N-S (Figure 7.22a) with direction indicators recording a flow direction towards the south (Figure 7.25c), overtopping 200m elevation. Although broadly exhibiting a single ice flow direction, the pattern is relatively discordant with variability in lineament orientation. This flow pattern is tentatively described as time

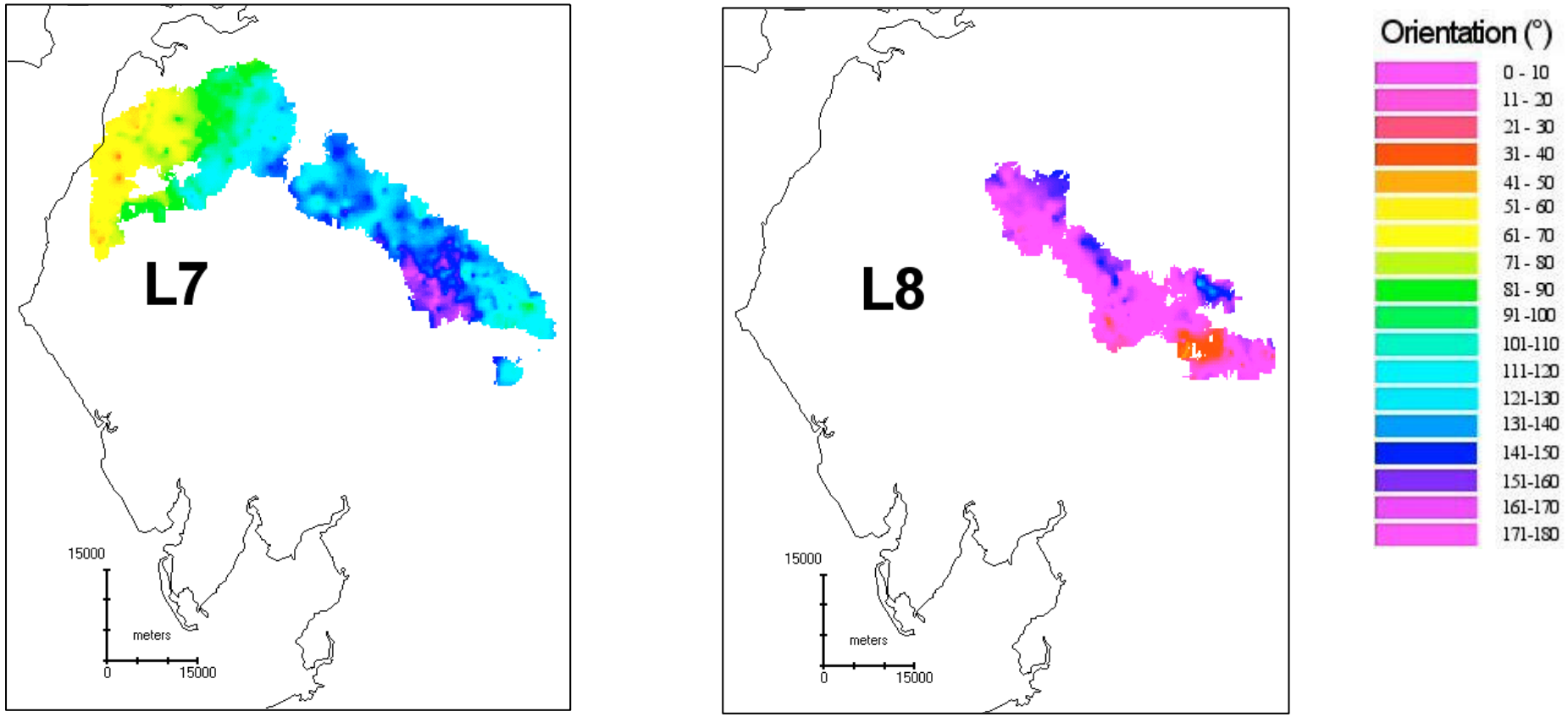

a

b

Figure 7.21 Surface plots of lineament orientation (300m resolution, 3 min data points, 3000m radii) for flow patterns L 7 (a) and L8 (b). L7 depicts a gradual change in orientation, curving around the northern Lake District. L8 is less conformable than L7 and is possibly time-transgressive.

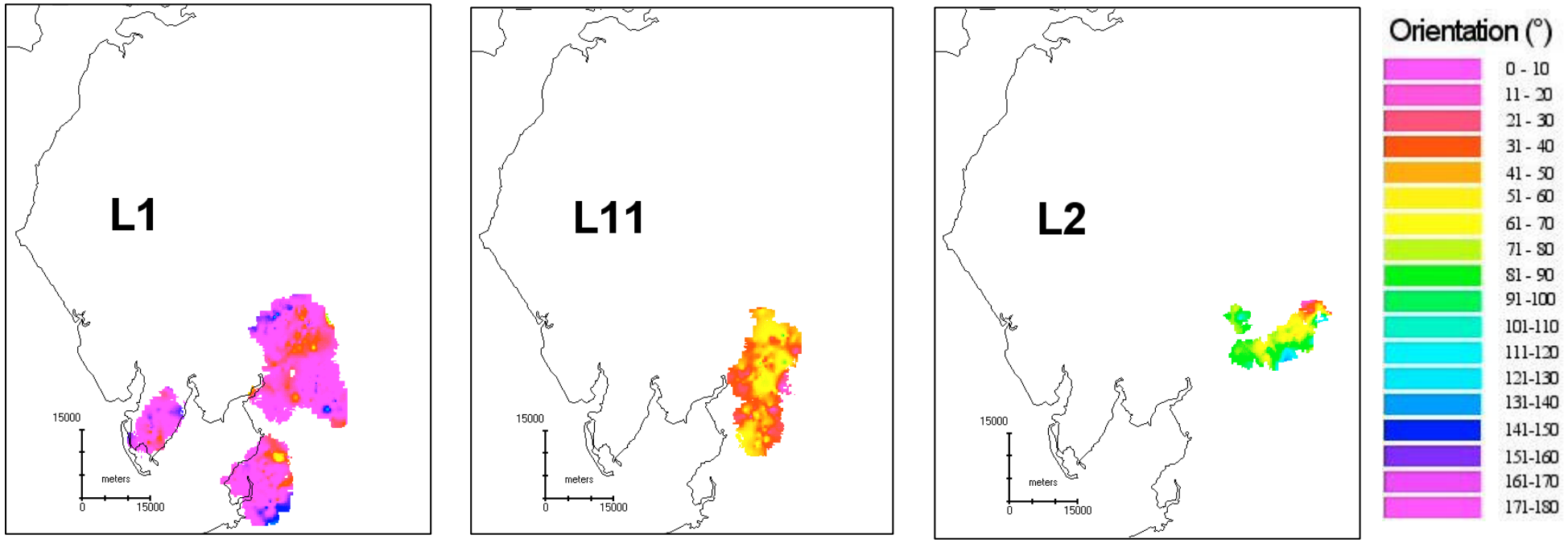

a b c

Figure 7.22 Surface plots of lineament orientation (300m resolution, 3 min data points, 3000m radii) for flow patterns L 1 (a), L11 (b) and L2 (c). L1 is dominated by a predominantly S oriented flow direction, although there are localised areas of inconsistency, possibly denoting a time-transgressive flow pattern. L11 and L2 both shown good orientation conformity, although the latter is effect by the constraints of topography.

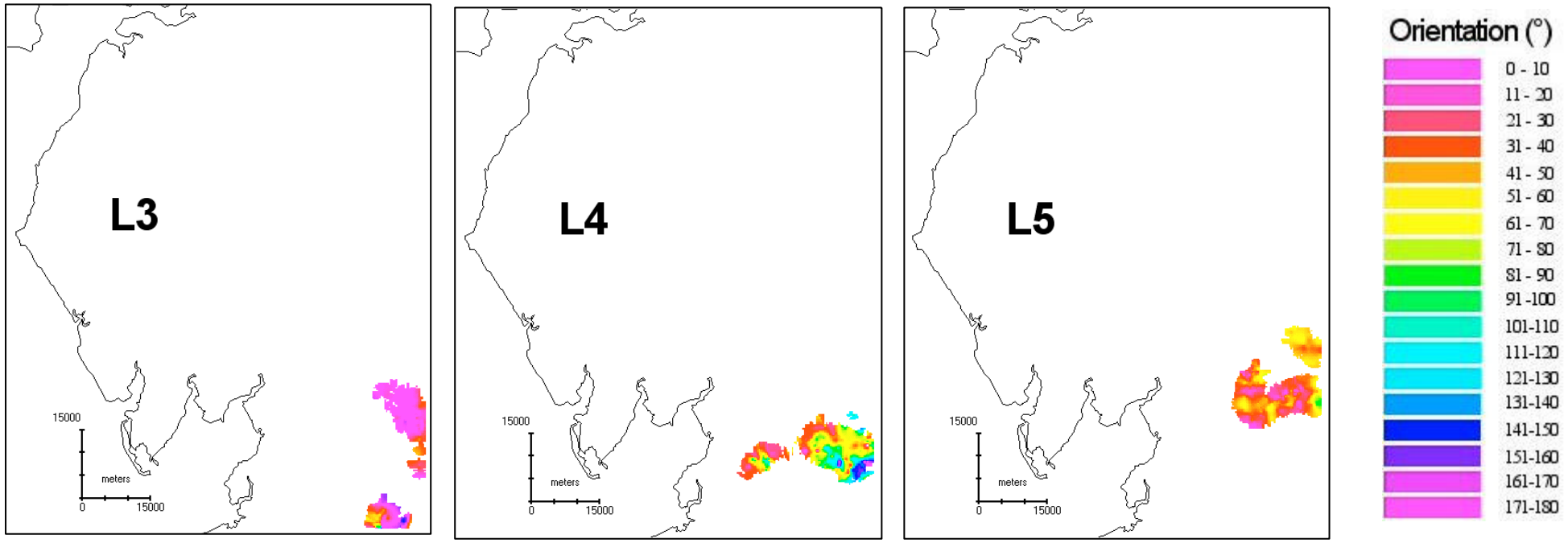

a b c

Figure 7.23 Surface plots of lineament orientation (300m resolution, 3 min data points, 3000m radii) for flow patterns L 3 (a), L4 (b) and L5 (c). L3 shows localised inconsistencies in orientation, although it is constrained by topography. L4 and L5 both show good orientation conformity, again they are both partly controlled by topography.

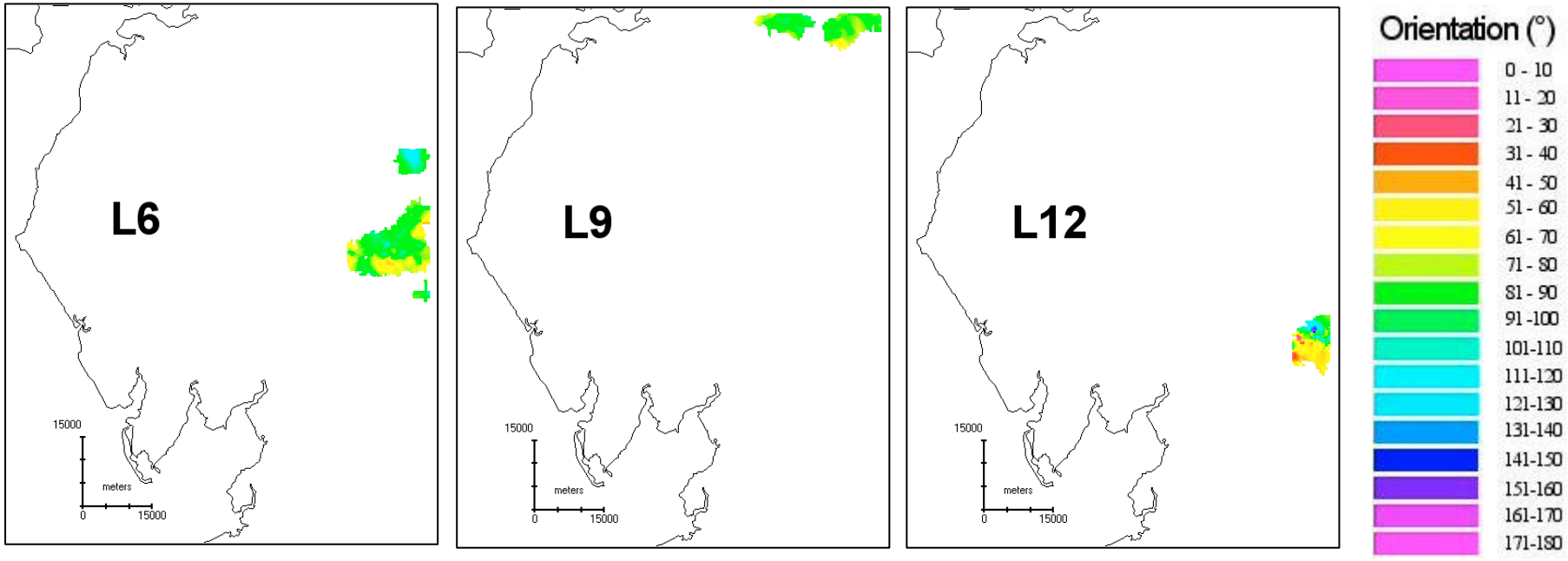

a b c

Figure 7.24 Surface plots of lineament orientation (300m resolution, 3 min data points, 3000m radii) for flow patterns L6 (a), L9 (b) and L12 (c). L6, L9 and L12 show good orientation conformity.

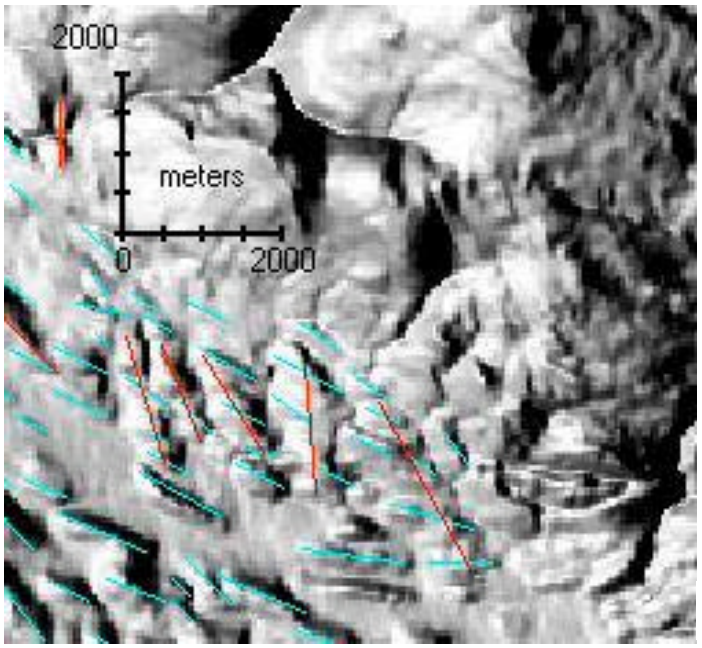

a

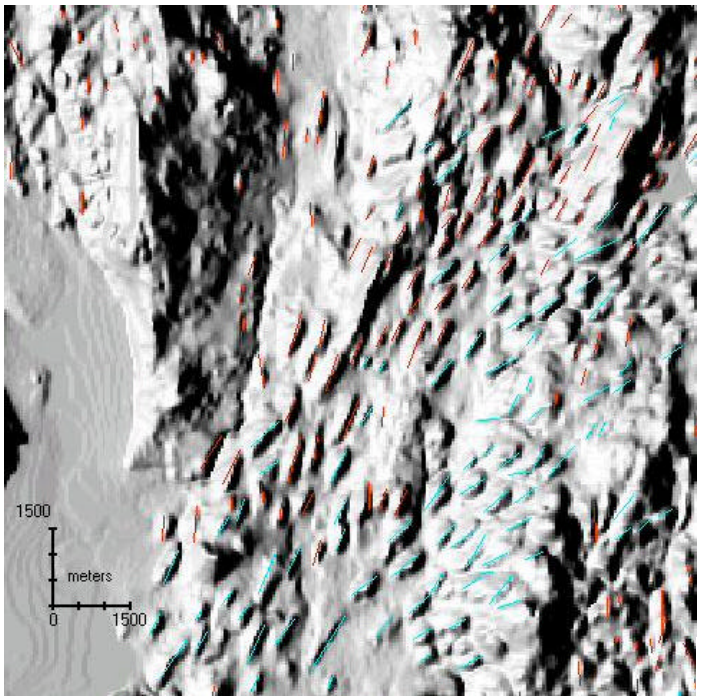

b

Figure 7.25 a. Example of cross-cutting showing smaller drumlins (L7) superimposed on larger, N-S trending, drumlins (L8).

b. Area of L1 showing traditional stoss-lee relationship with steeper, fatter, stoss end pointing upstream.

(©Ordnance Survey).

transgressive. The transverse bedforms located around Ingleton (RM1) are associated with, and are cross-cut by, L1.

L1 is intersected by L11 and L2. L11 exhibits strong orientation conformity (Figure 7.22b), with direction indicators confirming flow direction of NE to SW (and, as for L1, overtops 200m elevation). There are no clear signs of cross-cutting so a relative age relationship cannot be inferred. L2 (Figure 7.22c) exhibits good orientation conformity, although there are small changes in lineament orientation. This appears to be due the effects of topographic constraint (around 500m), with direction indicators tentatively suggesting ice flow broadly from E to W (supported by the convergence of topographically constrained drumlin patterns). L2 is cross-cut (i.e. older) by L11. L12 (Figure 7.24c) is also topographically constrained and, although there are no direction indicators, ice flow would be expected to flow to the lowlands in the east.

The remaining flow patterns (L3, L4 and L5) occupy the areas around Ribblesdale, Ingleton and Whernside, respectively, in the central and eastern parts of the southern region. L3 is located in an upland basin (~300m) and is trending N-S (Figure 7.23a), running incontinuously to the southern border of the DEM. These forms are relatively short, heavily modified and closely associated with the transverse bedforms located in the upper reaches of Ribblesdale. L4 forms part of a heavily modified lowland region that was partially mapped by Raistrick (1933). Although there are no direction indicators, lineaments are broadly trending E-W (Figure 7.23b). Finally, L5 is a NE-SW trending flow pattern (Figure 7.23c) which predominantly follows valleys but at its western extent climbs relief to 400m. It is also possible that RM1 has removed any previous bedforms beyond its current western extent. Again there are no direction indicators.

7.4.3 Geomorphological Ice Flow Direction Indicators from the Literature

It is appropriate to consult the literature to confirm the assessments of ice flow direction (using lineament stoss-lee relationships), as well as filling in areas where my assessments are not available. In the northern area the most prolific fieldwork was performed by Hollingworth (1931) and summarised by Mitchell

and Clark (1994). This work confirms the existence and direction of flow pattern L7 (SE to NW) and provides new direction information for flow patterns L6 (W to E), L8 (SSE to NNW) and L9 (W to E). It is probable that L10 links with drumlin flow direction NE to SW identified by Hollingworth (1931) just north of the border. Mitchell and Clark (1994) also summarise regional patterns identified by the distribution of Shap granite erratics which broadly support these flow directions. Riley (1987) reports on cross-cutting drumlins in the east, suggesting that flow pattern L7 is succeeded by L6. Whiteman (1981) is unable confirm ice flow direction, although concurs with Riley (1987) that it was probably broadly south to north. His morphological mapping confirms the cross-cutting of L7 on L8 (i.e. L8 is older). Boardman (1981) also confirms the northerly flow of L8 from the Lake District. The drumlin mapping of Burgess (1979) covered from Appleby to Brough. Unlike Riley (1987), he did not identify superimposition within the drumlin assemblage. However he suggests ice flow directions of west to east (as for flow pattern L6) linking with ice flow from NW to SE. This is opposite to the ice flow assigned to L7. He confirms this interpretation with erratic evidence east of Stainmore which shows evidence of Lake District and Scottish ice (Shap and Galloway erratics). Arthurton (1981) confirms the northward ice flow direction around Penrith (consistent with flow patterns L7 and L8) although his he was not able to confirm the existence of two different flow patterns. Erratic evidence shows the presence of both Lake District and Scottish ice. In the northern part of his region he specifically notes the existence of rough ground made up of irregularly shaped bedforms as possibly indicating where Lake District and Scottish ice sheets may have converged.

Far less landform data is available for the southern Lake District. Vincent (1985) reports broad ice flow patterns which simply depict southward flowing ice. For the Ribblesdale Valley and the area around Settle Raistrict (1933) reported striae orientations of NW to SE (my flow pattern L4), whilst Arthurton (1988) suggests ice flow from N to S, however he provides no corroborative evidence. For the area around Lancaster, Brandon (1998) identifies two tills in the region and suggests that they demarcate two ice flow events, supported by erratic evidence. One ice flow from an ice divide centred over the Howgill Fells (representative of my L5) and the other from the Lake District (representative of

my L1). He also notes the presence of a section of hummocky terrain which forms part of my flow set tentatively identified as ribbed moraine. Mitchell (1994) mapped drumlins in the Baugh Fell region (Wensleydale/Garsdale) where the cross-cutting and ice flow direction indicators are more complex. In general, he identifies a convergence of drumlins in Wensleydale and Garsdale indicating ice flow *down* these valleys (equivalent to L2 and L12). However these drumlins are superimposed upon larger drumlins which indicate ice flow from SW to NE. This ice flow direction is also supported by erratic evidence and drumlin mapping by Hollingworth (1931) in the Mallerstang area. It may link with my L5, although this flow pattern is more indicative of flow from NE to SW. §6.6.3 highlighted the reasons for poor correlation between the mapping of Mitchell and this work. It is possible that the DEM is unable to resolve the flow patterns Mitchell has mapped or that the bedforms identified as transverse forms in this region were mapped by Mitchell as drumlins. Mitchell confirms the easterly and westerly ice flow directions of L12 and L2 respectively, as well as southerly flow direction for L3 (the latter also confirmed by Hollingworth).

7.4.4 Summary of Flow Patterns

This section applies the techniques developed earlier in this chapter to the landform data mapped in Chapter 6. The use of orientation data was the primary tool in separating lineaments into individual flow patterns and was highlighted through the use of spatial variability plots of orientation and orientation conformity (i.e. vector strength of the interpolated dataset). Using this information, lineaments were separated into twelve flow patterns, according to their orientation and spatial continuity. This information needs to viewed within the context of ice thickness (where indicators are available) and the effect of topography for channelling ice flow. Further information that can be gained includes ice flow direction and relative age (through cross-cutting relationships).

The work concludes the grouping of lineaments into flow patterns and precedes the full glacial reconstruction. The latter would involve the grouping of flow patterns into flow sets and a subjective assessment of the timing of their formation (i.e. isochronous or time-transgressive). A thorough review of the available literature is required before a final reconstruction is performed.

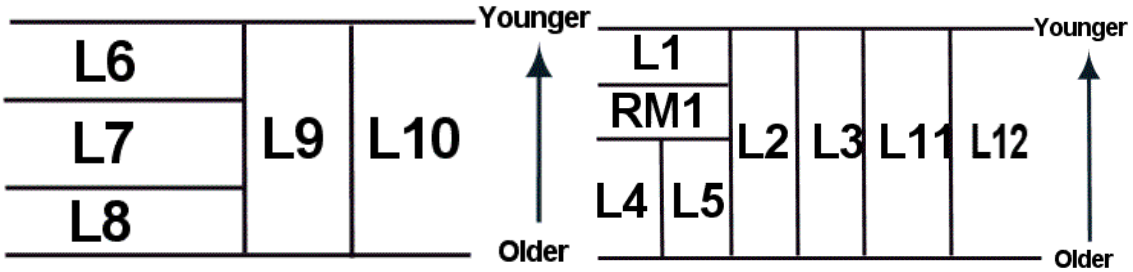

Table 7.2 Relative ages for the northern (left) and southern (right) Lake District. Horizontal lines denote a known or inferred (see text for further details) relative chronology. Vertical lines separate flow patterns where no relative chronology is known; for example L3 could "slide" up and down in time.

It is appropriate, at this stage, to comment on the data as it now stands. Initial evidence needs to be viewed within the constraints imposed by relative age relationships (Table 7.2) which, for example, broadly state that L8 precedes L7 in the north, whilst L4 precedes L1 in the south. L6 appears to have removed any past bedform traces of L8 and so is inferred to be younger; Riley (1987) has confirmed that L6 is younger than L7. In the south, RM1 is cross-cut by L1 and so precedes it. Their formation is thought to be closely linked (e.g. Clark and Meehan, 2001) and so they would probably have been formed during the same period. RM1 appears to have removed possible previous bedforms from L5 and L4, so these are inferred to be older.

Phase 1: Early expansion of Eastern lakes/Pennine/Howgill Fell ice.

For Phase one, L8 is proposed as the first recorded ice movement demonstrating the dominance of ice expanding out from the Pennines with a divide centred on the Eastern Lakes/Howgill Fells. The strong imprint of L8 on the landscape (with northward ice flow indicated by Hollingworth) does not extend beyond the Vale of Eden. Either such a trace has been removed or this early expansion was not extensive. This ice flow would have been followed by, or contemporaneous to, L11 and L3. These are again strongly imprinted upon the landscape and extend southwards. During this period there is no evidence for activity related to the central Lake District, however this must have had an ice dome and it is likely that any early traces of ice movement have been removed.

Phase 2: Major expansion of Pennine ice, confluent with Scottish ice, and a restricted Lake District ice dome.

Phase two would have seen the dramatic development of Pennine ice, forming the strongly curving flow pattern of L7. This is important as major westward flowing ice from the Pennines is not currently considered likely; this is, in part, because there is no evidence of Pennine erratic dispersal west of Stainmore. This flow pattern also suggests the presence of Scottish ice blocking the Solway Firth, as well as ice over the Lake District blocking a direct western passage. Hollingworth (1931) commented on the odd bedform shapes in the Carlisle region which show no preferred orientation. These *could* be indicative of the confluence of Scottish and Pennine ice. L10 and L9 indicate SW and E flowing Scottish ice respectively. Huddart (1994) presents erratic evidence to support the direction of L10, whilst Catt (1991) presents similar evidence for L9. Although these are tentatively grouped together, there are no constraints on their relative chronology and it is quite possible that L10 is representative of a re-advancing Scottish ice sheet in Phase 3 (this is also supported by Huddart, 1994). L5 is possibly contemporaneous. Finally L2 is possibly a late phase movement, as the flow pattern is contained within the valleys, before finally exiting west.

Phase 3: Expansion and subsequent retreat of Lake District ice.

Phase three is dominated by the strong imprint of L6 showing a possible expansion of Lake District ice, along with L12. L1 (including RM1) is possibly deglacial, demonstrating late phase retreat of ice towards the Lake District (i.e. it is *not* synchronous with L6 and L11). It should be noted that L4 (as shown in Figure 7.20) is somewhat of an anomaly. It is possible that L4 fits into the flow set formed by L6 and simply demonstrates the expansion of Lake District ice. The preservation of these landforms is poor and has been almost entirely erased by the transverse bedforms mapped further west.

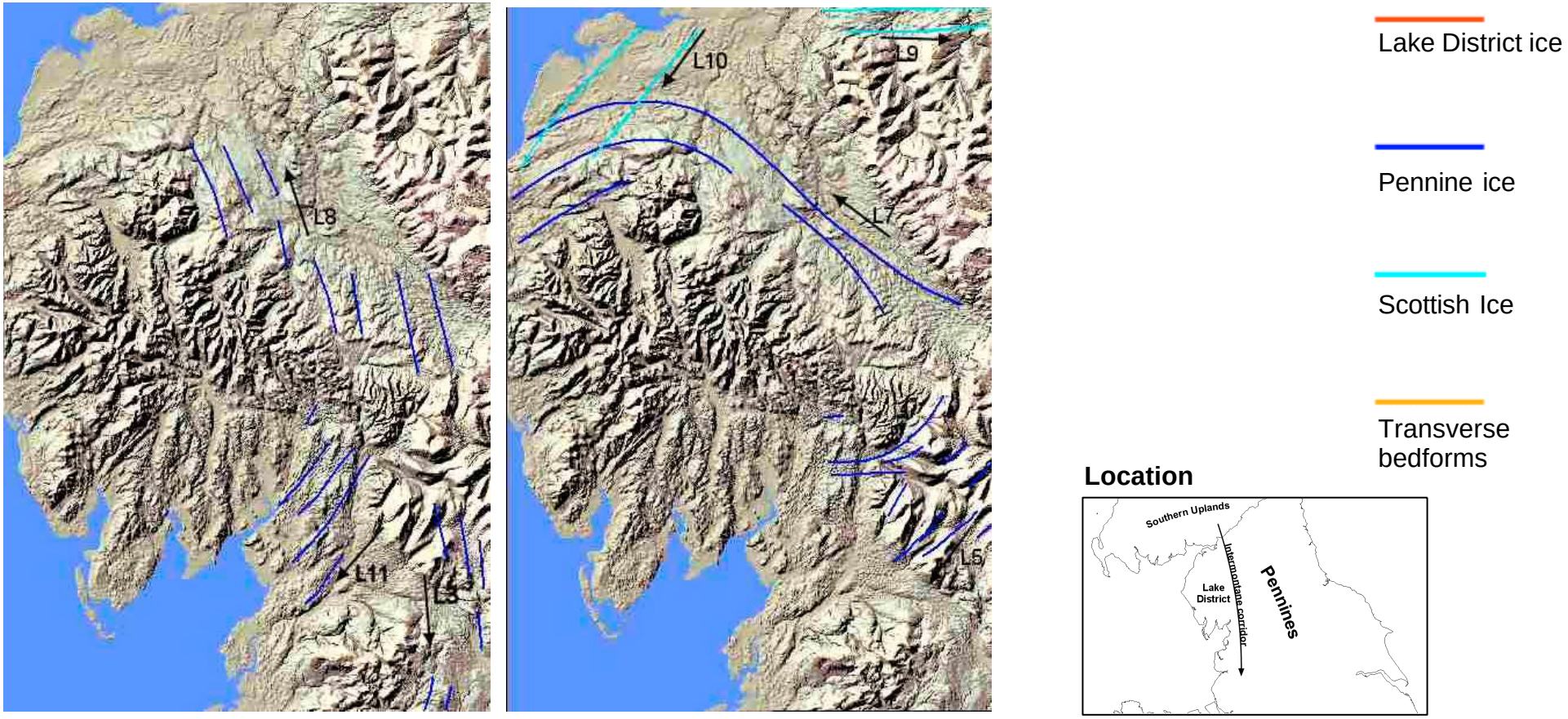

Phase 1 **Phase 2**

Figure 7.26a Preliminary ice sheet reconstruction reducing the 12 flow patterns to three main phases of ice flow. Phase 1 depicts the dominance Howgill Fell Ice (L8, L11 and L3) This expansion becomes a dominant pattern around the Lake District in Phase 2 with the formation of the curving ice flow around the north (L7). This is confluent with Scottish ice (L9 and L10) which is deflected eastwards and westwards. An ice dome over the Lake District probably blocked the direct westerly passage of L7.

Lake District ice

Pennine ice

Scottish Ice

Transverse bedforms

Phase 3

Figure 7.26b Phase 3 demonstrates the expansion of Lake District ice forming L6 and L12. Although in the same phase, L1 is representative of a waning ice dome over the Lake District and (in conjunction with the transverse bedforms of RM1) possibly shows of a deglacial pattern.

Discussion

The above phases are based upon ice flow directions and relative chronologies derived from the geomorphological record portrayed on the DEM and supported by similar evidence from the literature. It is important to understand the context of this work in relation to current ideas about the glacial history of the Lake District and surrounding region, as well as within the stratigraphic framework.

Two main hypotheses have been extended to interpret the evidence that have been reported. Huddart (1994) (see also Lezter, 1978) reviews and presents evidence for an early advance of Scottish ice penetrating the Eden Valley and crossing both the Tyne and Stainmore gaps to the east coast (see also Catt, 1991 and Douglas, 1991). This initial phase was followed by a build up of Lake District ice with northerly ice flow down the Eden Valley. Lake District and Scottish ice would have been confluent in the Carlisle region with both ice masses forced to flow east and westwards. The final phase saw a re-advance of Scottish ice; there is debate as to how extensive this was (e.g. did it penetrate the Vale of Eden?) and this is discussed further by Huddart (1994).

In comparison to this *ground based ice* model, Eyles and McCabe (1989) espouse a *glaciomarine* model which re-interprets sediments believed to represent re-advancing Scottish ice as marine in origin. This depicts the advance of a rising sea level (and so retreat of the Irish Sea glacier) into an isostatically depressed basin. High relative sea levels led to the rapid downdraw of ice, allowing fast ice flow and streaming. The sudden evacuation of ice would have led to a major collapse of ice domes with the probable stranding of dead ice in peripheral regions.

Stratigraphically, St Bees and Sellafield are important sites as detailed data is available for them, revealing a complex series of events. Their location is also significant as they are straddled between the Irish Sea and Lake District uplands and so have recorded major expansion and retreat of both Scottish and Lake District ice.

Huddart (1994) describes four main units at St Bees which are a succession of till (St Bees Till), silts and clays (St Bees Silts and Clays), sands and gravels (St Bees Sands and Gravels) and a final till (Lowca Till). The Lowca till is interpreted to be representative of the main Lake District glaciation which can be traced up the Eden Valley. The St Bees Silts and Clays and St Bees Sands and Gravels are interpreted as different facies of proglacial deposition from eastward advancing ice in the Irish Sea. The St Bees Till is interpreted as deposition from a re-advancing Irish Sea ice sheet, probably synchronous with (and part of) the Scottish Re-advance. This tripartite division of Cumbrian stratigraphy dates back to Hollingworth (1931) and other workers of the period.

Merritt *et al* (2000) interpret the sequences at Sellafield during the last glacial maximum as representative of a major incursion of Irish Sea ice (coalescing with Lake District valley glaciers), followed by a significant retreat, possibly deglaciating the northern Irish Sea basin (synchronous retreat of Lake District ice also occurred). A major re-expansion ('Gosforth Oscillation') of Irish Sea ice then occurred, and coalesced, with ice from the Lake District. They believe that most of the drumlinisation occurred during this period. This was followed by a series of re-advances, the most significant being the 'Scottish Re-advance', although there was probably no re-advance of ice from the Lake District.

Huddart (1994) and Merritt *et al* (2000) do not support the glaciomarine model. They found no evidence to support high marine still stands and refer to isostasy modelling by Lambeck (1996) as further confirmation. Additionally, sequences that Eyles and McCabe (1989) identify as glaciomarine, they interpret as glaciotectonic (and so ground based). McCarroll (2001) critically reviews, and rejects, the evidence for the glaciomarine model, however this is countered by critical support from Knight (2001).

With reference to this work, the simplest explanation for the evidence is an interplay between the Lake District ice dome and the competing ice divides located over the northern Pennines and Southern Uplands of Scotland. As such, the generation of subglacial bedforms would have been strongly influenced by the dominance of these different ice masses at different times.

It is natural to expect early ice flow to emanate from Scotland given the generally high elevations and northerly latitude, however the only evidence of Scottish ice flow in the bedform record is found in the very north of the region (L9 and L10; although these are tentatively placed in Phase 2). Given the erratic and stratigraphic evidence recording Scottish ice flow through Stainmore, the Eden Valley might be expected to retain geomorphic evidence. However a lack of evidence is not unusual as subsequent ice flow from both the Pennines and Lake District may well have erased the previous bedform record.

The first geomorphic evidence is recorded in Phase 1 which places an ice divide over the eastern Lake District, Howgill Fells and Pennines. The Lake District ice dome must have expanded to a significant size in order to support such ice flow (and indeed L8 may have been confluent with Scottish ice), however it suggests a shift in the centre of ice mass *towards* the Pennines. Phase 2 shows the classic curving ice flow around the north of the Lake District (L7); this suggests a centre of mass over the Pennines and, unusually, westwards ice flow *across* Stainmore. There is no supporting erratic evidence for such an ice flow, however the geomorphic signature strongly suggests this. The curving ice flow also suggests the presence of both a Lake District ice dome and confluent Scottish ice in the Carlisle region. L9 and L10 are tentatively placed here as representative of such a configuration, however L10 could easily fit into Phase 3 as part of the Scottish re-advance.

Phase 3 again shows the dominance of a Lake District ice dome with easterly flow over Stainmore and southerly flow towards Lancaster. It is possible that L6 may represent early Scottish ice flow across Stainmore, however it has a strong E-W orientation which suggests a Lake District origin, also supported by the distribution of Shap erratics (Mitchell and Clark, 1994). As noted above, L10 may well fit in this phase as most researchers agree Scottish ice did penetrate down the western Lake District, with limited invasion into the Eden Valley.

The three phases developed in this chapter depict a major ice mass over the Lake District that gradually expands eastwards forming a major ice divide that

causes the diversion of incursive Scottish ice both eastwards and westwards, before contracting into a final deglacial pattern. It is also conceivable that the extent of this ice mass remained fairly static until final deglaciation and that the Howgill Fells region operated as an important switch in initiating active ice flow and drumlinisation. Scottish ice is recorded in Phase 2 and, possibly, in Phase 3. In correlation to the simple, tripartite, classification, Phase 3 could be correlated with the Scottish Re-advance (and a deglaciating Lake District ice sheet). This places Phase 2 as the glacial maximum, with phase 1 representative of early build of Lake District ice. The early Scottish glacial advance is not recorded. Unfortunately the detailed stratigraphies from St Bees and Sellafield do not record the complex interaction that occurred in the upper Eden Valley. Further evidence will be needed to help resolve the complex series of ice flows that occurred here. The geomorphological evidence appears not to support the glaciomarine model. The final phase suggests deglaciation through a retreating ice margin in the south, with possible Scottish ice incursive into the Irish Sea. There is no support for ice streaming and subsequent drumlinisation as a result of rapid downdraw during this period.

It should be stressed that the above suppositions are based upon available landform data and the literature. In particular, only relative age assessments have been made so there is no knowledge of how this history fits within an absolute timescale. However, this procedure demonstrates that a complex pattern of landforms can be generalised into a fairly simple set of flow patterns which can then be interpreted into a glacial history.

7.5 Development of an Automated Flow Set Classification Technique

7.5.1 Introduction

The formation of flow patterns requires the generalisation and/or grouping of individual lineaments. These groups show strong similarity in orientation, with other diagnostic features including length, density and spatial continuity. This chapter has reviewed the visual methodology by which researchers have traditionally performed this stage and gone on to develop techniques to help identify flow patterns and to quantitatively validate their grouping. Earlier

discussion stressed the need to use objective and quantitative measures to help perform this stage in order to make it verifiable and comparable with other research. It was suggested that a fully automated technique would help alleviate this problem, however it is not a simple process to automate within current GIS and would require extensive testing to accommodate the complex glaciological scenarios it would be required to operate in. It is, however, appropriate to outline and review the broad aspects of such an approach. This section now performs this.

7.5.2 Development of a Fully Automated Flow Pattern Algorithm

This chapter has emphasised the requirement for locally based assessment of lineament grouping and it is therefore appropriate that an automated technique incorporates similar ideas. Indeed such “region growing” techniques are used in remote sensing for classifying imagery. However lineament data are vector, rather than raster based, and require a modified approach in order to work. The initial development of an algorithm centred upon the requirement to manually “seed” a region, from which flow patterns could be “grown” (a technique somewhat analogous to supervised classification by seeding within remote sensing). This would add adjacent lineaments into a flow pattern if they met certain criteria (e.g. deviation of orientation) until no more could be added. The remaining lineaments would remain unidentified and could be explored further if necessary. More specifically such an algorithm would involve the following steps (Figure 7.27):

1. Set threshold values:
a. Number of nearest lineaments to compare (n)
b. Length deviation (L)
c. Orientation deviation (α)
d. Maximum distance to nearest lineaments (M)

2. Choose a seed lineament that visually falls within the middle of a suspected flow pattern.

3. Look at *n* nearest lineaments:
Check M is not exceeded
Check L and α are not exceeded
If found within these thresholds *include* within the flow pattern
If outside threshold, *ignore*

4. Of this set of N lineaments (original seed and n nearest lineaments) take the two that are furthest apart and use these as *new* seeds within the current flow pattern and perform the routine in (3)
- If one of the two new seeds is the original then this is discounted, but no new seed is selected.

4. The procedure in (3) and (4) is continued until no new lineaments can be added.

The use of farthest apart secondary seeds is designed to reduce the number of nearest neighbour calculations whilst allowing expansion of the algorithm into all parts of the study area. If a primary seed is selected as a secondary seed then this would repeat calculations and therefore this seed is removed. Otherwise the algorithm simply operates by testing all lineaments for spacing (i.e. distance to nearest neighbour), orientation conformity and length conformity. The following section provides an initial assessment of the algorithm and then suggests areas for further development.

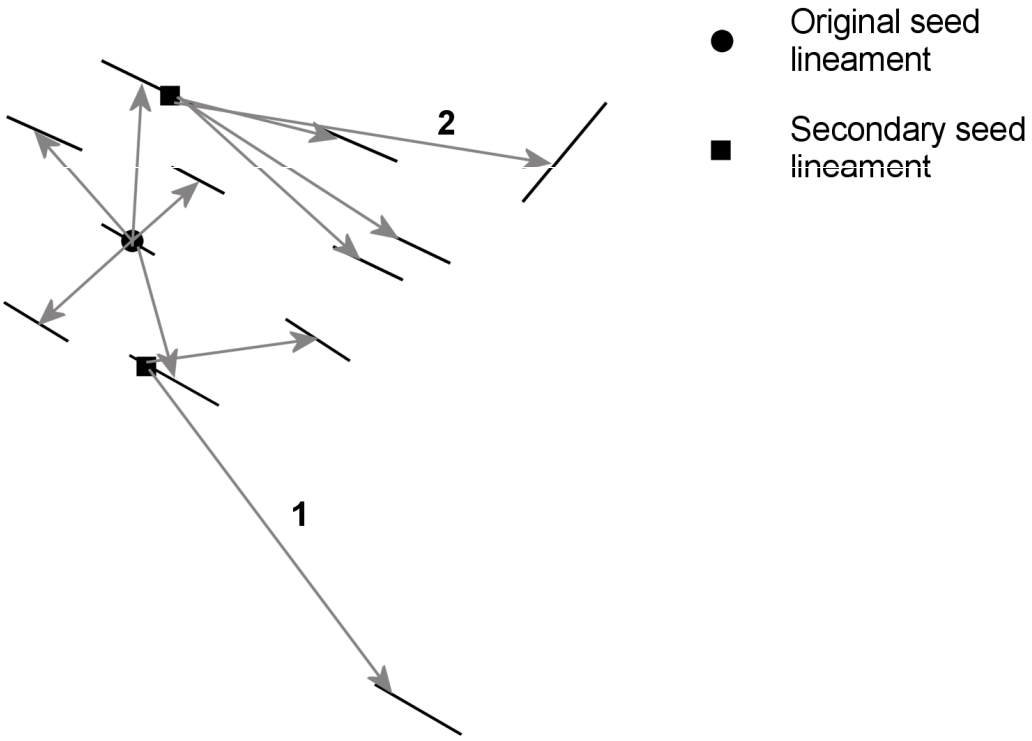

Figure 7.27 Idealised example of the automated flow pattern technique. The original seed lineament is selected and the five nearest lineaments located. Of these lineaments, the two furthest apart become secondary seed lineaments and the five closest unallocated lineaments are then selected. However at (1) the maximum distance to a lineament is exceeded and so cannot be selected. At (2), the maximum deviation in orientation is exceeded and so cannot be selected.

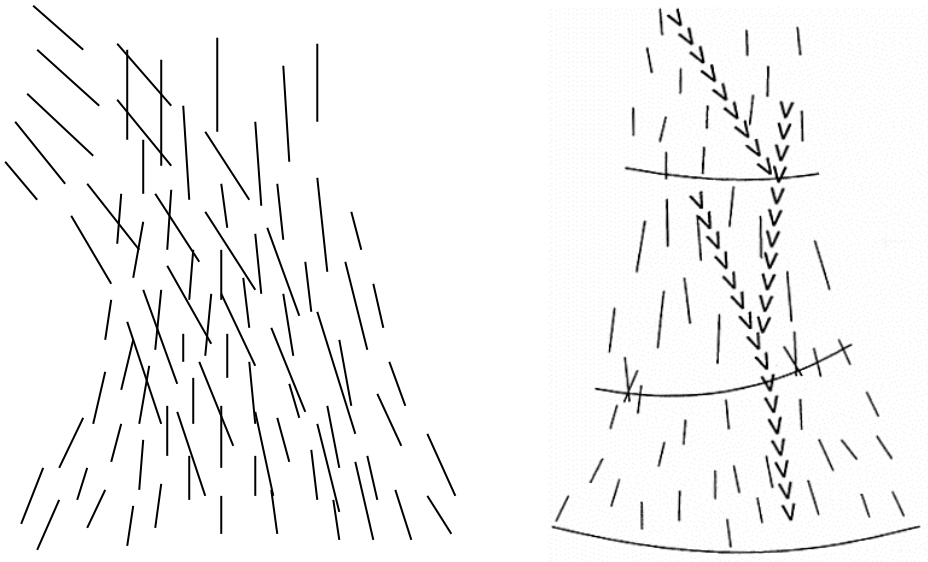

Figure 7.28 Low-angular cross-cutting (left) makes distinguishing flow sets difficult, particularly when lineament orientations coincide, as in the southern part of this example. Time-transgressive (right) flow sets display cross-cutting, low orientation conformity and abrupt morphometric changes yet are a single flow set (modified from Clark, 1999).

7.5.3 Initial Algorithm Testing

The above procedure was manually applied to the idealised dataset (Figure 7.8) used in previous sections. It performed satisfactorily, splitting lineaments into the two principal flow patterns. However it is probably self-evident that the algorithm will perform well in such a simplistic scenario. The full complexity of genuine mapped data needs to be fully explored in order to test how effective it is and develop a routine that will perform satisfactorily in a variety of situations. The algorithm was developed on the assumption that similarity of form suggests similarity of formation. More specifically, it is important to understand the different glaciological scenarios thought to be able to generate flow patterns and the traces they leave (Clark, 1999). In general, isochronous flow sets are easily identified, even when they are cross-cutting as they have high orientation conformity and gradual changes in morphometry. However, there are two scenarios which are more complex and so difficult to identify (Figure 7.28):

1. Low Angular Cross-cutting – lineaments which cross-cut at low angles are very difficult to identify, even by manual techniques. If cross-cutting involved re-moulding, then there may be little morphological trace of pre-existing lineament patterns. Superimposition may have left more morphological traces, but these can still be difficult to determine. In the example illustrated, an isochronous flow set has low-angular cross-cutting with another isochronous flow set. They may be distinguishable through differences in orientation, but at the lobe itself lineaments may be oriented in the same direction. In this instance spacing and length variations may provide further diagnostic information.

2. Time-Transgressive – the diagnostic criteria for time-transgressive flow sets (§3.7) are contrary to all the techniques used to identify isochronous flow sets. There can be cross-cutting (low to medium angular differences) within flow patterns, abrupt changes in morphometry and low orientation conformity. This can be complicated by lineaments being constrained by topography, particularly if the lineament record is not complete. However other associated evidence which can be useful, include the alignment of

eskers and end moraines. Such a situation would clearly become more complicated if there were, *in addition*, low-angular cross-cutting.

As well as the above glaciological scenarios, there may be morphological situations in which the automated procedure may not work. For example, threshold values for lineament length are not always appropriate as there can be scenarios when long lineaments are surrounded by many smaller lineaments.

7.5.4 Review

This section has attempted to develop an algorithm which could eventually be improved to perform fully automated flow set development. Initial development suggests that it is able to satisfactorily separate high-angular cross-cutting isochronous flow sets. However lineament data can be more complex, particularly where low-angular cross-cutting and time-transgressive flow sets are concerned. It would be necessary to perform additional testing and development to ensure such scenarios could be successfully handled. It is not appropriate at this stage to move on and develop this algorithm, however this section has provided a “proof-of-concept” which would allow later integration within a GIS workflow.

7.6 Conclusions

Generalisation is a complex procedure that is difficult to automate and consequently visually based, manual, techniques are preferred. The process of generalisation, as applied to glacial landform data, is poorly documented, relying upon a mixture of an assessment of “parallelness” and interpretation. This is inappropriate as it combines interpretative and non-interpretative stages together such that reproducibility becomes difficult. Two main approaches can be used in defining flow patterns:

- **Manual** - use of spatial variability plots to guide the observer into the classification of flow patterns and then to provide quantitative checks on manual flow pattern classification.
- **Automated** - a fully automated, locally adaptive, algorithm for classifying flow patterns.

The former procedure has been illustrated in this chapter and provides a common set of tools that can be applied by researchers to help generalise their data and then provide a quantitative assessment as to its applicability. This approach worked satisfactorily for both idealised data sets and real data for the Irish Midlands. Orientation and orientation conformity are the most important variables in generalising data into flow patterns, however it is important to supplement them with information on length and density where necessary. This approach was then applied to the landforms that were mapped from the DEM in Chapter 6. This is probably one of the most difficult landscapes not only to map landforms in, but also to create flow patterns. However the complex bedform traces were generalised into 11 flow patterns. Initial assessment of these data suggests that as few as 3 ice flow phases can be formed to explain the bedform pattern that is currently visible today (Figure 7.26).

The chapter was completed with the initial exploration of an automated flow set procedure. It was recognised that, like visually based techniques, any procedure needed to be based upon localised similarity of form. The algorithm therefore operates on a nearest neighbour procedure that assesses similarity in length and orientation. The procedure provides a “proof-of-concept”, however the section went on to explore scenarios where further development would be necessary. Ideally the technique would be implemented within a GIS workflow.

In conclusion, generalisation is an important part of ice sheet reconstructions as it helps devolve complex landforms into simpler flow patterns that can then be interpreted. This stage should ideally be as objective as possible, such that it is reproducible by others. The techniques outlined provide tools by which the researcher can assess landforms before they are generalised into flow patterns, as well as substantiate their division.

8 Conclusions

8.1 Introduction

Ice sheet reconstructions are an important part of glaciology, serving to provide information on how palaeo ice sheets both responded to, and influenced, climate change. This thesis has provided a study of the methods by which ice sheet reconstructions are performed through geomorphological mapping and has highlighted areas where improvements to this methodology could be made. The following sections summarise the results of this research and suggest future research topics.

8.2 ResultsSummary

8.2.1 Primary Data Acquisition: Satellite Imagery

Chapter 5 investigated the sensitivity of *relative size*, *landform signal strength* and *azimuth biasing* on satellite imagery with respect to landform mapping. Broadly, the results can summarised as:

- **Relative Size** - the effects of relative size are commonly appreciated (and compensated for) by researchers (i.e. higher spatial resolution data is required to map spatially smaller landforms). Early studies could not map individual landforms, however higher resolution satellite imagery now means detailed mapping is possible. The Russian study area showed a 170% increase in the number of lineaments mapped as a result of increasing the spatial resolution from 30m to 15m. For the Lough Gara region, relative size was the dominant control on landform detectability, resulting in a 220% increase in the number of lineaments mapped when resolution was increased from 80m to 10m. The effect of relative size is not considered a problem for the current range of earth resources satellites used by glacial researchers to perform landform mapping. Resolutions of <30m produce reliable results.

- **Landform Signal Strength** - is generally linked to the illumination elevation. For VIR imagery, low solar elevation is required and, as satellite overpass

time is fixed, it means that seasonal changes must be used in order to achieve variation in elevation. Solar elevation needs to be in the 5º-20º range in order to provide sufficient contrast to perform mapping. Solar elevations as low as 5º are available, but require optimum imaging conditions. For mid-latitudes this is difficult to achieve due to the high frequency of low pressure weather systems (i.e. cloudy days). For high latitudes, heavy snow cover will typically be present and may mask the terrain. Close investigation of archives will be necessary in order to select the best imagery.

- **Azimuth Biasing -** the illumination of an image *parallel* to the dominant lineament orientation causes those lineaments to appear altered in shape or to disappear altogether. In comparison to the dataset representative of all lineaments around Lough Gara ("truth"), the relief shaded DEM data illuminated orthogonal and parallel to the dominant lineament direction represented 84% and 40% of all lineaments, respectively. This dramatic difference is solely attributable to azimuth biasing and is unsatisfactory as it selectively removes information from the data used for landform mapping such that important features might be missed. This can be mitigated against by acquiring alternately illuminated imagery (either SAR or DEM data) or by having a broad knowledge of the study area. It is important to note that the parallel image selectively highlighted transverse landforms that *were not* visible on the orthogonal image.

It is recommended to use Landsat ETM+ imagery as it delivers the most appropriate data, however it may be necessary to use Landsat TM or MSS where satisfactory imagery is not available or there are economic constraints. To this end, the accompanying CD (and Appendix 2) provides the details necessary to calculate solar azimuth and elevation. This allows the researcher to highlight the best time of year to acquire imagery for, as well as note possible azimuth biasing effects. Although these results are principally aimed at VIR satellite imagery, the special case of SAR imagery is briefly addressed.

- **Synthetic Aperture Radar (SAR)** - this is particularly appropriate for mapping topographic features due to the side-looking sensor, however landform detectability is also affected by relative size, landform signal strength (although this is fixed) and azimuth biasing. Whilst the 25m resolution of the sensor is satisfactory for landform mapping, azimuth biasing can be a serious problem. The case study around Strangford Lough, Ireland, showed a dramatic difference in the lineaments represented for SAR and Landsat TM, with a vector mean of 141º and 98º respectively. In addition, the results of lineament mapping in Ireland were very poor and, in this instance, SAR was not an appropriate data source, although it has been used successfully elsewhere (e.g. Clark *et al*, 2000).

8.2.2 Primary Data Acquisition: DEM Data

DEM data have been available in various formats for over 30 years, initially based upon contour maps, but now directly measured. For the glacial researcher the issue is not whether data is available or how best to go about converting height data into a DEM, but rather *which* data is best suited to the research task and how to utilise it. The former question has a much wider remit to anyone using height data and is therefore beyond the scope of this thesis (this is discussed further in the final section), however the latter topic has pertinence within landform mapping itself. That is, we have absolute data concerning surface elevation (within set accuracy constraints); how do we best visualise this surface to allow accurate and consistent landform mapping. This might initially appear a simple task as almost all GIS, remote sensing and heightfield software allow the rendering of "2.5D" data through the use of relief shading. However this introduces an illumination source and therefore suffers very similar problems to those discussed above for satellite imagery. Clearly then we need to use height data in a robust manner.

Chapter 6 assessed the ability of a variety of standard and developed methods to visualise the landscape. Methods that were assessed included relief shading (parallel and orthogonal to the dominant lineament direction), principal components analysis (PCA), false colour composites, animated relief shading, slope curvature, 3D viewing and localised spatial enhancements. Ideally a

single visualisation method is required that optimally enhances the terrain, but without introducing bias. However no single visualisation method was able to provide optimal viewing. The following broad results were obtained:

- **Azimuth Biased:** relief shading is based upon an illuminated landscape and so contains azimuth biasing. Parallel and orthogonal relief shaded images contained 40% and 84% of the lineaments mapped on truth. Whilst landforms oriented parallel to the illumination azimuth were selectively diminished, those oriented perpendicular were selectively *enhanced*. So although individual relief shaded images were not satisfactory alone, in combination they have great utility.
- **Non-Azimuth Biased:** slope curvature, overhead illumination, PCA and localised spatial enhancements are preferable as they do not introduce illumination bias'. They contained 82%, 60%, 61% and 62%, respectively, of the lineaments mapped on truth. Whilst slope curvature performed well, the remaining methods were unsatisfactory.

Overall recommendations are that non-azimuth biased methods should be used for initial landform mapping. Azimuth biased methods can then be used to complete the mapping procedure. This method was then used to map glacial landforms, including over 2,600 lineaments, for the Lake District. After initial trial and error in their application, a satisfactory workflow was established in their use, finally producing the first complete bedform map of the Lake District. In comparison to published data, there are many more lineaments identified, including the presence of previously unmapped cross-cutting patterns and ribbed moraine.

8.2.3 Generalisation

The generalisation of landform data into summary flow patterns is currently a visual, qualitative, method. Chapter 7 developed a technique based around the provision of a set of maps that generalise the raw lineament data. These maps are interpolated surfaces based upon the length and orientation of the original lineaments. They are straight forward to interpret and allow the researcher to make informed decisions during the generalisation process. Once the

lineaments have been “split” into individual flow patterns, they can be visualised using the same method. This should help confirm that the flow patterns can be established as genuine. If not, they allow the process to be repeated. This is an important technique as it allows this stage of an ice sheet reconstruction to be objectively verified.

The above technique is implemented on the set of data mapped from the Lake District in chapter 6. The complex series of landforms proved difficult to generalise, however the 2,600 lineaments were reduced to a series of 12 flow patterns. Initial investigation suggests that this may reduce to as few as 3 flow sets that show a shift in ice mass away from the Lake District (towards the Pennines) before an increase, and expansion, in the dominance of Lake District ice. To conclude the chapter, a “proof-of-concept” algorithm was developed to show that it should be possible to automate such a procedure, however further development is required.

8.3 FutureResearch

During this work I have identified further avenues of research which would be appropriate to pursue and these are now discussed.

1. **Comparison of Landform Mapping Methods** - satellite images are one of several earth observation techniques that include, aerial photography, DEMs and field mapping. With regards to landform mapping, each method has its own strengths and weaknesses. The large areal coverage, low cost and manageability make satellite imagery ideal for rapidly mapping landforms over large areas. The opposite is true for field mapping which is slow, high cost and very detailed. Although these generalisations are broadly correct, this research has highlighted how satellite imagery can have serious errors of omission. Can similar problems affect the use of aerial photography or field mapping? For instance, aerial photos are normally acquired with high solar elevations and (in the northern hemisphere) with solar azimuth from the south. These effects seriously reduce the benefits of the high spatial resolution. It would be constructive and informative to compare landform mapping for these four methods over the same area. Although satellite

imagery can detect broad regional trends in landform assemblages, are all methods comparative when detailed morphometric information is collected? Might it be more appropriate to use DEMs for regional mapping and aerial photography for detailed mapping to confirm, for instance, cross-cutting and ice flow direction

2. **Comparison of DEM Data** – the different types of DEM data have briefly been discussed, however it is the source from which it is produced that determines their appropriateness and therefore usability for a particular purpose. The data used in this research was the Ordnance Survey's Panorama™ data, which is a 50m resolution product produced from original contour map data. The contour data is based upon a product that is designed to represent a "bald earth", that is, an earth surface devoid of buildings and vegetation. And because it's a bald earth and generated from contour data, the DEM surface has been smoothed. The same is not true of radar generated DEMs which generally measure a "visible surface". That is, they include buildings and vegetation (and anything else on the surface). Clearly, if a surface of interest is heavily forested, then the detectability of landforms will be severely degraded. Even in "clean" areas (i.e. bald) the difference in the type of point sampling used and method of collection means that landscapes can appear differently. Further work would be required to review the different types of DEM products available and then compare and contrast their applicability for landform mapping.

3. **Automated Lineament Generalisation** - Chapter 7 provided initial "proof-of-concept" development of an algorithm that can be used for generating flow patterns. This could potentially be automated and would allow a fast and truly interactive and iterative approach to flow pattern development. As such it is a computer programming exercise that would require refinement within the problem areas identified in Chapter 7.

8.4 Final Thoughts

This research began as an exercise in the application of a set of techniques and has progressed through to a refinement of these techniques. The previous

section highlights the areas where research can be pursued and all are based around technical enhancements, particularly in the arena of DEM data. DEMs will undoubtedly become one of the most important research tools of the next decade and further understanding of their use and weaknesses is vital to their acceptance by the greater research community. One topic which hasn't been touched upon is the original aim of this thesis; that is the reconstruction of the British and Irish ice sheet. This still awaits to be done, although Clark and Meehan (2001) have made a start, utilising DEMs rather than satellite imagery, whilst the BRITICE project (Clark, 2002) is making a contribution to the summation of mapped glacial landforms in the UK. The availability of OS Panorama™ and Landmap DEM data for Britain and Ireland means that there is now a free (for academic use) source of data available. All that is required is the appropriate mapping of landforms.

Bibliography

Aber, J. S., Spellman, E. E. and Webster, M. P. (1993) Landsat remote sensing of glacial terrain. In Glaciotectonics and Mapping Glacial Deposits. *Proceedings of the INQUA Commission on Formation and Properties of Glacial Deposits.* (Ed, Aber, J.) Canadian Plains Research Center, University of Regina.

Agassiz, L. (1840) On the evidence of the former existence of glaciers in Scotland, Ireland and England. *Proceedings of the Geological Society of London*, **3,** 327-332.

Aronoff, S. (1989) *Geographic Information Systems: a management perspective*. WDL Publications, Ottawa.

Arthurton, R. S. (1981) *Geology of the country around Penrith.* British Geological Survey.

Arthurton, R. S. (1988) *Geology of the country around Settle.* British Geological Survey.

Benn, D. I. and Evans, D. J. A. (1998) *Glaciers and Glaciation*. Arnold, London.

Black, S. M. (1995) *The development of a lineament identification/analysis technique in Northern Scotland.* Unpublished PhD Thesis, Department of Geography, University of Sheffield.

Boardman, J. (Ed.) (1981) *Field guide to Eastern Cumbria*. Quaternary Research Association, Oxford.

Boardman, J. (1991) Glacial deposits of the English Lake District. In *Glacial deposits in Great Britain and Ireland.* (Eds, Ehlers, J., Gibbard, P. L. and Rose, J.) Balkema, Rotterdam.

Boulton, G. S. and Clark, C. D. (1990) The Laurentide Ice Sheet through the last glacial cycle: the topology of drift lineations as a key to the dynamic behaviour of former ice sheets. *Transactions of the Royal Society of Edinburgh: Earth Sciences*, **81,** 327-347.

Boulton, G. S., Dongelmans, P., Punkari, M. and Broadgate, M. (2001) Palaeoglaciology of an ice sheet through a glacial cycle: the European ice sheet through the Weichselian. *Quaternary Science Reviews* , **20,** 591-625.

Brandon, A. (1998) *Geology of the country around Lancaster.* British Geological Survey.

Broadgate, M. L. (1997) *An integrated approach to palaeoenvironmental reconstruction using a GIS.* Unpublished PhD Thesis, Department of Department of Geology and Geophysics, University of Edinburgh.

Burgess, I. C. (1979) *Geology of the country around Brough-under-Stainmore.* British Geological Survey.

Campbell, J. (1984) *Introductory Cartography*, Prentice-Hall, London.

Catt, J. A. (1991) The Quaternary history and glacial deposits of East Yorkshire. In *Glacial deposits in Great Britain and Ireland.* (Eds, Ehlers, J., Gibbard, P. L. and Rose, J.) Balkema, Rotterdam.

Chrisman, N. R. (1983) The role of quality information in the long-term functioning of a GIS. In *Proceedings of AUTOCARTO*, Vol. 2 Falls Church, pp. 303-321.

Chrisman, N. R. (1994) The Error Component in Spatial Data In *Geographic Information Systems Volume 1: Principles* (Eds, Maguire, D. J., Goodchild, M. F. and Rhind, D. W.) Longman, London.

Clark, C. D. (1993) Mega-scale glacial lineations and cross-cutting ice-flow landforms. *Earth Surface Processes and Landforms*, **18,** 1-29.

Clark, C. D. (1997) Reconstructing the evolutionary dynamics of palaeo-ice sheets using multi-temporal evidence, remote sensing and GIS. *Quaternary Science Reviews* , **16,** 1067-1092.

Clark, C. D. (1999) Glaciodynamic context of subglacial bedform generation. *Annals of Glaciology*, **28,** 23-32.

Clark, C. D., Evans, D. J. A., Mitchell, W.A., Jordan, C., Merritt, J. and Bradwell, T. (2002) BRITICE: a GIS database of palaeoglaciological evidence of the last British Ice Sheet. Final progress report to the British Geological Survey. pp. 19.

Clark, C. D. and Knight, J. K. (1994) ERS SAR data as a tool for landform and lineament identification in previously glaciated areas. In *Proceedings of the First ERS-1 Pilot Project Workshop*, Vol. 356 European Space Agency Special Publication, Toledo, Spain, pp. 211-215.

Clark, C. D., Knight, J. K. and Gray, J. T. (2000) Geomorphological reconstruction of the Labrador Sector of the Laurentide Ice Sheet. *Quaternary Science Reviews* , **19,** 1343-1366.

Clark, C. D. and Meehan, R. T. (2001) Subglacial bedform geomorphology of the Irish Ice Sheet reveals major configuration changes during growth and decay. *Journal of Quaternary Science*, **16,** 483-496.

Close, M. H. (1867) Notes on the general glaciation of Ireland. *Journal of the Royal Geographical Society of London Dublin*, **1,** 207-242.

Colwell, R. N. (Ed.) (1960) *Manual of Photographic Interpretation*. American Society of Photogrammetry, Falls Church, Virginia, USA.

Colwell, R. N. (Ed.) (1983) *Manual of Photographic Interpretation*. American Society of Photogrammetry.

Cox, N. (2001) Analysing circular data in Stata [online]. No 5.3 in North American Stata Users' Group Meetings 2001. Available from: http://fmwww.bc.edu/RePEc/nasug2001/nasugnjc.pdf [Accessed: 3rd February 2003].

Dongelmans, P. (1996) *Glacial dynamics of the Fennoscandian ice sheet: a remote sensing study*. Unpublished PhD Thesis, Department of Department of Geology and Geophysics, University of Edinburgh.

Douglas, R. (1991) Glacial deposits of Northumbria. In *Glacial deposits in Great Britain and Ireland.* (Eds, Ehlers, J., Gibbard, P. L. and Rose, J.) Balkema, Rotterdam.

Estes, J. E., Hajic, E. J. and Tinney, L. R. (1983) Fundamentals of image analysis: analysis of visible and thermal infrared data. In *Manual of Remote Sensing* (Ed, Colwell, R. N.) American Society of Photogrammetry, Falls Church, Virginia.

Evans, I. S. (1972) General Geomorphometry, derivatives of altitude and descriptive statistics. In *Spatial Analysis in Geomorphology* (Ed, Chorley, R. J.) Harper and Row, New York, pp. 17-90.

Eyles, C. H., Eyles, N. and Miall, A. D. (1985) Models of glaciomarine sedimentation and their application to the interpretation of ancient glacial sequences. *Palaeogeography, Palaeoclimatography, Palaeoecology*, **51,** 15-84.

Eyles, N. and McCabe, A. M. (1989) The late Devensian Irish Sea basin: a sedimentary record of a collapsed ice-sheet margin. *Quaternary Science Reviews*, **8,** 307-352.

Fahnestock, J. D. and Schowengerdt, R. A. (1983) Spatially variant contrast enhancement using local range modification. *Optical Engineering*, **22,** 378-381.

Florinsky, I. V. (1998) Accuracy of local topographic variables derived from digital elevation models. *International Journal of Geographic Information Science*, **12,** 47-62.

Foley, J. D., van Dam, A., Feiner, S. K. and Hughes, J. F. (1990) *Computer Graphics: Principles and Practice*. Addison-Wesley, Wokingham.

Ford, J. P. (1981) Mapping of glacial landforms from Seasat radar images. *Quaternary Research*, **22,** 314-327.

Goodchild, M. F. and Kemp, K. K. (Eds) (1990) NCGIA Core Curriculum in GIS. [online]. National Center for Geographic Information and Analysis, University of California, Santa Barbara CA. Available from: http://www.geog.ubc.ca/courses/klink/gis.notes/ncgia/toc.html [Accessed: 3rd February 2003].

Goodwillie, D. (1995) *Two cross-cutting drumlin swarms in northern Sweden: geomorphology as a key to palaeoglaciology*. Unpublished report, Department of Geography, Stockholm University,

Graham, D. F. and Grant, D. R. (1991) A test of airborne, side-looking synthetic-aperture radar in central Newfoundland for geological reconnaissance. *Canadian Journal of Earth Sciences*, **28,** 257-265.

Guzzetti, F. and Reichenbach, P. (1994) Towards a definition of topographic divisions for Italy. *Geomorphology*, **11,** 57-74.

Hättestrand, C. (1997) Ribbed moraines in Sweden - distribution pattern and Palaeoglaciological implications. *Sedimentary Geology*, **111,** 41-56.

Hill, A. R. and Prior, D. B. (1968) Directions of ice movement in north-east Ireland. *Proceedings of the Royal Irish Academy*, **66B,** 71-84.

Hollingworth, S. E. (1931) Glaciation of western Edenside and adjoining areas and the drumlins of Edenside and the Solway Plain. *Quarterly Journal of the Geological Society of London*, **87,** 281-357.

Huddart, D. (1994) The Late Quaternary glacigenic sequence: landforms and environments in coastal Cumbria. In *Cumbria: field guide.* (Ed, Boardman, J.) Quaternary Research Association, Oxford.

Huddart, D. and N. F. Glasser (Ed.) (2002). *Quaternary of Northern England.* Peterborough, JNCC.

Hull, E. (1878) *Physical geology and geography of Ireland.* Stanford, London.

Irons, J. R. and Peterson, G. W. (1981) Texture transforms of remote sensing data. *Remote Sensing of the Environment*, **11,** 359-370.

Jackson, P. and Steyn, D. (1994) Gap winds in a fjord. Part II:Hydraulic analog. *Monthly Weather Review*, **122,** 2668-2667.

Jones, C. (1997) *Geographical information systems and computer cartography.* Longman, Singapore.

King, C. A. M. (1976) *Northern England*. Methuen.

Kitmitto, K., Cooper, M., Venters, C. C., Muller, J. P., Morley, J. G., Walker, A. and Rana, S. (2000) LANDMAP: Serving satellite imagery to the UK academic community. In *RSS2000: Adding Value to Remotely Sensed Data*, University of Leicester.

Kleman, J. (1990) On the use of glacial striae for reconstruction of palaeo-ice sheet flow patterns. *Geograska Annaler*, **72A,** 217-236.

Kleman, J. (1994) Preservation of landforms under ice sheets and ice caps. *Geomorphology*, **9,** 19-32.

Kleman, J. and Borgström, I. (1996) Reconstruction of palaeo-ice sheets: the use of geomorphological data. *Earth Surface Processes and Landforms*, **21,** 893-909.

Kleman, J., Hätterstrand, C., Borgström, I. and Stroeven, A. (1997) Fennoscandian palaeoglaciology reconstructed using a glacial geological inversion model. *Journal of Glaciology*, **43,** 283-299.

Knight, J. (1997) Morphological and morphometric analyses of drumlin bedforms in the Omagh Basin, north central Ireland. *Geografiska Annaler*, **79A,** 255-266.

Knight, J. (2001) Glaciomarine deposition around the Irish Sea basin: some problems and solutions. *Journal of Quaternary Science,* **16,** 405-418.

Knight, J. and McCabe, A. M. (1997) Drumlin evolution and ice sheet oscillations along the NE Atlantic margin, Donegal Bay, western Ireland. *Sedimentary Geology*, **111,** 57-72.

Knight, J. and McCabe, A. M. (1997) Identification and significance of ice-flow-transverse subglacial ridges (Rogen moraines) in northern central Ireland. *Journal of Quaternary Science*, **12,** 519-524.

Knight, J. K. (1996) *A geographical information system-based synthesis of the Labrador sector of the Laurentide Ice Sheet*. Unpublished PhD Thesis, Department of Geography, Sheffield University.

Lambeck, K. (1996) Glaciation and sea-level change for Ireland and the Irish Sea since Late Devensian/Midlandian time. *Journal of the Geological Society of London,* **153,** 853-872.

Letzer, J. M. (1978) *The glacial geomorphology of the region bounded by Shap Fells, Stainmore and the Howgill Fells in east Cumbria.* Unpublished MPhil Thesis, Department of Geography, London University.

Lidmar-Bergström, K., Elvhage, C. and Ringberg, B. (1991) Landforms in Skane, south Sweden. *Geografiska Annaler*, **73A,** 61-91.

Lillesand, T. M. and Kiefer, R. W. (2000) *Remote Sensing and Image Interpretation.* Wiley.

Lundqvist, J. (1989) Rogen (ribbed) moraine – identification and possible origin. *Sedimentary Geology*, **62,** 281-292.

McCabe, A. M., Knight, J. and McCarron, S. G. (1998) Ice-flow stages and glacial bedforms in north central Ireland: a record of rapid environmental change during the last glacial termination. *Journal of the Geological Society of London*, **155**, 63-72.

McCarroll, D. (2001) Deglaciation of the Irish Sea Basin: a critique of the glaciomarine hypothesis. *Journal of Quaternary Science,* **16,** 393-404.

Menzies, J. and Rose, J. (Eds.) (1987) *DrumlinSymposium*. Balkema, Rotterdam.

Merritt, J. W. and Auton, C. A. (2000) An outline of the lithostratigraphy and depositional history of Quaternary deposits in the Sellafield district, west Cumbria. *Proceedings of the Yorkshire Geological Society,* **53,** 129-154.

Mitchell, W. A. (1994) Drumlins in ice sheet reconstructions, with reference to the western Pennines, northern England. *Sedimentary Geology*, **91,** 313-331.

Mitchell, W. A. and Clark, C. D. (1994) The last ice sheet in Cumbria. In *The Quaternary of Cumbria: Field Guide*. (Eds, Boardman, J. and Walden, J.) Quaternary Research Association, Oxford, pp. 4-14.

Muller, E. H. and Pair, D. L. (1992) Comment and reply on "Evidence for large scale subglacial meltwater flood events in southern Ontario and northern New York State." *Nature*, **20,** 90-91.

Muneer, T. (1997) *Solar radiation and daylight models for the energy efficient design of buildings*. Butterworth-Heinemann, Oxford.

Olson, C. E. (1960) Elements of photographic interpretation common to several sensors. *Photogrammetric Engineering*, **26,** 651-656.

Ordnance Survey (1995) *Ordnance Survey Digital Map Data and Customised Services.* Ordnance Survey, Southampton.

Podwysocki, M. H., Moik, J. G. and Shoup, W. C. (1975) Quantification of geologic lineaments by manual and machine processing techniques. In *Proceedings of the NASA Earth Resources Survey Symposium*, Vol. TMX-58168 v1B NASA, Greenbelt, Maryland, pp. 885-905.

Pohl, C. and Van Genderen, J. L. (1998) Multisensor image fusion in remote sensing: concepts, methods and applications. *International Journal of Remote Sensing*, **19,** 823-885.

Prest, V. K., Grant, D. R. and Rampton, V. N. (1968) *The Glacial Map of Canada*. Geological Survey of Canada.

Punkari, M. (1982) Glacial geomorphology and dynamics in the eastern parts of the Baltic Shield interpreted using Landsat imagery. *Photogrammetric Journal of Finland*, **9,** 77-93.

Punkari, M. (1985) Glacial geomorphology and dynamics in Soviet Karelia interpreted by means of satellite imagery. *Fennia*, **163,** 287-307.

Punkari, M. (1989) *Glacial dynamics and related erosion-deposition processes in the Scandinavian ice sheet in south-western Finland: A remote sensing fieldwork and computer modelling study*. Research Council for the Natural Sciences, Academy of Finland, Helsinki, pp. 86.

Punkari, M. (1993) Modelling of the dynamics of the Scandinavian ice sheet using remote sensing and GIS methods. In *Glaciotectonics and Mapping Glacial Deposits* (Ed, Aber, J.) Proceedings of the INQUA Commission

on Formation and Properties of Glacial Deposits, Canadian Plains Research Center, University of Regina, pp. 232-250.

Punkari, M. (1995) Glacial flow systems in the zone of confluence between the Scandinavian and Novaya Zemlya ice sheets. *Quaternary Science Reviews*, **14,** 589-603.

Punkari, M. (1996) *Glacial dynamics of the northern European ice sheets.* Unpublished PhD Thesis, Department of Geology, University of Helsinki.

Raistrick, A. (1933) The glacial and post-glacial periods in west Yorkshire. *Proceedings of the Yorkshire Geological Society*, **44,** 263-269.

Rhoads, B. L. and Thorn, C. E. (1993) Geomorphology as science: the role of theory. *Geomorphology*, **6,** 287-307.

Riley, J. M. (1987) Drumlins of the southern Vale of Eden, Cumbria, England. In *Drumlin Symposium* (Eds, Menzies, J. and Rose, J.) Balkema, Rotterdam, pp. 323-333.

Rolando, L. J., Edward, R. C., Yunjin, K. and Yushen, S. (1996) Design of Shuttle Radar Topography Mapper (SRTM). JPL-NASA, Pasadena.

Siegal, B. S. (1977) Significance of operator variation and the angle of illumination in lineament analysis of synoptic images. *Modern Geology*, **6,** 75-85.

Slaney, V. R. (1981) Landsat images of Canada - a geological appraisal. Paper 80-5, Geological Survey Canada.

Smith, M.J., Clark, C.D. and Wise, S.M. (2001) Mapping glacial lineaments from satellite imagery: an assessment of the problems and development of best procedure. *Slovak Geological Magazine*, **7,** 263-274

Stokes, C.R. (2001) *The geomorphology of palaeo-ice streams: identification, characterisation and implications for ice stream functioning*. Unpublished PhD Thesis, Department of Geography, University of Sheffield.

Stokes, C.R. and Clark, C.D. (1999) Geomorphological criteria for identifying Pleistocene ice streams. *Annals of Glaciology*, **28,** 67-74.

Sugden, D. and John, B. S. (1976) *Glaciers and Landscape*. Edward Arnold, London.

Sugden, D. E. (1978) Glacial erosion by the Laurentide Ice Sheet at its maximum. *Journal of Glaciology*, **20,** 367-391.

Syverson, K. M. (1995) The ability of ice flow indicators to record complex, historic deglaciation events, Burroughs-Glacier, Alaska. *Boreas*, **24,** 232-244.

Tragheim, D. and Westhead, K. (1996) Seeing the lie of the land: digital photogrammetry aids geological mapping. *Mapping Awareness*, **10,** 34-37.

Vencatasawmy, C. (1997) *Statistical assessment and development of tools for mapping lineaments and landforms from synthetic aperture radar (SAR) images*. Unpublished PhD Thesis, Department of Geography, University of Sheffield.

Vencatasawmy, C. P., Clark, C. D. and Martin, R. J. (1998) Landform and lineament mapping using radar remote sensing. In *Landform Monitoring and Analysis* (Eds, Lane, S. N., Richards, K. S. and Chandler, J. H.) Wiley, Chichester.

Vincent, P. (1985) Quaternary geomorphology of the southern Lake District and the Morecambe Bay area. In *The geomorphology of north-west England* (Ed, Johnson, R. H.), Manchester University Press, Manchester.

Warren, W. P. (1992) Drumlin orientation and the pattern of glaciation in Ireland. *Sveriges Geologiska Undersökning*, **81,** 359-366.

Whiteman, C.A. (1981) “19” in *Field guide to Eastern Cumbria* (Ed. Boardman, J.). Quaternary Research Association, Oxford.

Wilson, J. P. and Gallant, J. C. (Eds.) (2000) *Terrain Analysis*. John Wiley and Sons, New York.

Yallop, B. D. (1992) A simple algorithm to calculate times of sunrise and sunset. Technical Note 70, Nautical Almanac Office.

Zevenbergen, L. W. and Thorne, C. R. (1987) Quantitative Analysis of Land Surface Topography. *Earth Surface Processes and Landforms*, **12,** 47-56.

Appendix 1 Graphical Rendering

1.1 Introduction

Rendering is the drawing of a real world object as it actually appears and, within computer graphics, specifically refers to the creation of a 3-D image that incorporates lighting effects to achieve this.

This section will briefly discuss the different models used to graphically render 3-D images. These models are based upon the position, orientation and characteristics of the surfaces and light sources illuminating them, however the actual physical interaction between visible light and surfaces is complex and consequently

graphics researchers have often approximated the underlying rules of optics and thermal radiation... Consequently many of the illumination and shading models traditionally used in computer graphics include a multiple of kludges, "hacks," and simplifications that have no firm grounding in theory, but that work well in practice. (Foley et al, 1990).

1.2 Rendering Models

The following sections discuss the two main rendering techniques, termed *local* and *global* illumination models. All models are, in general, physically based, being derived from physical principles of light and its interaction with different surfaces. A purely physically based model would be computationally intensive and so *localillumination* algorithms tend to incorporate approximations and simplifications to produce a graphically pleasing image. This method works on the principle of taking a surface and then incorporating visual enhancements where appropriate (e.g. directional light source, ambient light, material properties, reflections and transparency).

Globalillumination attempts to incorporate data on all reflected and transmitted light to produce a realistic image; this is opposed to using a simple ambient illumination term.

Both techniques require an input model (i.e. 3-D description) for the objects of interest, specification of the viewing and lighting geometry, calculation of the viewable surfaces (from the rendering viewpoint) and object colour assignment.

Local Illumination

This section describes the main techniques used in local illumination models, starting with simple illumination and slowly adding more complex effects.

1. Illumination

At its simplest, illumination is incorporated into a 3-D model by using non-directional light (i.e. no direct light source). This can be *self-luminosity* or, more realistically, *ambient light*, the latter of which can incorporate the reflective properties of an object. Most environments, however, have some kind of *point light source*, be it the sun or a lamp, from which light emanates in all directions. Object brightness depends upon the distance to, and direction of, the light source, whilst the object material properties control the type of reflection. Surface reflectance can be modelled using two main reflectance types:

1. *Diffuse (Lambertian) reflection* describes matte surfaces which appear equally bright from all angles. Diffuse light and colour can be added to make the shading more realistic. Further corrections can be added for atmospheric attenuation whereby more distant objects appear less intense than closer ones.

2. *Specular reflection* can be used to simulate shiny surfaces; simpler models assume equally radiating light (e.g. Phong), whilst newer models allow directionality to be introduced, in a manner similar to a spotlight.

2. Polygon Shading

Shading can be defined as *the calculation of light leaving a point*. To produce an image this can be performed by applying an illumination model at every visible point throughout a landscape, however this is computationally intensive

and so programmers have devised more efficient algorithms to approximate the visual rendering of this method for polygon models. These include:

1. *Constant shading* applies one illumination calculation to each polygon within a wire frame model; this is simply a method of sampling within the landscape.

2. *Interpolated shading* calculates illumination values at polygon vertices and then interpolates across the polygon between these values.

The above two methods suffer from the assumption that a polygon accurately represents the modelled surface, however for curved surfaces faceted banding becomes evident, an effect that is accentuated by the eye. However polygon wire frames are popular as visible surface algorithms are very efficient in this environment. *Gouraud shading* attempts to overcome these problems by interpolating polygon vertex illumination values. Polygon vertex normals are averaged from the surface normals of the polygon facets, vertex intensities (using a desired illumination model) are calculated and then intensities are linearly interpolated along and between edges.

Phong shading uses an alternative approach by interpolating the surface normal vectors rather than the intensity, a method which yields better results when using specular reflectance illumination models. As in the Gouraud shading, vertex normals can be averaged and then used to interpolate edge normals before going onto interpolate surface normals.

3. Surface Detail

Surface detail can be added to rendered polygons to make the final image more realistic. This can involve the overlay of *surface-detail polygons* which are ignored during the visible surface procedure, but then applies detail when the base polygon is shaded. This method is only suitable for gross detail and when more detailed textures are required a separate image is mapped onto the surface, a process known as *texture mapping*. *Bump mapping* modifies texture

mapping to take into account differences between the texture map and surface illumination conditions.

The above steps follow the production of a basic rendered image, however further details need to be considered in order to produce a realistic image. These include:

a. **Shadow** - shadow algorithms operate in relation to the point light source used in a scene; where multiple light sources are used, a relative shadow effect must be calculated for each surface.

b. **Transparency** - surface materials can be transparent or translucent. Simpler models ignore light refraction as the algorithms are significantly simpler and, through interpolation or filtering, calculate the colouring of the surface.

c. **Interobject Reflection** - where one surface reflects off another within an image, interobject reflection occurs and this can range from diffuse to specular. *Reflection mapping* attempts to address these issues however *it only provides an approximation to the correct reflection information* (Foley, *et al*, 1990).

4. Physically Based Shading

The Torrance-Sparrow model is a physically based model of a reflecting surface and has shown good correspondence to actual measurements. It assumes an isotropic collection of planar microscopic facets, each a perfect specular reflector. It has since been modified for computer graphics and incorporates the Fresnel equation for the specular reflection of unpolarized light of a non-conducting surface. Two further enhancements include the development of anisotropic illumination models which are better able to render preferentially oriented surface microfeatures and a correction for polarisation of light after it is reflected.

5. Further Enhancements

a. Extended Light Sources - models that are able to render “soft” shadows where there is only partial blocking of the point light source.

b. Camera Effects - post processing methods can add the effects of *depth of field* and *motion blur*.

Global Illumination

Global illumination models calculate the colour of a point using incoming light and light reflected and transmitted through different surfaces. Local illumination is concerned only with incoming light. The illumination models dealt with above have tended to use an single ambient light term in them and did not consider the position of the object or viewer or the effect of nearby objects in blocking ambient light. The *Ray Tracing* (view-dependent) and *Radiosity* (view-independent) methods are designed to incorporate these more complex interactions in a manner which hasn’t been achieved in the above models and are discussed below.

1. Ray Tracing

Ray tracing determines surface visibility by tracing imaginary rays of light from the centre of projection, through a viewing window to the objects of interest. For each pixel in the viewing window the colour is set to that of the object of *first intersection*. To calculate *shadow*, an additional ray is fired from the point of intersection to the light source and if a further intersection takes place then the area is in shadow and its colour contribution is ignored. A conditional statement within the algorithm can then go on to spawn *refraction* and *reflection* for specified objects. Each of these subsequent rays can then also spawn shadow, reflection and refraction rays which continues to a user specified maximum or until no object is intersected. Intensity is then computed from the last ray up, a node being a function of its children’s intensities.

Many modifications to conventional ray tracing have been made to increase efficiency, to more accurately model specular reflection and provide a better method than the simple point sampling. This final area has spawned methods

such as cone, beam and pencil tracing. Distributed ray tracing is a variation that uses a stochastic approach to ray tracing; it is able to offset the obvious effects of *temporal aliasing* (jagged edges) for the less obvious effects of noise.

One problem of these tracing methods is that they fail to account for indirect reflected and refracted light sources; to overcome this problem *backward ray tracing* attempts to trace the ray from the light sources to the viewer, however this method is usually used in tandem with conventional ray tracing, known as *bi-directional ray tracing*, in order to increase efficiency.

2. Radiosity

Ray tracing is able to model specular reflection and dispersionless refractive transparency effectively, however it still uses a single term to account for ambient light. *Radiosity* is the rate at which an object emits radiation and can be modelled within a closed environment such that all energy is either absorbed or reflected. This method removes the need to have an ambient light term as all interactions of radiation with a surface are accounted for. The method requires the computation of all light interactions, before a viewing position is selected and visible-surface and shading performed. This method has been refined since its introduction into computer graphics and can allow the progressive refinement of a rendered image with increasing iterations, rather than having to perform all the radiosity calculations first. Specular reflection has also been added into the radiosity calculations, however the computational overhead is quite high.

3. Hybrid Algorithms

Some authors have combined the radiosity and ray tracing methods to take advantage of each method's strengths in modelling ambient light and specular reflection respectively.

Ray tracing calculates the illumination signal for *each* shading point which means that even small or distant objects are captured as sharp images, however it is unable to trace indirect (ambient) illumination as it is coming from *all* objects and the method is only point sampling. It is therefore possible to miss significant sources of light. Conversely, radiosity algorithms are able to model

indirect light well, particularly multiple diffuse light sources. Such effects as soft shadows and colour bleeding are more easily produced, however specular reflection is reproduced less well due to a limiting resolution for the calculations of radiance.

Most hybrid algorithms begin with the view-independent radiosity calculations first in order to determine the ambient light. This is followed by the ray tracing to calculate the specular reflection.

1.3 DiscussionandConclusions

This appendix has given a brief introduction to computer based graphical rendering and so provided a framework with which to discuss its relevance to relief shading within GIS. Relief shading provides a special, simplified, situation for rendering. The object of interest (i.e. the DEM) is already a sampled surface. Simple shadow algorithms can determine whether any point on the surface is in shadow from a direct illumination source and then apply an interpolated shading algorithm. A constant term can also be used so that ambient light can be added. This *localillumination* model provides a fast and efficient solution for most scenarios. Unfortunately it is unable to accurately reproduce real world illumination conditions particularly those under low solar elevation angles; although the shadow algorithms are able to handle line-of-sight viewing adequately, the ambient light level is far too high as, in reality, this term is very sensitive in low light conditions. In addition, the algorithms do not add surface detail to account for the reflectance properties of the surface. A set specular reflector is assumed, generating high levels of reflected light. Ideally the lower levels of incident radiation associated with low solar elevation angles would be modelled, along with emitted and reflected light within the environment.

In conclusion, it is not surprising that computer relief shading is inappropriate for modelling earth surface radiation interactions as it is only broadly physically based with many simplifications designed to make the calculations more efficient. It is appropriate for the simple azimuth based experiments described in Chapter 5, however it is not suitable for modelling the effects of low solar

elevation of a topographically complex landscape with surfaces of varying reflectance characteristics.

Appendix 2 Solar Azimuth and Elevation Calculations

2.1 Introduction

Chapter 5 has presented conclusions for understanding the bias of lineament representation on satellite imagery. It went on to recommend the conditions through which optimum imagery can be obtained and presented calculations of solar azimuth and elevation (for Landsat ETM+) to help with this.

The following Appendix contains the algorithms necessary to calculate the solar azimuth and elevation angles for any given location, on any given day. This is specifically for the purpose of calculating these values for the days and times that a given satellite passes over a specific location. For example, Landsat ETM+, a near polar-orbiting satellite, has a swath width of ~180km. It has 233 paths which it takes 16 days to overfly, arriving back at its starting position. Each path is split into 248 rows (~180km long), covering the lit descending path (north pole to south pole) and unlit ascending path (south pole to north pole). The resulting grid is called the World Reference System (WRS) and is used to refer to all images. Each orbit takes approximately 90mins to complete and, due to the near-polar orbit and earth rotation, the paths aren't overflown in strict numerical order. Rather they follow a 7-day interval period, such that path 1 is overflown on day 1 and path 2 is overflown on day 8. As a result, satellite overpass times vary with both longitude and latitude, although adjacent paths have similar overpass times. In addition, the inclination of the satellite degrades through the year slightly altering the overpass times, although this is corrected once a year. Between years overpass times can vary by as much as 5 minutes.

The calculations have been summarised from Muneer (1997) where binaries and source code are available for individual use, and mainly utilise the work of Yallop (1992). The calculations below are based upon UTC time and require the latitude and longitude of the location and the time and day, month and year of the satellite overpass.

2.2 Solar Declination and the Equation of Time

All calculations are based around the *solar day*, which is measured as the time elapsed between the sun crossing a local meridian and the next time it crosses the same meridian. The solar day varies in length throughout the year, principally due to the tilt of the earth's axis and the angle swept by the earth-sun vector during a given period of time.

All calculations of solar position are relative to the position of the earth in its orbit around the sun and require the use of solar time. The *Equation of Time* (EOT) is used to calculate the difference between clock time and solar time. Once computed, this is then corrected for the local time of the area of interest and the difference between this position and that of the longitude of the standard time meridian. Finally the *solar declination* (DEC) can be calculated. This is the angle between the earth-sun vector and the equatorial plane.

A variety of equations are available to calculate both the equation of time and the solar declination at varying degrees of accuracy. For ease of use and accuracy the methods of Yallop (1992) are followed, as reported by Muneer (1997). Although the calculations are simple to follow, many of the variables do not have a physical meaning, however they are described for completeness. The calculations are as follows:

```
t = { (UT/24) + d + [30.6m + 0.5] + [ 365.25(y – 1976)] – 8707.5 } /
36525
```

where

```
UT = Universal Time
y = year
m = month
d = day
min = minutes
s = seconds
t = day count from epoch J2000.0 (noon on 1 January 2000)

UT = h + (min/60) + (s/3600)
```

In addition if m > 2 then y = y and m = m – 3, otherwise y = y –1 and m = m + 9.

The following terms are then calculated. It may be necessary to add or subtract multiples of 360 (for G, L and GHA) to set them in the range of 0-360.

```
G     = 357.528 + 35999.05t
C     = 1.915 sin G + 0.020 sin 2G
L     = 280.460 + 36000.770t + C
a     = L – 2.466 sin 2L + 0.053 sin 4L
GHA   = 15UT – 180 – C + L – a
SHA   = [ 15(UT-12) ] + 180
e     = 23.4393 – 0.013t
DEC   = tan-1 (tan e sin a)
EOT   = (L – C – a)/15
```

where

```
G = mean anomaly
C = correction to centre
L = mean longitude
a = right ascension of sun (apparent) in degrees
GHA = Greenwich hour angle of sun in degrees
SHA = Solar Hour Angle
e = obliquity of the ecliptic
DEC = declination of sun (apparent) in degrees
EOT = Equation of Time
```

2.3 Solar azimuth and elevation

Once the above calculations are complete, the following algorithms are used to calculate solar azimuth (AZ) and elevation (ELE):

```
sin ELE     = sin Lat sin DEC – cos LAT cos DEC cos SHA

cos AZ      = [cos DEC (cosLAT tan DEC + sin LAT cos SHA)] / cos ELE
```

2.4 WorkedExample

The worked example uses a WRS scene from Ireland (Path:207. Row:23) for 1st December 2000. The overpass time was 11:20GMT and the scene centre co-ordinates are N53.104º and W8.203º. The following calculations are then made:

```
Longitude Correction = 8.203/15 = 0.5468

UT    = 11.03
UT Corrected = 11.03 + 0.5468 = 11.57
d     =  1
m     = 9
y     = 2000

t     = [ (11.57/24) + 1 + 275.9 + 8766 – 8707.5 ] / 36525
      = 0.009196

G     = 688.58
G (reset range) = 328.58

C     = -1.01610

L     = 610.5070
L (reset range) = 250.5070

a     = 249.0074

GHA   = -3.93
SHA   = 165.45

e     = 23.4392

DEC   = -22.0369

EOT   = 0.1677 x 60 =  10.062mins

ALT   = 13.81º
AZ    = 166.13º
```

2.5 Conclusions

Although the above calculations are straightforward, they can be lengthy. The purpose of calculating solar elevation and azimuth is not for images that have already been acquired (as this information is usually provided with the meta-data) but rather to perform these calculations over a series of dates to ascertain the best images to acquire. This can be performed manually, however the user will probably want to use the algorithms with the supplied Microsoft Excel spreadsheet to calculate these values. This has already been performed for every Landsat ETM+ WRS cell for the 1st of each month, based around an overpass cycle starting 13th August 2000. Finally, the above algorithms can be programmed manually to allow the user to perform their own calculations on any location for any satellite overpass time.

Appendix 3 Spatial Data Accuracy, Error and Error Assessment

3.1 Introduction

Geography is the study of phenomena with regard to their location. This is operational in both 3-dimensional space, as well as over time. As a result, a phenomenon's characteristics can change in space and time, which consequently affects relationships with other phenomena.

Geographical study tries to simplify the complex nature of relationships between phenomena in space and time by observing them and providing a rational framework through which they can be described and understood. It is the process of observation (phenomena location and attributes) that leads to the recording of spatial data. As geographers attempt to simplify (or abstract) the environment through their description of spatial data, it follows that spatial data are themselves necessary simplifications of our complex environment. Any simplification will incorporate error, whether the recording techniques are analogue or digital, precise or approximate.

This section is concerned with the issue of data quality; the manner in which errors are manifested, their propagation and how to minimise their effect. The phrase *data quality* assumes some standard by which a data set can be judged. Chrisman (1983) suggests that this should simply be a measure of the fitness for purpose. Data only becomes information when there is meaning attached to it and, for this to occur, it must happen within the context of the area of study. In addition to the discussion below, further general texts include Jones (1997), Chrisman (1994), and Aronoff (1989).

3.2 Accuracy

If spatial data are an abstraction of the real world, then a measure of data quality is the accuracy with which the real world are represented. *Error*, or the difference between observed and real values, is a measure of accuracy. Although simple in concept, accuracy assessment is actually more complicated

as it assumes that there is a truth or real world value which can ultimately be known. This very much depends upon the type and scale of the data which is collected. For example categorical attribute data can be considered ultimately knowable (i.e. a person is male or female), whereas numerical measurements (e.g. locational data) are only known to some degree of certainty. Consequently we cannot know what the real or true values are and so accuracy assessment can only be accomplished by comparison with the most accurate measurement available.

The terms *precision* and *accuracy*, are often used interchangeably and as a consequence, incorrectly. Precision refers to the detail used to report an observation (e.g. for numerical data this is the number of significant figures), whereas accuracy is the closeness to the real value. Observations should be reported at a precision equivalent to their accuracy.

3.3 Data Quality

Datasets are comprised of any number of phenomena (or data elements) which have characteristics that affect data quality. In addition, the dataset as a whole has characteristics that also affect data quality. This section will now discuss these elements.

3.3.1 Data Elements

Spatial data elements are made up of locational and attribute data. Locational data can be comprised of points and lines, both of which can suffer from positional error (i.e. a deviation in observed position from the actual position). Positional error can be of two main types:

1. Systematic
2. Random

A *systematic error*, also termed a *bias*, refers to systematic or regular deviations between the observed values and true values. Although ideally these should be zero, if the systematic error is recognised then it can be corrected. *Random errors* are more problematic as, due to their randomness, they are more difficult

to correct and consequently affect the accuracy of the data in unpredictable ways.

Attribute error is concerned with *logical consistency,* which is the maintenance of logical relationships between individual data elements, such that they are all observed in the same manner. For example a road can be mapped at its centre line or either boundary; for consistency the same method needs to be applied throughout.

3.3.2 Data Sets

At the dataset level there are four main elements that affect data quality. These are:

1. Completeness
2. Applicability
3. Compatibility
4. Consistency

Completeness refers to the overall inclusivity of all real elements that are required to be mapped. Datasets can be incomplete yet have high accuracy; again, quality is concerned with fitness for purpose and incomplete data may be suitable for certain applications. Although a separate measure of quality, completeness does involve elements of accuracy which are similar to logical consistency and attribute accuracy.

Resolution is an important element of completeness as it refers to the minimum recording distance. Although a separate concept from accuracy, it is normal practice to make this value smaller than the desired accuracy of the system. In comparison to vector systems, raster based systems often apply the term slightly differently, suggesting it is concerned with the smallest distance over which change is detectable. Regardless of which definition is used, phenomena of different sizes will be detectable with data of varying resolutions. In addition to resolution, systematic and random error may also affect completeness as they can cause the omission or commission of phenomena.

Applicability refers to the overall suitability of data for an intended purpose, analysis or manipulation. For example certain interpolation routines may be inappropriate when converting digitised contours to digital elevation models, whilst population data is inappropriate to map glacial landforms. Data therefore has to be fit for purpose and suitable for whatever techniques are to be applied to the data.

Compatibility refers to the appropriate integration and use of different data sets within a study. For example, the same co-ordinate system should be used between data sets. Data sets should therefore be consistent in the way that they are captured, stored and analysed.

Finally, *consistency* requires the maintenance of a logical relationship between phenomena. Within a GIS this is typically enforced through the topological model (e.g. all polygons must be complete).

3.4 Sources of Errors

So accuracy and error have been discussed with respect to the observations and their real values. However spatial data, and its use, is concerned with more than simply recording values, but storing, analysing and displaying them. At every stage in the process of using spatial data, error can be introduced and, as such, data quality is concerned not so much with removing error, but understanding and managing it. The following section briefly describes the different stages at which error can be incorporated.

Data collection is concerned the initial acquisition of a primary data source from which spatial data will be mapped. Much primary data will be remotely sensed and can contain inaccuracies or biases. The operator may have little control over how the data are collected, but an appreciation of data limitations and management is essential. Secondary data may also be used and these will have their own data collection errors, as well as errors incorporated through their production.

The following stage is *data input* and involves an operator extracting appropriate elements from the input data. Data input is usually of high precision, but accuracy will depend upon the quality of the input data and the experience and ability of the operator.

After data has been captured in an appropriate manner, it will be in a format which can be *manipulated and analysed*. It is at these stages that further error can be introduced; examples include co-ordinate transformations, raster to vector conversion, interpolation and overlay operations.

Finally, *data storage* requires an appropriate number of significant digits otherwise numerical degradation occurs, whilst data transfer can cause the loss of data between different data formats.

3.5 Accuracy Assessment

Accuracy is defined as the deviation of our observations from the real or actual values and, for numerical data (e.g. locational data), these real values will not be exactly known. Accuracy assessment still requires some measure of accuracy and this can be dealt with statistically by providing a numerical assessment of the expected accuracy. In this scenario, observations can be viewed as experiments involving repeated observations. If these measurements are Normally (Gaussian) distributed then we can use the dataset characteristics to provide estimates of expected accuracy. An alternative solution is to compare the dataset values with ones of higher accuracy and so use them as a surrogate for the real values. In this manner we can gain a better understanding of the types of error present.

Attribute data can be numerical or categorical; numerical data can be assessed in a manner similar to that used for locational data. Categorical data are treated according to accuracy classification methods developed within the remote sensing community through the use of a misclassification matrix. Using higher accuracy data, a matrix of correctly and incorrectly classified phenomena or objects can be drawn up and give an indication of the overall accuracy.

Although attribute and locational error are often treated separately they can be intimately linked. Where attributes are applied to phenomena such as soil units, changing an attribute because it has been incorrectly classified can lead to a locational change of that unit. Other boundaries (e.g. political) are fixed and so attribute changes do not affect location.

3.6 Conclusions

Although spatial researchers are particularly concerned with accuracy, it is error that is the central topic. All spatial data are inherently wrong and contain errors. It is the job of the researcher to understand error and minimise it to a level where it is fit for the purpose it is to be used for. Spatial data cover a wide variety of disciplines and as such methods for dealing with error are various. The earliest approaches to error management came from surveying, photogrammetry and geodesy, where reliable measurements are obtained through repeated measures and the use of least-squares estimation. In contrast, social scientists have developed statistical tools from other disciplines to meet their needs and have consequently inherited their approaches. These are mostly designed to deal with errors from sampling.

GIS has to take these approaches and provide a way of incorporating and using them within a technical environment. It will then be possible to make users aware of the error that is inherent in their data and so provide methods of managing it. Within earth science this can provide minimum error guidelines, whilst for social science an awareness of the error can be reported and incorporated into the result.

Subglacial bedforms of the English Lake District and surrounding area

M.J. Smith and C.D. Clark, Department of Geography, University of Sheffield
in Smith (2002) "Techniques for the Geomorphological Reconstruction of Palaeo Ice Sheets from Remotely Sensed Data." Unpublished PhD Thesis, University of Sheffield

Key

- Circular to ovoid subglacial bedforms
- Glacial lineament, mostly drumlins
- Transverse bedform ridges, possibly Rogen Moraine

This map was produced using OS Panorama© DEM data at a resolution of 50m. Landform mapping was performed from the DEM, which was relief shaded using multiple azimuth illuminations in order to fully visualise the landscape. Further discussion can be found in Smith (2002) "Techniques for the Geomorphological Reconstruction of Palaeo Ice Sheets from Remotely Sensed Data." Unpublished PhD Thesis., University of Sheffield.

Relief shaded from the north

Relief shaded from the west

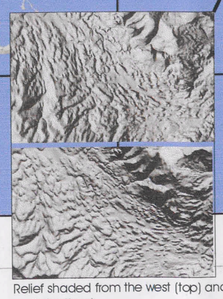

Relief shaded from the west (top) and north (bottom).

Background map is a relief shaded image coloured according to altitude and relief shaded from the NW.
© Crown Copyright Ordnance Survey. An EDINA Digimap / JISC supplied service.